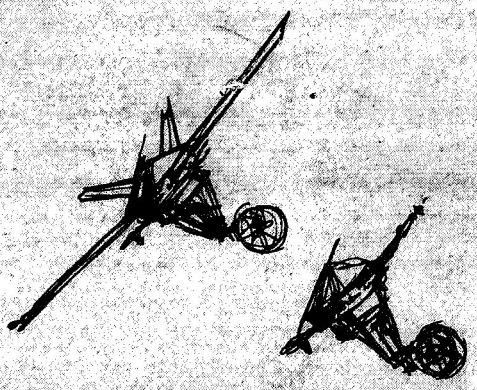

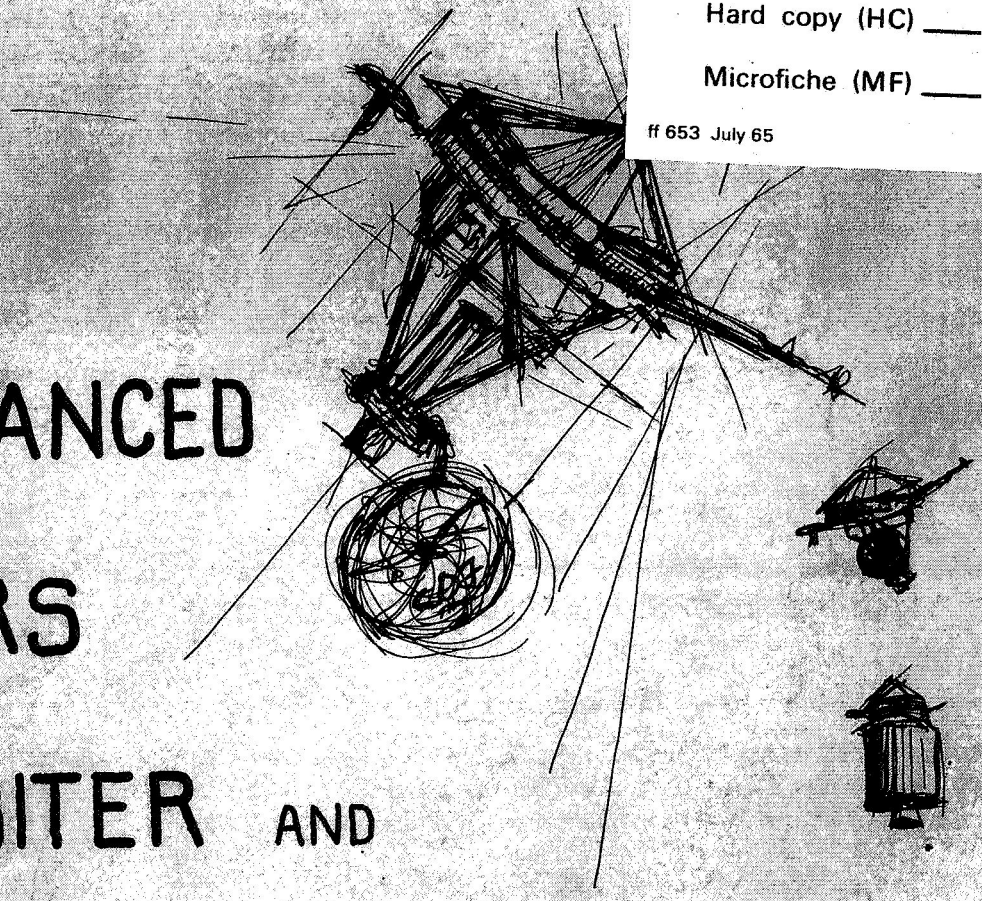

ADVANCED MARS ORBITER AND SURVEYOR

A CONCEPTUAL DESIGN BY THE NASA SPACE TECHNOLOGY SUMMER INSTITUTE

1968

FOREWORD

The Space Technology Summer Institute was sponsored by the National Aeronautics and Space Administration. It was held at the University of California at Santa Barbara under the direction of the Department of Mechanical Engineering. The program was designed for a duration of six weeks beginning on June 24th and ending on August 2nd.

The Institute was composed of thirty-five students, each of whom had completed his junior or senior year in college. Graduate student assistance was available in technical areas if needed. The students' major fields of study ranged from all areas of engineering to mathematics and physics. This wide variety of backgrounds gave the diversity needed for a successful program. Someone was always present who was familiar with the problems which were encountered and ultimately solved.

The purpose of the Summer Institute was to provide the fundamental background in the field of space technology which the ordinary university does not offer. After completion of this program, it is hoped that the students will have sufficient interest and background to further pursue their studies in the space field, either in graduate school or in industry.

The main project of the program was a systems engineering course in which the members were to create a preliminary design for an advanced Mars orbiter scheduled for launch in the late 1970's. Due to the extremely short six week time period, a conceptual design, rather than a detailed engineering analysis was undertaken. Consequently, some aspects of the design were only given a minimal amount of attention.

The students working on this program would like to express their thanks and appreciation to the people whose assistance made it possible to design a workable and technically correct spacecraft: to Dr. William Bollay for guiding the entire project and for giving vital technical information and assistance; to our own lecturers, Dr. Gray, Dr. Kuby, Dr. Mitchell, and Dr. Wyatt for the background information which their classes provided; to our guest lecturers Dr. H. Schuerch from Astro Research Corp., Mr. R.F. Hummer from the Santa Barbara Research Center of Hughes Aircraft Co. and to Dr. A.T. Nordsieck from the General Research Corporation; to the people at the Jet Propulsion Laboratory, T.R.W. and Rocketdyne for their valuable technical aid in the areas of communications, propulsion, and observation techniques; to A.C. Electronics for their design of the spacecraft lander; and finally to Professor Thomson, head of the Mechanical Engineering Department and Program Director, whose time and effort made the entire Institute possible.

SPACE TECHNOLOGY SUMMER INSTITUTE 1968

DESIGN GROUPS

Systems Integration Group

Project Manager--H. Laird Parry, U.C. Davis
Brian Boswell, U. C. Santa Barbara
Charles Franklin, Oregon State
Robert Fischer, U. C. Santa Barbara
Gil McCoy, University of Washington
Lawrence Trupo, University of Redlands
James Wolf, University of Portland

Propulsions Group

Group Leader--Eric Laine, U. C. Berkeley
Group Editor--John Quella, University of Colorado
Steve Body, U. C. Santa Barbara
Craig Hanson, University of Utah
Donald Miller, U. C. Santa Barbara
Jim Rexroad, Northern Arizona University

Power Generation Group

Group Leader--Mark Perra, U. C. Davis
Group Editor--Daniel Harkins, Seattle University
Greg Buchaj, Calif. State College at Los Angeles
Earl Kami, University of Hawaii
Daniel Murphy, Loyola University at Los Angeles
Joseph Riley, U. C. Santa Barbara
Russell Rosinsky, University of Wisconsin

Communications Group

Group Leader--Steven Cowen, U. C. Santa Barbara
Group Editor--Bruce Donsker, California State Polytechnic College
Robert Hamilton, U. C. Santa Barbara
Marc Krigel, Los Angeles City College
Steven Majoewsky, U. C. Santa Barbara
Don Ollis, U. C. Santa Barbara
Kenneth Takemoto, University of Hawaii
Edwin Wrench, U. C. Santa Barbara

Observations Group

Group Leader--Bob Elmore, U. C. Santa Barbara
Group Editor--Milton Lau, University of Southern California
Jerry Becker, San Fernando Valley State College
Gaston Chan, U. C. Santa Barbara
Dennis Cooper, U. C. Davis
Marty Fegley, University of Colorado
Carl Hindman, University of Colorado

TABLE OF CONTENTS

TABLE OF CONTENTS

Note: Detailed Tables of Contents appear before each Appendix.

PROJECT ORGANIZATION

To achieve the objective of designing an advanced Mars orbiter in the short time available, the class was divided into five groups for maximum efficiency. Each group had its own particular area of research and design. This type of organization allowed a more detailed analysis and in the end provided a workable and feasible spacecraft design.

Each individual group had a group leader and an editor who were selected by the group members. A periodic progress report was turned in by the leader of each group to the project manager so that all the work being done could be organized and coordinated.

The groups included Systems Integration, Propulsion and Performance, Power Generation, Communications, and Observation and Sensors. The role of the Systems Integration Group was to coordinate the work of the other four groups and to make final decisions on which systems were to be included in the final design. They were also responsible for the structural design and configuration of the spacecraft. The systems group received the reports from each individual group and compiled the final spacecraft systems report. The work of the Propulsion and Performance group included the choice of the launch vehicle design of the retro system for orbital insertion and design of the midcourse propulsion and attitude control systems. Computation of the Earth-Mars trajectory, Mars orbital characteristics, and launch window dates were also the responsibility of this group. The power Generation group was concerned with supplying the necessary onboard electrical power needed by the spacecraft systems, both while in orbit and in flight. The Communications group designed the transmitting systems for relaying the engineering and scientific data from the spacecraft to earth. This group also designed the systems for receiving the spacecraft command signals from earth. Some research was done concerning the earthbound tracking stations needed to receive the data transmitted from the orbiter. The Communications group also was in charge of the onboard data storage system which is to be used when the position of the spacecraft makes it impossible to transmit data in real time. The Observation and Sensors group did the actual design of the scientific payload which would be carried on the orbiter and were responsible for the lander which is to make a soft landing on the Martian surface. They also made the decision on the type of Mars orbit which was to be used in order to obtain the maximum efficiency from the observation and sensing devices onboard the spacecraft.

The project report is divided into two sections. The first is a summary of the proposed spacecraft design. The second consists of a series of appendices which describe the proposed system in greater detail and discuss alternate systems that were considered.

MISSION DEFINITION AND DESIGN PHILOSOPHY

One of the goals of the Summer Institute was the conceptual design of an advanced Mars orbiter to be launched in the late 1970's. In fulfilling this purpose it was necessary to look ahead and determine what the probable state-of-the-art in planetary exploration would be during this period. It was assumed that the Voyager Program would be completed as scheduled. This program would result in low resolution photographs of the Martian surface from an orbiter and the completion of preliminary geological and biological experiments by a lander.

Using these considerations as a starting point, it was decided that our orbiter should produce extremely high quality and high resolution photographs of different regions of the Martian surface and a topographical map (a light radar system was used). Also, the orbiter should have a lander capable not only of a soft landing but also of independent movement across the planetary surface to perform scientific experiments at various locations. In addition, several onboard scientific experiments during both the Mars intercept trajectory and Mars orbit should be performed.

A conservative approach was used and attempts were made to use already existing and proven design concepts. When existing designs were not adequate for the proposed systems, advanced designs were adopted. Advanced designs are most notable in the areas of observation techniques and communications. Whenever an untried system was incorporated into the spacecraft, a detailed analysis of the system was performed in order to insure maximum reliability and complete research and development before the production freeze date. The exact launch date was kept flexible in order to achieve the maximum payload which could be inserted into a Mars orbit. Time was not available for making a detailed three-dimensional orbit calculation using the digital computer. It was possible, however, to perform the computations of the performance parameters to a sufficient accuracy for a preliminary design such as this. Due to the limited working time available, alternate systems were not provided for most areas of the final design. In some critical areas, such as communications and power conditioning, redundant systems were designed in order to insure maximum reliability.

SPACECRAFT DESIGN SUMMARY

SUMMARY

The spacecraft proposed by the Space Technology Summer Institute for advanced Mars exploration has been designed with three major goals in mind: 1) obtaining high resolution pictures of portions of the planet, 2) obtaining an accurate surface profile of the planet, and 3) landing a mobile laboratory on the Martian surface. Pictures of 2 meter resolution will be obtained using a multi-spectral line scanning camera. A laser radar profile mapping system incorporated into the multi-spectral camera will let it accomplish the first two project goals simultaneously. To accomplish the third goal the spacecraft is equipped with a lander which will soft-land a mobile laboratory designed by General Motors to carry out experiments on the surface of Mars.

The spacecraft has been designed to accomodate the camera and lander. In order to deal with the tremendous earthward data transmission rates required for high resolution pictures (on the order of 10^7 bits per second), laser communication will be used for the earth downlink. A more standard microwave system will provide the earth uplink, lander/orbiter communications, and the earth downlink during transit to Mars. Power for the spacecraft will be provided by large roll-out solar arrays. The large arrays will provide 2000 square feet of solar panel area, enough to supply the required 10 kilowatts at Mars. The spacecraft will be launched from earth using a Saturn V/Centaur launch vehicle. A bi-propellant rocket engine will provide for midcourse corrections and insertion into a Mars orbit, while cold gas jets will be used for attitude control and stabilization.

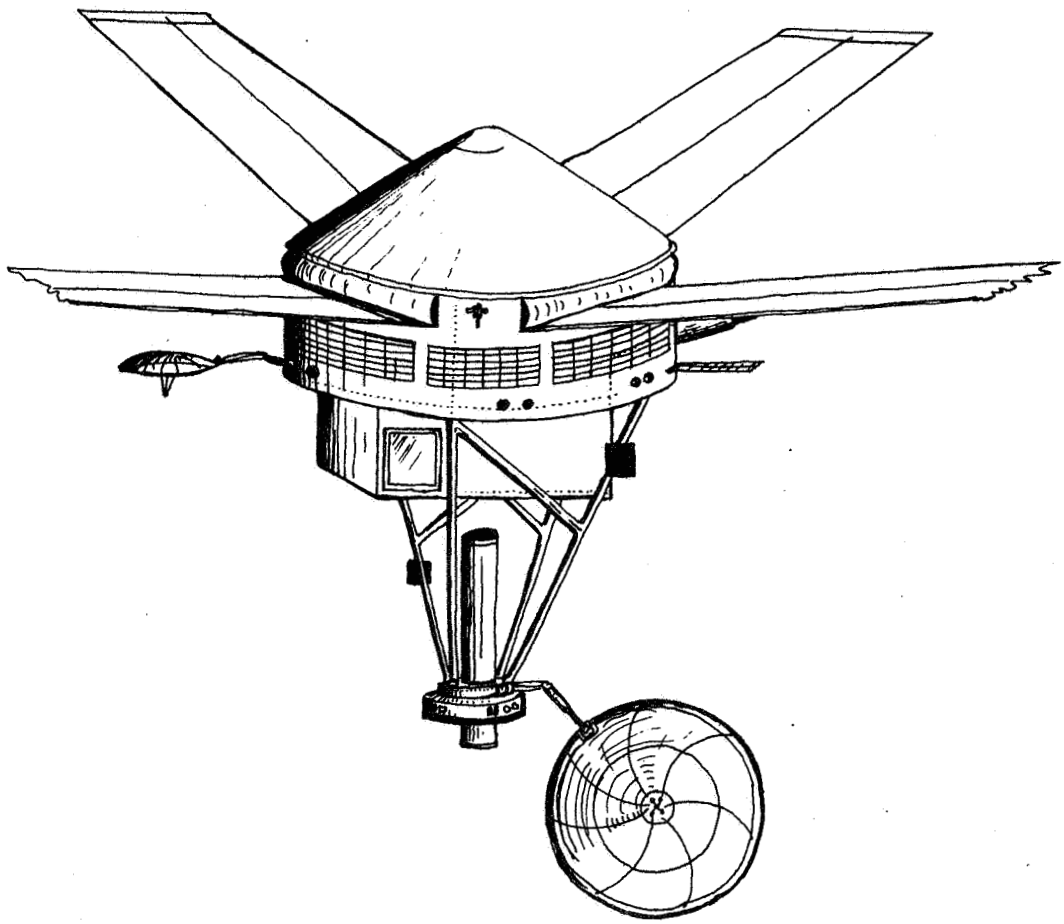

Advanced Mars Orbiter and Surveyor

CHAPTER 1

PROPULSION SYSTEM

SPACECRAFT DESIGN SUMMARY

PROPULSION SYSTEM

The objective of the Propulsion and Performance team was to choose a launch vehicle, design mid-course maneuver, retro, attitude control and stabilization propulsion systems, and to plan an appropriate Earth-Mars transfer orbit for a 1977-1979 scientific Mars orbiter. A design parameter of this project was the use of a Saturn V for the basic launch vehicle.

The final design of the propulsion system consisted of an uprated Saturn V/Centaur and chemical mid-course, retro, and attitude control and stabilization units. This system is capable of launching a Mars satellite with an initial payload of 87,000 pounds, placing this system into a parking orbit around the Earth if necessary, transferring the system from Earth to Mars, and placing it in a Mars orbit.

The mid-course and retro propulsion systems will use approximately 60,000 pounds of chemical bipropellant, hydrazine with UDMH and N_2O_4, in a single nozzle configuration. The attitude control and stabilization system will consist of twelve thrusters using either compressed nitrogen or hydrazine with UDMH and N_2O_4 bipropellant.

During the chosen launch window of September 4, 1977 to October 14, 1977, a scientific payload of 20,450 to 22,000 pounds will be placed in a Mars orbit. The transfer time for the Hohmann elliptical orbit used will vary from 230 to 260 days, depending on the launch date. A 200 kilometer sun synchronous, near polar Mars orbit will be used in order to make a maximum use of solar energy and still give complete planetary coverage.

Saturn V/Centaur Launch Vehicle

Our Mars mission dictates the use of a high performance propulsion system. The uprated Saturn V/Centaur system was chosen to produce the energy required to put an 87,000 pound payload on a Hohmann transfer orbit to Mars. This energy includes energy to escape the Earth's influence and give the approximate 3 km/sec initial velocity of the ideal Hohmann transfer ellipse to Mars. Additional energy requirements needed further in the trajectory will be obtained from rocket systems to be discussed later in this report.

The Saturn V is the largest, all chemical propulsion system available to U.S. engineers. It is a three stage rocket with a weight breakdown and engine configuration as shown in Table 1-1.

The burn time of the first stage is 150 seconds taking the vehicle to an altitude of approximately 30 nautical miles. Four of the five first stage rocket engines are gimballed for thrust vector control. Separation is performed by eight 80,000 pound thrust solid rocket motors.

The second stage burns for 375 seconds. Four of the five second

TABLE 1-1

WEIGHT BREAKDOWN AND ENGINE CONFIGURATION

OF THE STANDARD SATURN V CENTAUR

	Component	Weight (lb)	Engine	Thrust (lbf)	Fuel
Stage I					
	dry wt.	289,000	5-F1	$7.5\ 10^6$	Lox
	propellant	4,555,000	clustered		RP-1
	interstage	11,000			
Stage II					
	dry wt.	83,100	5-J2	$10.25\ 10^5$	Lox
	propellant	969,100	clustered		LH_2
	interstage	7,500			
Stage III					
	dry wt.	25,700	1-J2	225,000	Lox
	propellant	230,000			LH_2
	instrument unit	4,150			
Centaur					
	dry wt.	5,950	2	30,000	Lox
	propellant	30,000			LH_2

stage rocket motors are gimballed to provide thrust vector control during flight. Eight 22,500 pound thrust solid rocket motors are installed for ullage control. Four 35,000 pound thrust solid rocket motors are used for separation from the third stage. The second stage uses a programmed propellant mixture ratio sent from an instrument unit on the vehicle to optimize engine thrust/specific impulse history. The second stage has a shutdown-restart capability for possible orbit maneuvers.

The main engine on the third stage is gimballed in pitch and yaw to provide thrust vector control. Forward roll control is provided for by two fixed axis 150 pound thrust rocket motors. Roll, pitch, and yaw control is available during coast periods by fixed 150 pound thrust liquid rocket motors. Two solid rocket motors are used for initial ullage control, there are also two 72 pound thrust hypergolic engines for ullage control after any shut down and coasting period. Normally, the third stage is equipped with four 35,000 pound thrust retro rockets which would not be needed for this mission. These motors and associated propellants would be removed, reducing the third stage weight. This stage also has shut-down and restart capabilities which might be used for trajectory maneuvers.

The Centaur is a highly sophisticated propulsion system utilizing liquid oxygen and liquid hydrogen for propellants. It will be put on top of the Saturn V as a fourth stage. The Centaur has a diameter of ten feet, but by using a shroud this dimension will not limit the payload to a ten foot diameter. The Centaur has two 15,000 pound thrust engines gimballed $\pm$ 4 degrees to provide thrust vector control. It carries 30,000 pounds of propellants and has a firing time of 470 seconds. Restart capabilities are incorporated in the engines. Three axis attitude control is obtained from two thrust clusters each containing one 7 pound thrust pitch engine and two 3 pound thrust roll-yaw engines for ullage control. The reaction control engines use hydrogen peroxide monopropellant.

The basic Saturn V has its own instrument section located on top of the third stage. It includes five major subsystems; 1) Environmental control system which provides cooling of electronic equipment, 2) Guidance and control systems, 3) Measuring and telemetry systems which transmit signals from the vehicle or experiment transducers to Earth, 4) Radio frequency system to maintain contact between vehicle and Earth for tracking and command purposes, and 5) Electrical generation system. The Centaur also has its own guidance and control system.

Midcourse and Retro Propulsion

A storable liquid propellant system has been selected to execute mid-course maneuvers and retro-fire. The propellants selected are nitrogen tetroxide (N_2O_4) and a 50/50 mixture of hydrazine (N_2H_4) and unsymmetrical dimethyl hydrazine (UDMH). These liquids provide a high performance, space storable propellant that is relatively reliable and safely handled. They are hypergolic when mixed and, therefore, allow engine restart with a simplified system.

The proposed engine will develop about 100,000 pounds of thrust at

altitude with a chamber pressure of about 300 psi. Gimbal mounting will be used to allow additional control. Cooling will be accomplished by combined regenerative and ablative cooling. The chamber and throat will utilize the fuel as a coolant and the expansion nozzle will be ablative. Propellant pumps will be used to feed the engine because of the large quantity of fuel required on this mission. This presents a restart problem. One possible solution would be to add small pressure feed propellant tanks to provide fuel ullage and gas generator operation during initial start and restart. A schematic of such a system is shown in Figure 1-1.

Propellant loads vary with the change in velocity necessary to achieve Mars orbit. The change in velocity varies with the orbit and the launch date. Figure 1-2 shows the necessary fuel loads for velocity changes between 11,000 and 13,000 ft/sec. Fuel is consumed at a rate of 294 lb/sec with a 100,000 pound thrust engine. Total mid-course and retro burn times are shown for various velocity changes in Figure 1-3. Various propellant characteristics are given in Table 1-2.

The usable payload of the orbit vehicle varies between 16,800 and 29,680 pounds depending on the launch date. The total mid-course, retro system propellant tank volume would require a maximum of 812 cubic feet for usable fuel. This is broken down into 450 cubic feet for the oxidizer and 352 cubic feet for the fuel. The maximum burn time required would be about 6.5 minutes.

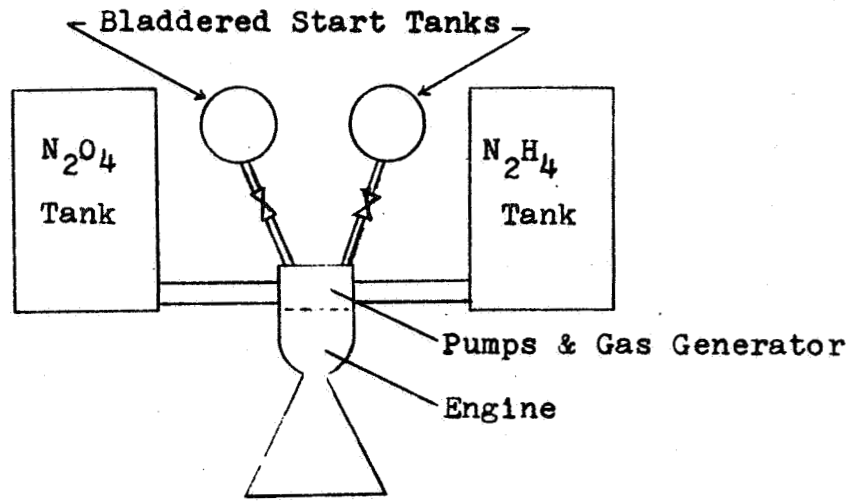

FIGURE 1-1

Schematic diagram of proposed mid-course and retro rocket system.

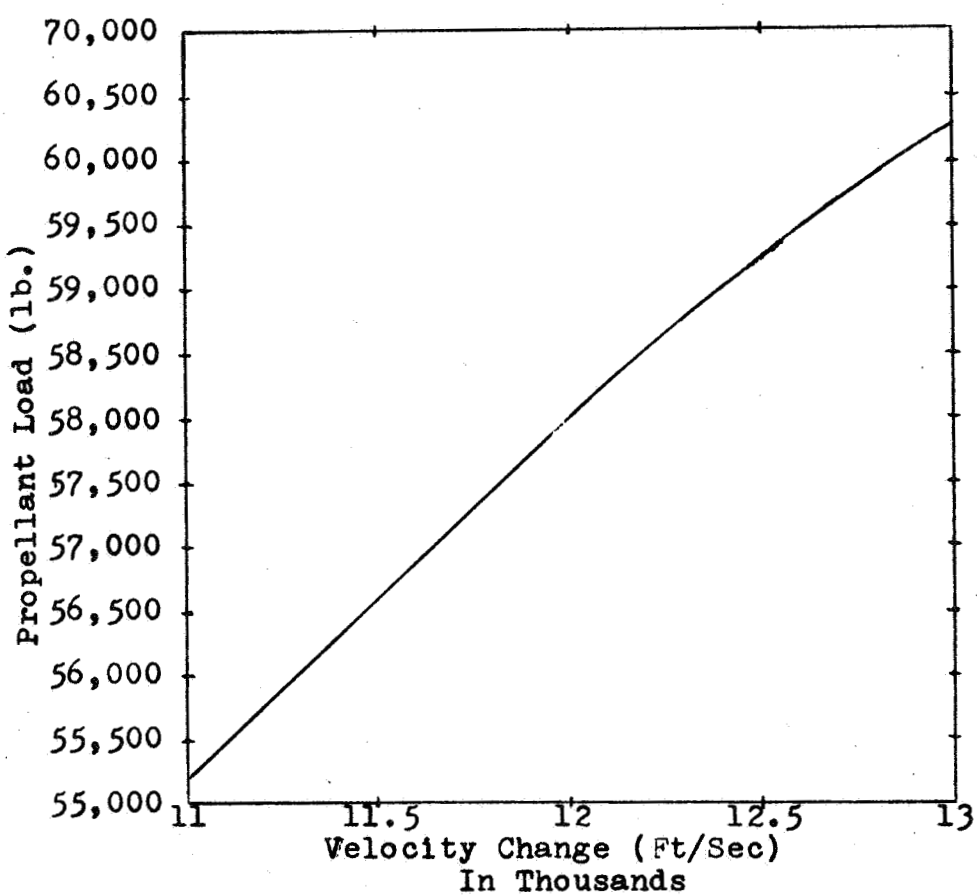

FIGURE 1-2

Propellant load vs. change of velocity.

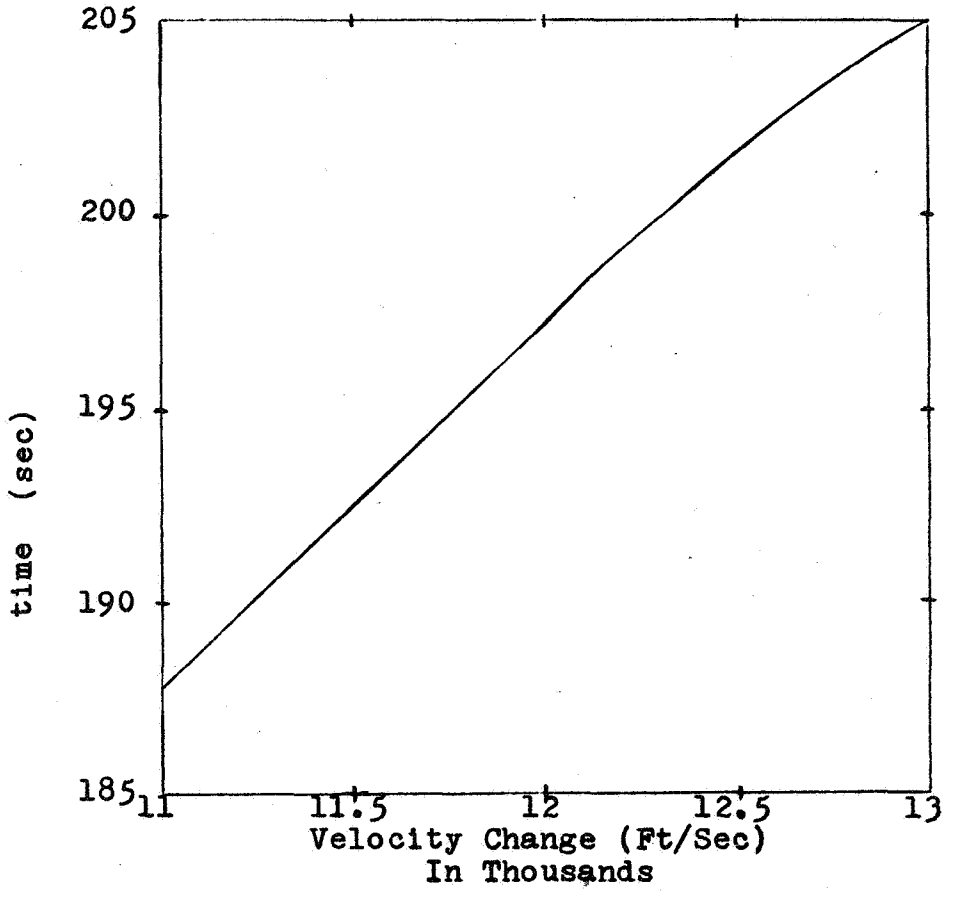

FIGURE 1-3

Burn time vs. velocity change.

TABLE 1-2

Propellant Characteristics

50/50 N_2H_4/UDMH Density =	56.1 lb/ft^3
N_2O_4 Density =	89.9 lb/ft^3
Combined Bulk Density =	74.3 lb/ft^3
Propellant Specific Impulse (I_{sp}) = (In vacuum with chamber press.=300psi.)	340 sec.
Propellant Burn Temperature =	5370 ^{o}F.

Stabilization and Attitude Control System

The propulsion system for zero gravity spacecraft attitude and stabilization control has four purposes: spacecraft stabilization following launch vehicle separation, navigation reference and sun acquisition, attitude orientation prior to mid-course maneuver and retro firing for orbit insertion, and sensor attitude maintenance during Martian orbit.

The propulsion system consists of twelve jets with 0.1 pounds of thrust directed along the three spacecraft axes. The jets shall be fired in couples or individually for roll, pitch, and yaw control. Two propellants should be considered for the final design, cold compressed nitrogen and a hydrazine with UDMH and N_2O_4 bipropellant. A description of both types of propulsion systems will be given in this report to facilitate a final decision.

All figures and calculations are based on a scaled Voyager spacecraft for which total impulse and flight times were known. The scaling was done by making a comparison between Mariner and Voyager crafts and applying that scale to the Mars mission. The total impulse required for the mission is 3600 pound-seconds. A safety factor of 1.5 was applied to yield an impulse of 5400 pound-seconds.

The compressed nitrogen propellant has a specific impulse of 71 seconds. Therefore, 76 pounds of propellant and twenty pounds of hardware are required, resulting in a 96 pound system with a volume of 5.6 cubic feet. The gas will be stored in spherical tanks at a pressure of 3000 psi.

The bipropellant has a specific impulse of 340 seconds. This requires 16 pounds of propellant and approximately 40 pounds of hardware, resulting in a system weight of 56 pounds. The nozzle will be cooled by radiation. Teflon bladders pressurized with helium gas will serve as the propellant expulsion system.

The cold gas system has the advantage of simplicity and reliability. Little hardware is required in a pressurized gas system. However, the low specific impulse of the propellant increases the weight of the system for a long duration, high total impulse mission. Although the bipropellant affords a lighter system, it does so at the expense of reliability and simplicity. Also, it is felt that the low thrust level required is below the optimum bipropellant range. Consequently, the cold gas system has been selected for our mission.

Mars Trajectory

Our proposed launch date is September 4, 1977, giving a flight time of 260 days. Ninty-seven days after launch, a mid-course plane change is required to account for the 1^{o} 51' difference between Earth and Mars' plane. The spacecraft orbit around Mars is circular and 200 km. above the surface. It is inclined 20^{o} with the Mars-Sun line and near polar. (This orbit meets the needs of the observations group.)

For the proposed 1977 launch date, a hyperbolic excess velocity leaving the Earth $V_{\infty E}$ = 15,720 feet per second is required. For this $V_{\infty E}$, the Saturn V-Centaur can launch a payload of 79,000 pounds toward Mars. The mid-course plane change requires an additional velocity increment of ΔV_1 = 2,730 feet per second. With this trajectory the spacecraft arrives with a hyperbolic excess velocity of $V_{\infty m}$ = 12,400 feet per second relative to Mars. This requires a velocity change near Mars of ΔV_2 = 8,920 feet per second in order to enter a 200 km. circular orbit around Mars. The total $\Delta V = \Delta V_1 + \Delta V_2$ = 11,650 feet per second. Using the proposed bi-propellant rocket system a total payload of 21,720 pounds can be injected into a Mars 200 km. orbit. It is proposed that the lander be included in this payload so that it can be directed to a desired location

For other launch dates the velocity requirements and payloads delivered to a 200 km. Mars orbit are shown in Table A-4.

CHAPTER 2

POWER GENERATION SYSTEM

SPACECRAFT DESIGN SUMMARY

POWER GENERATION SYSTEM

The preliminary power design for the craft employs the solar photovoltaic method of energy conversion. This system was considered to be the most feasible way of obtaining a ten kilowatt power source for the prescribed launch date. Such systems are currently in a state of the art and will require a minimal amount of design work to meet the mission requirements.

In-flight power will be supplied by a solar array covering the basic structure of the craft. This was done because the extended arrays would not be able to structurally withstand the accelerations caused by in-flight maneuvers.

Once in orbit, the space vehicle will deploy four thin-film roll out solar arrays. These arrays will be deployed from cylindrical containers mounted on the side of the structure in a position which will orientate the array surface towards the sun. The arrays will also be positioned in such a manner as to add over-all stability to the craft. This will be done by taking advantage of the solar pressure acting on a surface which is dynamically stable with respect to the center of mass of the entire system.

The solar arrays will be backed up by a support system consisting of a battery bank and a power conditioning unit. The batteries will be used during periods of solar occultation and on occasions which require more power than that delivered by the array. The power conditioning unit will regulate the power and provide the necessary voltage and current requirements for the proper operation of the control, communication and observation systems.

ARRAY DESCRIPTION

In-Flight-Power

In-flight power for the vehicle's guidance and communication subsystems is provided by three hundred square feet of conventional silicon solar cells bonded to the surface of the propulsion module. This will provide a power supply of three kilowatts at 1 A.U. or approximately 1.5 kilowatts in the vicinity of the Mars orbit. This array will be jettisoned after orbit insertion with the rest of the propulsion module.

Orbit Array

The solar arrays used for power during orbit will be of the thin film rolable type. The solar "blankets" consist ofcadmium sulfide solar cells deposited on a flexible organic sub-strata (Kapton).

Orbit Array Deployment

The solar array deployment technique for the spacecraft employs a roll-up storage system. Table 2-1 gives a display of the general design parameters of the system and Figures 2-1 and 2-2 show the general structural designs involved.

The advantages of this system are many. A folded array of comparable size could be made to compete with roll-up arrays in terms of weight, but storage space for such a system is prohibitive in our particular mission. In addition, the roll-up system can better withstand the acceleration and vibrational loads placed on it during launch and mid-course maneuvering operations, thus increasing the overall reliability of the system. Based on research studies by General Electric, Ryan Aviation, and Fairchild Aviation, the roll-out method of deployment is the most efficient in utilizing the extremely thin, lightweight, and flexible solar arrays made possible by the use of materials other than the now standard silicon.

The deployment system itself consists primarily of four aluminum drums 120 inches in length, mounted on smooth bearings and stub axles at the extremities. On each drum is wound a solar cell "blanket" whose dimensions are 120 inches wide by 600 inches long, providing a total deployment solar area of 2,000 square feet. At five foot intervals on the bottom surface of the "blanket", 120 inch long beryllium supports are incorporated, running the width of the solar arrays.

The solar "blankets" are deployed when a bi-stem boom of beryllium construction, extending 50 feet, is actuated after the Mars orbit is attained. The bi-stem boom is essentially a variation on the De Havilland boom, consisting of two circular segments which are stored prestressed in flat rolls and are extended to fit one inside the other. This boom is extremely compact and is extended by means of electric servo motors at a rate of 1.5 inches per second. At the leading edge of each solar blanket a reinforced beryllium support is installed and attached to the bi-stem boom.

The base support of the boom mechanism angles the boom (and the array) at an angle θ to the longitudinal centerline of the vehicle. This is done to provide for solar pressure stabilization of the craft. Such a configuration introduces a loss in efficiency of the array of $P_o \cos \theta$.

The design considerations and calculations for this system were performed while paying especially close attention to a study carried out by General Electric (Report #685D4246) on a similar system producing 10Kw. at 1 A.U.

Solar Array Design Parameters

Solar Panel Efficiency (percent)	10.0
Solar Panel Area (square feet)	2000
Power Generated per Square Foot Area - watts @ 1 A.U.	10
Total Power Generated - kilowatts @ 1 A.U. ..... - kilowatts @ 1.5A.U.	20 10
System Weight per Kilowatt Generated (lbs/Kw)...	30
System Weight (lbs)	600

Table 2-1

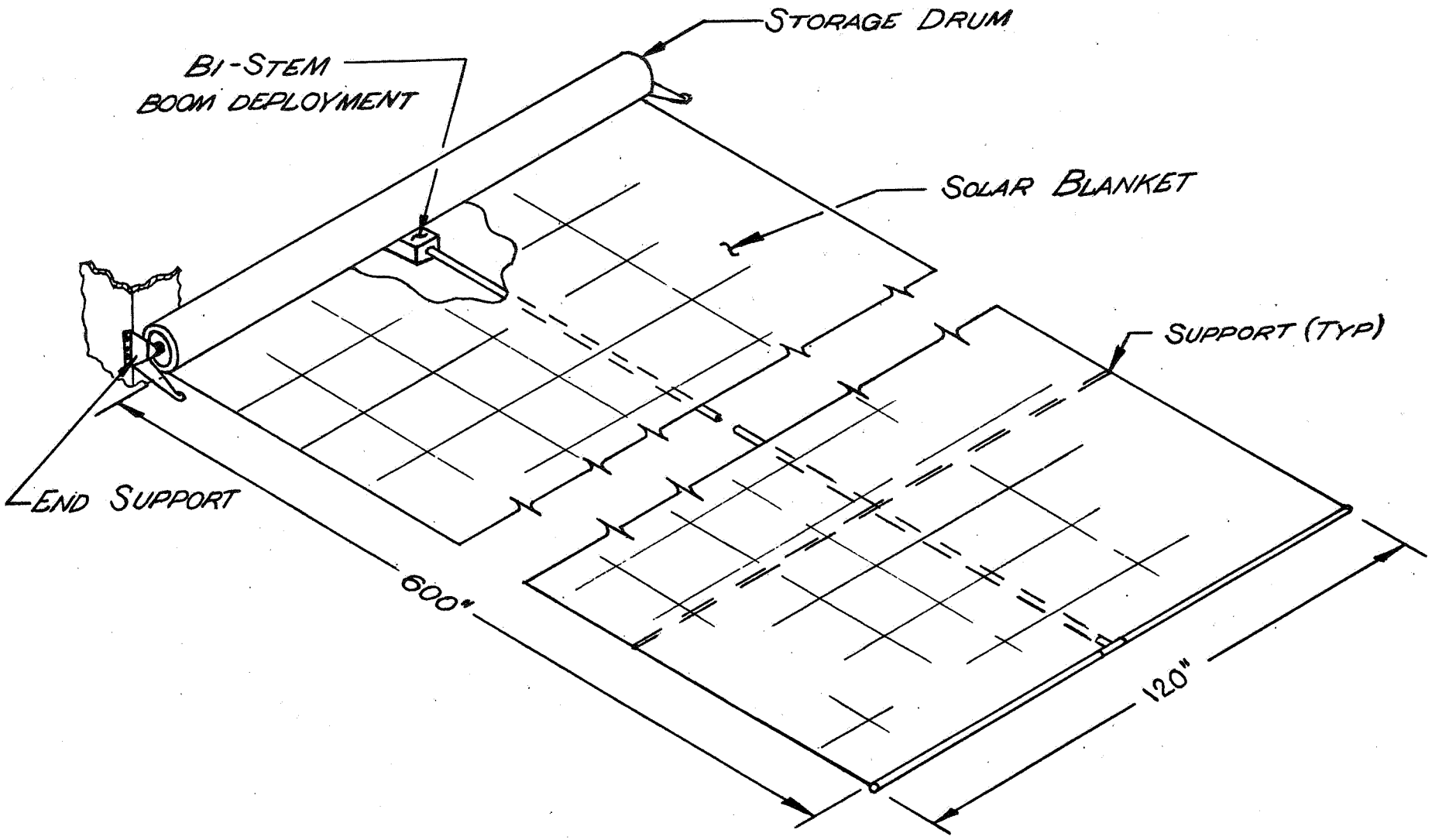

FIG. 2-1 DEPLOYMENT STRUCTURE SCALE 1"=2 2/3'

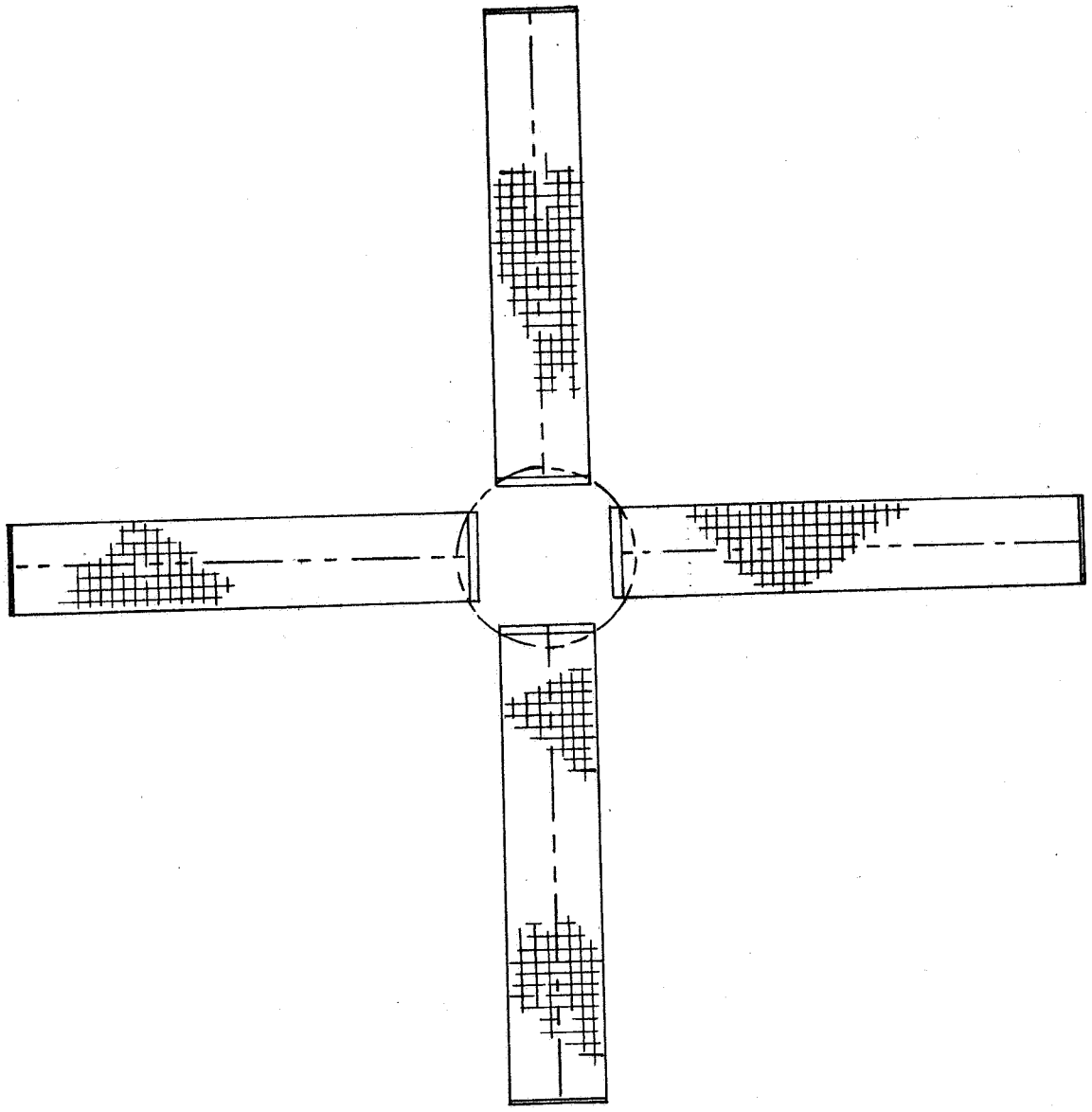

FIG 2-2 GENERAL CONFIGURATION SCALE: 1" = 1'

SECONDARY POWER SUPPLY

The purpose of the secondary power supply is to provide power for the experimental equipment during times the spacecraft is in eclipse. All of the power during eclipse must come from the secondary power supply since the solar cells are ineffective when not in the direct sunlight. The circular orbit of our spacecraft requires one hundred and ten minutes of which fifteen percent is in eclipse. In other words, during each orbit ninety-three minutes will be allowed for charging the batteries while for seventeen minutes they will be discharging.

Battery Description

The secondary power supply chosed for our spacecraft is the nickel-cadmium battery. This battery best fits the unique features encountered in our mission. The parameters determining the selection of this battery are included in the appendix.

During the four year orbit objective (each orbit being one hundred and ten minutes), the batteries have to go through approximately 20,000 charge-discharge cycles. In order that the battery achieve this high a number of recharge cycles, it is necessary that the depth of discharge be very low. For this reason a twenty per cent depth of discharge maximum is used. At this level the specific energy density of the battery is sacrificed leaving only three watt-hours per pound as compared to twelve watt-hours per pound at one hundred per cent discharge.

The battery power requirement is small because the spacecraft is in the sunlight eighty-five per cent of the time. Also, during periods of eclipse much of the observation equipment will not be used. Sufficient power is supplied because the synthetic aperature side-looking radar standby system uses six hundred thirty kilowatts of power for six nanoseconds approximately three thousand times per second. The solar array cannot supply this great an instantaneous power so that much power is drawn from the batteries. Also, much of the instrumentation cannot withstand the frigid temperatures of the Mars eclipse necessitating power consumption for the heating elements.

A significant characteristic of the nickel-cadmium battery is its ability to be recharged at a fast rate. With the proper controls it is possible to recharge a cell at a one hour rate. The energy for charging the batteries comes directly from the solar primary supply. A control unit regulates the charging current until the batteries are charged and then cuts it off.

All significant battery characteristics are listed in Table 2-2. It should be noted that although the minimum battery life requirement is four and three-quarters years, the nickel-cadmium cell has the potential of eight years operation if the other components of the spacecraft are still operational.

Secondary Battery Characteristics
Nickel-Cadmium Battery

No. of Batteries	2
No. of Cells per Battery	30
Voltage (volts)	37
Depth of Discharge (percent)	20
Specific Energy Density (WHr/Lb) ...	3.0
Capacity (WHr)	500
Weight (lb)	167
Volume (ft^3)	1.6
Cycle Life (minimum no. of cycles) .	20,000
Battery Life (minimum no. of years).	4.75
Time of Charge (minutes)	93
Time of Discharge (minutes)	17

Table 2-2

Power Conditioning

In addition to the primary solar array energy source and the secondary battery source, the power system requires a back up conditioning unit. This sub-system controls and regulates the raw power delivered by the source. It is the function of such a system to condition the raw power in such a manner that the power delivered to the onboard equipment is presented in a useable form.

The conditioning system used will be a de-centralized arrangement. In this process, the array output power will be regulated to a single DC component of the voltage. This single regulated DC voltage will then be bussed to the different power consuming sub-systems. Each sub-system will then be responsible for converting this DC voltage to a waveform suitable for the proper operation of their respective system.

The de-centralized system offers advantages in the fact that less cabling (and power loss) is involved in power transport as compared to having one central power conditioning unit for all sub-systems. Also, interference of various systems (such as magnetic interference) can be decreased by keeping the various individual sub-system power conditioning units isolated. Simplicity in distribution design is also an added advantage of the de-centralized system.

Figure 2-3 shows a basic distribution diagram of the electrical power subsystem.

The major piece of equipment in the conditioning sub-system is the "power switch and logic" section. This unit determines the source of the raw power being used (i.e. whether the batteries or the arrays are supplying the power). When the craft is in solar occultation and the arrays are useless, the batteries are switched into the source position. During solar orientation periods the arrays are used for power and the battery chargers are employed until the battery banks indicate a full charge. This same device also provides a means of dissipating extra amounts of power produced but not needed.

In addition to the switching system involved, the "DC Regulator" actually conditions the delivered raw power to meet the specifications of a true power supply. The resulting output of the system is a constant DC voltage with as little ripple involved as is feasible.

This system provides for a single DC regulated voltage and an unregulated DC voltage to be bussed to the necessary sub-systems. The regulated DC portion will go to the observation, communication, and control equipment. The unregulated power will go to such systems as capsule environmental control or heating units that will not require extremely exact reference voltages. Use is made of as much unregulated power as possible because there is a power loss factor involved in the DC regulator which if possible should be avoided.

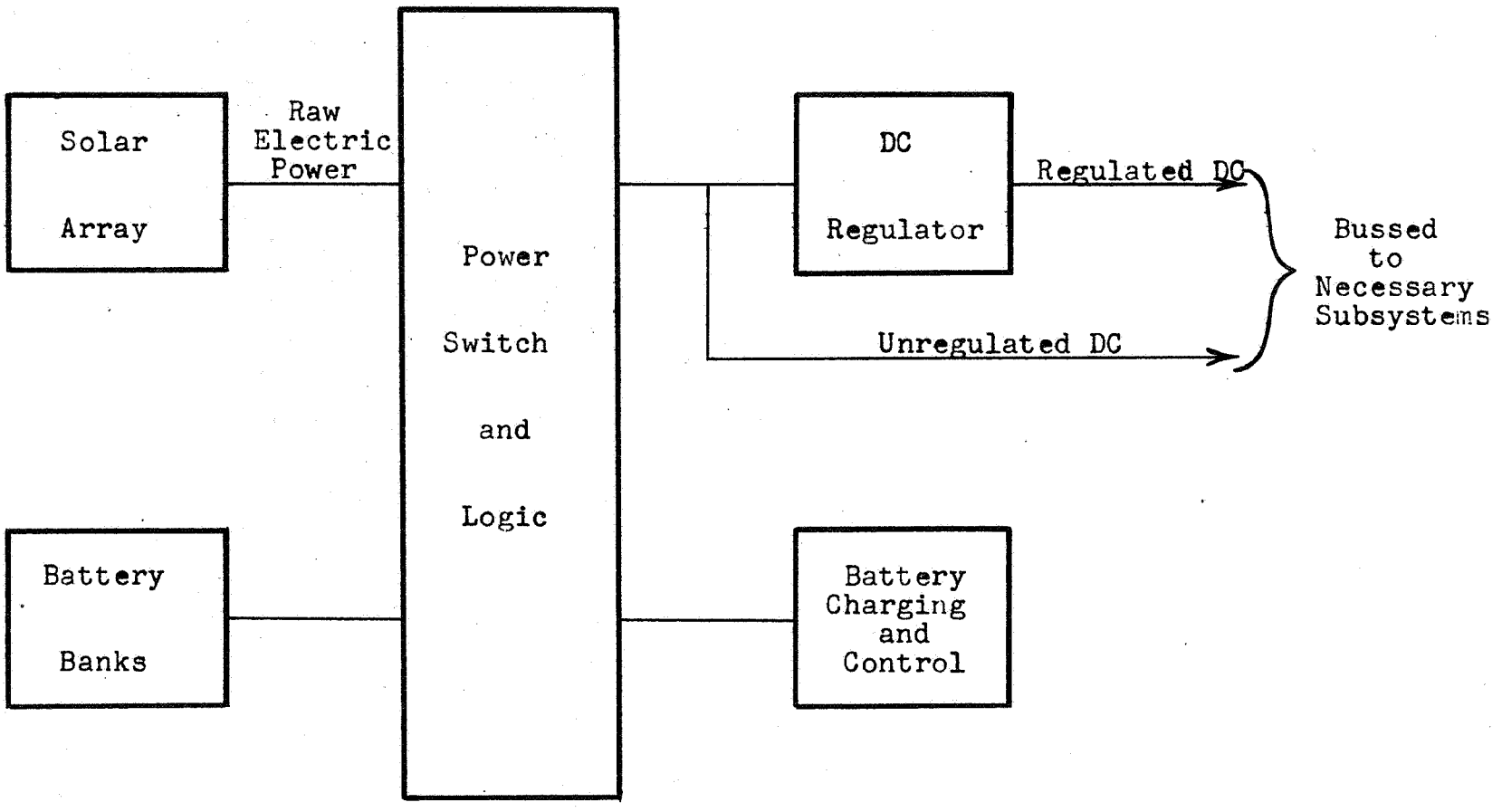

Figure 2-3 Elecrical Power System

CHAPTER 3

COMMUNICATIONS SYSTEM

SPACECRAFT DESIGN SUMMARY

COMMUNICATION SYSTEM

A necessary component of any space probe is the communications system. The funciton of any communication system is twofold. First, it must serve as a command link. The probe must be able to receive commands from Earth to initiate various phases and functions during the mission. Those controlling the mission must be able to make mid-course corrections, initiate experiments, and demand engineering telemetry when needed. Second, the communications system must provide for the transmission of gathered data back to the Earth where it can be interpreted. The quantity of data which can be collected on a given mission is primarily determined by the speed of the downlink, or the transmission rate.

Certain experiments obviously require that greater amounts of data be returned to Earth. A television picture, for example, requires that a great deal more intelligence be transmitted than, say, a temperature reading. It is common practice that the analog data from the sensors be converted to a discrete, or digital, form to facilitate transmission. When in digital form, intelligence is converted to a 1-0 or YES-NO format. Each one or zero is referred to as a "bit." Thus, the number of bits required to convey a given event is a measure of the event's complexity. To transmit a temperature would require, say, six bits... a television picture of extremely high resolution might require 10^9 bits. Thus, it is to our advantage to be able to transmit a large number of bits in a short amount of time.

Since, for complex intelligence, such a great many bits of information need to be sent, it is natural to attempt to find methods of transmitting the data in as convenient a manner as possible. One approach is to store the data as it is collected, perhaps at an extremely high rate compared to the proposed rate of transmission, in a magnetic tape recorder or thin film memory, and then play it back at a manageable rate. This was the approach used in the Mariner probes. It has the disadvantages of very limited data storage capacity in the case of a random access memory, and relatively low reliability and relatively slow record and playback rates in the case of a tape recorder. For instance, a high resolution television picture containing 10^9 bits would require 10^4 seconds to be transmitted at the rate of 10^5 bits/second, corresponding to 2 2/3 hours ... assuming that the recorder and data transmission link could satisfactorily operate at these speeds.

Another approach is to send only part of the data. Often a considerable saving in the amount of data to be sent can be obtained through the use of data compression techniques. By clever coding, one can reduce the redundancy in the data by a factor of 5 to 10 or more.

The third alternative is to use extremely high data transmission rates, transmitting the (compressed) data as fast as it is procured. This is referred to as real - time transmission. It has the disadvantage of requiring great amounts of bandwidth, and thus correspondingly great amounts of radiated power.

All space probes up to this date have employed S-band (2.3GHz) microwave links to transmit the downlink to Earth. These systems have proved to be an adequate means of communication up to the present. The S-band system's great reliability and moderate bit rates have sufficed to relay data from deep space probes so far. However, to this date we have contented ourselves with sending only a few million bits of information per mission. Since very high resolution television is one of the objectives of this mission, requiring data rates of 10^7 bits/sec even after data compression for real-time transmission, the present microwave system is seen to be entirely unsatisfactory. At the transmission rate of previous proves it would take years to send just a single high resolution picture!!

Of course, there are constant improvements being made on the current microwave system. Through the use of higher transmitting power, shorter wavelengths, and larger antennas the bit rate is being pushed upward. It is conceivable that, through the use of several kilowatts of radiated power, and huge, unfurlable transmitting antennas, that the bit rate from Mars could be pushed to the neighborhood of 10^6 bits/sec. This however, is a brute force technique ... and any real technological breakthroughs do not appear to be probable. Thus, one encounters innate limitations in the microwave system.

An alternate system is the use of a laser downlink. The extremely short wavelength at optical frequencies (e.g. 10^{-6} meters) allows one to collimate the coherent radiated power emanating from the device into a narrow beam, thus concentrating a far greater amount of power on the receiver than for conventional microwave systems. More power means greater bandwidths, and thus higher transmission rates. Bit rates of over 10^7 bits/sec are completely reasonable, and even 10^{10} bits/sec is foreseeable in the remote future. The laser system has far greater potential for deep space communications than microwave, and indeed may be a necessity for any meaningful communications at all for probes to Jupiter and beyond.

These tremendous bit rates do not come without a price, however. There are many problems that need to be solved before such a system can be feasible. Such drawbacks as low overall efficiency, multimode operation of injection lasers, atmospheric aberration and attenuation, and the great need for stability and pointing accuracy need to be overcome. This topic is discussed at some length in the appendix.

Despite the amount of technological refinement needed to make an operational laser link fulfill the communication function for this project, it was decided after considerable research, that the benefits to be obtained through the use of an optical system far outweighed the disadvantages projected to be with us still in ten years. The high transmission of very high resolution, real time television; and the voluminous quantities of data to be collected from the other experiments. Thus, a large portion of the group's research was concerned with designing and theoretically evaluating such a system.

A different set of circumstances are encountered when designing an uplink (for command) for the system. High bit rates are not at all necessary, or even desirable, since only short commands are to be sent.

Capacities of 1-10 bits/sec are entirely satisfactory. Great amounts of radiated power are available here on Earth, so transmitted power is no problem. The important requirement for an uplink is reliability. The message must get through to the probe with little probability of error. One mistake could, for example, fire the retrorockets at the wrong time and send the probe plunging to destruction on the Martian surface. From a reliability standpoint, all factors point to S-band microwave, and thus it is this mode which will be used on the uplink. S-band will allow communication with the probe whenever it is not eclipsed by Mars, since there are transmitting stations situated over the entire Earth, and because the S-band is relatively independent of ambient weather conditions.

Since this mission will involve a relatively sophisticated lander, the need for communications with the surface is also a requirement of the system. Reasonably high bit rates will be returned from the lander, and commands will need to be sent. Microwave communications over this relatively short distance are entirely adequate, and thus will be employed for two-way communications with the Martian surface. This system will be outfitted with a 10 foot diameter directional antenna so that in event of downlink failure on the part of the laser, the microwave system can serve as an emergency back-up and transmit to Earth at a reduced bit rate. This adds a certain amount of redundancy to the system. It is planned to use X-band (8.5 GHz) on this link. The reduced beamwidth offered by X-band is seen as an advantage in case Earth communication must be initiated in the event of emergency.

Stabilization Requirements

Stabilization and pointing control for the laser downlink will be kept within $\pm$ 0.1 arcsecond. This will be accomplished through the use of an onboard feedback and control system fed by a star-tracker locked on a laser beacon from the vicinity of the receiver. No excess fuel for stabilization will be required, since the tracking system involves movement of only the telescope lens. One should note that the platform will be held inertially within about 1 degree of Earth at all times after insertion.

Optical Receiver and Laser Power

The receiver chosen for our system is a direct detection static crossed-field photomultiplier with an S-25 photocathode surface. The system is cooled to an overall equivalent system temperature of 50° K. The assumed effective transmitter aperture is 36 cm. The assumed effective receiver aperture is 200 cm. The transmitted beam divergence is assumed to be diffraction limited (2.88μ radians). Using typical present parameters for the receiving system, the required maximum laser transmitter power to give a probability of error less than 10^{-6} at an S/N of 20 db is 43 watts.

Downlink

The transmitter for the downlink will consist of a cryogenically cooled array of gallium arsenide lasers, modulated in a PCM:CW fashion. The beam will be spread to 12 inches initially, giving a beamwidth of

about 3 microradians. This system, using a proposed peak output power of 100 watts, is capable of transmitting 10^7 bits/sec over the maximum Mars-Earth distance. The downlink system will include a microwave backup link (employing a far lower bit rate) for redundancy in the event of a primary component failure.

CHAPTER 4

SCIENCE PAYLOAD

SPACECRAFT DESIGN SUMMARY

SCIENCE PAYLOAD-PRIMARY SYSTEMS

The primary objective of this mission is to obtain high resolution maps, including topography data, and bio-geological information of the Martian surface. Instrumental in achieving the objectives, the following systems are proposed:

1. Multi-spectral Line Scan Camera
2. Laser Radar Profile Mapping System
3. Mobile Surface Laboratory

Multi-spectral Line Scan Camera

The primary instrument chosen for the mission is a 5 band, 16 channel multi-spectral line scanning camera. It utilizes a 120 cm. telescope f/4 optical system. This system scans a 1 km wide strip of the planet's surface from an altitude of 200 km. The ground resolution of the instrument at this altitude is two meters although the diffraction limit of the telescope is 10 cm, offering considerable growth potential for higher resolution work. The images are formed on a fiber optic array using optical fibers of 22 microns diameter. The fibers are stacked in a semi-circular configuration which is swept by fiber optical pipes mounted on a motor armature. Band splitting is performed by prisms after scanning and the light is detected by photomultiplier tubes and silicon photodiodes. The unreduced data production rate is @ 3×10^7 bits per second utilizing all 5 bands with 6 binary bit coding for each point. The 2m resolution , 1 km swath width combination offers reasonable coverage of the planet and produces data at a rate that, with compression, is compatible with the communication capabilities of the satellite for real-time video transmission, thus circumventing the need for large data storage facilities and maintaining a high duty cycle factor for the camera system.

In order to achieve 2m resolution of the Martian surface, approximately 10^{14} points must be covered. Using the five band six bit word format approximately 10^{15} bits would be required to describe the surface. Given our communications rate of 10^7 bits/sec, complete coverage of the planet cannot be achieved in a 1500 day mission, thus we must trade off our coverage for resolution.

For our mission a 200 km sun synchronous polar orbit inclined approximately 20° from the plane perpendicular to the Mars-Sun line was selected. The 200 km figure was selected because we felt it was as close as was permissible under conditions of orbital life time and current contamination criteria. At this altitude sufficient light is available for video and infrared scanning at the high rates required for high

resolution photography. Given the ground velocity of the satellite of 3.2 km/sec and the 1 km swath, eight hundred thousand data points are covered each second. That is, 2.4×10^7 bits/sec are continuously produced. Appropriate digital logic can be applied to reduce this figure to 10^7 bits/sec with use of a relatively small amount of storage.

The camera itself is mounted in such a way as to allow two degrees of freedom, thus, permitting scan outside the path of the satellite. This permits more selective coverage of the planet and allows reduction in the amount of redundancy of the orbital path coverage, although at somewhat lower resolution. We feel that all components of the camera system excluding the scanning apparatus, can be classified as state of the art for 1968.

General Configuration

A multispectral line scan camera that will take pictures of the surface of Mars in five wavelength bands with a ground resolution of two meters is proposed for this mission. A conceptual diagram of the configuration is shown in Figure 4-1. Ground reflected sunlight is imaged by a reflecting mirror optical system into an array of optical fibers. The fibers are arranged in a semi-circle and scanned by a rotating disk.* Optic fiber pipes supported in the disk direct the light into parabolic collimating mirrors, also shaped in semi-circular strips. These mirrors, along with the lens, focus the light onto a prism where it is divided into a frequency spectrum. Fiber optic bundles relay the light from certain wavelength bands to various visible and infrared detectors. The signal is detected and sent to a data bus for encoding and transmission.

Optical Mirror System

A mirror with a 1.2 meter aperature and a 4.8 meter focal length is proposed in this design. The 1.2 meter aperature is necessary so that the detectors will have sufficient illumination. A focal length of 4.8 meters has been selected for two reasons. First, it allows for an acceptance half angle in the fiber optics of 14.5° which is sufficiently small for acceptable transmittance and minimal spreading. Also, the f/4 mirror system is capable of focusing the image onto an image plane of fiber optics which is sufficiently large, from the standpoint of fiber packing, for 2m resolution and 1000m swath width. A Ritchey-Chretien telescope optical system is proposed, since the field coverage is the best and the angular image blur is minimal. [1] Beryllium was selected as the mirror and structural material because of its high strength and thermal merit.[2] A servo mechanism is proposed for use on the secondary mirror for fine adjustment and thermal compensation.

Fiber Optic Array

A 4.8m focal length project a 1 km swath width, at a satellite altitude of 200 km, into an image plane of 2.4 cm in length. A ground resolution element of 2m x 2m must image onto a cell area of $48\,\mu \times 48\,\mu$. Due to packing efficiency and optical fiber coupling, this area must be four optical fibers in diameter. [3] Using a spacing of $2\,\mu$ for coating thickness, the optical fiber diameter used for transmission is $22\,\mu$. However, a transmittance loss of o.67 is incurred due to this packing arrangement.

* The rotating scanner concept was originally proposed by the Stanford group of reference 4.

In order to decrease the rate of the scan motor, 16 channels are proposed. These 16 channels are arranged in an array of 32 by 1000 fibers. Due to the motion of the satellite the ground image moves across this array. A diagram of this fiber optic array is shown in Figure 4-2.

Scanning Process

The array of 32 by 1000 fiber optics is bent into a semi-circle for rotary scanning. In order to increase the time allowed for detection by the photo-multiplier tubes and the silicon photodiode, four channels will be scanned simultaneously. The four channels are spread in a semi-circular strip, with four sets of semi-circular strips mounted vertically, thus giving a total of 16 channels. This semi-circular configuration is shown in Figure 4-3.

A spinning armature supporting eight fiber optic pipes, as shown in figure 4, scans the ends of the semi-circular fiber optic array. To accept the light, at a disk to array spacing of 30 μ, the eight fiber optic pipes used for scanning are 63 μ in diameter. At a 3.2 km/sec orbital velocity of the satellite, 1600 two meter wide lines must be scanned per second. Since 32 lines are scanned during each revolution, 50 revolutions per second is the spinning rate of the disk. 50 rps is equivalent to 3000 rpm, and it seems reasonable that a motor lifetime of 40,000 hours could be expected at this operating speed. [4]

Dispersive Optics

A conceptual diagram of the light dispersive system is shown in Figure 4-4. The outlets to the eight 63 u diameter fiber optic pipes supported in the arm of the scanner are spaced about one cm apart. The light from four of these fiber optic pipes will be projected onto four parabolic collimating mirrors which are cut into a semi-circular configuration. These four beams of light are focused to a point impinging upon four prisms. These prisms disperse the light into multiple fiber optic bundles which terminate at the appropriate detectors.

Wavelength Intervals and Detectors

Coverage in both the visible and the near infrared is desired. Therefore, five wavelength intervals were chosen in the following regions:

Visible	Near Infrared
0.45μ-0.55μ	0.75u-0.85u
0.55u-0.65u	0.80u-1.2u
0.65μ-0.75u	

Photomultiplier tubes were selected as detectors for the three visible and first infrared region, and a silicon photodiode was selected in the infrared region (0.8μ-1.2μ). [5] These detectors are the most sensitive available, have fast reaction times and afford good signal to noise ratio for the intensities available. The technology in this area is well advanced and was not explored in detail by the group.

Power and Weight Requirements

The systems weight allotment for the multi-spectral scanner was approximately 2000 lbs. This number is rather conservative. Assuming that the primary mirror and camera supporting structure is constructed of beryllium (density .80), a crude estimate can be made of the weight of the system. The breakdown is:

1.	primary lens (120cm)	900 lbs
2.	support structure	600 lbs
3.	scanning detectors and supports	40 lbs
4.	secondary mirror, servo and support	40 lbs
5.	scanning mirror	100 lbs
	Total	1680 lbs

The power required for scanning and detection is less than 50 watts. These estimates do not include the weight or power requirements of external servo machanisms, which if present could be as much as 10% of the overall system weight. The above breakdown is conservative by current standards in that the total volume calculated for the primary mirror was based on that of a cut cylinder with a center thickness of 10 cm without edge trimming which represents considerably greater volume than is actually required. Also the external structure weight was estimated using guidelines appropriate for earth-based telescopes rather than space systems. Our weight figures should by no means be considered an efficient payload weight schedule, however, they do demonstrate the feasibility of such a system if the Saturn V vehicle is utilized.

REFERENCES

1. Hughes,MSPS Report; SBRC page 2-35

2. Hughes, MSPS Report; SBRC page 2-39

3. M.S. Kapany, Fiber Optics, 1967, Academic Press, page 83.

4. "Demeter," Stanford Project on a Multi-spectral Line Scanner

5. Hughes, MSPS Report; SBRC, pages 2-46 to 2-49

Figure 4-1 MSLS

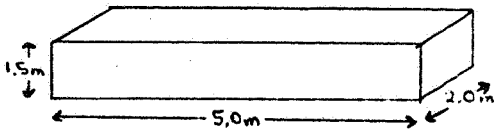

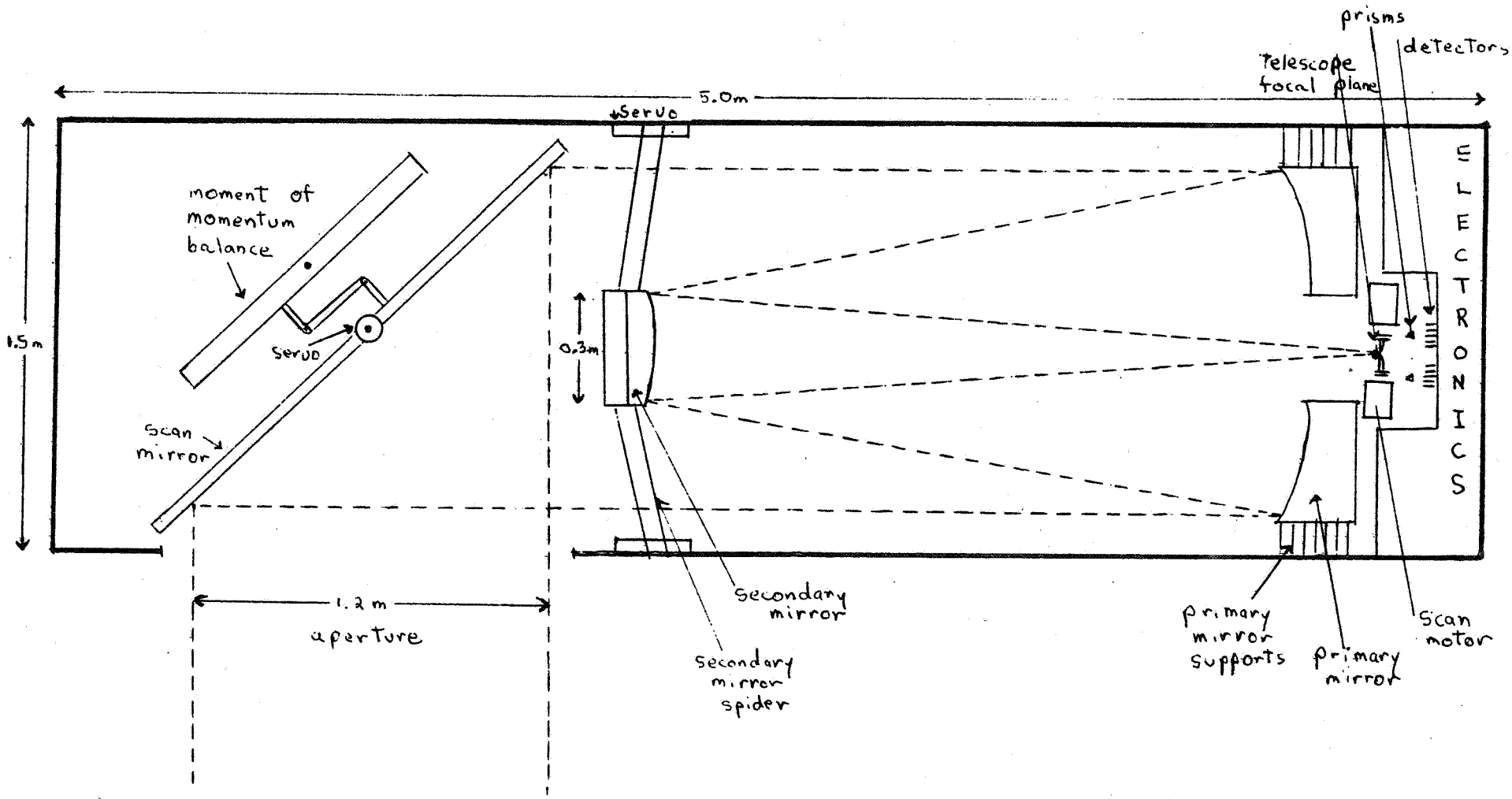

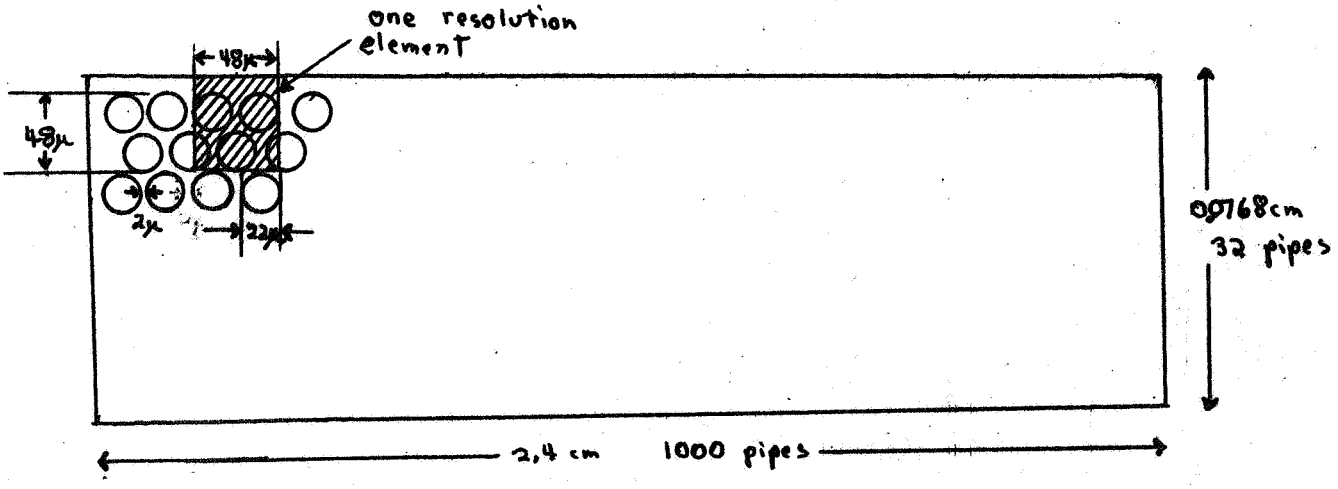

Fiber Optic Pattern on Image Plane

Figure 4-2

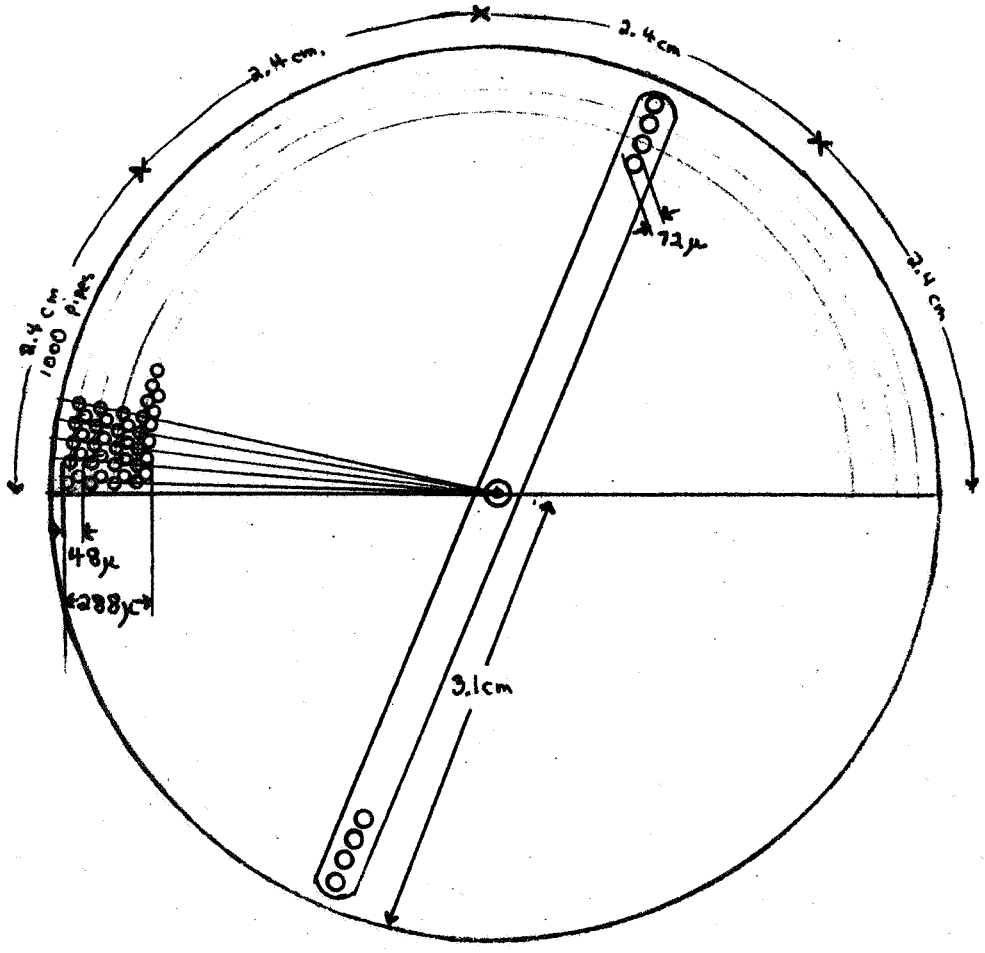

Semi-circular Fiber Optic Pattern and Scanning Shaft

Figure 4-3

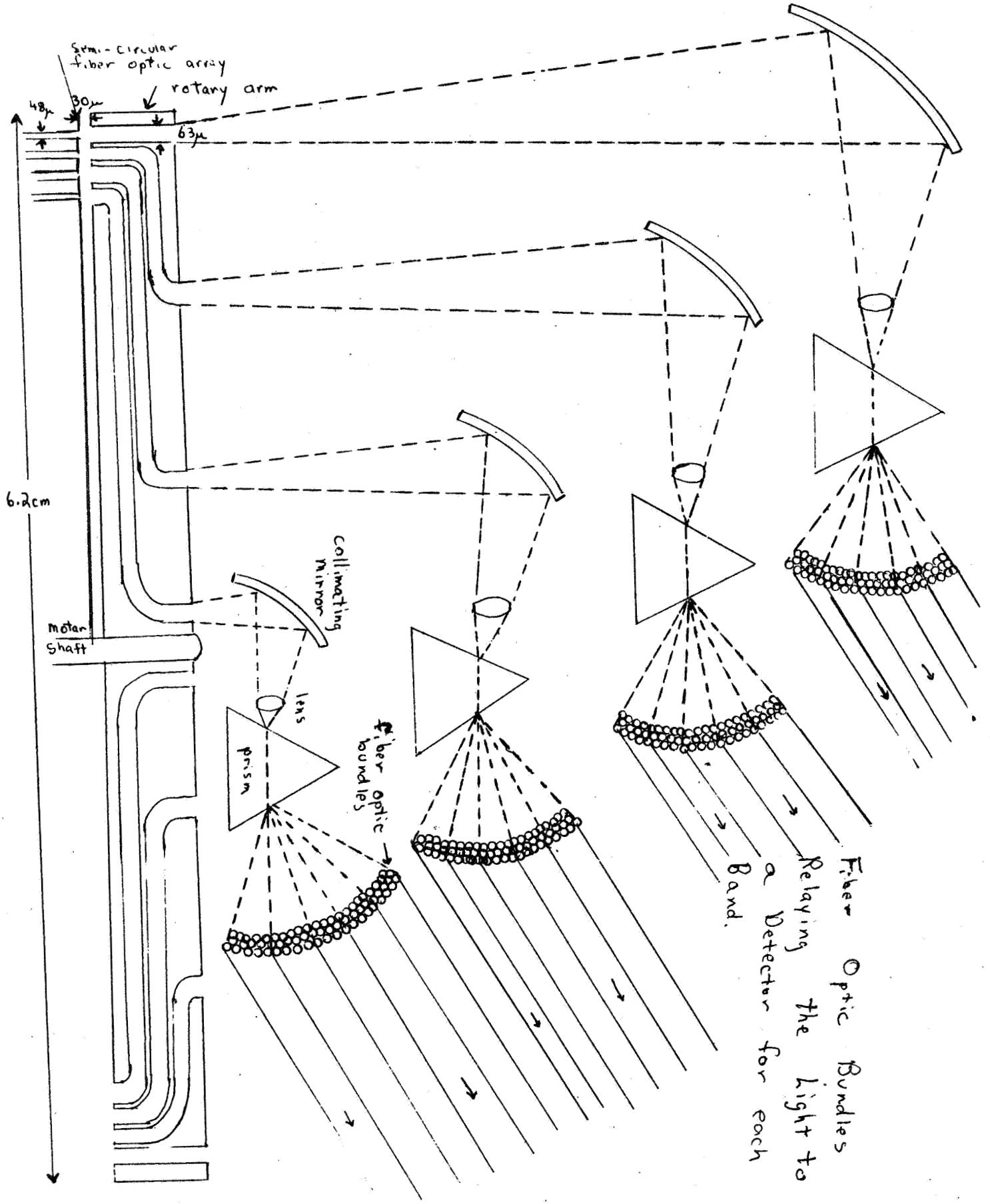

Light Dispersion Process

Figure 4-4

Laser Radar Profile Mapping System

One of the primary purposes of the mission to Mars is to obtain high resolution pictures of the planet's surface. To make these photographs more rewarding, it is often desirable to supplement them with profile mappings, i.e. high resolution altitude measurements of the surface. The proposed optical laser mapping system will do just that. The laser radar system, commonly known as "lidar," uses a frequency modulated continous wave laser beam to give a profile map of the Martian surface. This map will have two meter resolution to be consistent with the Multi-spectral camera system. Range measurements will be accurate to within a few centimeters.

The FM-CW laser radar chiefly consists of a transmitting system, receiving system, and signal processing system. A continuous wave gas or solid state laser capable of 2 to 3 watts ouput at wavelengths ranging from 2.3-2.6μ or 2.8-3.5μ should be used for a transmitting source. A modulator (frequency modulation at 1.14 khz.) and an optical system (chiefly a focusing lens and rotating mirror) provide the remaining components of the transmitter. The receiving system contains a one meter squared Cassegrainian optical system and a scanning system using optical fiber techniques. Signal processing is done by amplification, detection, mixing, counting, and conversion systems.

The total system requires 1102 watts of power. This figure, of course, is subject to change depending on improvements in laser efficiency over the next ten years. The total system weighs 216 pounds and has a total volume of approximately 21 cubic feet. System stability should be maintained to within one second of arc in roll and pitch directions to provide adequate stability of laser transmitting and receiving systems.

This system will map the terrain of Mars at a rate of 3.20 square kilometers per second assuming a 200 km orbit. Considering a 16 gray scale level is used for mapping, the data rate is on the order of 3.2 mega bits per second.

It does seem feasible to combine scanning equipment of both the multi-spectral camera and lidar systems into one in order to reduce redundancy and also provide bit by bit correlation between camera and laser profile pictures.

For a detailed analysis of the above proposals, refer to Appendix D.

Mobile Surface Laboratory

The lander system, known in most technical literature as the "Mobile Surface Laboratory" (MSL), is primarily a biologically oriented roving vehicle although it does contain apparatus for geological and physical experiments. It is a six wheeled machine of very high mobility and low center of gravity, and capable of motion over most kinds of soils and terrains. Four wheels are rigidly connected by a frame and the other two, plus frame, carry the power supply. Carrying its own communications equipment, it is capable of transmitting 50,000 to 200,000 bits per

second of information to the orbiter. The MSL contains an on-board computer which controls the various experiments while also making decisions as to actions it should take to avoid obstacles or potential dangerous situations that have been sensed by its TV cameras, infrared radiometer, etc.

The vehicle is delivered to the Martian surface by McDonnell designed system of ejection from a sterilized "pod" in which it is carried to the planet. A series of retro-fires, attitude readjustments jettisons, and parachute maneuvers lower the lander to the ground on a "rocket propelled" platform controlled by radar altimeters. Once on the surface the rover is deployed simply by crawling from the platform. By Earth control, it then proceeds to its first experimentation site and begins relaying data. After experimentation has ceased or a series of negative results are returned , the MSL may move again and again to give scientists a very varied and useful array of information concerning the surface and atmosphere of Mars.

A detailed description of the MSL appears in Appendix D.

SCIENCE PAYLOAD SECONDARY SYSTEMS

Should the weight and spacial limitations of the mission permit, a number of secondary systems are proposed to conduct experiments which may not be included on prior missions or may be of interest to repeat. These experiments may be broken down into two categories--those to be executed while in a Martian orbit and those in an Earth-Mars transfer orbit. The experiement utilizing the Infrared Spectrometer falls in the first category, and the following, in the second:

a. Magnetometer
b. Cosmic Dust Collector
c. Gamma Ray Spectrometer
d. Solar Plasma Probe
e. Cosmic Ray Detector
f. Trapped Radiation Detector

Planetary Experiment-Infrared Spectrometer

While infrared (IR) detection systems may be used for mapping purposes and for the determination of surface composition on Mars, the principal use of an IR spectrometer as a secondary observation technique will be to conduct temperature studies of both the Martian surface and atmosphere and to determine the presence and concentration of IR active constituents in the atmosphere.

Carbon dioxide is believed to be the principal IR active constituent in the Martian atmosphere. Therefore, the CO_2 absorption band in the 4.3 micron region is of significance in our temperature studies. [1,2]

In addition to the above spectral region specified, four other bands to be examined are proposed: [3]

0.2-4u	includes all reflected radiation
5.6-7u	water vapor absorption window
8-12u	atmospheric window
6-40u	includes all emitted radiation

With such ranges, the presence and concentration of the IR active gases in the atmosphere may be determined. In addition, some of the Sinton bands in the 5-16μ range, indicative of organic molecules on the surface, may be detected.

To skirt the critical temperature requirements of detection elements within the specified spectral bands, Lead-Selenide detectors are proposed for the 0.2-4 and 4.3μ bands, and thermistor bolometers, for the others.

Estimated specifications are as follows:

weight - 16 lbs
power - 7 watts
size - 10 x 13 x 16 inches

A diagram of the spectrometer is shown in Figure 4-5. It is similar to that proposed in the JOVE study [4] with the exceptions of the addition of a rotating, multi-sided mirror to sweep the beam of radiation across the row of detectors and of the requirement of having highly reflective surfaces attached to the tines of the tuning fork chopper, such that, when it cuts off the incident radiation from the planet, an internal source is reflected upon the detectors, thus serving as a temperature reference.

This proposed system is designed for continuous observation of the planet from a Sun-Canopus oriented stabilized platform.

Interplanetary Experiments

Experiments for the observation of interplanetary phenomena will be performed in transit. These will include measurement of the interplanetary matter such as cosmic dust, gamma rays, solar plasma, cosmic rays and trapped radiation.

All these experiments will continue in operation when in orbit, acquiring data on the phenomena in the vicinity of Mars.

It is hoped that from the data obtained theories predicting phenomena such as the "Garden Hose Effect" of solar plasma flow [5] could be tested and the shock wave, with its corresponding cavity, [6] in the plasma flow caused by Mars' magnetic field detected and measured. These experiments will be described in more detail in the following pages.

Magnetometer

It is desirable to have a high resolution magnetometer which would measure the magnitude, direction and time variation of any fields present. To eliminate the necessity of rotating the spacecraft to measure the direction of the magnetic field, three mutually perpendicular sensors will be used. A magnetometer similar to the one designed for the SAMPLER mission would do admirable. This instrument is capable of measuring magnetic fields to an accuracy of 0.1 gamma and will follow time variations up to 1000 Hz.

To prevent the spacecraft magnetic field from interfering with the measurements the sensors will be extended on a boom to lower effective spacecraft magnetic field to less than 0.5 gamma.

Cosmic Dust Detector

Measurements of the number and momenta of the micro-meteorites in transit and around Mars may lead to an understanding of their origin.

Figure 4-5 Schematic of IR Spectrometer

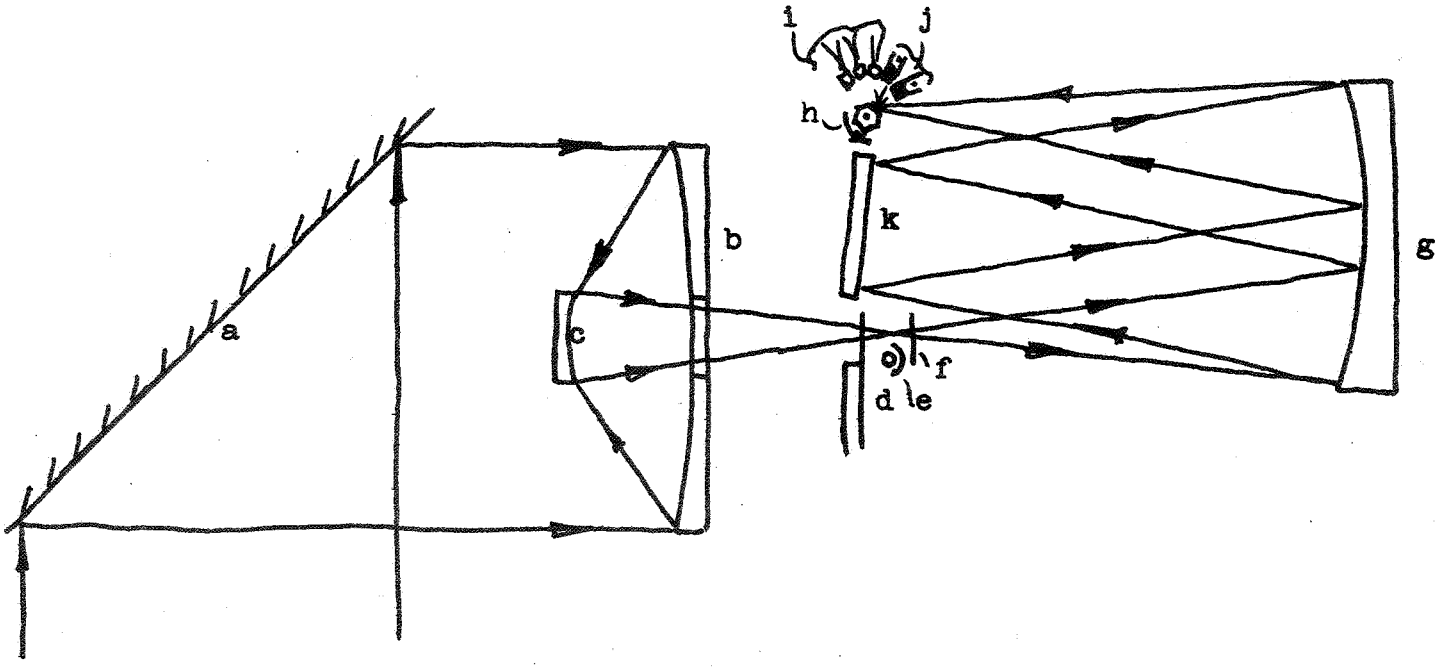

a. Plane Mirror
b. Collecting Mirror
c. Secondary Mirror
d. Tuning-fork Chopper
e. Internal Reference Radiation Source
f. Entrance Slit
g. Monochrometer Mirror
h. Rotating, Multi-sided Mirror
i. Thermistor Bolometers
j. PbSe Detectors
k. Diffraction Grating (200 lines/mm)

The spacecraft will have micro-meteorite sensors in the forward direction of travel and in the reverse direction. A third will be perpendicular to these two.

Each sensor consists of a metal plate with a piezoelectric transducer attached. The output will be fed to a high gain amplifier whose output at selected gain points will be fed into electronic counters. The information is read periodically into storage for transmission to earth and the counters reset.

The sensors will pick up any vibrations of the spacecraft consequently spacecraft noise should be kept to a minimum to prevent interference with this experiment.

Gamma Ray Spectrometer

This instrument will detect the presence of gamma rays and high energy particles in space. It will also detect the presence of solar photons.

The gamma ray spectrometer consists of a detector, photo-tube, and an analyzer. Gamma rays and charged particles will excite the detectors, which consists of a standard scintillator and a plastic scintillator, differently. The charged particles cause a flash that is fast compared to the pulse caused by gamma rays. The analyzer can thereby differentiate between them and also determine their magnitude.

Solar Plasma Probe

Solar plasma is an electrically neutral mixture of atomic ions and electrons and seems to be associated with magnetic fields.

This instrument will take data on particle direction, velocity, energy and time variation. Since laser communication will not be operational in transit, communication capability in this period will be limited, and only low speed response to variations will be possible. Measured currents will be correlated with the magnetometer readings to study the mechanisms involved in the propagation of particles from the sun.

It may be feasible to make measurements of high-speed variations when in orbit around Mars for detailed measurements of the magnetosphere and related shock wave. At this time it will take advantage of the capabilities of laser communication when the cameras are not in use.

Cosmic Ray Detector

This instrument will measure (1) the absolute and relative flux levels, and (2) the energy spectra of the two main components of primary cosmic radiation (protons and ionized helium) with energy that range from one to six hundred Mev/nucleon.

The sensors consists of six sets of scintillation telescopes facing six directions to measure variations in direction of the incident cosmic rays.

This experiment will acquire data on cosmic rays far from the influence of the Van Allen belts and in the vicinity of Mars. It will test the theory that cosmic rays of galactic origin enter the solar system with constant velocity in time and space.

Trapped Radiation Detector

This instrument will:

1. Monitor solar cosmic rays and energetic electrons in interplanetary space, and study their angular distribution, energy spectra, and time histories.

2. Search for trapped particle radiation in Mars orbit and measure it in the proton ranges from 10 thru 200 Mev and in the electron ranges from 50 thru 5 Kev. It will also determine their spatial distribution, energy spectra, and identities.

The possible presence of radiation belts around Mars similar to the Van Allen belts of the Earth will be investigated and measured.

BIBLIOGRAPHY

1. Jamieson, J.A., McFee, R.H., Plass, G.N., and Richards, R.G. Infrared Physics and Engineering, McGraw-Hill Book Co., Inc., New York, 1963.

2. Jupiter Orbiting Vehicle for Exploration (JOVE),NASA contract NSR 01-003-025, Report No. CR-61180, 1967.

3. McClatchey, R.A. "The Use of the 4.3 Micron Band to Sound the Temperature of a Planetary Atmosphere," Proceedings of the EM Sensing Symposium (Miami Beach, Florida, 22-24 November 1965).

4. Shaw, J.H. and Schaper, P.W. "Surface Temperature of Mars," JPL Space programs Summary 37-45, vol. IV.

5. Smith, R.A., Jones, F.E., and Chasmar, R.P. The Detection and Measurement of Infra-Red Radiation, Oxford University Press, London, England, 1957.

6. Stanford Advanced Mars Project for Life Detection, Exploration and Research (SAMPLER), 1965.

7. Tech. Rpt. no. 32-740, Jet Propulsion Laboratory, Pasadena, California.

8. Phase 1 Study Report, VOYAGER SPACECRAFT, Vol. 2.

9. TRW Systems Group, Redondo Beach, California.

REFERENCES

1. Shaw, JPL SPS 37-45, Vol IV, p. 203
2. McClatchey, Proceedings of the EM Sensing Symposium
3. SAMPLER, p. 72
4. JOVE, p. 3-45
5. NASA-University conference on the Science and Technology of Space Exploration, Vol. 1, p. 74
6. SAMPLER, p. 47
7. SAMPLER, p. 48

CHAPTER 5

SPACECRAFT CONFIGURATION
GUIDANCE AND CONTROL SYSTEM

and

MISSION SEQUENCE

SPACECRAFT DESIGN SUMMARY

SPACECRAFT CONFIGURATION

The controlling factors in the configuration design were the requirements of the camera (an unobstructed view and two degrees of rotational freedom) and the orientation of the laser communication telescope, solar panels, and antennas.

The final spacecraft design can be seen in Figures 5-1 and 5-2. The basic load supporting structure of the spacecraft is a circular equipment module divided into separate bays. The bays contain all the electronic equipment required for the spacecraft. Louvers on the outside of the ring will provide thermal control. The equipment module will support the lander, the multi-spectral camera and "lidar system", the radiator for cooling the laser telescope, and by a light framework the laser telescope and the ten foot diameter Mars link antenna. Four solar rolls will be inset and on opposing sides of the equipment module. Between the solar rolls on the edge of the module are four attitude control units. The two by four parabolic Earth link antenna, magnetometer and boom, and solar vanes are also inset in the module and deploy at the proper time. The propulsion module, which will be separated after orbital injection, is attached to the equipment module by a framework which surrounds the camera, laser, and ten foot antenna.

The camera is gimbaled for two degrees of rotation freedom of $\pm 10^{o}$. The laser is also gimbaled and located on an inertial platform as its Earth alignment is critical.

A solar array of three hundred square feet is located on the bottom end of the spacecraft to provide the required inflight power of $1\frac{1}{2}$ kilowatts.

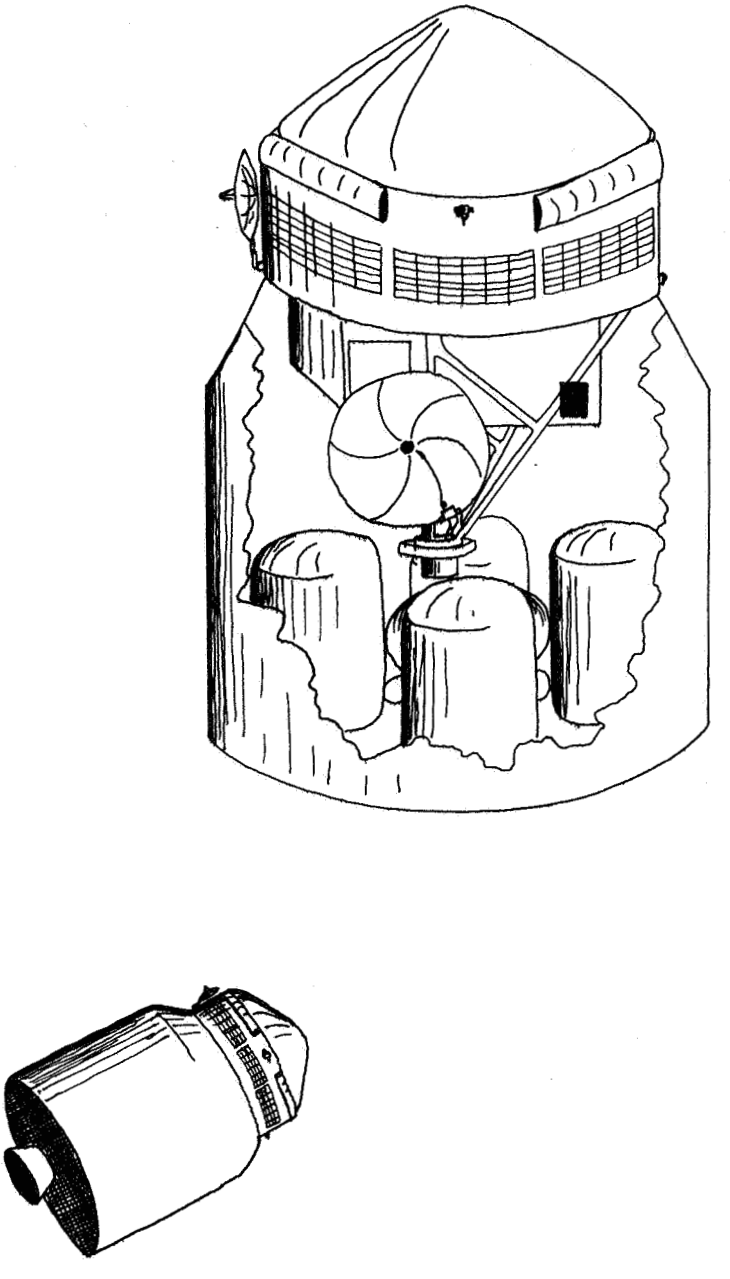

Figure 5-1 Spacecraft with Propulsion Module

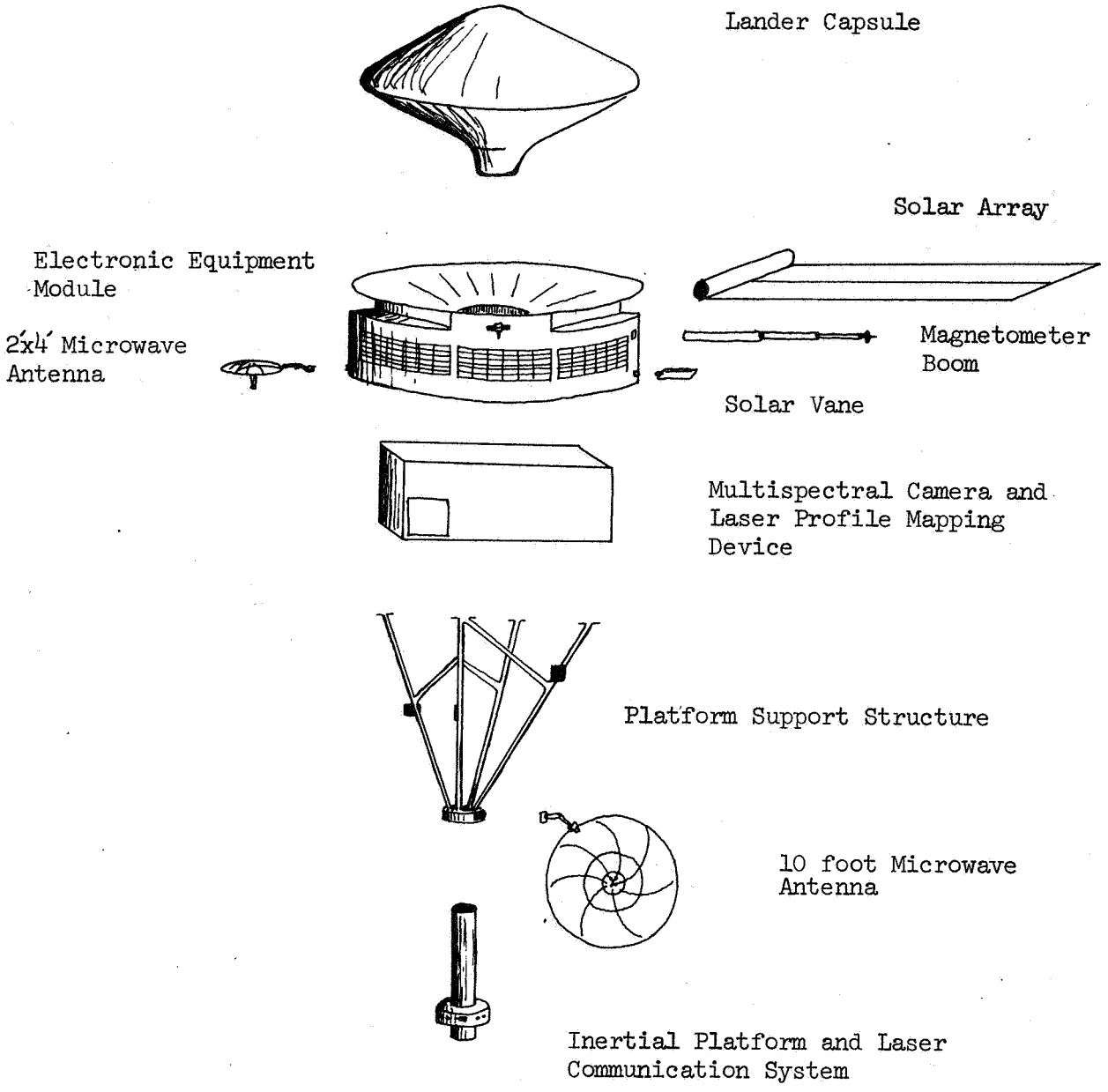

Figure 5-2 Spacecraft--Exploded View

GUIDANCE and CONTROL SYSTEM

The control system will be required to perform the functions of attitude control, mid-course guidance, Mars approach guidance, and correct orientation of antennas, camera, and other moveable devices. The system will consist of inertial and optical guidance, supplemented by Earth-based tracking and command.

This mission requires two basic modes of attitude control for the spacecraft:

1) Fixed attitude of the vehicle with respect to optical references, during cruise and motor firings (see Fig. 5-3).

2) Rotation of the vehicle about its principal axis during Mars orbit (see Fig. 5-4).

To carry out these operations will require the use of an inertial guidance system and two optical sensor systems. One set of sensors will be mounted on the bus; the other set of sensors, the stable platform, and the laser system will be attached to the main guidance and communications module, about which the bus may rotate.

During the flight, the vehicle will use a Sun-Canopus reference system. While in Mars orbit, sensors will normally be locked on the sun and Canopus, and there will also be Earth and Mars sensors in operation. The attitude of the vehicle toward Mars will be determined by means of an infrared linear scan system, similar to that used by the OGO satellite. Because the spacecraft is required to locate Earth with u radian accuracy for laser communications, a conventional optical scanner would not be adequate. Too large an optical system would be needed. The most appealing method is the use of the inertial platform, to which instruments could be slaved. The platform could supply the required accuracy. The use of this system is made possible through the use of the laser communication servo lock. The stable platform would be periodically corrected by means of a command signal from Earth which would know the laser communication platform attitude quite accurately at any given time. This platform would then serve as a reference for laser communication reacquisition when laser communication lock is lost by planet occulation or noise factors. Thus one integrated system would provide a constantly recorrected reference for the instruments and for spacecraft attitude maneuvers plus a reference for laser communication acquisition scanning.

Mechanisms of the accuracy required are now in existence, and long term reliability should not be a serious restriction. For example, an electric vacuum gyro now provides the following performance:

1) Drift: 10^{-5} deg/hr compensated at 0 g.

2) Reliability: Mean failure time is greater than 30,000 hrs.

3) Noise level: 0.5 arc second in 100 Hz band.

4) Weight and size: 1.5 lb, 40 cu in, less power supply *

In the event that laser communication should fail completely, the sun/canopus reference system would then be used, and as much data as possible would be collected by means of the 10 ft high-gain antenna.

The accuracy of orientation required by the laser telescope and the camera becomes a formidable problem when the spacecraft has relatively massive rotating parts (as the camera in this spacecraft). This problem is partially taken care of by mounting the laser on an independently oriented inertial platform. An additional method of ameliorating the problem would be to provide flywheels to cancel all or part of the angular momentum of the camera by spinning them in the opposite direction. The use of the fairly massive equipment module for the flywheel was considered but rejected because of the complexity introduced. The flywheel will introduce a weight penalty but this can be minimized by spinning the flywheel at a much greater rate than the camera and thus maximizing its effective angular momentum.

* Inventor, Dr. Arnold Nordsieck of General Research Corp.

FIGURE . MARS ORBIT CONFIGURATION

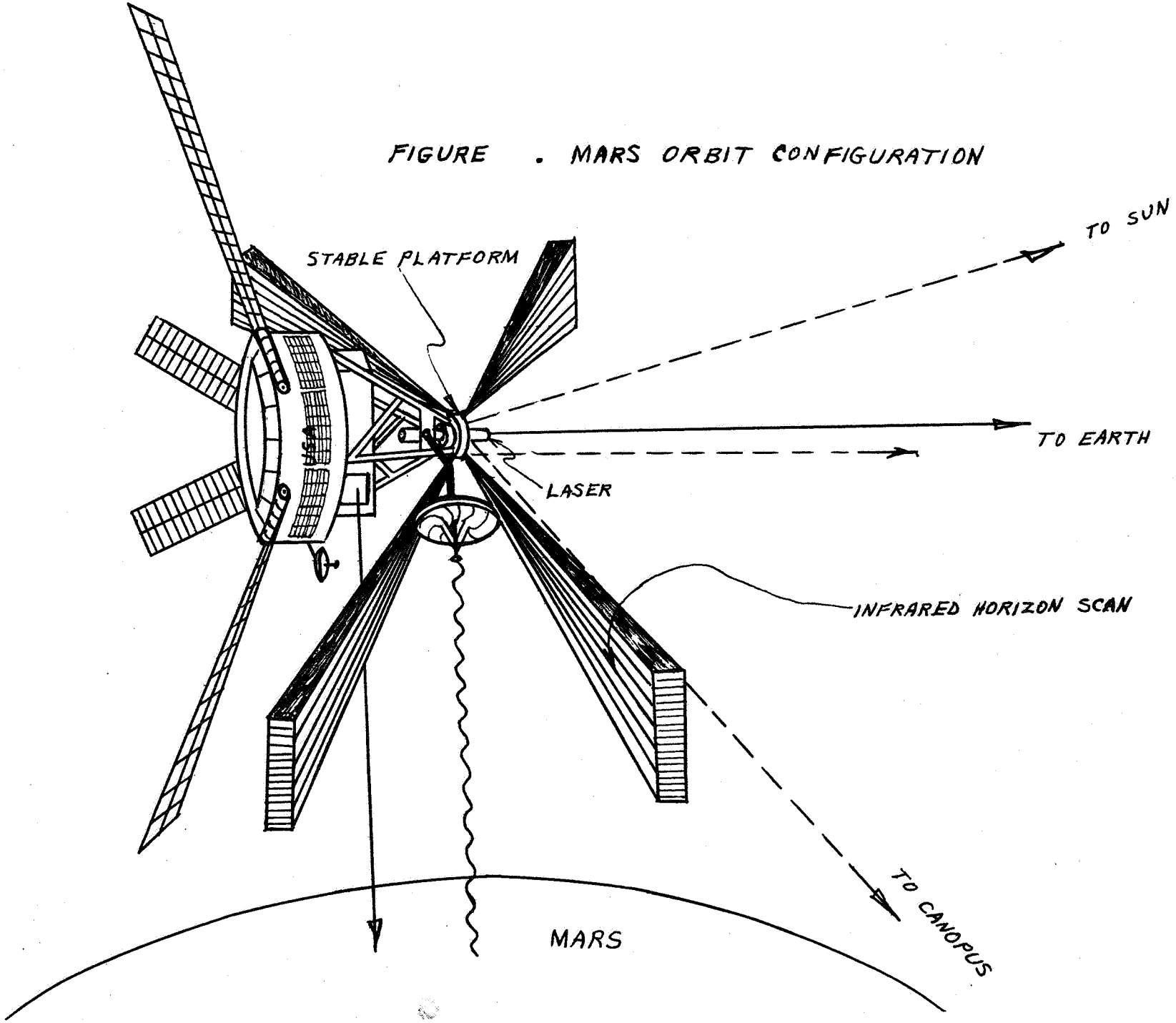

FIGURE . CRUISE CONFIGURATION

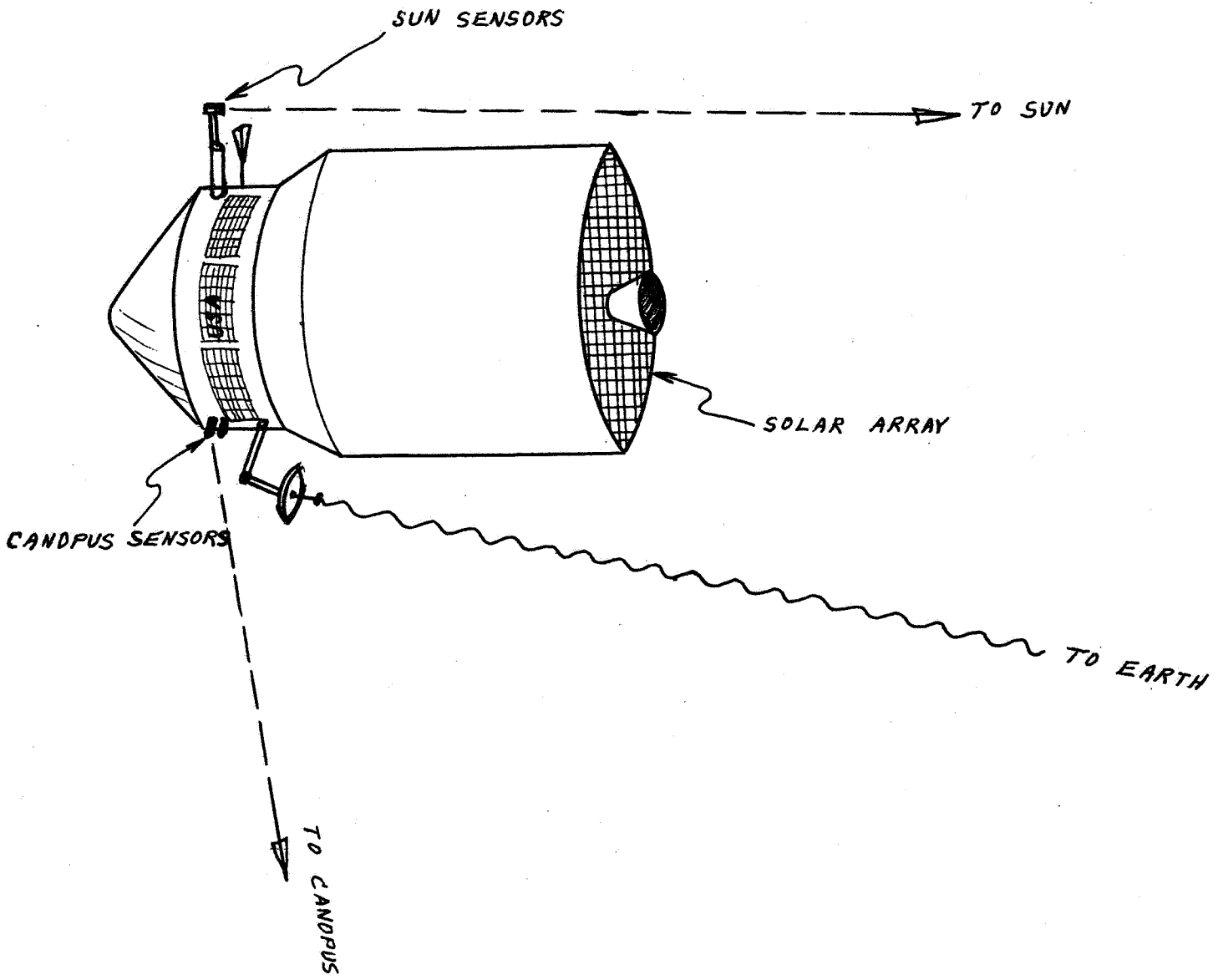

MISSION SEQUENCE

1. Lift off
2. 1st stage burnout and jetison--burn time 150 sec.
3. 2nd stage burnout and jetison--burn time 375 sec.
4. 3rd stage burnout and jetison--burn time 445 sec.
5. Centaur burnout and jetison--burn time 470 sec.
6. Sun-Canopus acquisition and orientation
7. Deploy: 1) solar vane
   2) magnetometer
   3) 2' by 4' antenna
8. Mid-course correction
9. Retro rocket fired--Mars orbital injection
10. Retro propulsion module jetisoned
11. Deploy: 1) 10 ft. antenna
    2) solar arrays
12. Earth acquisition by laser telescope
13. Picture taking and data transmission begins--target for lander chosen
14. Lander separated

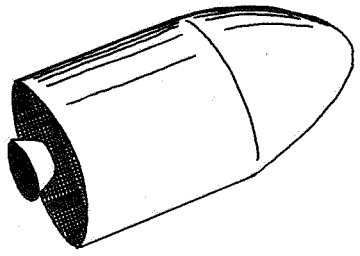

A. After Centaur is Jettisoned

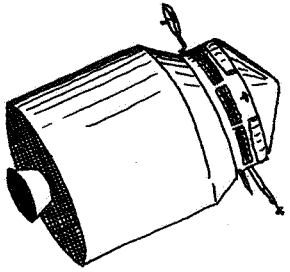

B. Cruise Configuration

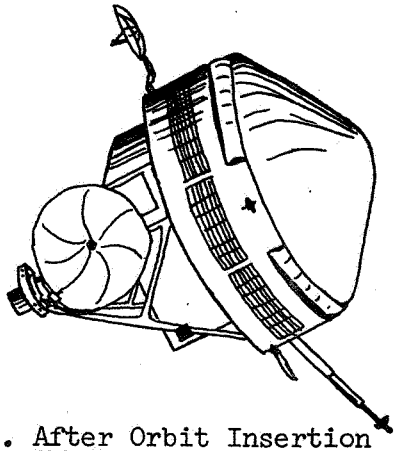

C. After Orbit Insertion

Figure 5-5 Mission Sequence

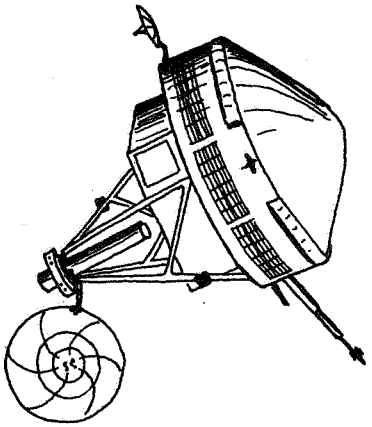

D. In Orbit--10' Antenna Deployed

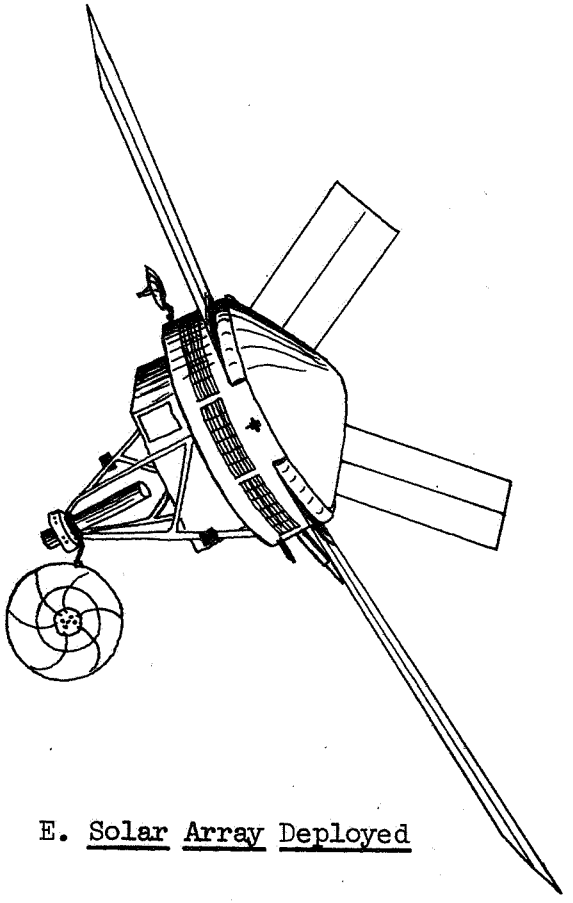

E. Solar Array Deployed

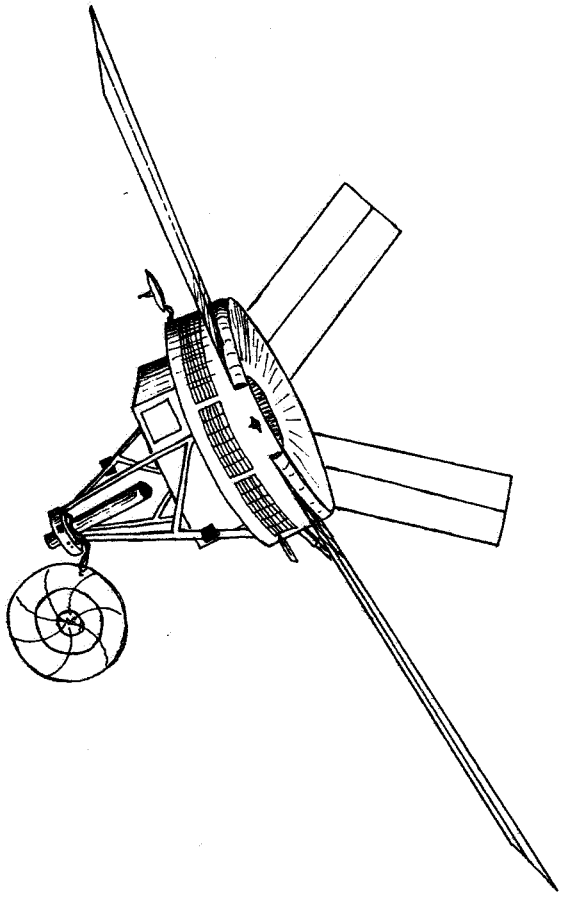

F. Orbiter After Landing Capsule Ejection

APPENDIX A: PROPULSION AND TRAJECTORY

PROPULSION AND TRAJECTORY

All Chemical Propulsion

There are basically only two all chemical propulsion systems to investigate for the high energy mission under study. These are the Saturn V and the Saturn V/Centaur systems. Along with these two systems one could consider as separate propulsion systems uprated versions of the Saturn V and Saturn V/Centaur. It will be assumed, however, that the uprated systems will be desired. The necessary research, development, and testing will have been completed and these uprated systems will be in the manufacturing stage. The additional cost of the uprated systems should not be excessive. Since both systems under investigation are essentially the same (on one system the Centaur is added to the Saturn V as a fourth stage) it will only be necessary to determine mission requirements. From these requirements, the necessity of using the Centaur will be determined.

The hyperbolic excess velocity can be determined from trajectory calculations and is found to lie between 12,000 and 15,000 ft/sec depending on the launch date. The payloads that can be injected into the Hohmann transfer trajectory are determined from Figures IV-7 and V-3 of the Payload Planners Guide from Douglas Aircraft. See Figure A-1. An uprating factor of 11.3% is used in determining the increased payload capabilities. This value is obtained from a table of missions and associated payloads of the standard and uprated systems. The results of the payload capability calculations are found in Table A-1. One can see it is advantageous to use the Saturn V/Centaur system due to the increased payloads.

TABLE A-1
COMPARISON OF STANDARD AND UPRATED
SATURN V PROPULSION SYSTEMS

EXCESS HYPERBOLIC VELOCITY (fps)	STANDARD SYSTEM PAYLOAD LESS CENTAUR (lb)	UPRATED SYSTEM PAYLOAD LESS CENTAUR (lb)
12,000	70,000	77,000
15,000	60,000	66,600

EXCESS HYPERBOLIC VELOCITY (fps)	STANDARD SYSTEM PAYLOAD WITH CENTAUR (lb)	UPRATED SYSTEM PAYLOAD WITH CENTAUR (lb)
12,000	78,000	86,600
15,000	72,000	79,900

PAYLOAD VS HYPERBOLIC
EXCESS VELOCITY
SATURN V/CENTAUR

STANDARD SATURN V/ CENTAUR

Fig. A-1

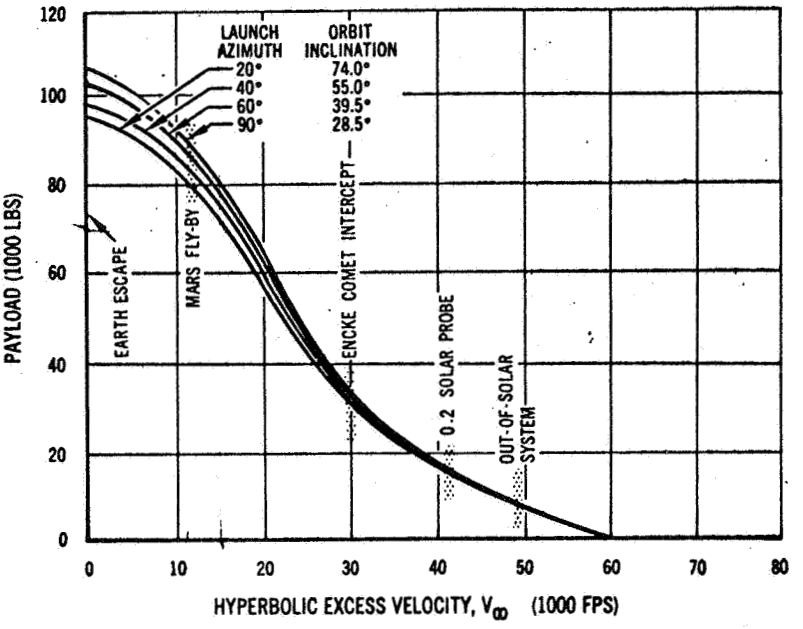

NOTES:
1. COPLANAR DIRECT ASCENT LAUNCH FROM E.T.R.
2. PARKING ORBIT ALTITUDE = 100 N. MI.
3. $V_\infty = \sqrt{(V_f)^2 - (V_{esc})^2}$

WHERE:
V_f = VEHICLE CUT-OFF VELOCITY INERTIAL, (FT/SEC)
V_{esc} = ESCAPE VELOCITY AT A CUT-OFF ALTITUDE (FT/SEC)
$V_\infty = \sqrt{C_3}$ = ENERGY PARAMETER

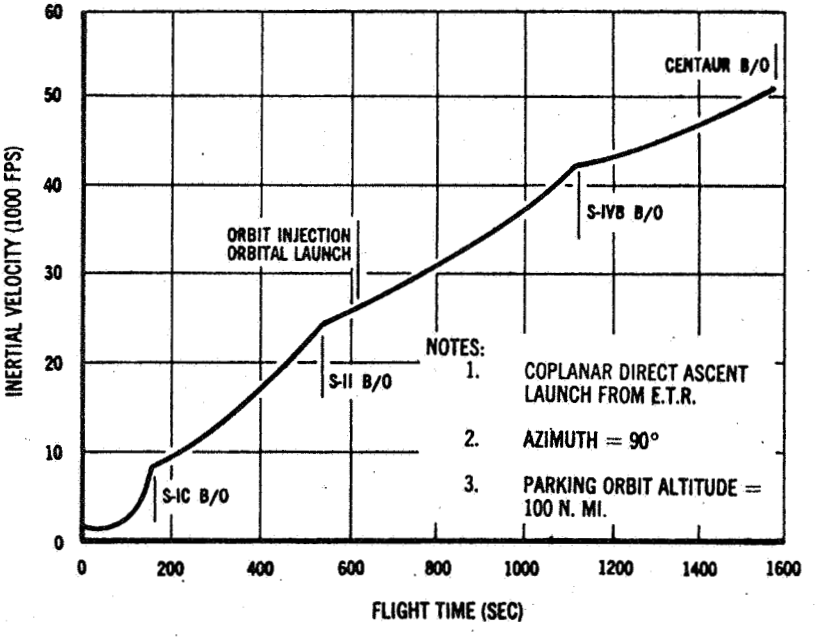

SATURN V/CENTAUR INERTIAL

Nuclear Rocket Systems

Nuclear propulsion was considered as a replacement for the Saturn V third stage and the Centaur. The decision to disregard nuclear propulsion was based on unavailability. We do not feel that a suitable nuclear rocket engine will be operational by the projected launch date because the NERVA program has been cut from the present budget. If such a system becomes operational by the launch date it should be reconsidered.

The NERVA engine is to be a 200,000 to 250,000 pound thrust nuclear rocket motor with a specific impulse of 825 seconds. It will be a graphite reactor-hydrogen system operating at a chamber temperature of about $4,500^{\circ}R$.

Because this type of engine develops a high thrust with a high specific impulse it has many advantages. It would increase the usable payload of this mission approximately 88% if used as a Saturn V third stage. Present tests indicate it would be light enough and reliable enough for large, long range missions. It also could be used as a power supply for other systems and there is some possibility of making it recoverable.

The main disadvantages of such a system are high development cost, safety in space, and the short time available for adequate development.

The cost of using nuclear propulsion would be a major factor in a decision about future use. If the payload were much larger, the cost per pound for nuclear propulsion, neglecting development cost, would make its use feasible but the payload may be too small to give nuclear propulsion an economic advantage over chemical.

Electric Propulsion Systems

The Saturn V/Centaur is capable of placing a maximum of 261,000 lbs. in a 100 mile Earth orbit. A 350 day mission, out in orbit with acceleration on the order of 10^{-3} ft/sec^2 would require a thrust of 8.8 lb_f. Since the maximum available thrust is equal to 1 lb_f (restricted by max power = 125 KW) acceleration would be on the order of 10^{-4} ft/sec^2. Transfer time would be on the order of 7 years, and ion propulsion for this transfer is impractical.

If the necessary power was available, 1100 KW, 15% of the total weight would be fuel = 37,500 lb, storage tanks, $\frac{0.065 \text{ lb}}{\text{lbm fuel}}$, power generation, 150 lb/KW, power conditioning, 30 lb/thruster, and engine weight = 78,000 lb, leaving a nonpropulsion payload = 145,000 lb.

Mid-course and Retro Propulsion Theory

Mid-course and retro propulsion are necessary to change the vehicle speed in order to achieve the desired Mars orbit. The use of the mid-course system in conjunction with the attitude control system allows trajectory correction to be made during the long Earth-Mars coast period, as well as altering the vehicle speed.

The necessary velocity change, vehicle weight, and propellant determine the amount of propellant necessary by the relation $\Delta V = I_{sp} \cdot g_o \cdot \ln \frac{w_i}{w_b}$

where w_i is the gross vehicle weight and w_b is the burnout weight. The propellant weight is then $w_p = w_i - w_b$

The weight of the propellant tanks and engine is estimated to be ten percent of the propellant weight, giving a total mid-course and retro propulsion system weight of $w_{syst} = 1.10 w_p$

and the usable payload is then $w_{pay} = w_i - w_{syst}$

Payloads calculated for various propellants can then be used as a figure of merit for propellant selection.

Once the propellant is chosen and a thrust level is set a burn time can be calculated from $I_{sp} = \frac{F}{\dot{w}}$

where $\dot{w}$ is the propellant weight flow rate. The thrust is limited by acceleration limits on the payload and normally is chosen for near maximum acceleration to reduce burn time.

Chemical Mid-course and Retro Propulsion

Three types of chemical propellants are available for auxiliary propulsion systems. They are cryogenic liquids, solid propellants, and storable liquid propellants.

Cryogenic liquids develop high specific impulse but present storage problems when applied to long space flights. This type of fuel requires insulation and a refrigeration system in order to store it for any length of time. The predicted storage time of a refrigerated system adapted for space use is limited to about five days which is far below the time required for this mission. Cryogenic propellants were, therefore, eliminated from the list of possible propellants.

Solid propellants were seriously considered for the auxiliary propulsion system because of the high reliability of solid rocket motors. It was found that the performance of the solid motors was far below that of storable liquid systems when applied to the large payload and velocity change required by the mission.

The major advantages of solid rockets are their simplicity and reliability. They also eliminate pumps and plumbing problems inherent in liquid systems and pre-set firing times can be accurately controlled by grain design.

The disadvantages, as applied to the proposed mission, are low performance, poor restart capability,and lack of controlled variable firing time.

Five of the better performing solid propellants were eliminated because they compared unfavorably with most of the storable liquid systems available. The best performing solid is retained in Table A-2 for comparison.

Further development in high performance solid propellants and solid engines that can be throttled and restarted may produce a system that will compare favorably with storable liquids for large payload applications. If this should come about, the use of solid auxiliary propulsion should be re-evaluated.

Both monopropellant and bipropellant storable liquid systems were considered for the proposed design but the monopropellant systems were eliminated by preliminary calculations because of low performance and lack of development of large monopropellant systems.

Preliminary calculations eliminated several bipropellant combinations and left ten combinations with adequate performance for our application. These are listed in Table A-2 for performance comparison.

Final propellant selection was based on getting the highest performance possible from a reliable and safe propulsion system. Table A-2 shows the usable payload for several propellants based on a select launch date and a gross payload weight of 97,000 pound. . (This figure was later changed to 87,000 pounds.) The first seven fuel-oxidizer combinations in Table A-2 give nearly the same performance and all are adequate for the proposed design.

The seven fuel-oxidizer combinations were selected as possible propellants and their characteristics studied. Hydrazine in pure form was eliminated because of its possible use as a monopropellant. This lowered the number of possible combinations to three, all of which contain a form of hydrazine and use nitrogen tetroxide as an oxidizer.

Nitrogen tetroxide and a 50/50 mixture of hydrazine and UDMH was selected on the basis of performance, handling characteristics, and present development. From the present development of N_2O_4-50/50 engines it is speculated that reliable high performance engines will be readily available by our launch date.

The proposed system will provide adequate restart capability, thrust, and control to allow precision trajectory corrections and short burn retro fire. It will have a capability of more than one mid-course maneuver if necessary.

PROPELLANT			Oct. 4, 1977 LAUNCH			Nov. 3, 1979 LAUNCH		
Oxidizer	Fuel	Mixture Ratio (O/F)	Propellant Weight (lb)	System Weight (lb)	Usable Payload (lb)	Propellant Weight (lb)	System Weight (lb)	Usable Payload (lb)
N_2O_4	N_2H_4	1.20	65,750	72,330	24,670	71,050	78,150	18,850
ClF_3	N_2H_4	2.77	65,810	72,390	24,610	71,200	78,320	18,680
N_2O_4	50/50 N_2H_4/UDMH	2.00	65,900	72,490	24,510	71,250	78,370	18,630
N_2O_4	MMH	2.20	65,900	72,490	24,510	71,250	78,370	18,630
IRFNA	N_2H_4	1.40	66,150	72,770	24,230	71,450	78,590	18,410
90%H_2O_2	N_2H_4	2.00	66,250	72,870	24,130	71,600	78,760	18,240
N_2O_4	UDMH	2.60	66,250	72,870	24,130	71,600	78,760	18,240
ClF_3	NH_3	3.93	66,500	73,150	23,850	71,950	79,150	17,850
ClF_3	86/14 MMH/N_2H_4	2.80	66,950	73,650	23,350	72,550	79,810	17,190
IRFNA	UDMH	3.00	67,500	74,250	22,750	72,800	80,080	16,920
Double Base Ammonium Perchlorate Composite, Aluminized (Solid)			70,650	77,710	19,290	74,850	82,330	15,670

TABLE A-2

Usable Payload Comparison for Selected Propellants

Calculations based on $\Delta V = I_{sp} g_o \ln \frac{W_i}{W_b}$, $W_i = 97{,}000$ lb.

(Solid propellant shown for comparison only.)

Calculations of fuel loads and burn times were made based on the following equations and specifications:

$$\Delta V = I_{sp}\, g_o \, Ln \frac{W_i}{W_b}$$

W_i = 87,000 lb. = gross payload

W_b = burnout payload

$W_p = W_i - W_b$

$W_{pay} = W_i - 1.1(W_p)$ = usable payload

$I_{sp} = \frac{F}{\dot{w}}$ = 340 sec. $\dot{w}$ = propellant weight flow rate

F = 100,000 lb.

$$t = \frac{W_p}{\dot{w}}$$

The results of these calculations are shown earlier in the report in Figures 1-2 and 1-3.

Electrical Mid-course and Retro Propulsion

Of the three varieties of electric propulsion, electrostatic, electromagnetic, and electrothermal, only electrostatic devices are sufficiently developed to warrant consideration. To date, two electrostatic thrusters have been developed, mercury bombardment and cesium contact. The mercury bombardment thrustor is much more efficient than the cesium contact thruster, as can be seen from Figures A-2 and A-3. State of the art 20 x 10^{-3} lb. thrust devices are considered as the basic element when clustering engines. The following mass-thrust estimates are based on 1 lbf/28,000 lbm with an acceleration of 3×10^{-4} to 10^{-3} ft/sec. The thrust level is limited by the maximum available power, approximately 1 lbf/125 kw. We note that an uprated Saturn V/Centaur is capable of placing 87,000 pounds into a transfer orbit to Mars, which requires 3.1 pounds thrust for adequate acceleration. Thus we cannot use electric propulsion for mid-course maneuvers or retro propulsion.

Given the necessary power, 380 kw, we can estimate the nonpropulsion payload. Fuel weight = $W_{INITIAL} - W_{BURNOUT} = W_i (1 - e^{-\Delta V / I_{sp} \cdot g})$ = = 67,000 pounds. Storage tanks (0.065 lbm/lbm fuel), feed system plumbing (31bm/thruster), power generation (50 lbm/kw), and thrusters (8 lbm/thruster) give a toatl weight of 33,000 pounds. The nonpropulsion payload is thus 54,000 pounds. We would need a nuclear power supply to achieve the necessary thrust level.

Fig. A-2

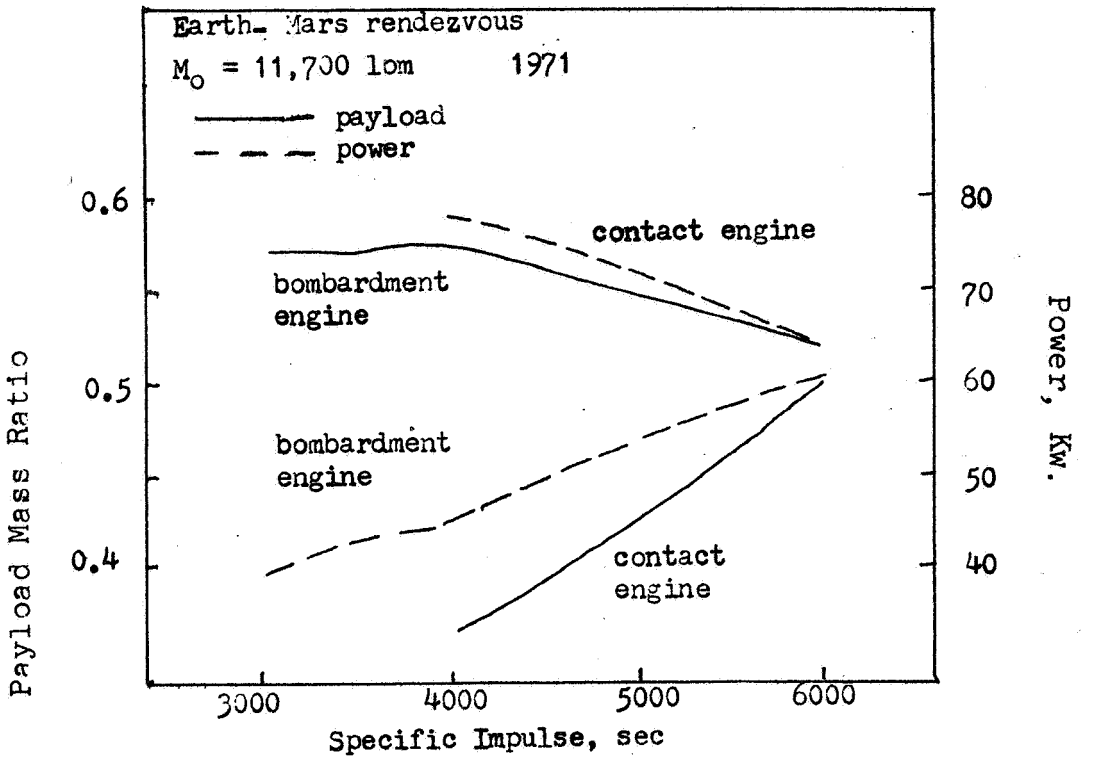

mercury bombardment and cesium contact ion engine performance capability

Fig. A-3

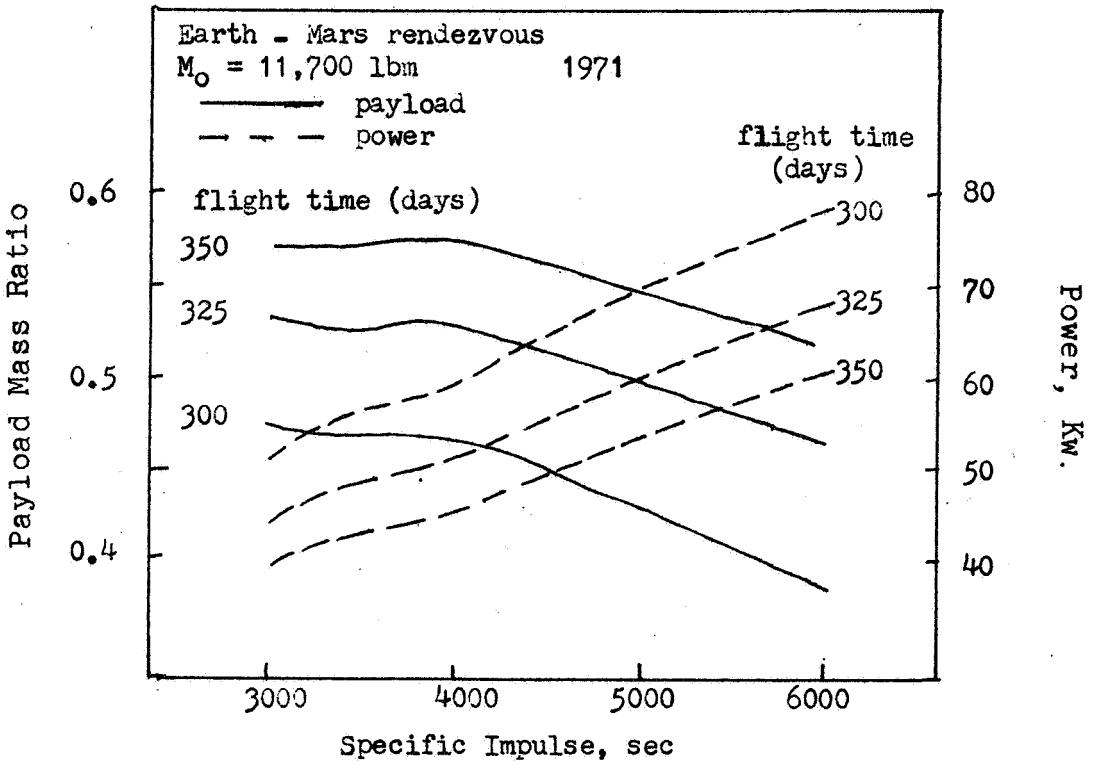

effect of flight time on ion engine performance

Graphs from ion rocket systems and applications
UCLA course X458.1
Jerome H. Molitor Hughes Research Laboritories

Stabilization and Attitude Control

Three systems were considered for an attitude control system: ion propulsion, cold compressed gas propulsion, and storable liquid bipropellant propulsion.

The ion system is ideally suited for attitude control operations. The low thrust levels are adequate and the high specific impulses allow long duration, high total impulse missions with a low fuel weight. However, the high power requirements (on the order of 1 lb thrust/125 kw) make the system entirely unfeasible. A minimum of two operating thrustors would demand too great a solar array. Deployment and structure problems involved in the high acceleration mid-course and retro maneuvers also limit the feasibility of such a system. The development of high power to weight ratio nuclear power supplies would allow the ion system to be reconsidered.

A cold compressed gas propulsion system offers the advantage of simple, reliable operation. Very little hardware is needed for a gas system, but the specific impulse of such a propulsion system is much lower than bipropellant or ion systems. If a mission is of long duration or high complexity a large total impulse will be required of the attitude control system. Thus, due to the low specific impulse, a high propellant weight is needed.

A number of bipropellants were considered for the attitude control system. Due to its high specific impulse, the 50/50 hydrazine with UDMH and N_2O_4 propellant was chosen. State-of-the-art has eliminated thermal instability and many reliability problems. The high specific impulse of the bipropellant requires less propellant weight, but the system is more complex and has a greater hardware weight. The result is a high weight system when the total impulse requirements are low.

The problem of choosing a complete system becomes a trade-off between propellant weights and hardware weights, with some reliability considerations for the cold gas and bipropellant arrangements. A graph of total weights as a function of total impulse for the two arrangements is shown in Figure A-4. As is seen, there is a total impulse at which the more complex bipropellant system has a lower weight than the gas system. Above this impulse the bipropellant system would be more desirable. Problems of reliability may demand the serious consideration of a gas system even though it is heavier. An overall comparison of the system can be seen in Table A-3.

Figure A-4

System Weight as a Function of Total Weight

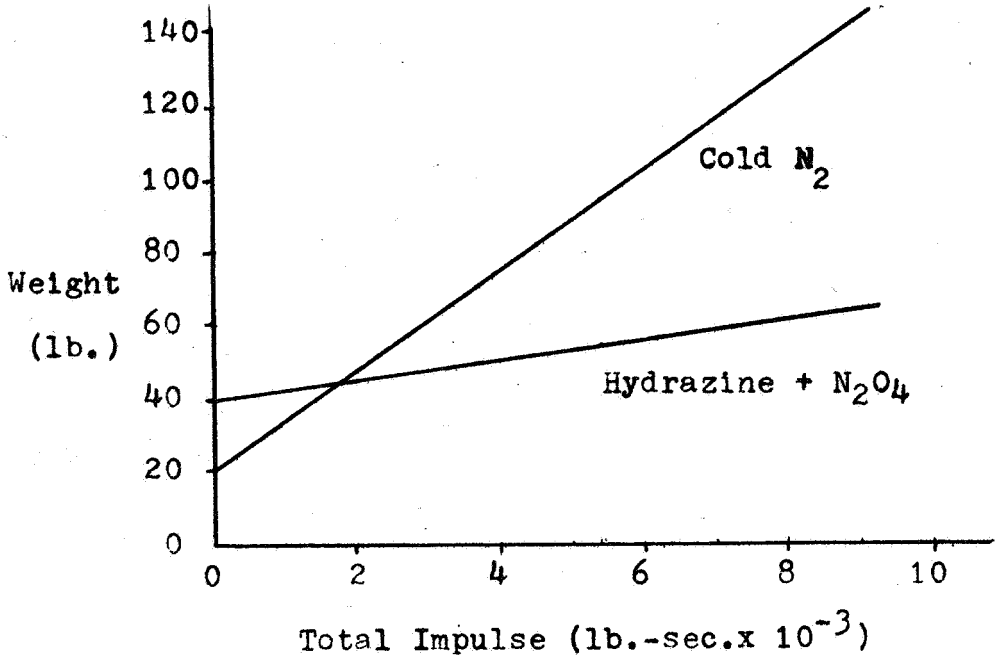

Table A-3

Alternate Systems Comparison

	Cold N_2	Hydrazine + N_2O_4
Specific Impulse	71 sec	340 sec
Propellant Wght.	76 lb.	16 lb.
Hardware Wght.	20 lb.	40 lb.
Volume	5.6 ft^3	.22 ft^3

TRAJECTORY

To plan a Mars orbit, it is necessary to look at several factors which affect the mission. There are not only mid-course corrections in orbital planes and stabilization, but also a final ΔV for a Mars orbit. All of these need to be minimized so a maximum payload may be put into Mars orbit.

There are many possible transfer orbits to Mars (different ways of obtaining a Mars mission). Some have shorter transfer time but require more energy; others take longer but use less energy. In planning this mission, it was determined that the required energy was the determining factor. Hohmann Transfer Orbit is a transfer using the least amount of energy and was therefore used in calculation the trajectory for this mission.

NASA publishes the Planetary Flight Handbook which takes into consideration many orbital affects caused by planets in the solar system, i.e., spheres of activity. The numbers used for the calculation of the values for mid-course ΔV, total ΔV, and other orbital speeds are taken from this handbook.

An analysis of other dates, as shown by Table A-4, reveals why we chose the date we did. Another reason for choosing a launch date of September 4, 1977 was a "safety" period of about one month when we could make the launch.

Calculations showing how to determine necessary speeds and weights are as follows:

Hyperbolic excess speed = 0.161# * 29.78 km/sec = 4.79 km/sec = 15,720 ft/sec

Mid-course ΔV = .028# * 29.78 km/sec = .834 km/sec = 2,730 ft/sec

Arrival speed = .126# * 29.78 km/sec = 3.75 km/sec = 12,400 ft/sec

Circular velocity of Mars at surface, V_{co} = 3.548 km/sec

Circular velocity at a height of 200 km = $\frac{V_{c_o}}{\sqrt{\frac{r}{r_o}}} = \frac{3.548}{1.029}$

where r = 3615 km; r_o = 3415 km

V_c AT $h = 200$ km $= \sqrt{2}\, V_c = 4.88$ km/sec

$V_p^2 = V_{cp}^2 + V_\infty^2$

$V_p = 6.16$ km/sec ; $V_p - V_{cp} = 2.72$ km/sec = 8,920 ft/sec

#Figures from NASA Planetary Flight Handbook.

$8,920 + 2,730 =$ Total ΔV of 11,650 ft/sec

$\Delta V = I_{sp} \cdot g \ln \frac{w_1}{w_2}$; $\frac{w_1}{w_2} = e^{\frac{\Delta V}{I_{sp} \cdot g}}$

$I_{sp} = 340$ sec ; $I_{sp} \cdot g = 10,890$; $\frac{\Delta V}{I_{sp} \cdot g} = 1.071$

$\frac{w_1}{w_2} = e^{1.071} = 2.92$ $\quad w_2 = \frac{w_1}{2.92} = \frac{79,930}{2.93} = 27,000$ lb.

79,930 - 27,000 = 52,930 = W_p = Weight of propellant tanks plus propellant structure = 10% W_p = 5,290 lb.
∴ useable payload = 27,000 - 5,290 = 21, 720 lb.

TABLE A-4

Launch Date	ΔT (days)	Useable Payload (pounds)	$V_{\infty E}$ (ft/sec)	Arrival Speed (ft/sec)	Mid ΔV (ft/sec)
9/4/77	260	21,720	15,720	12,400	2,730
10/4/77	230	22,000	12,300	14,070	2,440
10/14/77	220	20,450	12,200	14,450	2,540
10/4/79	250	18,520	15,400	16,100	1,660
11/3/79	220	16,500	11,900	18,460	1,270
11/2/81	280	29,680	12,500	12,140	880

APPENDIX B: POWER GENERATION SYSTEMS

POWER SYSTEMS INVESTIGATED

Nuclear Sources

An adequate source of electric power is essential to all space missions, and in this discussion nuclear power systems are considered. Radioisotope decay and fission in nuclear reactors produces heat, which can be converted partially to electrical energy in a variety of ways, with the remainder of the heat being radiated to the external environment. The mission under consideration requires about 10 kw of electrical power. The most promising radioisotope and nuclear reactor power systems in this power range, namely, the isotope Brayton and the SNAP 8 thermoelectric, will be presented.

Isotopes

The Brayton cycle gas turbine is of particular interest for use with radioisotopes because of a potential cycle efficiency as high as 25%. Figure B1 shows a likely Large Heat Source (LHS) electric power system. The Brayton cycle utilizes argon, neon, krypton, helium, xenon or mixtures of inert gases as the working fluid. There is no boiling or condensing; consequently, there are no two phase zero gravity startup problems or material corrosion problems. In this system, the working fluid remains in the gaseous state throughout the cycle. "Cold" gas is compressed in the compressor and passes through a regenerator where it is preheated by gas from the turbine exhaust. The gas is then heated to its maximum temperature in the isotope heater and expanded in a turbine which drives a compressor and an electric generator. The turbine exhaust gas then passes through the "hot side" of the regenerator where it gives up some of its heat to the gas leaving the compressor. Additional waste heat is transferred to the radiator where it is radiated to space. The "cool" gas leaving the radiator enters the compressor and passes through the cycle again. This isotope Brayton system will be available by 1972 to be used initially in MORL and Advanced Lunar Exploration.

Reactors

In connection with the isotope power program, much work has gone into thermoelectric conversion system technology; this technology, coupled with the 600 thermal kilowatt SNAP 8 reactor will result in a system with the power range of 10-25 kw. The upper limit is predicted because of the low system efficiency (3-4%) of thermoelectrics at the SNAP 8 operating temperatures and the relatively large radiator required. A thermoelectric space power conversion system using the heat from a nuclear reactor is shown schematically in Figure B2. The heat is extracted from the source by a liquid metal loop. This primary loop is connected to a secondary loop by a heat exchanger, double action, thermoelectric electromagnetic pump. The secondary

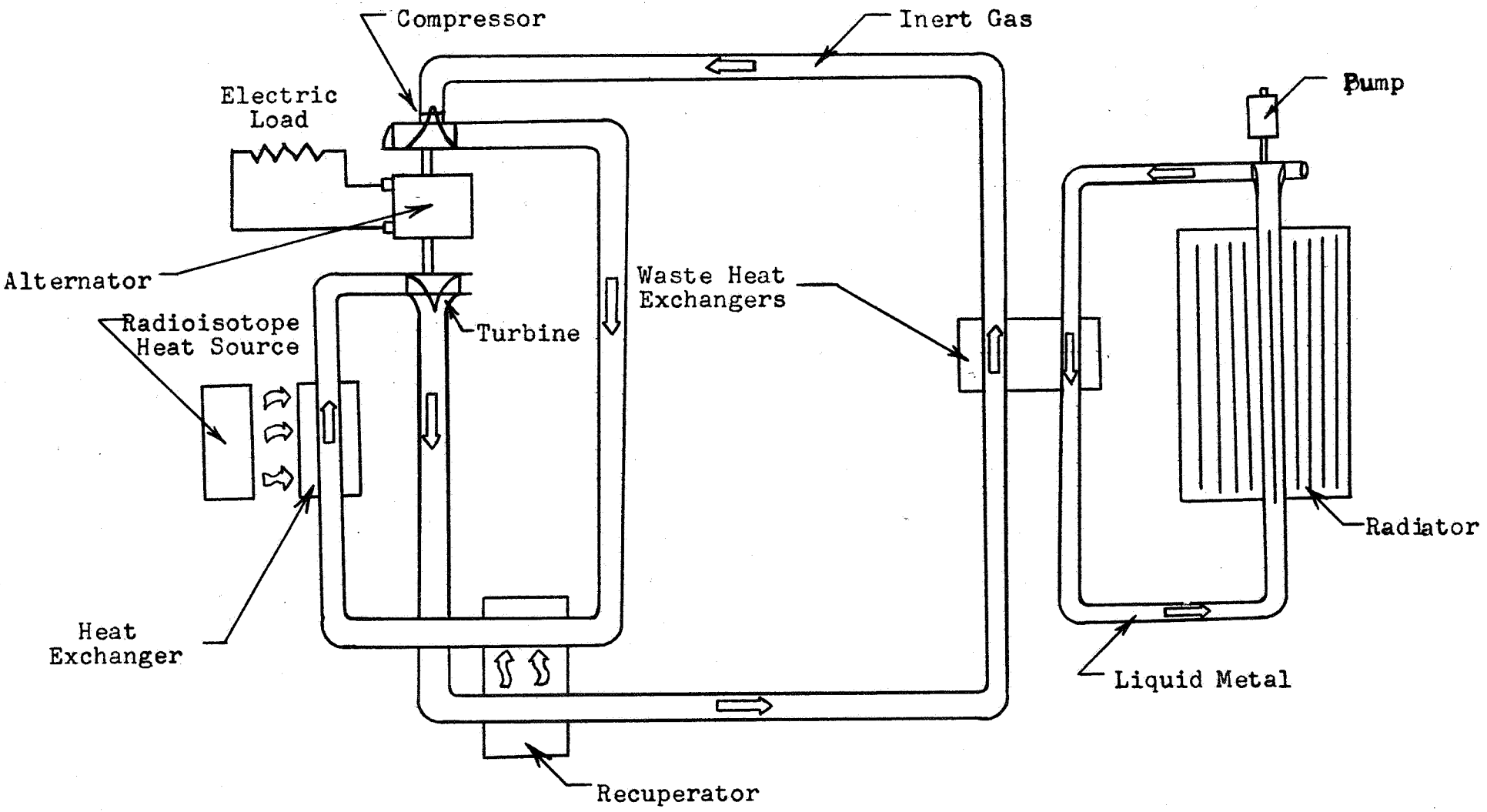

Figure B1 Large Heat Source (LHS), Brayton Cycle

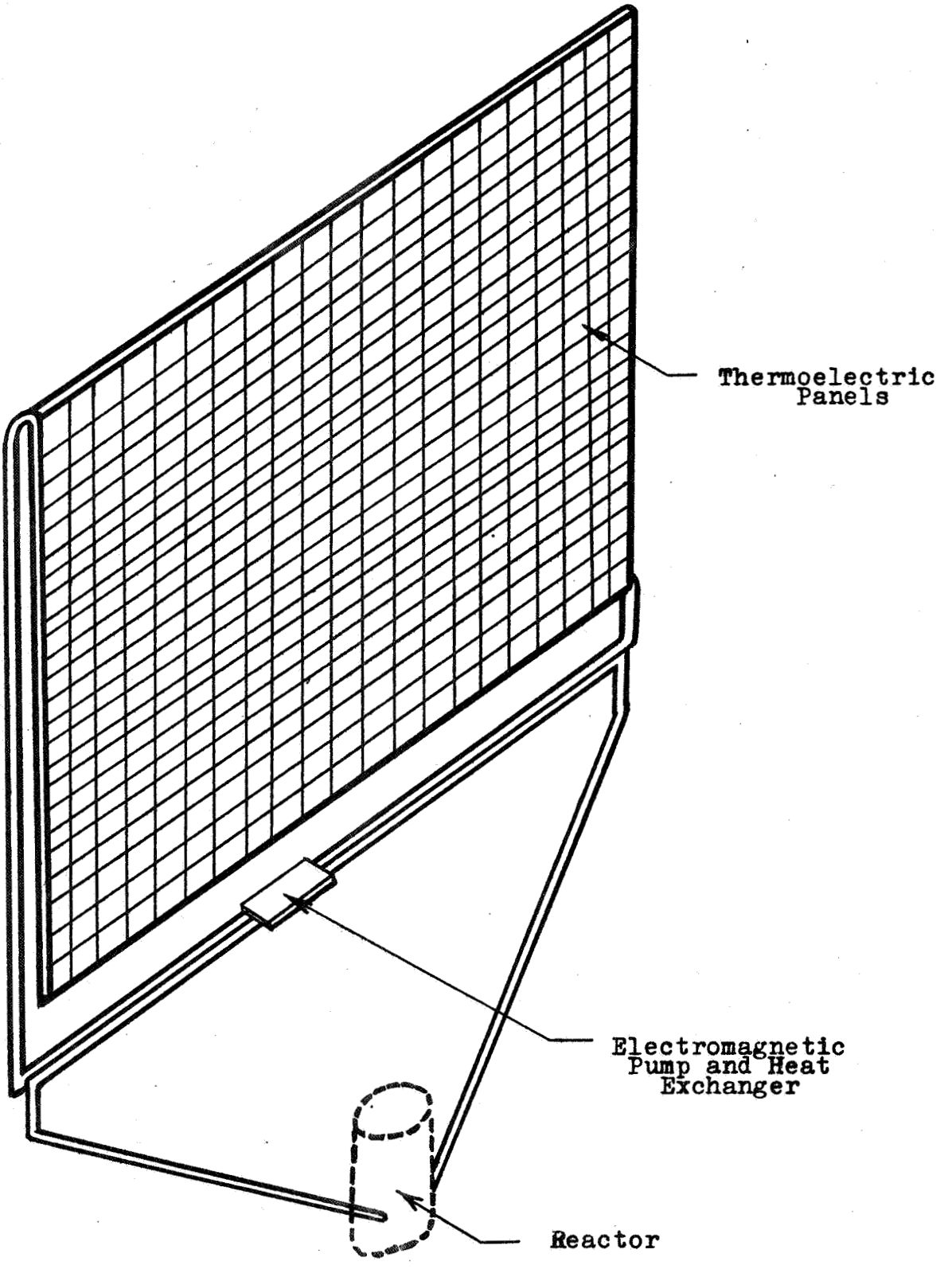

Figure B2 Thermoelectric Space Power System

loop supplies heat to the converter radiator panel. The reactor loop can work at a higher temperature than is permitted by the thermoelectric converter. The mass flow of coolant is held to a minimum, and a larger temperature difference between inlet and outlet is used. On the converter side, the temperature of operation is lower. The temperature difference is small, and mass flow is not limited. The temperature difference between the two loops can be used for power generation for the electromagnetic pump. The converter for the pump consists of two large elements, which permit higher temperature operation. The efficiency of conversion in the pump is not important, since the waste heat is used in the power conversion panel which consists of converter and radiator integrated into one unit. Even though thermoelectric power conversion systems have overall efficiencies of only a few percent, they are attractive since they have no moving parts and thus a reliably long life.

Photovoltaic Systems

Another prominent system in the field of space power sources is photovoltaic energy conversion. In this process, solar cell arrays convert the solar energy radiated by the sun directly into electrical energy. Consequently, use is made of the readily available energy of the photons that are present in space.

Theory

The photovoltaic method of energy conversion takes advantage of the high energy photons radiated by the sun. These photons are used to create free electrons in a semiconductor material. The free electrons result in a current flow.

Photons with enough energy ($E=h\nu$) excite electron-hole pairs in a semiconductor PN junction causing a diffusion process. The result of this action is a minority carrier flow in which holes cross the junction into the P region and electrons into the N region. This minority carrier motion produces a charge flow (or current) across the junction region. When an external load is attached to the junction, part of the current involved flows through it and the rest flows through the internal resistance of the semiconductor device. Consequently, the photovoltaic cell becomes a current source.

The highest radiation photons from the sun occur in the green light region with a magnitude of approximately 2.5 electron volts. A solar cell designed to produce electron hole pairs with 1.0 to 1.5 electron volt photons (ie. the forbidden energy band between the bound and conduction electron states of the material is 1.0 to 1.5 ev.) will produce the greatest cell efficiency since the greatest number of incident solar photons will be effective in the process.

In the overall array system, the individual cells are mounted in a sun oriented direction. They are connected in series and parallel combinations in a configuration that will deliver the desired voltages

to the power conditioning and battery storage systems. From this point the power is regulated and bussed to the various subsystems.

Cell Materials

Although single-crystal silicon cells are the most commonly utilized cell today, extensive research is being conducted on CdS and GaAs cells. The best conversion efficiencies for these solar cell materials are shown in table B1. These efficiencies are for single crystal, single PN junction experimental cells. They have not improved very much during the past four years and only small improvements should be expected in the future.

Two important material properties relating to the efficiency of the photovoltaic effect are the optical absorption and the diffusion length L of the semiconductor. The short circuit current I_s of a solar cell is given by the expression:[16]

$$I_s = Q(1-e^{-\alpha\gamma})(1-r)eN_{PH}(E_g) \approx eN_{PH}L$$

where Q is the collection efficiency, r the reflection coefficient, l the thickness of the semiconductor, N_{PH} (EG) the number of photons absorbed by a semiconductor of band gap energy Eg, and N_{PH} is the total number of photons in the solar spectrum. For high efficiency, L must be as great as the spread depth over which the solar photons are absorbed. For Si and GaAs, L must be 100 and 2 respectively. Even if L≈X, and neglecting other lossess such as reflection, the solar conversion efficiency of the photovoltaic effect is limited by the relative number of solar photons absorbed and the potential at which the electrons absorbed and the potential at which the electrons are delivered compared with the energy of the photons.

The simplified expression for the maximum efficiency of a solar cell is given by:[16]

$$\eta_{MAX} \cong N_{PH}(E_g)V_{mp}/N_{PH}E_{av}$$

where Vmp is the voltage at maximum power, and Eav is the average energy of solar photons, about 1.5ev. For silicon N_{PH} (Eg) is $2/3N_{PH}$, and Vmp is about 1/3 Eav, which gives 0.22 as the maximum theoretical efficiency.[26]

Table B1 also lists the theoretical efficiencies of some of the more common photovoltaic materials and the best reported experimental efficiencies. Silicon and gallium arsenide have given the most promising results to date. Silicon is the material nearly exclusively used for commercial solar cells at present. The results for GaAs represent many years of effort applied to a very stubborn material, but improvement in efficiency and reduction in cost are still necessary before it can challenge the position of silicon. However, for high temperature operation and for high radiation areas, GaAs cells may offer advantages over Si Cells.

As a description of typical cell parameters, silicon solar cells are produced in large quantities with sunlight efficiencies (at air mass one)

TABLE B1

EFFICIENCIES OF SOME SOLAR CELL MATERIALS

Material	Bandgap Energy, ev	Theoretical Efficiency, %	Experimental Max. Efficiency*, %
Si	1.11	22	14
GaAs	1.40	26	11
CdTe	1.45	23	6
CdS	2.40	18	8

*1 A. U., A. M., 25 C

TABLE B2

MINIMUM FILM THICKNESS REQUIRED FOR VARIOUS MATERIALS

Material	Thickness (μ)	Utilization (%)
Si	100	85
GaAs	2	90
CdTe	10	90
CdS	1	Anomalus Behavior

of better than 13% and air mass zero efficiencies of better than 11%.[26] At 25°C single cells with a base resistivity of 1-2 ohm-cm yield open circuit voltage of 0.58V, short circuit currents of 27-33 ma/cm^2 (AM1; 100mw/cm^2 solar intensity) and 32-40 ma/cm^2 (AM0; 140mw/cm^2 solar intensity). The voltage and maximum power output in such cells degrade with increasing temperature at the rate of 2.3 mv/°C and 0.1mv/°C respectively. The spectral response per photon of silicon solar cells peaks at 0.72μ when the junction depth is 1μ (the so-called red-shift cell), and 0.66-0.70μ for a junction depth of $\frac{1}{4}$ to $\frac{1}{2}$μ (the so-called blue shift cell). In general, blue shifted cells are preferred because of radiation damage effects in outer space. On a relative basis there is more blue light in outer space sunlight than in terrestrial sunlight.

Cell Structures

The great majority of silicon solar cells made today are 1x2 or 2x2 cm in area and about 8 to 14 mils thick. The front layer of the cell is usually N-type silicon with the base material being P-type. This is the so-called N-on-P radiation resistance cell. The N-on-P cell is considerably more resistant to radiation than the P-on-N cell, and yet is not electrically inferior to the P-on-N cell.

Silicon cells can be made as thin as 2 to 4 mils. These have an advantage in terms of weight, and a disadvantage in terms of decreased output and susceptibility to breakage. An optimum cell thickness may be about 8 to 12 mils. Although the sintered contact seems to be the most reliable to date, the problem of contacts to solar cells is still one of the most difficult to solve. Techniques for connecting cells in series and in parallel as well as in series-parrallel are well in hand, using either shingling or flat lay-down methods, with the latter applied in the majority of the recent systems.

The chief reason for the present high cost of solar cells is the need for single crystal material which limits the production size of individual solar cells. Non-single crystal films can be used for solar cells. The multi-crystal selenium and copper oxide photo-electric exposure meter has long been in use. More recently, CdS and CdTe film-type solar cells have been developed.[20] The CdS cells have yielded over 8% efficiency.

Claimed advantages of thin film cells include:[6]

1) Lower specific weights than about one third of the thinnest silicon cell.

2) Relative immunity to radiation, eliminating the need for heavy glass shielding.

3) Flexibility permitting compact launch stowage in roll-up arrays.

4) Economical manufacturing and installation costs in large size units.

Unresolved problems include:

1) Stability, (degradation occuring under storage, humidity, thermal cycling and UV light).

2) Prerequisite of extreme cell materials purity and high conductivity.

Film devices offer weight reduction because only very thin layers (microns) of most semiconductors are needed for the conversion of solar protons in electricity. Most of the 12 to 14 mils of Si used in single crystal devices serve as structural support. The film thickness required is given by the semiconductors optical absorption. Table B2 shows approximate minimum film thickness for various materials based on the indicated estimates of percentage utilizations of the possible material absorption of solar photons. Silicon does not appear very promising since diffusion lengths of about 100μ are required, whereas the grain size may be no more than 10μ, and diffusion of carriers across grain boundaries is not expected to be very efficient. The materials CdS and CdTe are receiving considerable attention. CdS cells of 50cm area (3x3in.), made by evaporating CdS and then forming a barrier layer with copper, having yielded efficiencies up to 6.9% on plastic substrates and up to 8.2% on Mo substrates.[20]

A difficulty with both CdS and CdTe is a deterioration caused by moisture in the air. For space purposes this may not be serious, but for terrestial storage a hermetic seal may be required.

Films have been made on relatively flexible organic (Kapton) or metallic substances. The metal substrates required construction of a front-wall cell since light cannot penetrate the conducting metal substrates. This problem has been solved by several companies.

Power to weight ratios up to 100 w/lb are reported for individual 3x3 in. CdS cells (neglecting a significant part of the total solar cell array weight such as deployment and support structure and electric cabling). This is to be compared with 75 and 150 w/lb for individual 0.8x0.8 in. Si cells (in this case neglecting cover glass, adhesives, electrical interconnectors, support structure, thermal control paint, electric cabling, etc.) ranging in thickness from 12 mils down to 4mils. The power to weight ratio for such Si cells is reduced to 40 to 80w/lb when all components are included except deployment and support structure and electric cabling.

Design Problems

Semiconductor devices in general are sensitive to radiation, and solar cells are especially vulnerable because of their placement on the outer surfaces of the satellite. The radiation in space consists of electrons with energies from a few kilo-electron volts to about 8 mev. The general effects of this radiation on solar cells are:

1) The power output of the cell is quite sensitive to radiation.

2) The current decreases more rapidly than the voltage for radiation absorbed below the top layer.

3) The decay is qualitively the same for all types of deeply penetrating particles of radiation.

4) Particle radiation of shallow penetration, e.g. protons with energies of not more than a few hundred kiloelectron volts affect the voltage and the shape of the current-voltage characteristic much more severely than through a decrease of the short wavelength portion of the spectral response.

Much effort has been applied toward understanding these effects. The radiation physically creates Frenkel-type effects in the semiconductor by actually knocking atoms out of their equilibrium lattic positions. These defects act either as intrinsic defects, or in combination with other impurities they act to form recombination centers that cause the photon-generated pairs to recombine before being collected (i.e. the life-time and diffusion length are reduced).

N-on-P cells withstand radiation about 30 times better than the P-on-N cells for electrons and about 3 times better for protons because the defects in P-type material are less effective as recombination centers than in N-type material. Because of the nature of the damage, it is possible to effectively increase "life" by adding to the area of array. For example, a 17% increase in array area would increase life by a factor of ten (i.e. the same power output would be achieved after intercepting ten times the particle flux per unit area).

Increasing the resistivity of the base material in silicon increases the radiation resistance of the cell. A factor of 2 or 3 in resistance to electron damage can be expected in going from 1 to 10Ωcm, although the efficiency of 10Ω^{cm} cells is such as to lower output voltages (0.53V as compared to 0.58V). Going above 20Ωcm can lead to other problems such as reduced voltage, increased series resistance, and temperature sensitivity. The optimum silicon resistivity for radiation resistance is probably near 10Ωcm.[16]

Also, thin film cells are two to three orders of magnitude more radiation resistant than their single crystal counterparts. Whereas heavy fused silica cover glasses are required to protect the single crystal cells from proton damage, no such protection is need for the thin film CdS cells.

In addition to radiation considerations, problems such as temperature cycling tend to place some limits on the design possibilities of the photovoltaic system. Figures B3 thru B5 show some projected characteristics concerned with solar cell design. These parameters were used in consideration of the basic power supply design requirements of this mission.

Deployment Considerations

One of the major problems in the development of high power solar arrays is the mechanism for deploying the array in a reliable fashion. The advanced array development programs with high power to weight ration

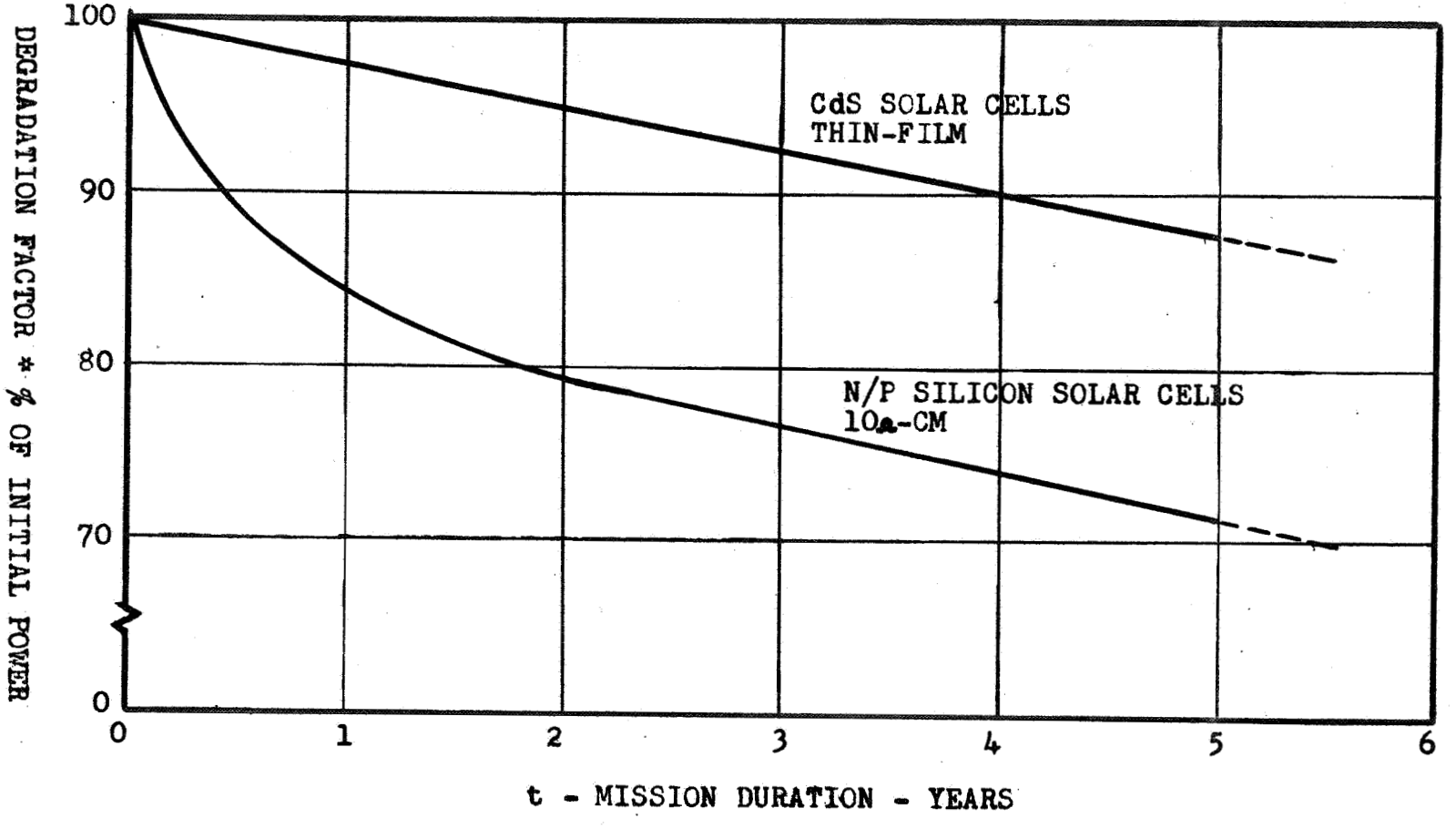

Fig. B3 Solar Cell Degradation Due To The Space Environment [26]

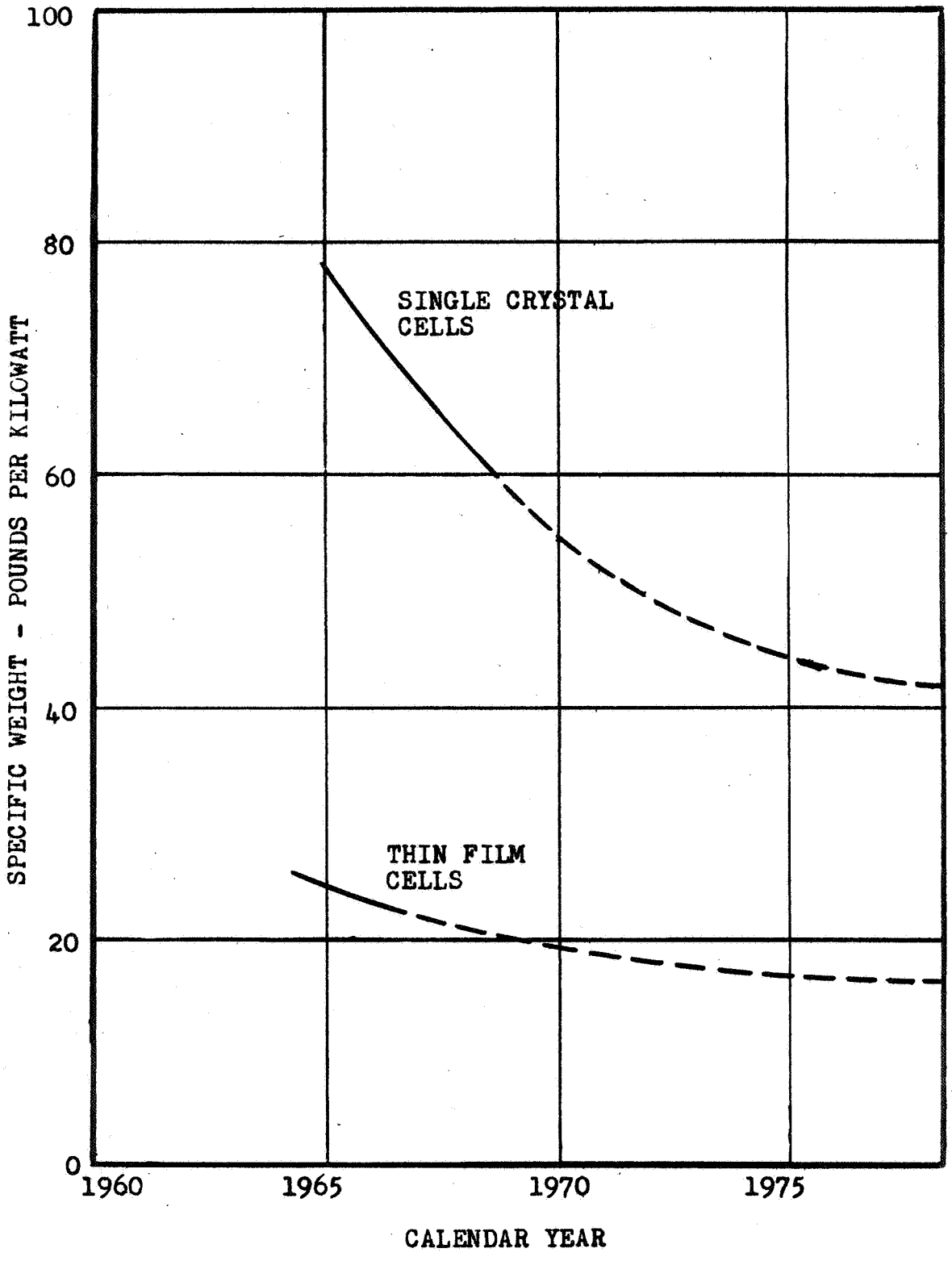

Fig. B4 Specific Weight--Solar Cell Arrays[26]

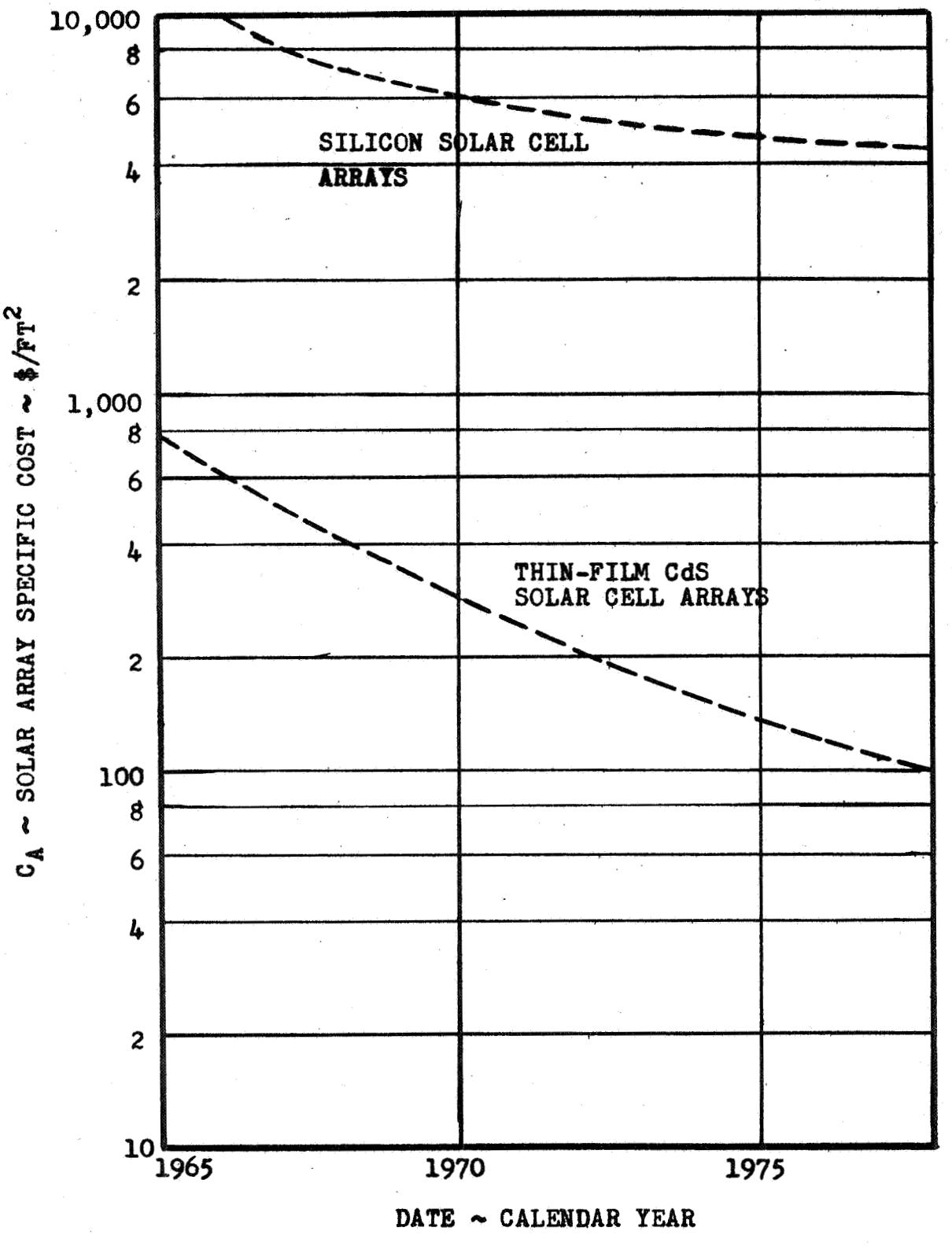

Fig.B5 Solar Cell Array Cost [26]

goals and extremely large array areas have had to utilize new structural design concepts more than previous spacecraft experience.

Two array techniques currently being studied are potentially capable of demonstrating a specific weight of less than 50 lbs/Kwe. The semi-rigid panel concept employs a rigid frame or truss which supports a thin, flexible membrane-like substrate. Evaluation of structural materials for this concept indicated that beryllium, because of its very high stiffness-to-weight ration, was most suitable for this concept.

The second technique, roll-up arrays, utilizes deployable booms to pull out a thin, flexible sheet substrate, which is rolled up securely around a drum for support during periods of high dynamic loading (eg. during launch). Once the spacecraft enters the orbit phase, the booms pull the array out much as one draws a window shade, and holds it extended. This technique affords the most flexible packaging concept and has the greatest potential for lightweight design.

The Jet Propulsion Laboratory has initiated efforts to determine the feasibility of developing the roll-out array techniques, aiming at a goal of 33 lbs/kwe for a 10 kw array. Contracts have been awarded to G.E., Ryan and Fairchild-Hiller for parallel investigations of their techniques to meet these roll-out array goals. The G.E. model has not only met most of the design requirements but has surpassed the weight to power ratio initially hoped for (33 lbs/kw) by obtaining 30 lbs/kw.[9]

Conclusion

Solar cell arrays offer the following characteristics;

1) A 10% conversion erficiency.

2) Minimum power conditioning required.

3) Relative insensitivity to solar orientation (power = k cos ϕ where ϕ is the angle of light incidence to the solar array).

4) Light weight, with 30 lbs/kw a reasonable goal.

5) Ruggedness and reliability for lifetimes up to 10 years.

6) No special collectors or radiators required.

7) Need for energy storage.

8) Large area causing drag.

Recent excellent progress in lightweight array design, improved radiation resistance, and improved CdS efficiency indicates that photovoltaic power systems will continue to be a basic source of space power throughout the next decade.

SYSTEM CHOICE DECISIONS

Primary Power Source Selection
(Alternates were selected on the basis of a 10kw system at 1.5A.U.)

Electric power systems can be classified by the source from which they derive their energy: solar or nuclear. The nuclear classification is further divided into two important types. The first type, reactor systems, were eliminated because of the extremely high weight to power ratio-350 lb/kw for the SNAP-8 thermoelectric system. In addition, the relatively short productive lifetime of the SNAP-8 placed undesirable limitations on the duration of our mission; we would not be able to observe Mars during a complete season cycle of about two years using the SNAP-8 system. This system, however, does provide a high degree of mission adaptability, since it has no orientation requirements associated with it.

The radioisotope Brayton cycle system offers advantages similar to those of the reactor systems. The nuclear systems are all insensitive to solar distance and radiation environment. However, the prohibitive cost of the plutonium fuel, together with the relatively high weight to power ratio, forced the elimination of this alternative power system. The relatively short lifetime is a direct result of our limited technological capability in dealing with the Brayton cycle subsystems. This also placed undesirable limitations on the duration of our mission.

Solar photovoltaic power production offers several advantages for the selected power range. Recently developed thin film solar cells are highly pliable and highly resistant to radiation. Also, advancements in roll-out arrays have reduced the specific weight of a solar power system to 30 lbs/kw.

Table B3 presents various competing factors of the three alternative power systems. It is clear from the table that the SNAP-8 and LHS systems possess several desirable features. However, since some of the most fundamental considerations in choosing a space power system are weight, cost, development status, and fuel availability, it was decided that the nuclear power systems are not optimum for this mission. It is interesting that a few years ago it was generally believed that the use of photovoltaic solar cell arrays would be limited to applications requiring less than one kilowatt of power and that larger spacecraft auxiliary power requirements would be satisfied by the use of more sophisticated energy sources using nuclear systems. However, this conclusion was largely based on comparisons between existing photovoltaic arrays and the projected designs of other systems. Since that time, photovoltaic cells technology has advanced while much of the expected capability of other systems still remains to be demonstrated. This has resulted in the reconsideration and adoption of photovoltaic systems for high-power applications. Table B4 displays the major trade-offs

Table B3

Summary of Competitive Factors

Consideration	LHS Radioisotope-Brayton	Snap-8 Reactor	Solar Photovoltaic
Power Capacity	2-10 Kwe	10-30 Kwe	1-50 Kwe
Weight	925 lbs @ η = 20%	3500 lbs	650 lbs @ 30 lbs/Kwe slight degradation with time
Mission Life	1.1 Years		
Solar Occultation	No Affect		Requires Battery Plus 25% Solar Array Increment
Vehicle Configuration	No Affect		Requires Storage and Deployment
Attitude Control	No Dynamic Effect and No Orientation Required		Orientation Required
Effect on Orbit Selection	No Drag at Mars. Lower Periapsis Allowed		Panel Drag Restricts Orbit to One High Enough to Assure Long Life
Sterilization	Possible		Possible but Battery Questionable
Cost: Fuel	$160,000,000	Small	None
Cost: Developement	$ 50,000,000	$63,000,000	$30,000,000
Availability	1970-72	1975	1970-72
Previous Experience	None	Little	Extensive
Environmental Effect: Radiation and Meteorites	None		Neg. for CdS System Appreciable for Si

Table B4

Electrical Power Trade Studies

TOP LEVEL TRADES

Candidate Concepts	Intermediate Selection	Selected Concept
Nuclear Reactor System	Reactor Thermoelectric	Solar Photovoltaic with Storage Battery
Isotopic System	Radioisotope Brayton (LHS)	
Solar System	Solar Photovoltaic Rechargeable Storage Battery	
Characteristics Determining Selection	Cost Availability	Weight Reliability

SECOND LEVEL TRADES

Candidate Concepts	Intermediate Selection	Selected Concept
Solar Array	Fold - Out Roll - Out	Roll - Out
Storage Battery	Nickel - Cadmium Silver - Cadmium Silver - Zinc	Nickel - Cadmium
Conditioning and Distribution	Centralized De-centralized	De-centralized
Characteristics Determining Selection	Reliability Electrical Efficiency Availability Weight Magnetics	

involved in the decision of the particular mission system used.

SECONDARY POWER SOURCE DECISION

Choice of Battery

Three types of batteries were considered as the secondary power supply for our mission: nickel-cadium, silver-cadmium, and silver-zinc. The selection of battery type was based on:

1) Reliability

2) Cycle life required

3) Specific energy density

4) Battery life required for the mission

5) Temperature sensitivity

The battery which best fits these requirements is the nickel-cadmium battery.

Where high reliability and completely automatic operation is essential, the nickel-cadmium cell has been the most widely used system. In the temperature range from forty-eight to ninety degrees Fahrenheit the probability is 0.9999 that a power package consisting of one operating battery and two redundant standby batteries can survive 8000 cycles or two years of orbital life. Roughly eighty percent of all NASA spacecraft use nickel-cadmium batteries.

Electro-Optical presented the data of Figure B6 in its report of July 7, 1967. The comparison is given for orbit times approximating the one hundred and ten minutes it will take our mission. Assuming an orbit life of four years, the secondary battery must withstand 20,000 charge-discharge cycles. On the basis of the data in Figure B7 the nickel-cadmium battery is capable of 20,000 cycles providing the depth of discharge is low.

If considering specific energy density as the sole criterion for the choice of battery, then the silver-zinc battery would be chosen. Figure B8 indicates that at all levels of discharge the silver-zinc battery is superior and the nickel-cadmium lags all three. At a depth of discharge of twenty percent, for example, the nickel-cadmium battery has an actual specific energy density of three watt-hours per pound. This compares to ten watt-hours per pound for silver-cadmium and eighteen for silver-zinc.

The orbiting life of our mission was designed for four years. Adding to this the two hundred sixty days in transit gives a minimum battery life requirement of four and three-quarter years. Typical silver-zinc batteries are rated at one to two years because their separator material is subject to electrolyte deterioration. Deterioration of the silver-cadmium battery is not as critical with its life being prolonged

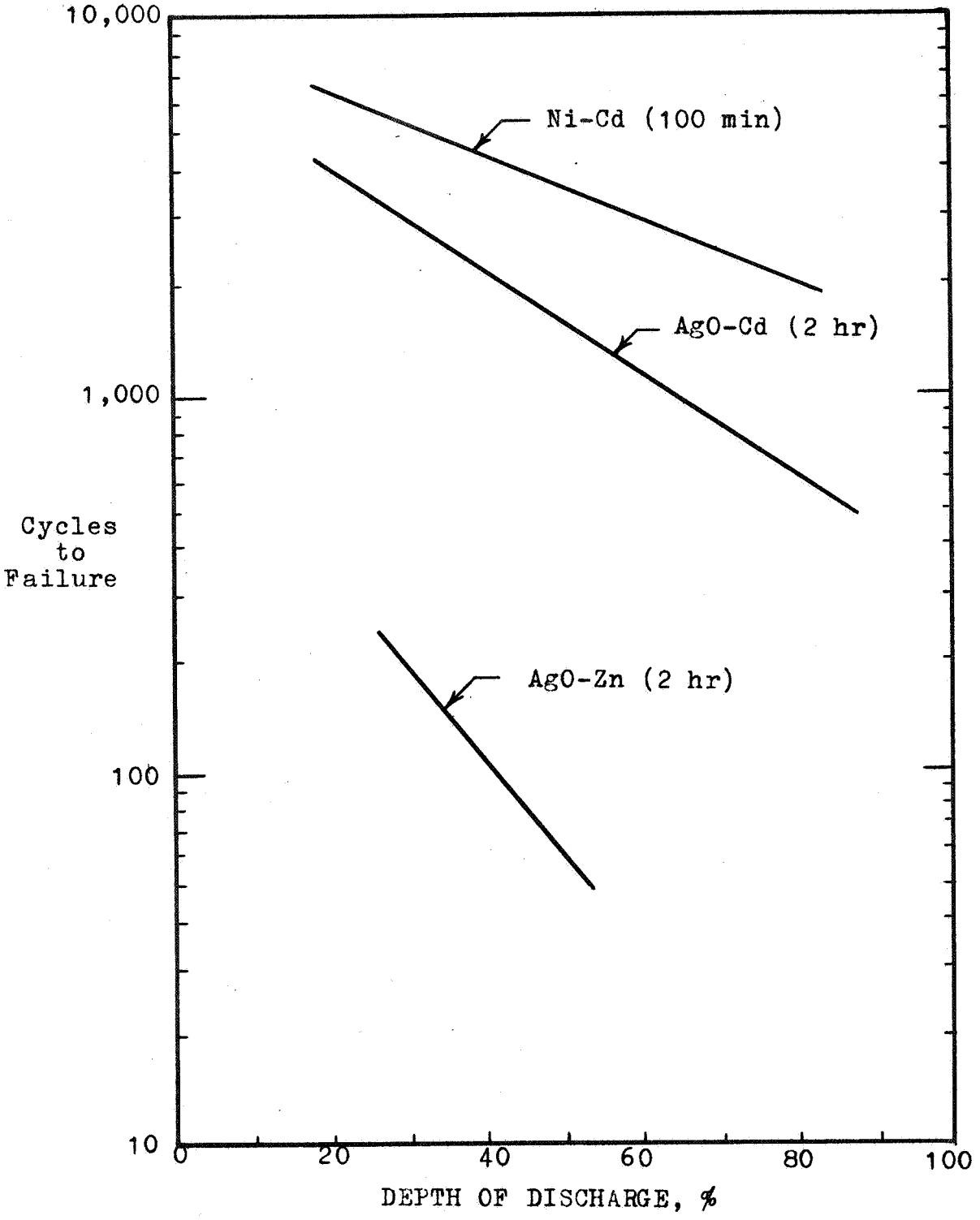

Figure B6 Cycle life to failure for various orbital times.

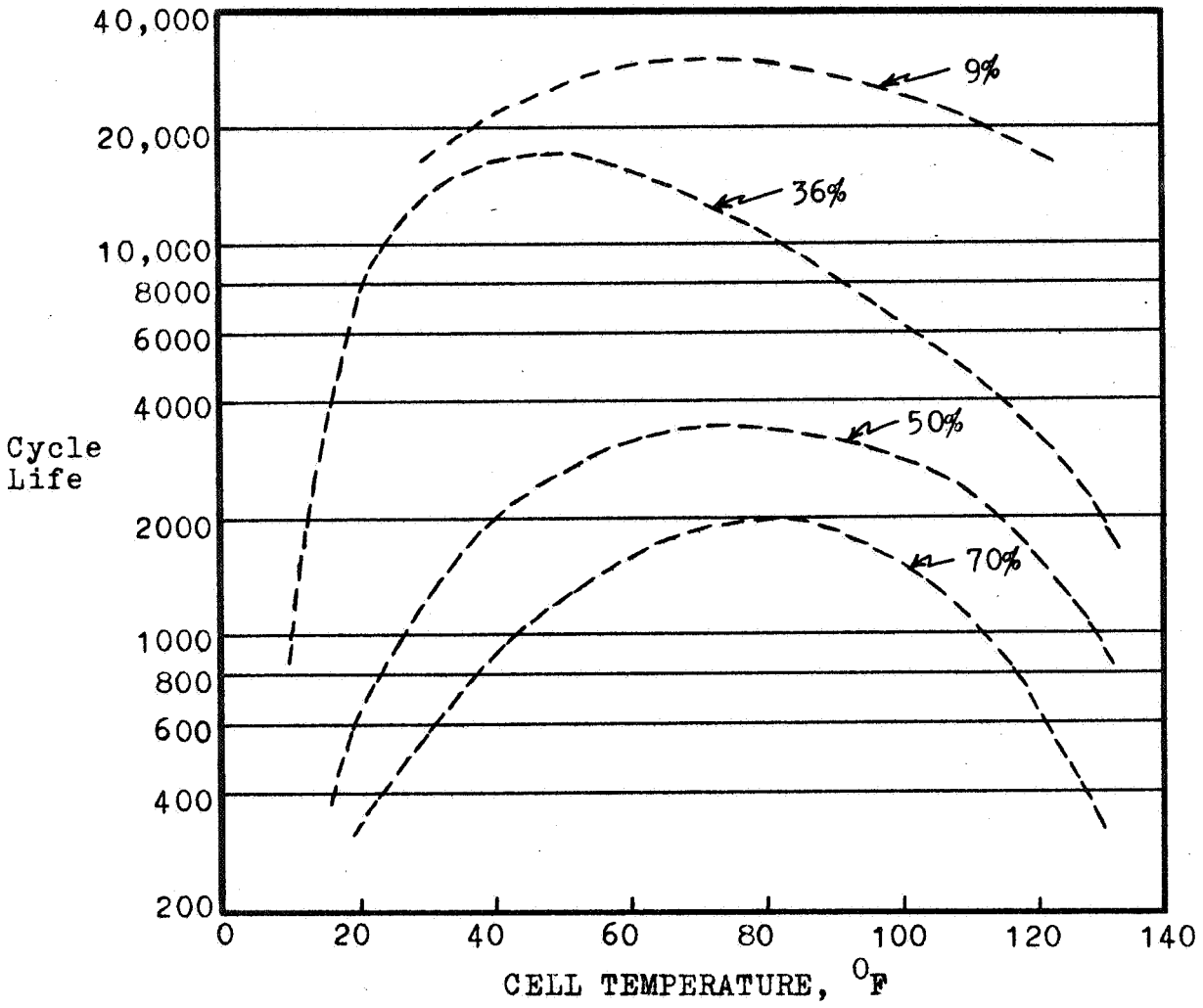

Figure B7 Estimated cycle life of nickel-cadmium cells as a function of temperature for various depths of discharge.

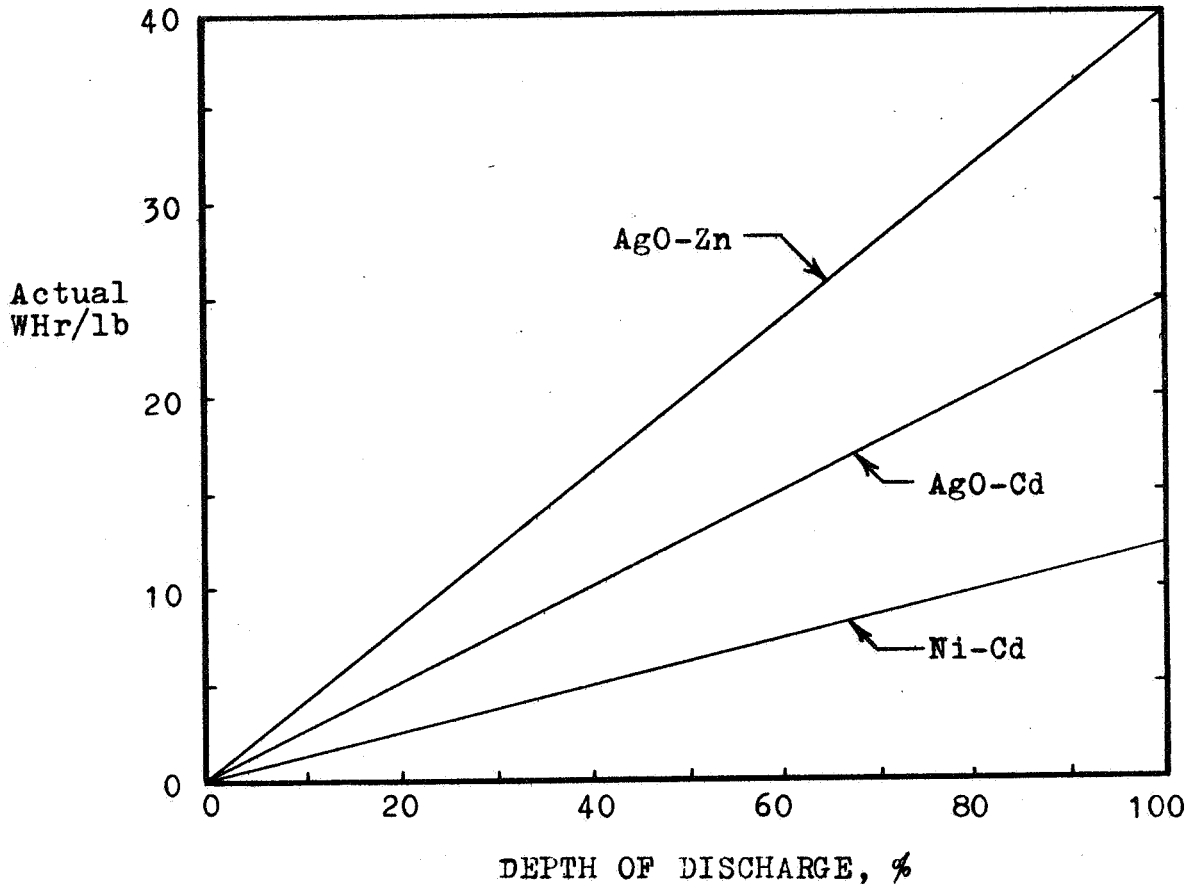

Figure B8

Temperature	Condition	AgO-Zn	AgO-Cd	Ni-Cd
32^0F	Discharged	1-3	3-4	8
	Charged	1	2-3	8
75^0F	Discharged	1-2	2-3	8
	Charged	.5-.7	1-2	8
120^0F	Discharged	.4-.5	1-2	4
	Charged	.2-.3	.5-1	4

WET LIFES OF SECONDARY BATTERIES (YEARS)

Table B5

if maintained at a low enough temperature as indicated in Table B5. The nickel-cadmium battery does not seem to have any major difficulties in meeting the life requirement. As the table shows, silver-zinc and silver-cadmium batteries are very sensitive to temperature changes whereas the nickel-cadmium battery has significant loss only when subjected to high temperatures (one hundred twenty degrees Fahrenheit). Nickel-cadmium batteries can be operated at temperatures as low as minus sixty-five degrees Fahrenheit with heaters.

In summary, nickel-cadmium batteries were chosen because of their proven reliability, long cycle life possible if the depth of discharge is low, long battery life, and effective operation at low temperatures. These factors far outweigh its low specific energy density.

FUTURE AREAS OF DEVELOPMENT

Nuclear Sources

In the future, advanced reactor electric power systems will be required for auxiliary power and electric propulsion. Goals such as light weight, 3000°F. operation, and long life require the technological investigation of advanced liquid metal Rankine turbogenerator systems, direct conversion thermionic systems, and magnetohydrodynamic generator systems. Nuclear thermionic generators look particularly promising in the 300 to 1000 kw range. In this conversion system, heat is applied to one metal electrode from an energy source such as a nuclear fuel. As the metal temperature increases, electrons are emitted and are captured on a cooler electrode. The difference between the work functions of the electrodes constitutes the energy per electron converted directly from heat to electrical energy. Usually very high emitter temperatures are required (like 3000°F.). A single converter provides about 5-10 watts/cm^2 of emitter surface area, requiring several thousand for a large system. The converters can be connected in a manner similar to solar cells so that failure in one or a group of converters will not shut down the system; therefore, a high degree reliability is possible. In the power range exceeding 1000 kw, nuclear magnetohydrodynamic converters look promising. A simple MHD converter consists of a duct through which gaseous working fluid flows, colls which produce a magnetic field across the duct, and electrodes at the top and bottom of the duct. The gas, by virtue of its motion through the magnetic field, has an EMF generated in it which drives a current throught it, the electrodes, and the external load. The thermionic and MHD conversion systems, with no moving mechanical parts and very high efficiency at large power outputs, appear very promising for future large size space missions.

Photovoltaic Sources

Solar cell arrays have been one of the major sources of power for space systems. There is no doubt that with further technical advancements, the solar array will continue to play an important role in the success of space exploration.

An investigation into new materials could result in several important advancements. The most prominent areas of research should include development of high efficiency cells which are thinner and show less sensitivity to radiation effects and thermal cycling. In the over-all array system, better cell design would tend to improve the life of the system as well as adding to the weight, cost, and reliability factos involved.

In addition to material research, there is much to be learned about the field of array deployment. It is entirely feasible that extremely large photovoltaic arrays ;will someday be used as large power sources for a multitude of different purposes. These systems

may be several orders of magnitude larger in size and power output than that configuration considered for this mission. Consequently, due to the extremely large areas involved, new methods of deployment must be considered. This may lead to such methods as: centrifugal force deployment and support, mounting arrays on an inflatible surface, or array construction in space. Also, a circular deployment configuration would take the greatest advantage of the space used.

Packaging of extremely large arrays will be a large problem. It is more than likely that a thin film roll type array material will be used. Therefore, an analysis of foldable or rollable geometric configurations should be considered in order to take advantage of the flexibility of the system. A method of rolling (or unrolling) a large surface area easily into a small manageable configuration would solve one of the major engineering problems involved with large size photovoltaic systems.

With the use of large arrays, problems will also arise in the support systems. Bussing power over the large distances involved and regulating the large quantities of raw power will present engineering problems that would be a challenge to solve. Careful consideration will have to be paid to such problems as voltage drops and magnetic interference.

With the increasing technology of solid state devices, it may be possible that small instruments may be able to be implanted in certain critical areas of an array to help control operational parameters. It may even be feasible to mount the actual instruments in a particular mission at different points throughout the array. With this system, specific array areas could be designated to supply the power to a specific piece of equipment.

It is apparent that there is a great deal to be learned about the technology of photovoltaic systems. It is also quite reasonable to be sure that such systems will be used for further inter-planetary space missions. Consequently, the new technology and extended research is necessary to keep up with the growing demands for a more powerful and efficient system.

SELECTED REFERENCES

1. Advances in Energy Conversion Engineering, Intersociety Energy Conversion Engineering Conference, New York, American Society of Mechanical Engineers, 1967.

2. Barber, t.a., et. al. "Spacecraft Electric Propulsion-Now?", Astronautics & Aeronautics. June, 1968.

3. Batz, D.R., Kerrisk, D.J. Primary Electric Propulsion Technology-Toward Flight Programs for the Mid-1970's. June, 1968

4. Bernatowicz, D.R., et. al. "Solar and Chemical Power Systems", Space/Aeronautics (Research & Development Issue). Mid 1966.

5. Burnett, J., et. al. "Selected Notes on Solar Power Systems". Electro-Optical Systems pub. July 7, 1967.

6. "Cell Studies Spur Solar Power Advances", Aviation Week. August 25, 1967.

7. Collins, D.H. Batteries. Macmillan Company, New York: 1963.

8. Faget, M.A., Purser, P.E., Smith, N.F. Manned Spacecraft: Engineering Design and Operation. 1965.

9. "Feasibility Study of a 30 Watts Per Pound Roll-Up Solar Array. Report 3." General Electric Company, Missile & Space Division, March, 1968.

10. Hearings before the Committee on Aeronautical and Space Sciences United States Senate. 90th Congress, 1st Session on S. 1296. April, 1967.

11. Holbeck, H. "A Structural View of Solar Array Developments", Advances in Energy Conversion Engineering (ASME Conference Papers). August, 1967.

12. Jasinske, R. High Energy Batteries. Plenum Press, New York: 1967.

13. NASA FACTS. December, 1967.

14. Newstein, J., et. al. "Selected Notes on Space Power Systems". Electro-Optical System pub. Feb. 23, 1965.

15. Pederson, Erik S. Nuclear Energy in Space. Prentice-Hall Inc. Englewood Cliffs, N.J. 1964.

16. Rappaport, P. "Photovoltaic Power", J. Spacecraft. July, 1967. Vol. 4.

17. "Selected Notes of a Solar Power System for Weather Observation", Electro-Optical Systems pub. Feb., 1966.

18. "Selected Notes on Space Power Systems", Electro-Optical Systems pub. Feb., 1965.

19. Shair, R.C., et. al. "A Review of Batteries and Fuel Cells for Space Power Systems", Journal of Spacecraft and Rockets. July, 1967. Vol. 4, No. 7.

20. Shirland, F.A. and Hietenan, J.R. "Thin-Film CdS Solar Cells", Proceedings of the 5th Photovoltaic Specialist Conference, 1965.

21. Snyder, Nathan W. Energy Conversion for Space Power. Vol. 3. Academic Press, New York: 1961.

22. Snyder, Nathan W. Space Power Systems, Vol. 4. Sept., 1960.

23. "Voyager Spacecraft Final Technical Report", Vol. A. Boeing Co. Pub. (Prepared for JPL under contract No. 951111). July, 1965.

24. Ibid., Vol. B.

25. "Voyager Spacecraft System Preliminary Design", General Electric pub. Vol. F. July 30, 1968

26. Weiner, H. "Solar Cell/Battery Power Systems For Advance Applications", Advances in Energy Conversion Engineering. (ASME Conference Papers). August, 1967.

APPENDIX C: COMMUNICATIONS

COMMUNICATIONS
TABLE OF CONTENTS

TABLE OF CONTENTS CONT'D

MEMORY

An important part of the communication facilities on board the spacecraft is the storage capability. During periods of occultation, data from the scientific experiments must be stored on board to be transmitted back to earth at a later time. Several types of storage systems were considered for this mission. They were: photographic film, magnetic tape, and thin-film magnetic core.

Photographic data processing such as used by Surveyor and Orbiter, allows high resolution pictures to be transmitted at a convenient data rate. This is possible since no digitation occurs until the actual transmission of the picture. The main disadvantage of such a system is its non-reusability. To carry enough film for a two year mission might be very impractical.

Magnetic tape is a commonly used system. Tape is reliable, reusable, and is now space-qualified. The main disadvantage with magnetic tape is the data rate. The output from the multi-spectral camera and high-resolution television experiments will be on the order of 10^7 bits per second. The maximum packing density of information on a tape is 10^3 bits/in. Assuming 100 ips tape speed, the result is 10^5 bits/sec. A data rate of 10^5 bits/sec would be compatible with a microwave communication system, but could not keep up with a 10^7 bit/sec laser system. Another disadvantage of a tape storage system is mechanical vibration. Since the laser down-link contemplated for this mission requires a platform stable to within 10^{-6} radian, extreme care would be needed to keep a 100 ips tape transport from introducing pointing inaccuracies.

Finally there is the magnetic core, or thin-film type of memory. The main advantages of this type of memory are high speed (10^7 bits/sec is common) and the absence of moving parts. Disadvantages are large power and space requirements. Also this type of memory is volatile (the information is stored only while power is supplied). Even so, this seems like the best memory for the high-speed "data dump" system proposed for this mission.

Typical size for a thin-film memory element is about 0.01 in. square by 10^{-5} in. thick. Allowing for spacing between elements, a memory could easily be constructed with 50 elements per inch. Using this as a basis for calculations, a 2 megabit (250,000 data points, 8 bits/data point) memory would require 10"x10"x1". It would consist of 8 memory planes with a 500x500 grid in each plane. Allowing for connections and the transistor drivers necessary to actuate the memory, one frame would occupy 1 cu. ft. Most of this space is driver, so by proper selection of ground returns, many 1" thick memory banks would require little extra space. The thin-film elements require 750 ma. to switch them, so, allowing for amplifier and driver inefficiencies, a 20 megabit memory would draw approximately 20 watts at about 10 volts. It would occupy 2 cu. ft. A similar (2 megabit) memory could be used for command decoding and data compression. It would require an additional 1 cu. ft. and an additional 20 watts.

MODULATION AND CODING

In choosing a modulation and coding system, many factors must be taken into account, such as information rate, distance, power, allowable error and noise. Analog systems have a distinct disadvantage in two areas: high error probabilities due to background noise, and higher power requirements for a given amount of information. Digital systems have one disadvantage but several major advantages. The disadvantage is the necessity of very complex electronic encoding equipment. The advantages include error detecting and correcting techniques, as well as time multiplexing for high transmission rates and time-sharing techniques.

Of the possible digital systems (PAM, PDM, PFM, PPM, FSK, PSK, PCM), PCM (Pulse Code Modulation) has an advantage for our mission due to its low power level at high bit rates on the down-link and the fact that PCM approaches the theoretical limit in exchange of bandwidth for signal to noise ratio.

Since video requirements dominate the down-link with 10^7 bits per second and there will be 64 levels of intensity, a 6 bit PCM system could be used ($2^6 = 64$) to quantize the video information and transmit it.

Three methods of PCM have been suggested:

PCM/CW would involve switching a gallium arsenide laser on and off corresponding to a zero or a one in the binary system. This method has a distinct power advantage in that the 100 watts developed by the laser is transmitted directly without being partially absorbed by optical equipment. However, it is possible that a fading in the intensity of a "one" due to noise or interference might be interpreted as a zero at the receiver. This would be especially true if it was decided to go through the atmosphere.

PCM/LPL (linear polarized light) involves changing the direction of polarization by 90 degrees and assigning a value of one to the first polarization and zero to the other. This method will not be described in detail for two reasons: First, the effects of the sun's magnetic field or the earth's atmosphere could rotate the two 90° vectors and cause errors. Secondly, the only difference between this system and the system to be described is that this system has neither a quarter wave plate at the receiver nor the same voltages on the Pockel or Kerr Cell. There is also a negligible loss of power through a ¼-wave plate.[9]

PCM/CPL (circularly polarized light) appears very promising, especially if it is decided to go through the Earth's atmosphere. Any continuous wave laser could be used and the only loss at the transmitter (assuming the laser can be built to put out linear polarized light using Brewster windows) would be less than 15% in the electro-optic modulator. At the receiver, however, there would be a small loss in the Rochon prism or Wollenstat prism. Basically, linear polarized light from the polarized laser or non-polarized laser plus polarizer

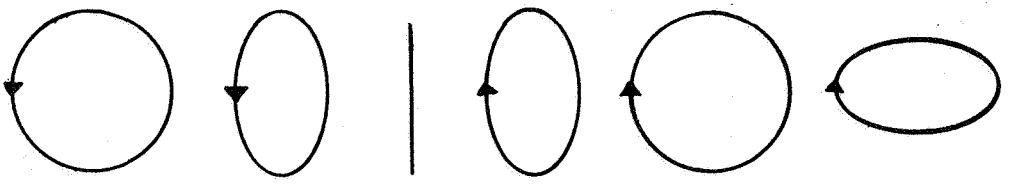

a "one" a "zero"

Figure One Circular Polarized Light

would be beamed into an electro-optical modulator having a voltage impressed accross it such that the birefringent medium has a fast and slow axis at 90° with respect to each other (fast refers to relative index of refraction). Since the LPL can be divided into two orthogonal components, one of these will be delayed. When the components are recombined at the output, circular polarized light results. As the voltage is linearly increased, the output will look as shown in Figure One.[9, 16]

Thus for two particular voltages, we can get out CPL in either one direction or the other, corresponding to a zero or a one. The advantages are obvious; errors in direction of polarization would be very difficult to make and the absence of a signal would indicate trouble, not a binary zero. The faulty data could be sent again with no loss of information.

At the receiving end, the CPL is collected and passed through a quarter wave plate, which converts it to orthogonal LPL. This is then passed through a Rochon or Wollenstat prism which changes the angle of the output beam according to its polarization. These separate beams are aimed at photo multipliers which are fed into a difference amplifier, giving a binary output.[16]

In Table One, a distance of 50 million miles was assumed. Powers for other distances can be obtained from the following chart. MDSV stands for "Manned Deep Space Vehicle." Figure Four shows a possible system organization for PCM/PCL.

Coding

Coding can be thought of as the processing that lies between the data sources and the modulator. This includes analog to digital conversion, time multiplexing, data compression and mode switching. All of the above, except data compression, have been fairly well formulated and the systems used on the Mariner projects would suffice with no major changes. There is, however, a new method of data compression yielding compression ratios as high as 20:1, called Time Buffered Coarse Fine Video data compression. Using six-bit PCM, compression ratios of about 6:1 are typical. Basically, this method

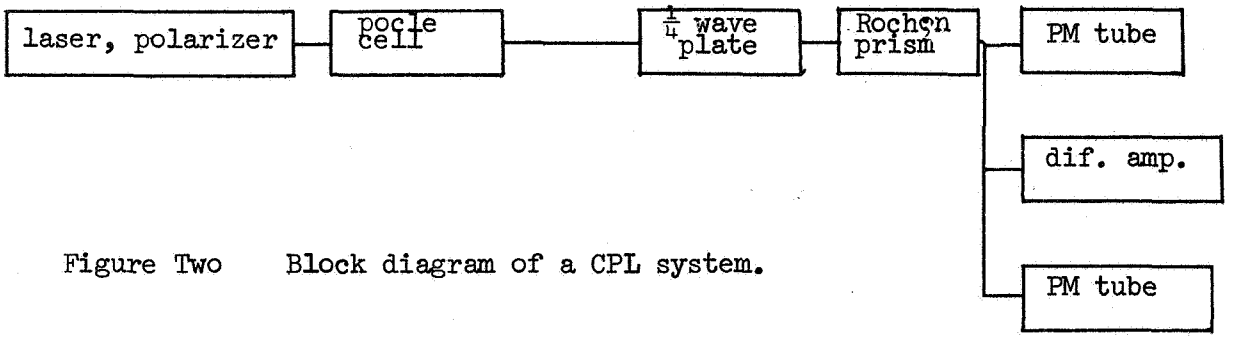

Figure Two Block diagram of a CPL system.

Table c-1
Modulation Systems

Data rate	Modulation	Earth Transmitter / MDSV Receiver	MDSV Transmitter / Earth Receiver
30 k bits/sec	PPM	5.4×10^{-3} watts	1.0×10^{-3}
	PCM/PL	2.5×10^{-1} "	7.1×10^{-2}
	Coherent FSK	2.3×10^{-1} "	2.3×10^{-2}
50 M bits/sec	PCM/PL	80	11
	Coherent FSK	340	34
		Satellite Transmitter / MDSV Receiver	MDSV Transmitter / Satellite Receiver
30 k bits/sec	PPM	5.4×10^{-3} watts	4.0×10^{-2}
	PCM/PL	2.5×10^{-1} "	3.2×10^{-2}
	Coherent FSK	2.3×10^{-1} "	2.3×10^{-1}
50 M bits/sec	PCM/PL	80	65
	Coherent FSK	340	340

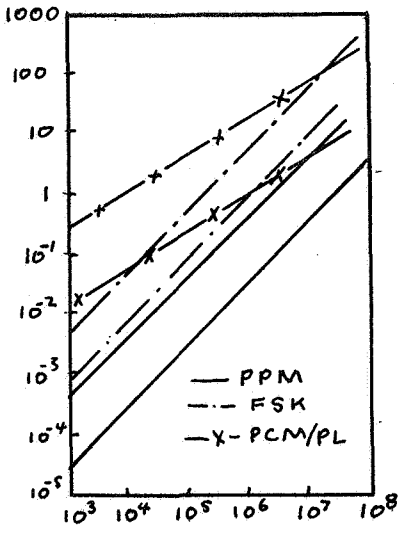

Figure c-3

MDSV Transmitter Powers

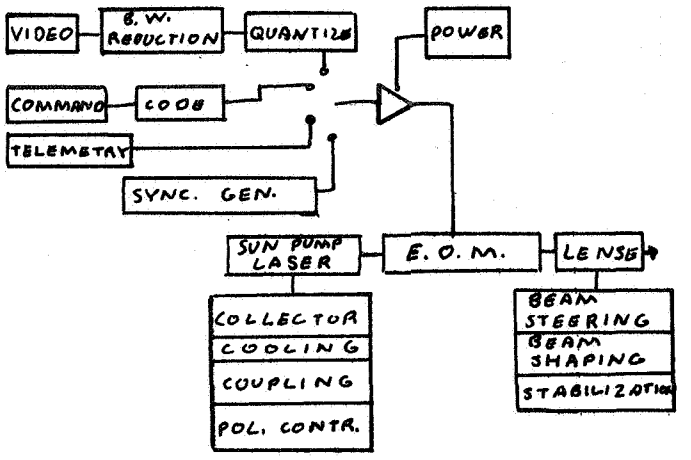

Figure c-4

MDSV PCM/PL Transmitter

lowers redundancy of data caused by large picture areas of the same shade by going into a run light level after two redundant element information words. An important part of the time-buffered compressor is the coarse-fine system, which is a non-time buffering technique that gives a 2:1 compression ratio and provides high accuracy. For most pictures, about 85% of the elements are accurate to 6 bits while the rest are only to three bits at the intensity edges. Either the three most significant or the three least significant bits are transmitted, depending on the amplitude and speed of swing of the information. An interword coding method is used in order to tell the receiver the coarse-fine status changes. The large number of fine levels in a typical CF coded video signal suggests the use of a redundancy removal method operating within the CF code but just on the fine elements. The transmitter contains hardware to define and recognize redundant element occurrences. The occurrence and number of element removals in the processed data stream is conveyed in the stream to the receiving decoder.

TRANSMITTERS

A number of different types of lasers were originally considered for the downlink. Due to efficiency and information carrying potential, the selection was reduced to three possible types: argon, carbon dioxide, and gallium arsenide.

Although some very distinct advantages are to be had at 0.5 microns (argon), the argon laser's very low efficiency of 0.1% eliminated consideration for its use as a downlink. This leaves CO_2 and GaAs for consideration.

The CO_2 laser boasts relatively high efficiency and an atmosphere "window" making it a reasonable choice for use as a downlink. Although the beamwidth obtainable with reasonably sized optics (1 meter parabolic reflector) is fairly broad, being on the order of 13 microradians, the high output power obtainable (i.e. 100 watts or more) tends to compensate for the divergence loss. Carbon dioxide's wave length of 10.6 microns suffers little atmospheric absorption (see Figure 5) and thus could be received on earth. A signal at 10.6 microns, however, offers a detection problem. Due to the low energy of a photon at this frequency, photomultiplier tubes cannot be utilized, since their operation involves overcoming a work function. Noise considerations tend to eliminate semiconductor devices, leaving only coherent heterodyne detection as an alternative. Since a laser beam passing through the earth's atmosphere tends to lose spatial coherency at the receiver, this means of detection cannot be used in practice as long as the receiver is located in the atmosphere. Thus, one would be forced to receive the signal from a position in space. Even then, the resulting Doppler shift would necessitate a very complex AFC (automatic frequency control) circuit at the receiver or a very wide I.F. bandwidth.

The gallium arsenide laser, operating at 0.86 microns, has high efficiency but is readily absorbed upon passing through the atmosphere, forcing it to also be received in space. Due to gallium arsenide's much shorter wavelength, much tighter collimation is obtainable than with CO_2, 2.8 microradians being representative for a one foot, difraction limited reflector. And, although marginal, 0.86 microns can be received using direct, noncoherent detection through the use of a photomultiplier tube. This allows very simple and effective detection schemes.

GaAs lasers are also very easy to modulate. Whereas a CO_2 laser would require an external electro-optic modulator, an injection laser can be modulated internally by verying the input current in the proper fashion. Therefore, an on-off, PCM-type modulation is readily obtainable by switching the input current on and off by suitable means, such as with a transistor or silicon controlled rectifier.

A program was run to calculate the effects of wavelength and range upon beam divergence and resulting spreading loss. It was decided that one foot and one meter berillium parabolic reflectors could be

Table c-2 Charateristics For GaAs And CO_2 By The Mid 1970's

	GaAs	CO_2
Laser Efficiency	40%	10%
Wavelenght	0.86 microns	10.6 microns
Detection	direct, noncoherent	heterodyne, coherent
Atmospheric Effect	absorption	coherency loss
Modulation Losses	0%	65%
Modulator	internal	external
Peak Output	100 watts	100 watts
Cooling	100 watts	100 watts
Raw Power Input	250 watts	3000 watts

used for GaAs amd CO_2 lasers respectively, since closer tolerances would be required for a difraction limited GaAs system than for CO_2. The results of this computation show that up to 13 dB gain can be obtained through the use of gallium arsenide and its resulting narrow beamwidth.

As can be seen in Table 2, both lasers require reception from outside the earth's atmosphere to realize their full advantages. The gallium arsenide laser, assuming present multimode operation is overcome, requires smaller optics, has higher overall efficiency, uses simpler detection techniques, and is easier to modulate than the carbon dioxide laser system. For this reason it was decided to concentrate on the development of a gallium arsenide downlink for the mission.

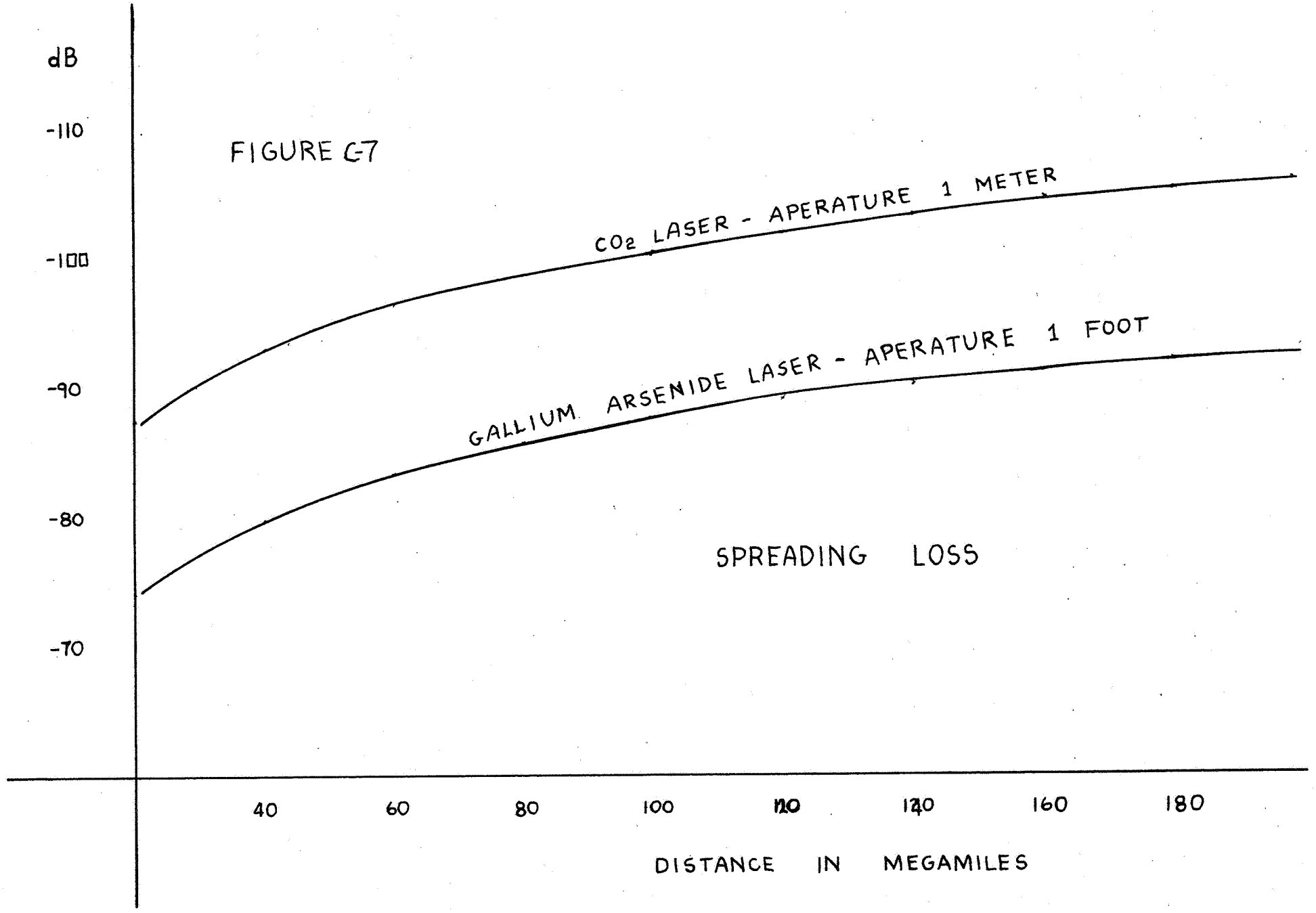
dB
-110
-100
-90
-80
-70
FIGURE G-7
CO2 LASER - APERATURE 1 METER
GALLIUM ARSENIDE LASER - APERATURE 1 FOOT
SPREADING LOSS
40
60
80
100
120
140
160
180
DISTANCE IN MEGAMILES

TRANSMITTER

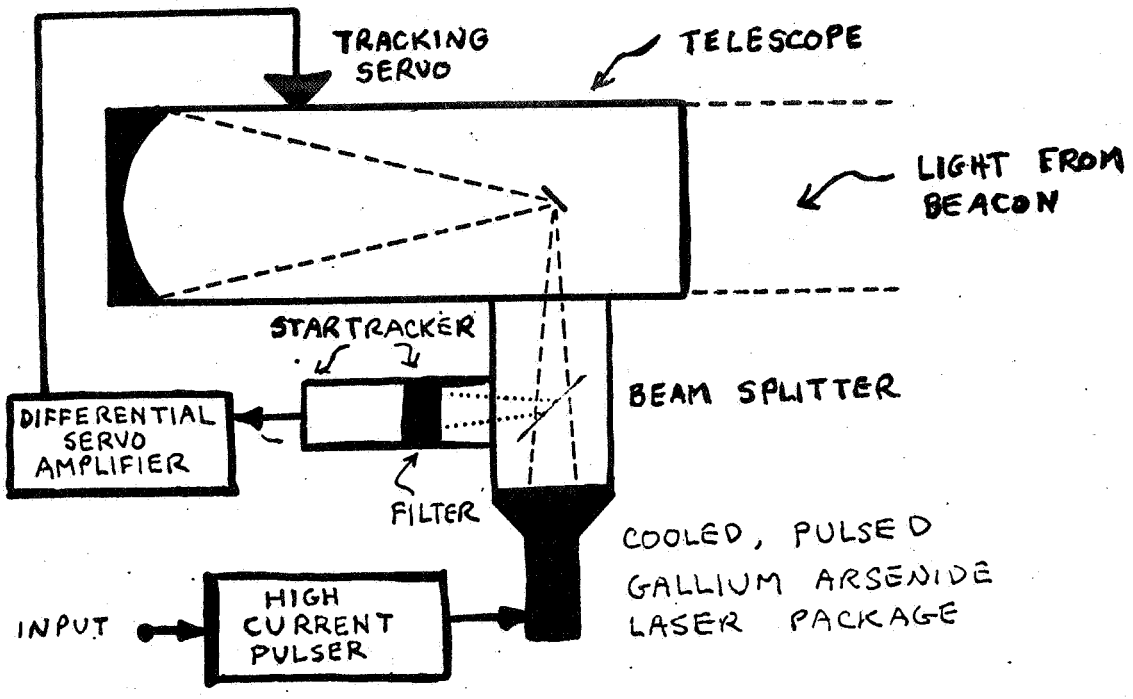

RECEIVER

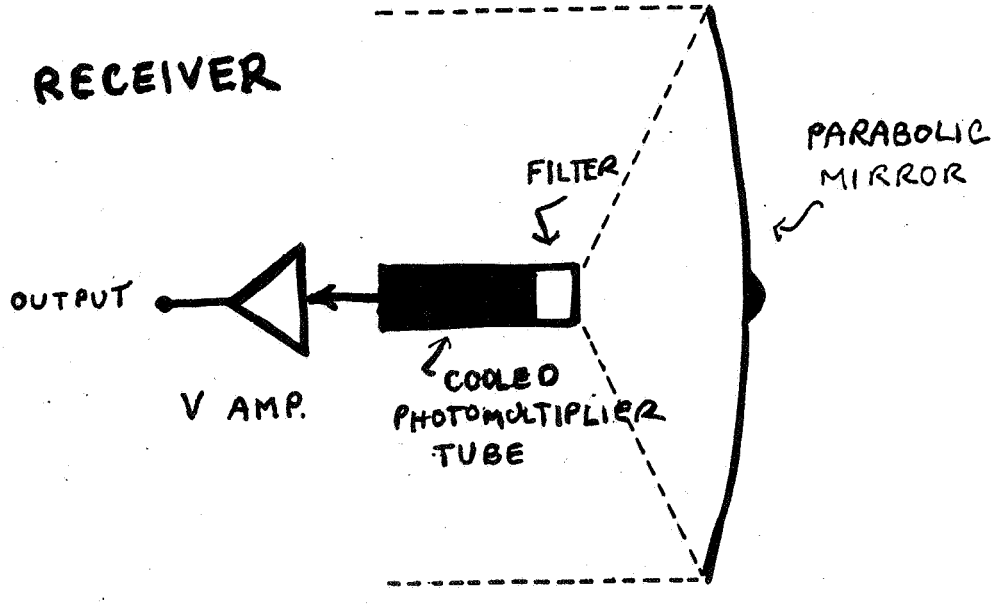

MODULATORS

Of the many types of light modulators to be discussed later in this section, the modulator chosen in this study, and also the modulator that has received the most attention for laser work, is the electro-optic modulator. In our study, a KDP (potassium dihydrogen phosphate) crystal was chosen for reasons which will be given later in this report.

In a typical electro-optic crystal (KDP) the application of an electric field causes a change in the refractive index. This change is proportional to the first power of the applied voltage; this is also one of the prime advantages of KDP modulators. An increase in the refractive index causes light to travel more slowly while a decrease causes light to travel faster. Since, with a change in the velocity of light, there is a corresponding change in phase, an electro-optic modulator is actually a phase modulator. The light is converted to amplitude modulated light by running it through a polarizer which is at 45 degrees with respect to the applied electric field.

A second type of modulator which was under study by our group is the magneto-optic or Faraday-effect modulator. The Faraday effect causes a rotation in the plane of polarization of light as it moves through a substance. The rotation is in a direction that is parallel to an applied magnetic field. The amount of rotation is directly proportional to the size of the applied magnetic field.[18] An effective modulator of this type requires a material that has a large rotation of polarization as a function of magnetic field. Since no very effective material is presently at hand, this modulator was not chosen for further development. Also, limitations in thickness and heating problems make this technique impractical. If used, the resulting change in plane angle could be converted to an A.M. signal by again passing the beam through a polarizer.

A third modulator of interest was that of the gallium phosphide diode. Modulation takes place in the diode's p-n junction, which is relatively small. Since our power considerations involve approximately 100 watts, and the diode's junction is of such a small size, this modulator cannot be used due to the extremely high power densites involved.

All forms of modulation mentioned thus far have been external systems. But one of the simplest and most direct methods of modulation involves direct "pumping" of the laser oscillator. This can be accomplished in a GaAs laser by turning its power source on and off. If a CO_2 laser is used, "pumping" can be obtained by switching the laser's r-f source. If a KDP modulator with a GaAs laser will be chosen, power requirements could be cut in half, efficiencies raised, and heat dissipation problems reduced, if the GaAs laser is pumped to give a transmission of all "ones". "Zeroes" could be formed by stopping transmission of "ones" with the KDP modulator.

As was stated earlier, for a KDP electro-optic light modulator (EOLM), the change in refractive index is proportional to the first power of the applied voltage. This difference in refractive index,

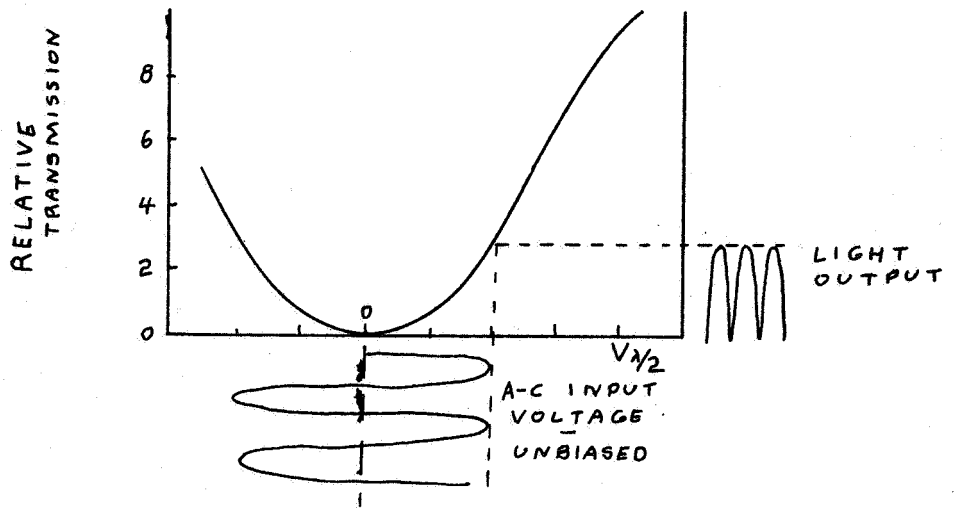

Figure c-5 Characteristics Of An Unbiased EOIM.

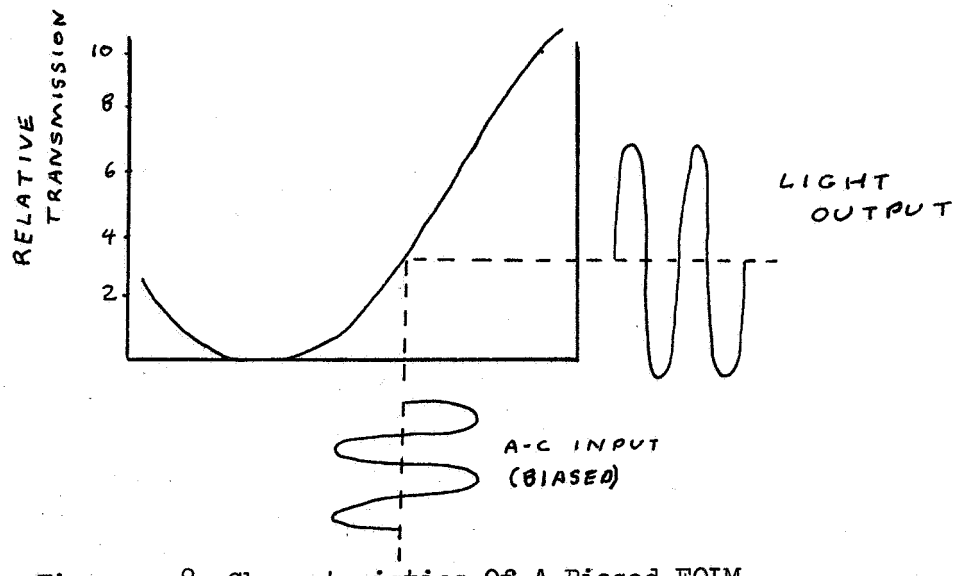

Figure c-8 Characteristics Of A Biased EOIM.

usually called birefringence, is given by

$$B = n_o^3 r_{63} E$$

where

n_o = ordinary index of refraction of the crystal

E = electric field in volts

r_{63} = constant describing Pockels effect

One problem with a KDP modulator is the fact that even though the refractive index is a linear function of applied voltage, the relative

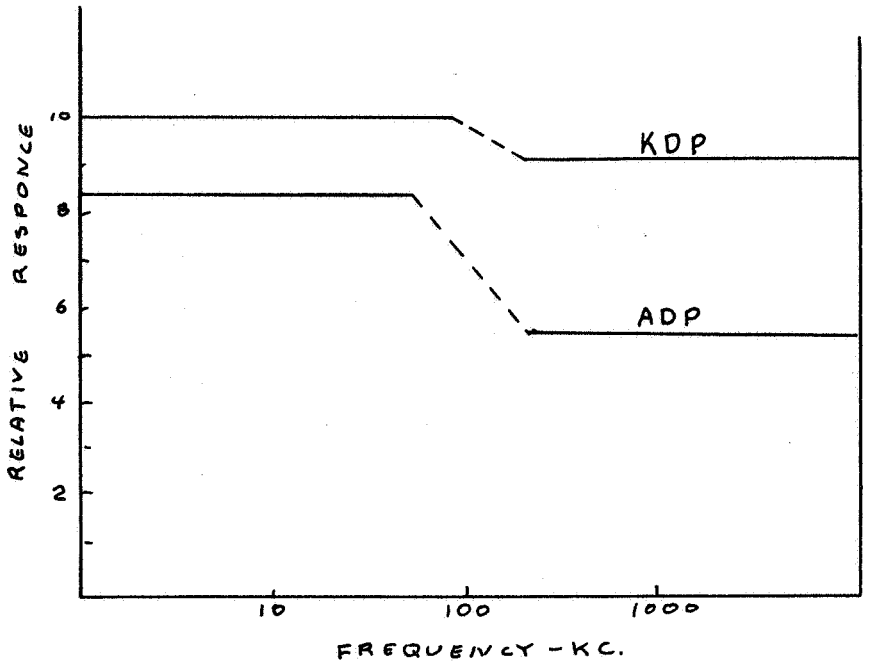

Figure c-10 Relative Response Of A KDP Modulator.

Table c-3 KDP Modulator Statistics

Transmission	.85	.85	.85	.85
Capacitance	40	10	10	10
Loss Tangent	.05	.05	.05	.05
$V_{\pi/2}$	8000	9000	9000	9000
Optical Attenuation	.1	.3	1.0	2.0
3 db. Bandwidth	4	10	5	100
Modulation power (w)	2.5	13	4	11
Weight (lb)	?	21	151	251
Size (in^3)	?	30	85	25

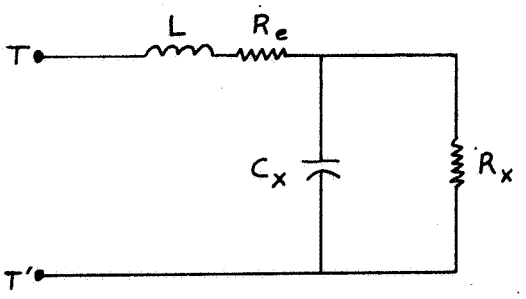

Figure c-9 Equivalent EOLM Circuit

transmission is only linear in a finite region. The relative transmission of a standard ELOM is given by:

$$T = \sin^2(\pi V)/(2V_{\lambda/2})$$

where

V = applied voltage

$V_{\lambda/2}$ = voltage for half-wave retardation

The transmission characteristics of unbiased and biased modulator units are shown in Figures 5 and 8. Only when biased to the half-wave retardation point $V_{\lambda/2}$, can a linear output be expected.

In the frequency range of 10^7 Hz., which is the modulation frequency we are proposing, the equivalent circuit for a EOLM is as shown in Figure 9, where:

T-T' = modulation terminals

L = lead capacitance

R_e = resistance in electrodes

C_x = KDP crystal capacitance

R_x = KDP internal resistance

From the previous circuit, the power dissipated in a KDP crystal can be found from:

$$P = V^2(2\pi f)C_x \tan\theta$$

where

V = applied voltage (rms)

f = frequency

$\tan\theta$ = loss tangent

The frequency response of a KDP modulator is shown in Figure 10. This is for a biased signal and one within the linear modulation of the KDP crystal.

Table 3 shows four KDP modulators that have been studied in this report. Values are typical of most KDP crystals made as of June 1966.

STABILIZATION

In order for a laser system to even be mentioned as a means of communication, and in order to fully utilize the narrow beamwidth of a laser, a very stable tracking network must be employed. Before going into a system of tracking to hold a laser beam within ±1/10 arc second, it will be assumed that a sun-canopus system can hold the ship within a ± 1 degree filed of view of the earth. The system described in this section for use by the communications group, has been designed by Perkin-Elmer for NASA and can be found in contract NASA-cr-252; "Determination of Optical Technology Experiments for a Satellite."

For this system, a CO_2 or Argon laser beacon from earth will be aimed at the satellite. CO_2 and Argon have been chosen since at both of these laser frequencies there are partial "windows" in the earth's atmosphere. The choice between these lasers has not been made in this report since the one with greatest c.w. power output should be used, without regard to efficiency.

Assuming the ship is oriented to within one degree of earth, light will enter the telescope and be reflected toward a four corner prism by the beamsplitter. Within one degree of earth, but not within 1/10th arc-second, the light will reflect off the four corner prism and on to the photomultipliers spaced around the prism. Since the light does not get broken evenly over all four surfaces of the prism, unless it is perfectly centered, the photomultipliers will generate unequal signal strengths which are then passed to the four-quadrant detector. This detector then senses the weaker and/or greater signals and sends the necessary commands to the very fine pointing subsystem for realignment of the telescope lens.

One fundamental problem that can be solved with additional equipment, but has not been discussed up to now, is that of "point-ahead" communications. As seen in Figure 12, if the laser signal is sent directly back to where the beacon is seen, the earth will be missed by 16,000 miles due to the relative motions and time lags involved. t_1 is the time a particular bundle of photons will leave the earth. At t_2 this bundle will arrive at the orbiter and at the same time, a signal is sent back to earth. With no point ahead angle, the signal will arrive at point A even though the earth has moved on to point t_3. The lead angle is given by:

$$\theta_L = S/R - a$$

where "a" is the aberration angle. Since the point ahead angle varies slowly with time, adjustments can be controlled by means of a small on board computer, or by signals from earth.

Perkin-Elmer's design was given to NASA in 1965, and it was assumed that it will be perfected by 1975.

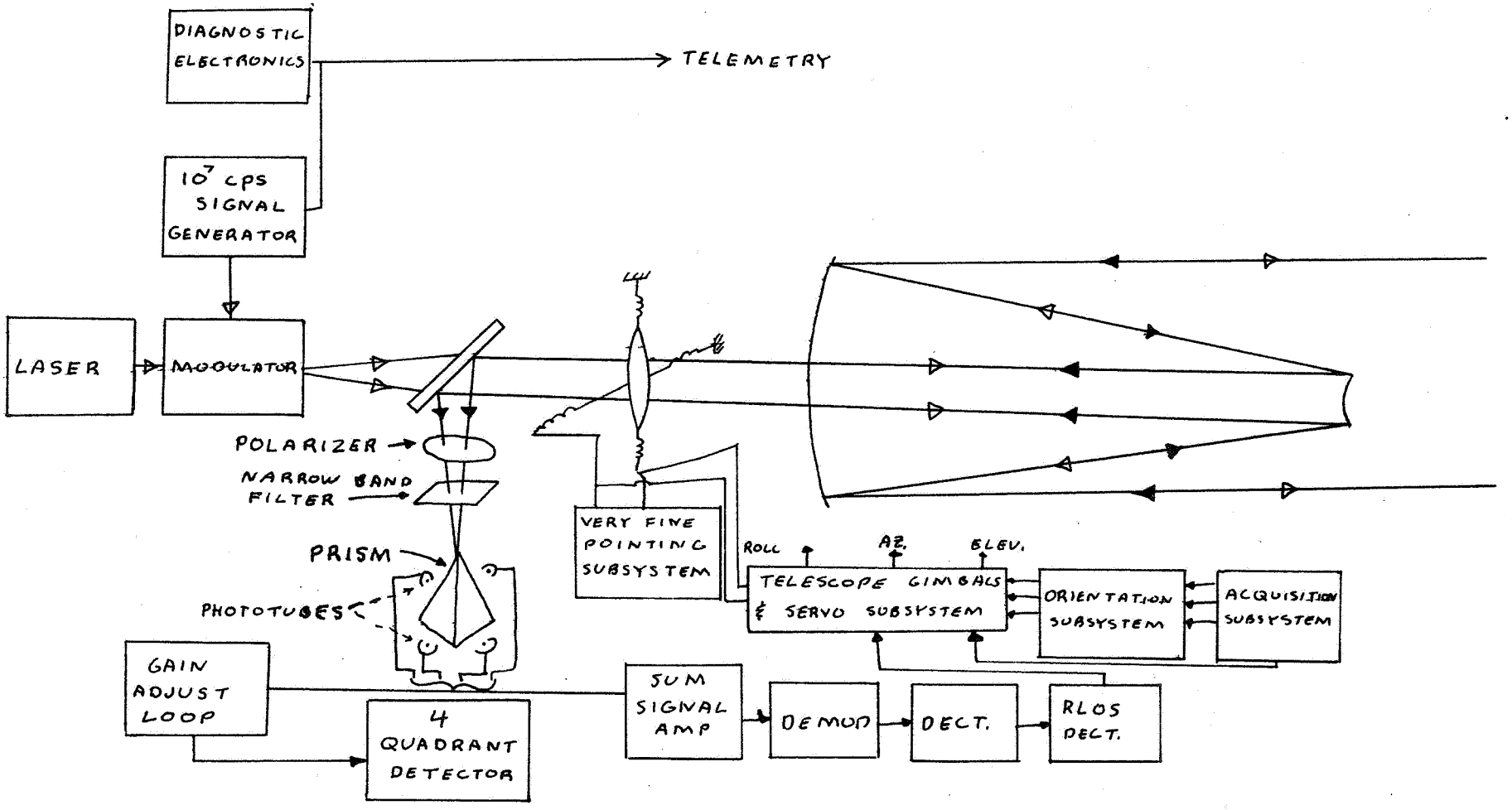

Figure c-11 1/10 Arc Second Earth Tracking System.

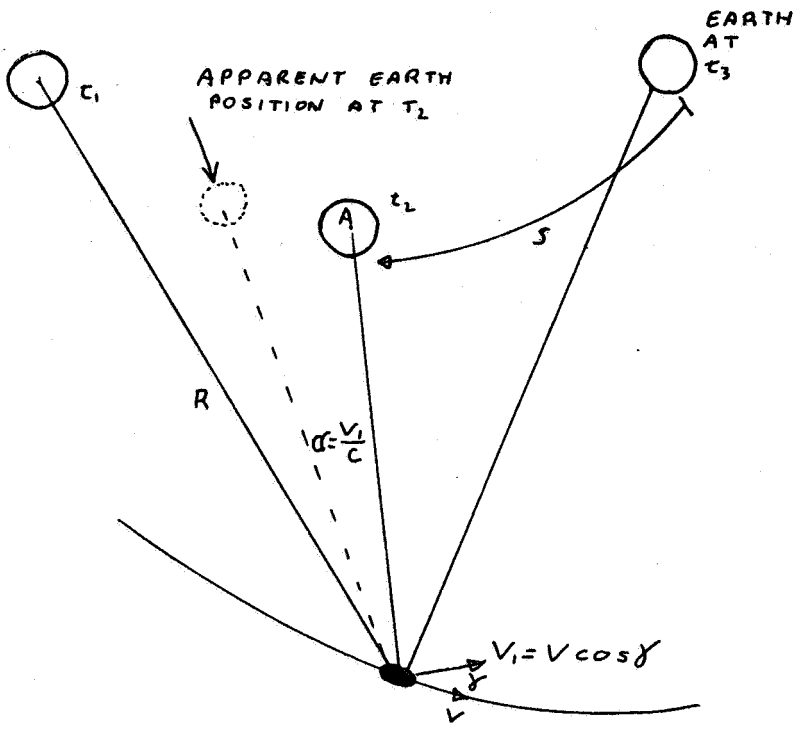

Figure c-12 Earth Position As A Function Of Time.

OPTICAL RECEIVER AND LASER POWER

The receiving system is assumed to be on the Moon or on an orbiting satellite. This eliminates the atmospheric effects on the laser beam and, using suitable station locations, can provide continuous, weather-independent communications. A microwave link could relay the information via standard S-band channels to any of the many proposed or existing earth receiving stations. The pointing requirements necessary for the antennae (approximately one microradian) are compatible with the tolerances on the Orbiting Astronomical Observation Satellites that are to be launced soon.

Since the required transmitter power is inversely proportional to the receiver effective area, a reduction in the required transmitter power can be obtained by increasing the receiver antenna. (A limit is reached where machining tolerances and nonlinearities take over). But a real reduction in the calculated power can be made. The assumed receiver aperture is that considered to be the maximum size presently feasible on a satellite. If the station is on the Moon, probably the aperture can be increased. A rough guess would be that the required transmitter power could be cut by fifty-percent at least -to 85 watts, which is close to the projected figures for a cryogenlly cooled, pulsed GaAs Laser.

Optical Receiving Systems

Optical detection systems are generally considered in three categories:[6] a) Heterodyne, b) Carrier-Frequency Preamplification, c). Direct Detection. The first two systems rely on the coherence of the incoming signal and, therefore, nothing in the system (including the transmitting medium) may significantly alter the coherence of the beam if proper operation is to be obtained. A heterodyne receiver mixes a strong local oscillator (LO) laser at a frequency near the signal frequency with the incoming signal. Hopefull, this photomixing will bring the output (IF) signal above the internal noise, while the LO shot noise maska the background noise. See Figure 1.[6] In carrier-frequency preamplification, an optical preamplifier, with a gain high enough to make noise introduced in detection negligible, is placed before the detection stages. Although preamplifiers are in principle possible, low-noise optical preamplifiers are not presently available. By far the simplest of the three systems in principle are the direct detection or incoherent devices. They respond directly to intensity variations in the incident light; they are photon counters. See Figure 2.

Ideally, the optical heterodyne receiver has a 3 db S/N advantage over a direct detector,[12] but there are also several disadvantages and unresolved problems.[11] There is a requirement for alignment of the received and LO beams within an angle $d\theta \leq \frac{L}{A_r}$ where $d\theta$ is the alignment angle, L is the wavelength and A_r is the receiver aperture. The LO power must be several orders of magnitude greater than the signal (microwatts vs. picowatts) and great care must be taken to prevent masking of the original signal. The LO instabilities and Doppler shift necessitate

very close frequency and power tolerances on the LO. The one-way Doppler shift has been shown to be .50 to 2.7 ($\times 10^{-5}$) microns in wavelength,[11] this limits the predetection filtering to 1 Angstrom bandwidth.[11] However, much research is being done on optical heterodyne receivers and a very practical 10.6u receiver is advertised in the literature. At the present time, the optical heterodyne receiver is the only practical system for the CO_2 gas laser at 10.6 microns, and there are doubts that a quanta limited direct detector will ever be available. Because of the problems of the heterodyne receiver and the antennae systems the CO_2 laser presently offers many problems in detection.

It has been shown that as the bandwidth and signal to noise ratio are increased, ideal signal-shot-noise operation is increasingly possible with direct detection.[12] It is shown in the power calculations that our system approaches (within an order of magnitude) "noise-in-signal" operation. This considerably lessens the appeal of optical heterodyne systems. It is for this reason, and for those of simplicity and proven reliability, that this group has chosen a direct detection system (at the higher frequencies, not CO_2).

It is often convenient[6] to consider the generalized detector operation as a three-step process. See Figure 3. In the first step, free carriers are created by the incident light; in the second step, these carriers are multiplied by a current-gain mechanism; and finally, the amplified current interacts with external circuitry to provide an output signal.

A great concern in any detection process is the amount of "noise" present. There are four general types of noise present in an optical system. 1. Quantum, or shot, noise is due to the quantum nature of light. It is explained in two ways: a. The probability of intercepting a photon (or the radiation field intensity) is proportional to the product of its amplitude vector and its complex conjugate ($\bar{A}\bar{A}^*$). Therefore, even if the received radiation is a coherent monochromatic wave of constant power, photons will still be received randomly, leading to noise. b. The Heisenberg Uncertainty Principle states that (Energy uncertainty) (Impingement time uncertainty) $\geq h/4\pi$. Therefore, the more precisely the photon energy is known, the less precisely the time of arrival can be determined. It is this uncertainty in time of arrival that contributes to the quantum moise.[11] 2. Flicker noise, or 1/f noise, is noise whose mechanism of modulation is unknown but is believed to have something to do with the recombination of the carriers in semiconductors. It has an approximate 1/f power density spectrum, and, due to the extremely high f associated with a laser, most authors ignore it. 3. Thermal noise is due to thermal agitation of the molecules or electric charge in the equivalent resistance (circuit elements). 4. Other noise is due to nonlinearities of the amplifier and perturbations of the system. Excess sho noise is quantum noise introduced either by the secondary-emissive nature of the multiplication dynodes, or the action of current carriers in a semiconductor device.

The above factors are specifically the "noise" terms in the detector. However, a great many factors contribute to the "signal-to-noise ratio" in any space communications system. Each process, from the photons

from Mars impinging on the camer lens, to the reproduction of the picture at the receiving station, changes the "S/N". Because of the limitations of this analysis, certain assumptions must be made. We assume the "signal" to be the encoded PCM pulses from the laser. Therefore, the "S/N" from the camera and data mechanisms is very high. The "signal" for the camera system would be photons from the section of Mars observed. (For our desired accuracy this is true. It has been shown that for 1^{0} resolution in infrared in a bank of clouds of approximately 200^{0}K, the S/N is better than 50 db)[10]. The encoding must, by design, be a faithful (low noise) reproduction of the original analogue signal. The modulator, or pulsing circuits, are assumed to add negligible noise.[14]

Considerable time and effort has been devoted to analysis of S/N for optical systems. Almost universally, a common equation is obtained (barring nomenclature differences), and the authors then attempt to eliminate terms by considering limiting cases)i.e. quantum limited, background limited, thermal limited, etc.). The author finds it difficult to determine offhand the limitations of our system. Therefore, we will consider the overall effects and then compare this result with the ideal, quantum limited case to see, if indeed, the system approaches the best limited case.

Presently, for large bandwidth, high-speed optical systems, there are three detectors available: the multiplier traveling-wave phototube (MTWP), the static crossed-field photomultiplier (SCFPM), and the silicon avalanche photodiode (APD). These devices were chosen as representing the present state-of-the-art.

The MTWP is a combination of three or four secondary-emissive surfaces with a helical output coupler. The main advantage of the MTWP is that relatively low multiplication is required to have a high $M^{2}R_{eq}$ (figure of merit) because of the very high equivalent resistance of a helix. This means that the dynamic range is large and the frequency maximum is greater than other devices. However, the MTWP is a passband detector with typical passbands of 1-4GHz. The MTWP finds the most use in optical heterodyne receivers. See Figure 4.

The SCFPM uses an arrangement of static electric and magnetic fields to make all secondary electrons emitted from rest follow congruent paths from one dynode to the next until reaching the output coupler. See Figure 5. The SCFPM is in an advanced state of development, and seems to be developable into a highly reliable, quantum limited, gigahertz bandwidth detector. Unlike the MTWP, the SCFPM is capable of receiving pulsed signals (PCM) without a subcarrier.

The silicon avalanche photodiode is the most promising solid-state detector presently available. See Figure 6. It uses impact ionization of the signal semiconductor with the carriers in the high field region of a reverse-biased p-n junction to achieve breakdown, or avalance operation. Control of this avalanche to produce useful current gain is primarily a problem of eliminating impurities in the junction region,

a similar problem to that which faced early transistor technology, and development of better fabrication techniques may make the APD a very useful detector for a system like ours. Because of the excessive noise in external amplifiers, a lack of definite parameters for our system, and the complexity of analysing the sensitivity of a photo avalanche detector, we have chosen to use a static crossed-field photomultiplier in our receiver. An attempt is made to look at the relative performance of the APD. See Figure 7.

Power Calculations for a GaAs Laser at .87u using a S-25 SCFPM

Assumptions and parameters for the system:

1) A S-25 photoemissive surface with a quantum efficiency (n) of 1% and a dark current $I_d = I_{d\,S\text{-}20} = 10^{-9}$ amps at the anode is used with a static crossed-field photomultiplier with the following figures of merit: $M^2 R_{eq} \triangleq 10^{12}$, F=1.3, and T≐ 50°K. The first two values are current experimentally measured values, and the last is approximately the system temperature in present S-band microwave systems, and can be reached optically by cooling the receiver and using advanced SCFPM tubes.

2) The system noise is assumed additive (not multiplicative), and Gaussian, so standard signal to noise ratio (S/N) techniques can be used. The overall S/N required is determined for a given uncorrelated received error rate.[8,9] We choose a S/N of 20 db for less than 10^{-6} probability of error. (Less than one error a second at a transmission rate of 10^7 bits/sec if the error checked at the receiver).[14]

3) The antenna and optical parameters are:
transmitter aperature (A_t)= 36cm, receiver aperature (A_r)=200cm, receiver field of view (Ω) 10^{-4} steradian.

4) The worst case of the background spectral density occurs when both Mars and Jupiter are in the field of view. $\mathbb{I} = 10^{-11}$ watts/cm^2-str-μ. The required signal-to-noise ratio is given by:

$$S/N = \frac{\frac{1}{2}m^2 I_s^2 M^2 R_{eq}}{2eBFM^2 R_{eq}(I_s + I_b + I_d) + kTB}$$

For convenience we define:

$$a = \frac{P_s}{P_t} \qquad b = \frac{n}{2hfF} \qquad y = B(S/N)$$

In our case:

$a = 4.65 \times 10^{16}$ unitless
$b = 5.85 \times 10^{16}$ joules
$y = 10^9$ hertz

m= modulation index
$I_s I_b I_d$= signal, background & dark currents at cathode
M= multiplication
R_{eq}= Equivalent resistance
F= excess noise factor
e= electronic charge
B= bandwidth
k= Boltzmann's constant
T= absolute temperature
n= quantum efficiency
f= frequency
h= Planck's constant
P_s= received signal power
P_t= transmitted power

The above formula assumes that the photo-mixing of the background and signal is negligible--a condition that is true if $\frac{\mathbb{I}L^2}{2}(10^{-23})$ is much less than $\frac{hf}{n}$ (10^{-16}).

Solving for the required transmitter power:

$$P_t = \frac{y^{\frac{1}{2}}}{2ab^{\frac{1}{2}}}\left\{\frac{y^{\frac{1}{2}}}{b^{\frac{1}{2}}} + \left[\frac{y}{b} + 4P_{ni}\right]^{\frac{1}{2}}\right\} \qquad L = \text{wavelength}$$

where:

$$P_{ni} = A_r \Omega_r B\Pi + \frac{I_d hf}{ne} + \frac{kThf}{2ne^2M^2R_{eq}} \doteq 1.02\text{x}10^{-16} + 4.75\text{x}10^{-13} + 3.02\text{x}10^{-13}$$

The required transmitter power output, assuming no filter, modulator or antenna loss is:

$$P_t \doteq 42.5 \text{ watts}$$

Now we shall look at the case where the receiver has a low enough noise figure (or large enough y) to be quantum limited. In that case for PCM direct detection:

$$P_s = \frac{(S/N)hfBF}{\frac{1}{2}n} \doteq 4.57\text{x}10^{-9} \text{ watts} \qquad P_t \doteq 10 \text{ watts}$$

This value is ideally the least possible power that could be used (assuming our antenna sizes, quantum efficiencies and S/N) regardless of the receiver. So, the transmitter power value will not be reduced greatly unless an improvement in quantum efficiency is developed.

An idea of the actual laser output power necessary can be obtained by assuming nominal values for antenna and optic efficiencies and filter efficiencies. We assume the following:

transmitter & receiver optics and antenna- 50%
filter efficiency (1 Angstrom)- 50%

Using these efficiencie we compute:

Power output required with losses -- 170 watts
Power output ideally with losses -- 40 watts

Optical Receiver and Power Calculations Summary

S/N overall -- 100 20 db
A_t effective -- 36cm.
divergence -- 2.88 microradians
A_r effective -- 200cm.
n_r efficiency -- 50%
xmtr & rcvr
antenna & optics
n_{S-25} -- 1%
I_d anode -- 10^{-9} amps
M^2R_{eq} -- 10^{12} ohms
F -- 1.3
T system -- 50°K.
Ω_r -- 10^{-4} str.

Uncorrelated error probability of 10^{-6}
⊕ background -- 10^{-11} watts/cm^2-str.-micron
B information -- 10^7 htz.
B filter -- 1 Angstrom
n filter -- 50%
P_t no loss -- 42.5 watts
P_t no loss ideal -- 10 watts
P_t loss --170 watts
P_t ideal loss -- 40 watts

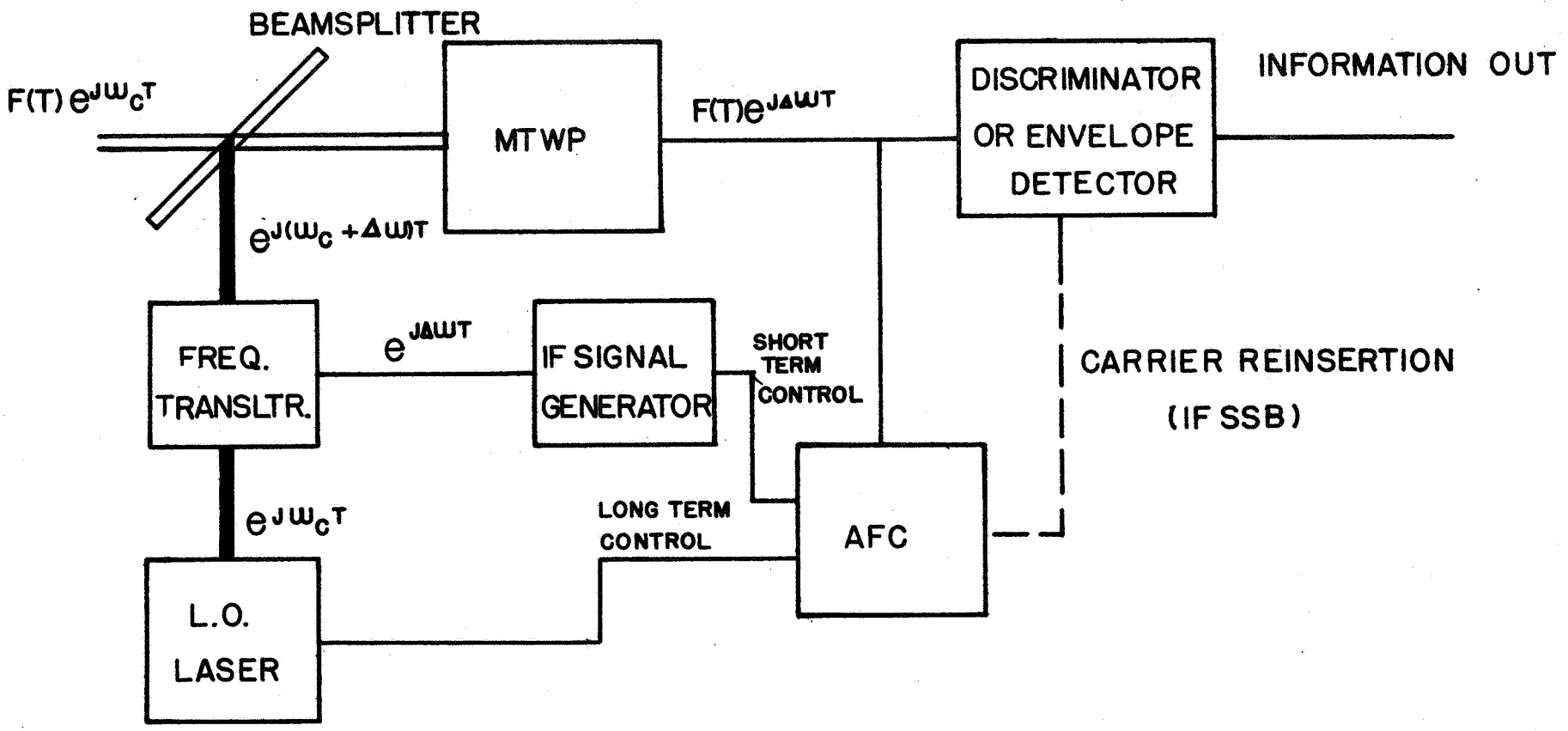

Figure c-13

BASIC MW. IF. OPTICAL HETERODYNE RECEIVER

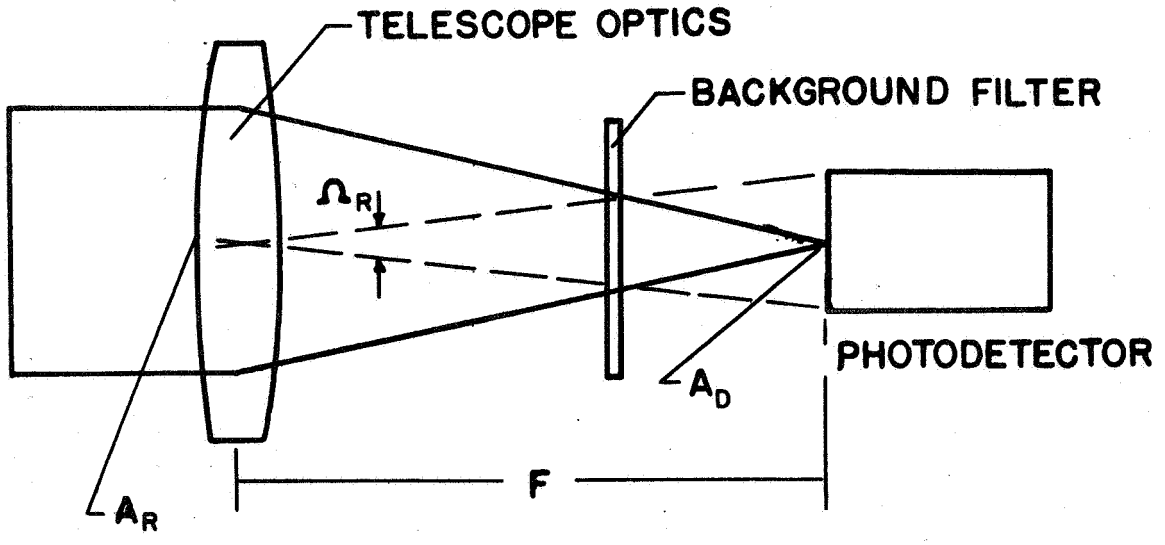

Figure c-14

DIRECT DETECTION

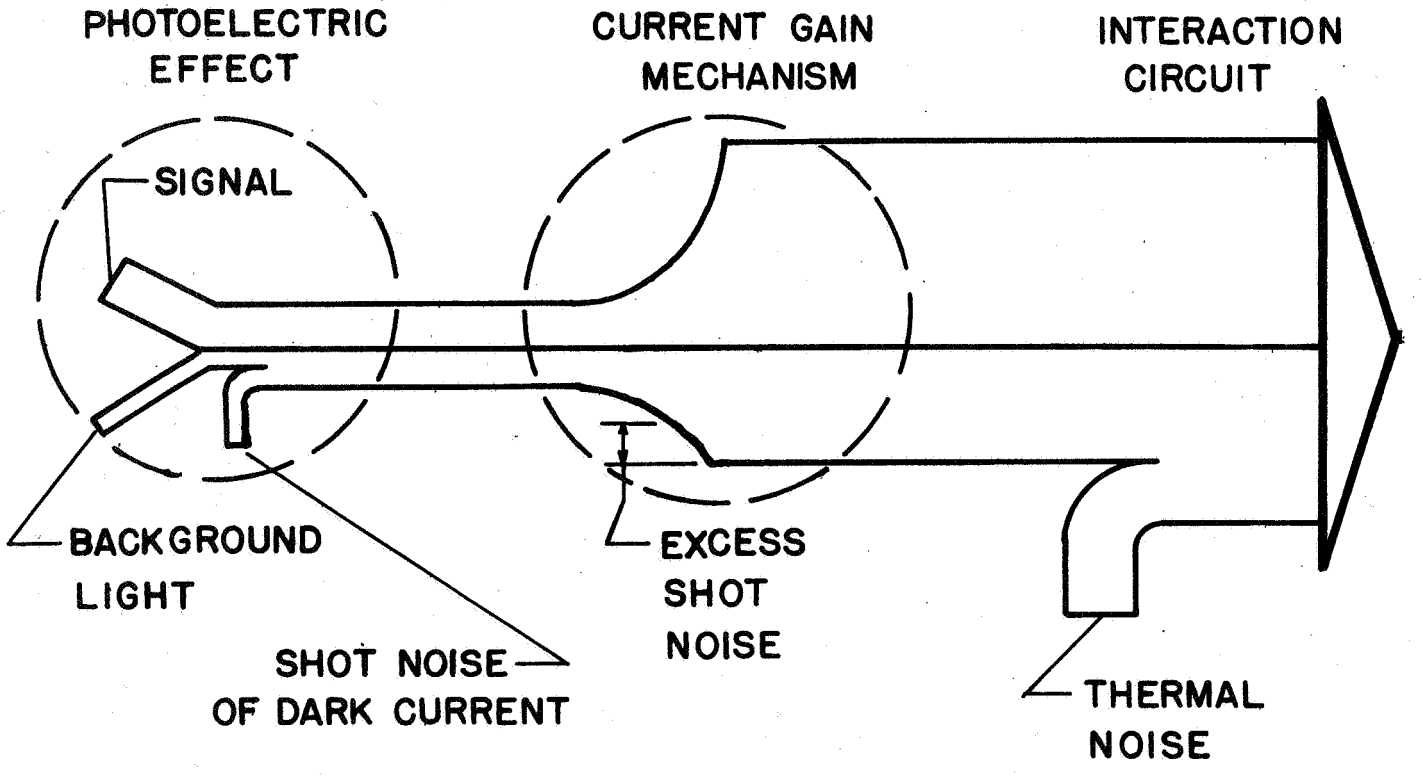

Figure c-15

PHOTODETECTION

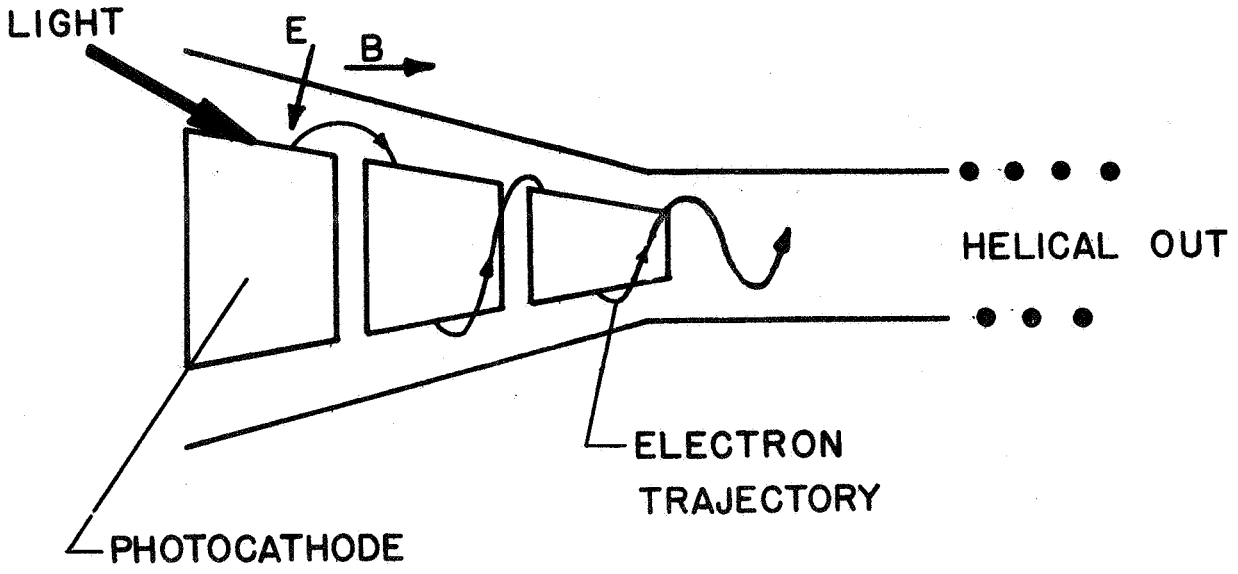

Figure c-16

MULTIPLIER
TRAVELING-WAVE PHOTOTUBE

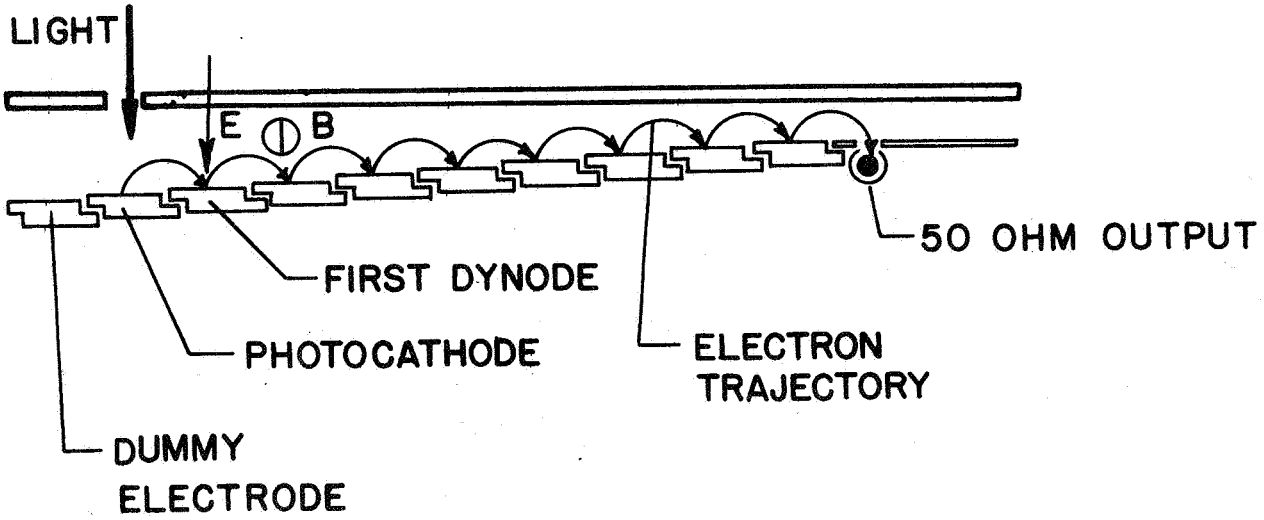

Figure c-17

STATIC CROSSED-FIELD
PHOTOMULTIPLIER

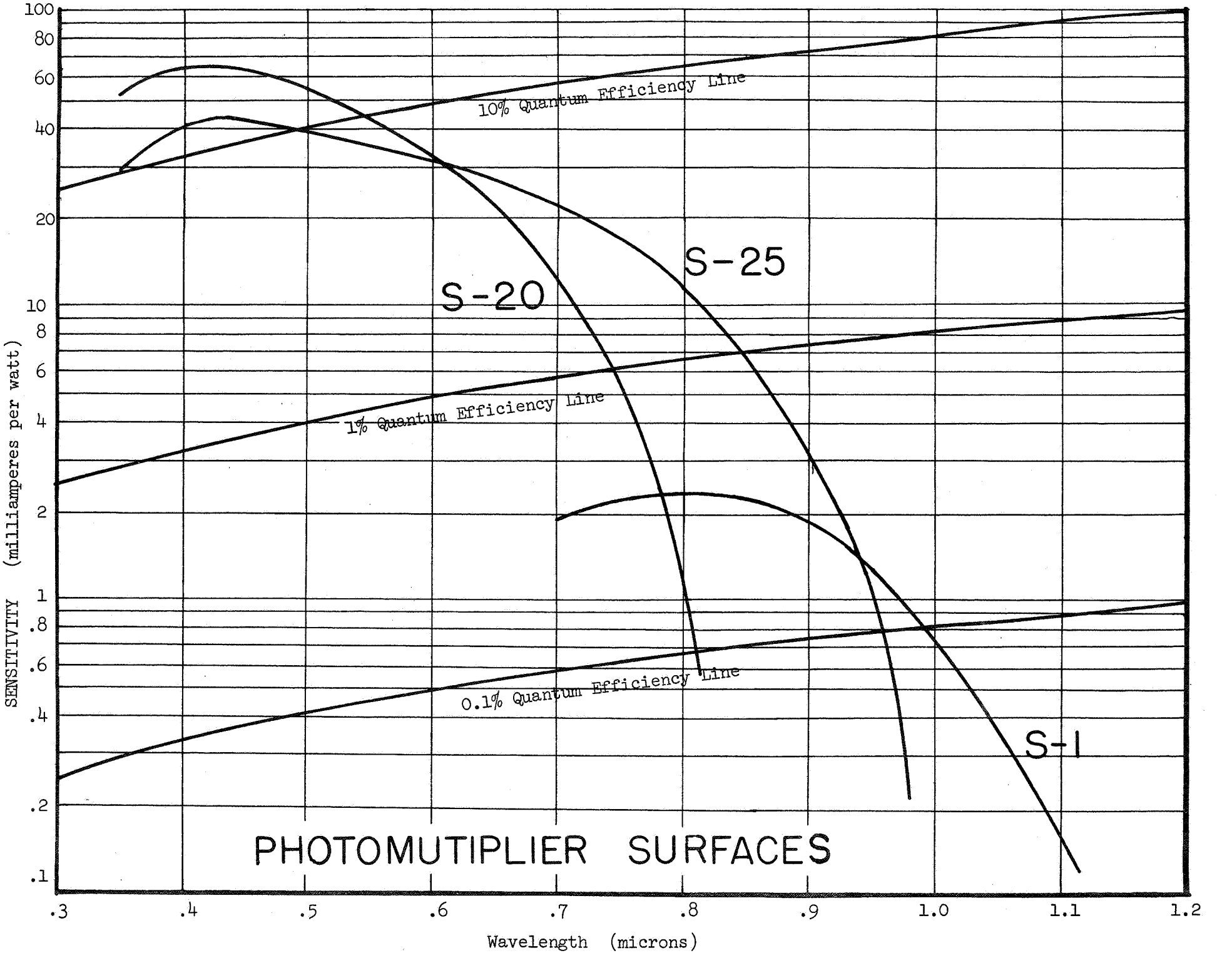
100
80
60
40
20
10
8
6
4
2
1
.8
.6
.4
.2
.1
SENSITIVITY (milliamperes per watt)
10% Quantum Efficiency Line
1% Quantum Efficiency Line
0.1% Quantum Efficiency Line
S-20
S-25
S-1
PHOTOMUTIPLIER SURFACES
.3
.4
.5
.6
.7
.8
.9
1.0
1.1
1.2
Wavelength (microns)

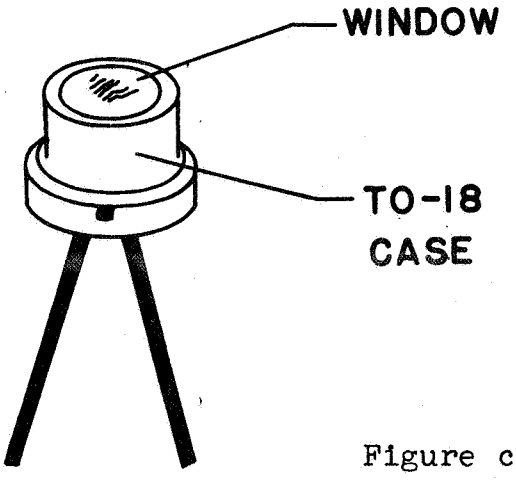

Figure c-18

APD OR OTHER SEMICONDUCTOR DEVICE

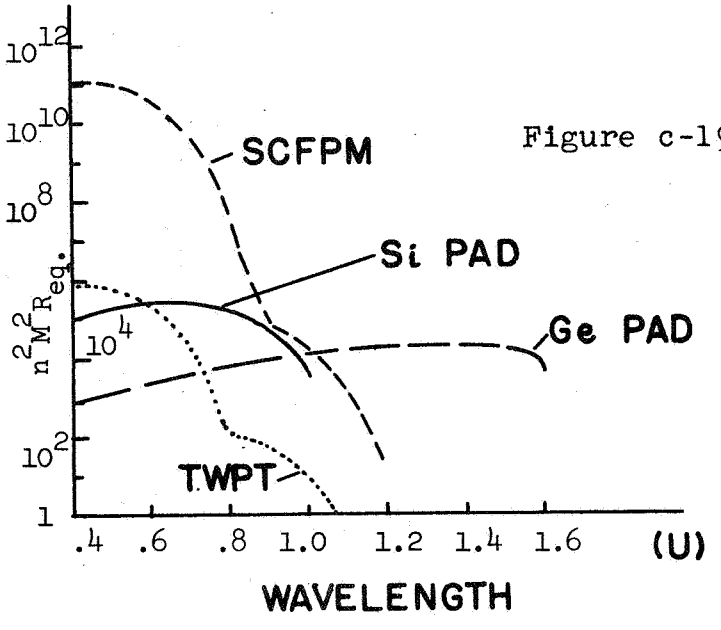

Figure c-19

FIGURES OF MERIT FOR DETECTORS

EXPERIMENTAL COMPARISON OF DEVICE FIGURES OF MERIT Table c-4

Photodetector	Wavelength Range	Diameter of active area	$M^2R_{eq.}$	Comments
Si Avalanche	.4- 1.0 u.	40 u.	2.5×10^6	Highest (Gain)(B.W.) of all solid-state detectors
Ge Avalanche	.6- 1.6 u.	40 u.	1.5×10^5	Most sensitive wide-band infrared detector
Dynamic Crossed-Field P.M. Tube	approx. .4- 1.2	Several cm.	5×10^{15}	Very Sensitive but needs a microwave pump source
Static Crossed-Field P.M. Tibe	" "	" "	2×10^{12}	Very sensitive & seems best for baseband uses
Reflection Dynode Multiplier T.W.P.	approx. .4- 1.1	" "	10^{10}	Very sensitive, wide-dynamic range- best for bandpass uses

Some Typical Experimental Parameters Table c-5

Device	Wavelength efficiency	$M^2R_{eq.}$	$B_{opt.}$	Θ_R	A_t	A_r	F	Comments
Direct Detection (S-20) MTWP	.4880 u. 15%	10^{10}	10 Å	10^{-4} str.	5.0 cm rad.	25	1.3	
Si Avalanche	.4880 25%	8×10^4	"	"	"	5	5.8	
(S-1) MTWP	1.06 5×10^{-4}	10^{10}	"	"	"	25	1.3	
Ge Avalanche	1.06 35%	8×10^4	"	"	"	5	33	$I_d = 10^{-7}$ amp
Heterodyne Detection (S-20) MTWP	.4880 15%	10^{10}	"	"	"	2	1.3	
Ge Photodiode	1.06 35%	80	"	"	"	4	1.0	$P_{lo} = 2 \times 10^{-3}$ watts overcome thermal noise

Note:
B= 1 GHz. was assumed
M_{opt} is based on a 6-dB noise figure for the following amplifier
All multiplier phototubes should, with further development, provide sufficient gain to be quantum limited with GHz. bandwidths

S/N FOR PCM ERRORS

Table c-6

Signal to Noise Ratio	Probability of Error	Average Time Between Errors at 10^5 pulses/sec
13.3 db.	10^{-2}	10^{-3} sec.
17.4 db.	10^{-4}	10^{-1} sec.
19.6 db.	10^{-6}	10 sec.
21.0 db.	10^{-8}	20 min.
22.0 db.	10^{-10}	1 day
23.0 db.	10^{-12}	3 months

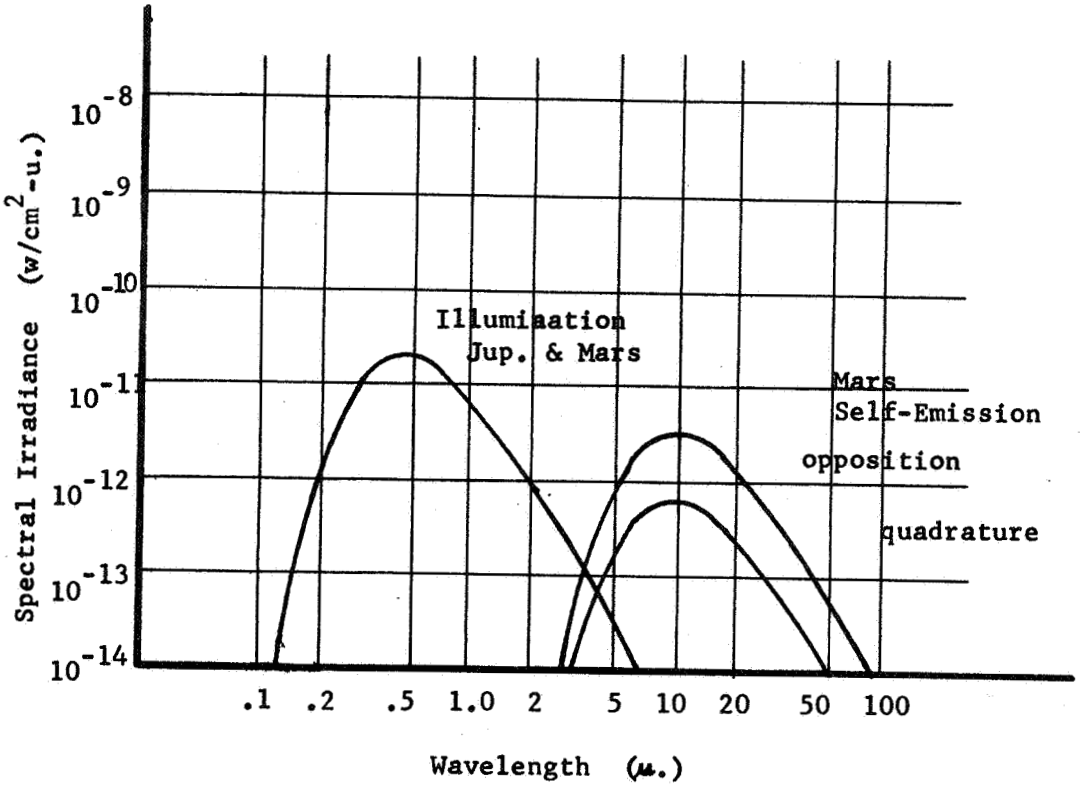

Figure c-20

PLANETARY SPECTRUM (NO ATMOSPHERE)

JPL OPTICAL COMMUNICATIONS SUMMARY Table c-7

("A Study of Weather Dependent Data Links for Deep-Space Applications")

Parameters:

$$M = \frac{(pB)R^2}{P}$$

$M_{JPL} = 5.3 \times 10^5$ AU^2/joule.

		OR
p = S/N for Mission	$= 10^2$	10^2
B = Bit Rate (BW)	$= 10^6$ b/sec.	10^7
R = Range (Mars)	= 2.3 AU.	2.3
P = Raw Power in	= 1 kw.	10 kw.
	$M = 5.3 \times 10^5$	$M = 5.3 \times 10^5$

The receiver system is assumed to be sophisticated enough to be quantum limited. Therefore, the noise spectral density ($\mathbb{D}$) is given by hc/l.

All calculations assume the above M, then range equations are solved for the necessary antennae sizes. $(N^{\frac{1}{2}} D_t D_r)$ where:

N = number of antennae in array
D_t = diameter of transmitter antenna
D_r = Diameter of receiver antenna

The receiving stations are based on the earth at selected places.

System efficiencies are estimates and may be within 20-50% of the actual values.

Atmosphere: CO_2 LASER OPTICAL SYSTEM AT 10.6 μ. Table c-8

transpariency	85 %
efficiency due to loss of coherence.	90%
atmospheric efficiency	76.5 %
unobsecured telescope aperture	88 %
transpariency & reflectivity of optics	82 %
Optics	72 %

For the entire system:

Transmitter power conversion	12 %
Transmitter optics	72 %
Atmosphere	76.5 %
Receiver optics	72 %
Detector quantum efficiency	40 %
N (system efficiency) =	1.9 %

$\mathbb{D} = hc/l = 2.0 \times 10^{-20}$ watts/Hz.

JPL SUMMARY (Cont.)

CO_2 Laser at 10.6 μ.

Wavelength	10.59 u.
Receiving System Noise Spectral Density	2.0×10^{-20} watts/Hz.
Overall System Efficiency	1.9 %
$N_r^{\frac{1}{2}} D_r D_t$	15.3 $ft.^2$

Table c-9 Gallium Arsenide Laser at .87 μ.

For the entire system:

Laser power conversion	4 %
Transmitter optics & antenna	50 %
Atmospheric transmission	85 %
Receiver optics & antenna	50 %
Narrow Band Filter	30 %
Postulated advanced photodetector	30 %

N (system efficiency) = .0765 %

Receiving System Noise Spectral Density ($\mathbb{D}$) =2hc/l = 4.566×10^{-19} watts/Hz

$N_r^{\frac{1}{2}} D_r D_t$ = 31.7 $ft.^2$

NASA/HUGHES OPTICAL COMMUNICATIONS SUMMARY Table c-10

("Optical and Microwave Communications")

Parameters:

The receivers are Earth based.

PCM is used.

Mars Vehicle to Earth-Based Ststion Laser Transmission Analysis

Parameter	Ionized Argon Laser		CO_2 Laser (8)	
Wavelength	0.5 μ.		10.6 μ.	
Range, R	1.852×10^8 km.		1.852×10^8 km.	
Transmitter power	4.0 w.	6.0 dbw.	130 w.	21.1 dbw.
Antenna gain (1) Trans.	12.7 cm.	115.3 db.	1 m.	106.7 db.
Transmission loss (2)	t= .85	-0.7 db.	t= 0.7	-1.4 db.
Spreading loss	$1/4\pi R^2$	-236.7 db/m^2	$1/4\pi R^2$	-236.7 db/m^2
Atmospheric Loss (3,7)	0.40	-4 db.	0.40	-4 db.
Receiver Aperture Area (4)	78.5 m^2	18.9 dbm^2	78.5 m^2	29.3 dbm^2
Receiver Loss (5)	0.27	-5.7 db.	0.27	-5.7 db.
Received Power		-106.4 dbw.		-100.6 dbw.
CNR		10.0 db.		10.0 db.
Detector quantum efficiency	0.20	-7.0 db.	0.20	-7.0 db.
Allowable Noise Power		-123.4 dbw.		-117.6 dbw.
hf	3.97×10^{-19}	-184.1 dbw/Hz.	1.88×10^{-20}	-197.3 dbw/Hz.
Noise Bandwidth (2 B_o)	1.15 MHz.	60.7 dbHz.	93 MHz.	79.7 dbHz.
Maximum Transmission Rate	1.15×10^6	Bits/ sec.	9.3×10^7	Bits/ sec.

Note:

(1) For defraction limited beamwidth of 1 arc sec at l=.5μ. & 2.67 arc sec at l= 10.6 μ.

(2) Beam deflector t_1= 0.85, modulator t_2= 0.85

(3) Rain losses 30 db, fog and snow losses 80 db

(4) Assuming 30-meter spherical antenna, effective diameter is 10 meters

(5) 10 Å filter, t_1= 0.35; antenna, t_2= 0.90; beam deflector, t_3= 0.85

(6) CNR= $nP_s/2hfB_o$, quantum noise limited; CNR= 10 db for $P_{e,s} = 2.3 \times 10^{-5}$

(7) Rain margins not included

(8) Assumes quantum noise limited and that suitable detectors will be available

WESTINGHOUSE OPTICAL COMMUNICATIONS SUMMARY

("Deep-Space Optical Communications")

Table c-10 (cont'd)

Parameters:

Both Earth and satellite based receiving systems are looked into.
PCM/PL is found to be the most advantageous modulation system.
The error rates are such that commercial video at real time is sent from Mars
The optical system postulated is at .60 u.

Down Link	Data Rate, Bits/sec.	Error Rate, Bits/sec.
Video	5×10^7	10^{-3}
Telemetry	1×10^3	10^{-6}
Voice	3×10^4	10^{-3}

TRANSMITTER POWERS

Data Rate	Modulation	Satellite Transmitter Power for Given Errors	
		Earth Receiver	Satellite Receiver
5×10^7	PCM/PL	11 watts	65 watts

Note: The larger power required for the satellite receiver is because a smaller antenna is possible in a satellite than on the Earth.

NASA/ L.C. VAN ATTA OPTICAL COMMUNICATIONS SUMMARY

("R&D for Future Deep Space Communications") (table c-10 cont't)

Parameters:

It is assumed that appropriate tracking techniques for heterodyne receivers, high speed detectors and efficient modulators are available at 10.6 u..

From the range equation, the use of an optical system improves the transmission gain, but degrades:

- P_t because the laser is less efficient than microwaves
- A_r because of atmospheric effects and diffraction limitations
- L (attenuation) would be greater, and intolerable in rain, fog or clouds
- T_r because of celestial noise and much less sensitivity in the detector than with microwaves.

These disadvantages in general rule out infrared or optical frequencies for deep space communications in the near future.

COMPARISON OF A 10.6 μ. OPTICAL SYSTEM WITH A 2.3GHz. M.W. SYSTEM

	2.3 GHz	10.6 U. Heterodyne	.53 U. Direct Detection
Efficiency (%)	40 (1 kw)	8	0.3
Transmitter gain (1000 lbs.)	51 db. (72')	111 db. (1.4m)	134 db. (1m)
Receiver dia.	64 m	1.4m	Relay Satellite 1.4m
Noise temp.	25 °K	1350 °K	27,000 °K
Quant. Effic.		0.5	0.2
Optical Effic.	loss 1 db.	0.8	0.5
Modulation	Coherent biorthogonal	Coherent biorthogonal	Incoherent polarization shift
Power	0 db.	-7 db.	-21 db.
Trans. gain	0	+60	+83
Receiv. area	0	-33	-33
Noise temp.	0	-17	-30
Receiv. losses	0	-4	-10
E/N_o	0	0	-2
	Net advantage:	-1 db.	-13 db.

NASA/VAN ATTA SUMMARY (Cont.) Table c-10 cont'd

Possible Improvements in db Over Present Parameters (Previous Comparison)			
	2.3 GHz.	10.6 μ.	0.53 μ.
Power	+1 db.	+2 db.	+11 db.
Trans. gain	+14	+9	0
Receiv. area	0	+9	+9
Noise Temp.	+2	0	0
Receiver losses	0	0	+3
E/N_o	+2	+2	+7
Net growth:	+19 db.	+22 db.	+30 db.

Assumptions To Derrive the Above Improvements			
Power	Amplifier effic. incrsd. from 40 to 50 %	Laser effic. inc. from 8 to 12 %	Laser effic. inc. from .3 to 4.0 %
Transmitting gain	Estab. of 1000lb.,300' inflatable antenna	Estab. of 1000lb, 4m aperture limited telescope	Tracking problem limited
Noise temp.	Reduct. of backgrnd. from 25 to 16°K	Quantum limited	Quantum limited
Receiver area	Cost limited	Same as trans. gain	Estab. of 1000lb, non-aperture limited telescope
Receiver losses	Already negligible	Losses already low	improved filters & photoemissive materials
E/N_o	Improved coding	Improved coding	Introduction of effic. pulse position modul.

Discussion of Other Optical Communication Reports

The other optical communication evaluations summarized in this section differ from our proposed system in some minute and some major ways. The changes thus arising in the analysis may effect the overall results. We will look at some possible differences.

JPL Report

The assumption that the system is quantum limited is close to the value that we calculated. The value of M used may be the same as our system (i.e. B=10^7, S/N=10^2, R=2.3 AU, P=10kw.). The atmospheric effects may be ig ored since our system is outside the atmosphere. The value of laser efficiency is lower than the value we assumed (4% vs projected 10% for GaAs). The efficiency of the GaAs detector is greater than our S-25 SCFPM. The final value of $N_r^2 D_r D_t$ is calculated to be 31.7 ft.^{2}. These are actual diameters, not effective diameters. Therefore, the approximate effective diameters are $D_r^* D_t^*$ are approximately 10 ft.^{2}, with a laser power output of 40 watts. Our system has a power output of 170 watts and a $D_r^* D_t^*$ of approximately 6.82 ft.^{2}. These values are very compatible and no drastic differences exist in the final calculations, even though slightly different overall parameters were used.

NASA/Hughes Report

No close comparison of our system and their system can be made since the only optical systems detailly looked into were Ionized Argon (.5u.) and CO_2 (10.6u.) laser systems. The efficiencies used for filters, modulators, antennae (when extrapolated to .87u.) yield results not in great conflict with our assumed values.

Westinghouse Report

The assumption made in this report is that a laser system is used at .60u. and postulated device efficiencies are used. The error rates used (10^{-3}) for commercial quality video is not near high enough for our high resolution purposes. The modulation is the same as ours, PCM/PL. They calculate a transmitter power of 65 watts necessary for a satellite receiver. Nothing can really be said about their assumptions or calculations, because they do not outline, in enough detail, the assumptions or calculations in the paper referred to. However, their power of 11 watts for an Earth based receiver seems a bit too low- a little too close to the ideal case.

NASA/Van Atta Report

The major assumptions ruling out optical communication systems for the near future were: P_t, A_r, L, and T_r. The atmospheric effects on A_r and L can be ignored since our system is in space. Celestial noise (Mars, Jupiter and stars) is negligible in our case. And the relative positions of the Earth, Mars and the Sun are such to eliminate the problem of direct solar radiation. In fact, the sunspot cycle will be at its height during our voyage, thus making optical communications look even better when compared with microwaves. Using these changes, it is difficult to rule out a system like ours easily, especially when the technology associated with optical communications is in its present state of flux.

UPLINK

The command uplink will provide control and guidance information to the spacecraft for trajectory maneuvers and corrections, and supply commands for correct functioning of subsystems. This earth-to-orbiter system is a vital link in the Mars probe which places stringent requirements on the use of microwaves. The 3-year mission demands a command capability of 10 bps with at least a 20 db S/N ratio up to distances of 2.5 AU. Environmental conditions include 50 degree K to 400 degree K temperature extremes and 5-G launch acceleration shocks. The system assumes the use of three 210-ft DSIF transmitting antennas on earth, each with a power output of 400 kw at 2.1 ghz, backed up by the 85-ft Az-El antennas with 100 kw output each.

The success of the Mars mission depends greatly on the performance of the uplink, and reliability is the first consideration in design. To decrease command errors, the system will be digital and will employ three PCM/PSK channels with a maximum bit error rate of 10^{-5} errors per bit. The orbiter will include three S-band 2.1 ghz solid state receivers, each capable of being addressed on independent channels for maximum redundancy. The three antennas--the low-gain slotted waveguide, the 10-ft parabolic dish and the medium-gain elliptical paraboloid--will be switched between the receivers to provide for normal and backup communications.

Assuming lossless transmission from earth, the command signal power received aboard the spacecraft is given by

$$P_r = (P_t A_r A_t)/(\lambda^2 D^2)$$

where

P_t = transmitted power on earth
A_r = effective area of receiving antenna
A_t = " " " transmitting antenna
λ = wavelength of transmitted signal
D = range

With a 210-ft. 60% efficient antenna transmitting 400 kw. on 2.3 ghz and a 2-ft. by 4-ft. elliptical parabolid on the spacecraft at 2.5 AU, the received power is 5×10^{-14} watts. Losses would reduce this signal strength, however, and the receiver must have at least a -160 dbm threshold level. This design is within the present state-of-the-art.

Typical values of each receiver package, exclusive of diplexing and associated equipment, will be:

Weight	10 lb.
Size	500 cu. in.
Power	10 watts

Work is presently being done on improving the receiver noise figure and reliability, and by 1978, technology should produce reliable receivers with noise figures of about 5db.

ANTENNAS

One of the vital links in the earth-spacecraft microwave communications system is the antenna. Earth antennas are used for data acquisition from the Mars probe, for tracking, and for command and control, while spacecraft antennas direct information signals back to earth. Improvements in deep space communications seem to lie in the direction of larger antennas and/or greater power levels. Antenna designs will be discussed in this section.

Earth Antennas

Presently the primary NASA tracking facility includes a worldwide network of 6 stations employing 85-ft. diplexed parabolic cassegrainian antennas for deep space communications, and construction of three 210-ft. parabolic reflectors is planned at DSIF stations in Australia, South Africa, and California. Although funds have not been appropriated for the completion of the Australian and the South African antennas, the 210-ft. network should be operational within a decade. For increased information rate and range, larger microwave antennas are being proposed, but the possibility of their erection by 1978 is remote.

The 210-ft. parabolic cassegrainian antenna increases the capabilities of deep space communications tremendously. The Goldstone antenna in California boasts a 62-db gain in the S band and a 177 dbm carrier threshold. Using the Goldstone installation, the Mars-Earth communications system is capable of a 30° K noise temperature at a S/N ratio of 10 db. Slight improvements of a few degrees may be expected by the launch date. The antenna pointing accuracy is 70 seconds of arc and the beamwidth is 9 minutes of arc. 400 kw of power can be transmitted from the antenna.

Although the 210-ft. Goldstone dish is presently being used for S-band communications, it is capable of being operated in the X band. However, sky noise is an important consideration, and although system gains are increased in the X band, system losses and atmospheric attenuation (see Figure 22) tradeoff studies indicate the 2.1-2.3 ghz band is optimum for a Mars mission. The uplink will be 2100 to 2120 mhz while the microwave backup downlink will be 2290 to 2300 mhz.

Spacecraft Antennas

The choice of spacecraft antennas is determined by the following considerations:

1. Size and weight limitations
2. Beamwidth and gain
3. Fabrication techniques--tolerances, strength, and reliability

The antenna must fit easily inside the spacecraft shroud without introducing undue deployment or weight problems. Ideally it should have a high gain and a narrow beamwidth in deep space but not cause tracking or earth-acquisition problems. On the otherhand the antenna should

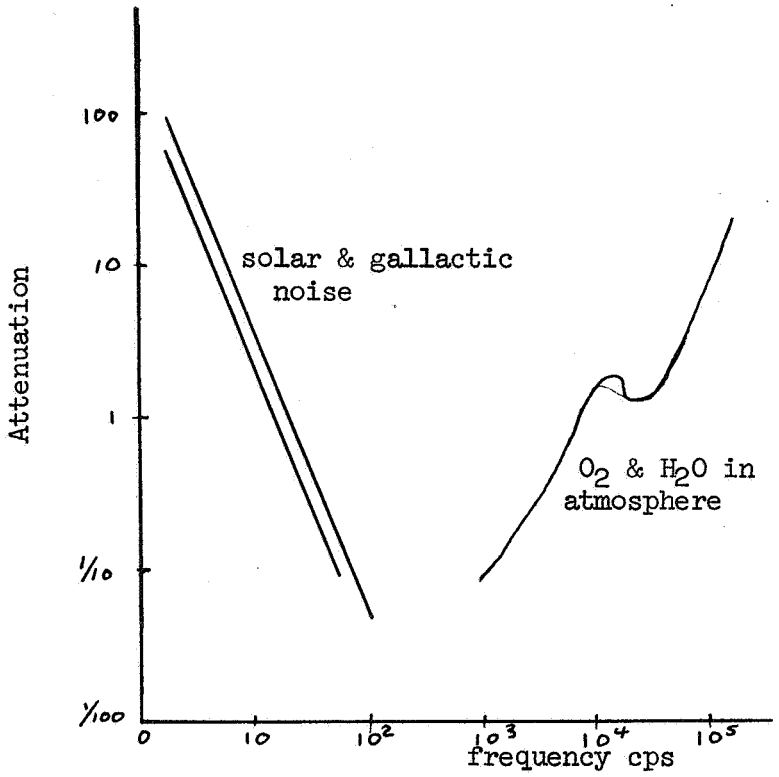

Figure c-22 Transmission Losses

be omnidirectional near the earth to accommodate vehicle maneuvers. Finally, construction must be within the capabilities of fabrication technology--for example, parabolic surfaces should be machined to optical tolerances, or within 1/16 of a wavelength while maintaining reasonable antenna strength and reliability.

Deep space vehicles usually carry three or more antennas--a low-gain omnidirectional antenna for use during the launch phase, a medium-gain antenna for use in the midcourse phase, and a high-gain parabolic dish for use in deep space. We have adopted this scheme to give maximum reliability and efficiency. Each antenna will be connected to a separate receiver, and provisions are made for switching the antennas between the receivers in a backup mode.

The low-gain antenna must possess an omnidirectional radiation pattern to maintain communications with the earth during launch and in early orbital maneuvers. We have chosen a cross-slotted circular 10-ft. waveguide as our low-gain antenna, getting a nearly hemispherical radiation characteristic. During early interplanetary flight this antenna will be diplexed for use with the 2.1-ghz uplink and the 2.3-ghz downlink. The slotted radiator must be capable of transmitting equipment, telemetry data at 100 bps and receiving 10 bps command until

Table c-10 Parabolic Antenna Beamwidths

Diameter	S Band	X Band
1 ft.	25°	5.6°
5	4.9	1.1
10	2.5	0.56
15	1.6	0.38
18	1.4	0.31
20	1.2	0.28
30	0.82	0.19
50	0.49	0.11
100	0.25	0.06

the midcourse maneuvers have been completed with a communications range of 1.2×10^7 km. After launch the medium-gain antenna will be deployed and available as a backup.

After flight stabilization and midcourse maneuvers, communications will be switched to the medium-gain antenna, which will remain the primary antenna in use until the Mars encounter. This antenna must have a beamwidth which can accommodate slight spacecraft flight instability. A 2-ft. by 4-ft. Mariner-type elliptical paraboloid is adequate for this purpose, since only 100 bps downlink and 10 bps uplink rates are required. This fixed reflector has a fan-shaped beam about 20 degrees by 10 degrees at the half-power points, permitting for vehicle alignment drifts. In case more gain is necessary, communications can be switched to the high-gain antenna, and the slotted radiator may be used to resume control after unexpected tumbling.

In the Mars orbit the laser downlink will be employed, and the

Table c-11 Parbolic Antenna Gains

Diameter	S Band	X Band
1 ft.	14.7 db	27.4 db
5	28.0	41.4
10	34.6	47.4
15	38.1	50.9
18	40.1	52.5
20	40.7	53.4
30	44.2	56.9
50	48.6	61.4
100	54.6	67.4

medium-gain reflector will remain operational on the uplink for command and control. In addition, a high-gain parabolic antenna will be used for the orbiter-lander link where it will be capable of handling the large bit rates necessary for observational information transmission. However, the large reflector must act as backup for the laser downlink, and in case of laser failure, the high-gain antenna will be switched to the earth downlink while the low-gain reflector maintains lander communications. Thus the high-gain reflector must be capable of high bit rates yet not introduce unreasonable tracking problems.

We have investigated the gain and beamwidth characteristics of circular microwave parabolic reflectors of different diameters to operate in the S-band (2.3 ghz) or the X-band (8.5 ghz) regions. The approximation:

$$\theta = \frac{\lambda}{d}$$

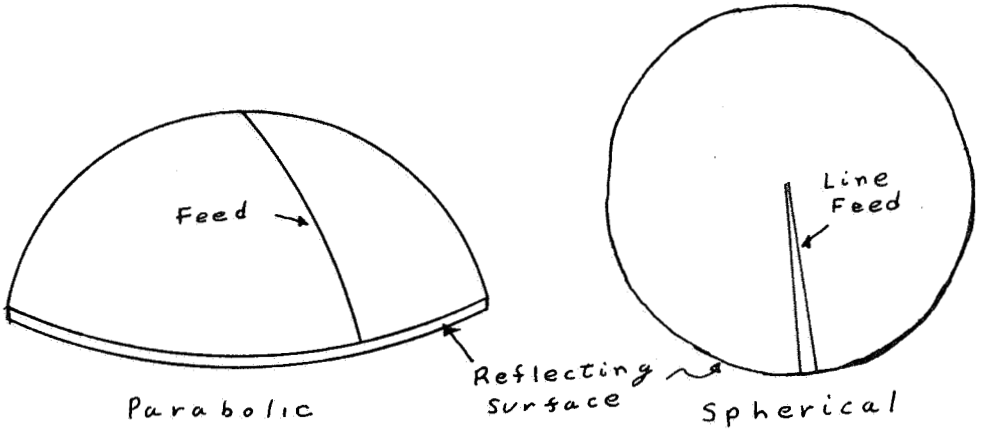

Figure c-23 Balloon Antennas

where

θ = antenna beamwidth

λ = wavelength

d = antenna diameter

gives the beamwidth values shown in Table 10.

Antenna gain, shown in Table 11, is given by

$$\text{Gain in db} = 20(\log f + \log d) - 52.6$$

where

f = frequency in mhz

d = diameter in feet

Parabolic microwave reflectors offer the advantages of high gain and narrow beamwidths, enabling the orbiter to transmit more information and increasing the effective range of the link. In addition, parabolic antennas are frequency insensitive and can be diplexed at 2.1 ghz and 2.3 ghz with no significant losses. We have investigated the possibility of using gimballed parabolic reflectors of up to 18 feet in diameter, the maximum size permitted in the spacecraft shroud. Problems arising from surface tolerances, mechanical strength, and reliability were considered in the high-gain antenna choice. Earth re-acquisition was judged a minor problem since the laser system would already incorporate adequate provisions for platform stability.

In our study of the telecommunications system to be used on the Mars probe, we have also considered employing various unfurlable parabolic and spherical antennas in the earth-orbiter backup link. Unfurlable antennas feature substantial gain advantages over conventional parabolic microwave antennas in deep space communications and are capable of greater information rates and range in both the up- and the downlink. Compared to a conventional parabolic S-band 18-ft. antenna with a gain of 40 db, unfurlable antennas will be capable of 50 db or more by 1976. The use of up to 50-ft parabolic antennas which fold to fit within the Saturn V shroud is still under study by industry, and further improvements in microwave space communications seem to lie in the direction of larger antennas.

Another design which was considered featured a large inflatable plastic balloon deployed in space. The balloon would either include a parabolic surface or would inflate to a sphere enclosing a line feed system, as shown in Fig. 23. However, both types of balloon antennas require close surface tolerances, and further development depends upon advances in industrial technology.

Despite the advantages of using these larger microwave antennas, our choice of the laser orbiter-earth downlink made the unfurlable paraboloids and balloons unnecessary. Even without resorting to large transmitting reflectors, the laser system will be able to handle information at a rate of 10^7 bps from a Mars orbit. On the uplink, a smaller microwave antenna will be able to receive the 1-10 bps required for control and guidance. Furthermore, the problems of unfurlable antenna fabrication, pointing accuracy, and surface tolerance seem to make it unjustifiable, at this stage anyway, to favor a large size microwave antenna system over lasers.

We have concluded that a 10-ft. steerable parabolic reflector for orbiter-lander communications and backup earth downlink would be most compatible with the high capacity laser downlink system. Spatial requirements and deployment problems limit the size of the antenna to 10 feet, which would accommodate a bit rate substantially less than that of the laser system. However, the primary mode of the high-gain paraboloid would be orbiter-lander communications in which large reflector size is unnecessary; the high-gain antenna would be deployed on the downlink only in the event of laser failure.

MILLIMETER WAVES

Millimeter waves were considered as an alternative communications system. In order to justify consideration of this system many extrapolations from sketchy reports had to be made. For this last reason, this report will deal with what has been done in the field of millimeter meters, theories and laboratory results.

Generation Techniques

Two basic techniques have been utilized for millimeter wave generation, these being scaled down versions of successful microwave systems and development of new methods to extract energy from electrons.

In concept, the simplest of these are the scaled down versions of microwave generators.[25] Generation has been successful using klystrons, magnetrons, backward wave oscillators (BWO), and traveling wave tubes (TWT's).[26]

The use of these systems has been limited to the lower bands of the mm-wave spectrum because of the extremely close tolerances required. These tolerances, when described in terms of operating efficiencies, result in efficiencies of from 15% to 25%, or in at least one report, a maximum of 30%.[14]

Some laboratory figures for such devices range from 150 watts at 50 gc continuous wave (CW),[25] to 6 KW at 5.5 mm (55 gc) CW operation using a TWT. However, at least one klystron can match this with 6 KW at 5 mm (60gc) CW and 3 KW at 3 mm (100 gc) pulsed.[26] Figure 24 helps to describe these systems of generation and gives comparative evaluations of operation.

New methods for mm-wave extraction have been developed and in some cases show great potential. These newer methods include varacter diodes and doubler diode techniques, tornadotrons, ferrites and rebatrons.

Theoretical possibilities for high energy radiation from rebatron devices have not yet been achieved. This system uses the interaction of a tightly bunched beam of electrons passing through a hole in a dielectric medium.

Tornadotrons and ferrites both use a spinning band of electrons from which to extract energy. The tornatrons using a cloud of electrons in a vacuum have successfully produced "a few" milliwatts of power at 70 gc, while the ferrites using a band in a solid material shows potential tens of watts at 300 gc.[25]

Harmonic generators have been developed to produce mm-waves from below mm-wave frequencies. Such a system theoretically can double the frequency with 100% efficiency. But because of conversion efficiency, loses decreasing quickly with increasing fundamental frequency, and increased harmonic number, this has not been possible.[27] Using

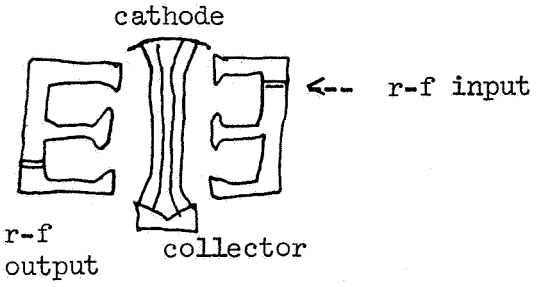

Klystron

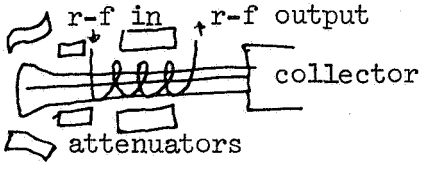

T.W.T.

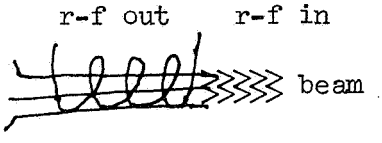

B.Y.O.

Figure c-24

Millimeter Wave Generators (schematic)

copper contacts in GaAs (gallium-arsenide) semiconductors, frequency doublers have been successful. However, for communication purposes the 1 mw. obtained as output power would not probably be useful.

In most cases, significant discoveries in mm-wave generation have been mentioned without regard to frequency. However, it should be noted that if either an Earth-orbiting spacecraft or a moon base equipped to receive mm-wave radiation are available, direct Mars-orbiter to Earth links will be necessary. In this case, frequency will play an important role in determining the millimeter system which is to be used. Lasers have higher attenuation in the atmosphere than do mm-waves. Microwaves have extremely low atmospheric loses but also have low bit rates as compared to mm-waves.

Millimeter waves, on the other hand, offer high bit rates (10^7 bits/sec) and definite "windows" at which attenuation is at a minimum. These windows occur at 30 gc, 95 gc, 140 gc, and 240 gc. The lowest attenuation figure is at 30 gc. This would therefore be the optimum frequency in such a mm-wave communication system.

Modulation

As in generation devices, modulation techniques stem mainly from the tried-and-true methods of scaled down microwave techniques. An alternately magnetized and demagnetized ferrite material which can change the direction of polarization used in conjunction with an absorbing disk to attenuate one direction of the polarized field, has been found to be an effective modulating device.[26] The draw-back

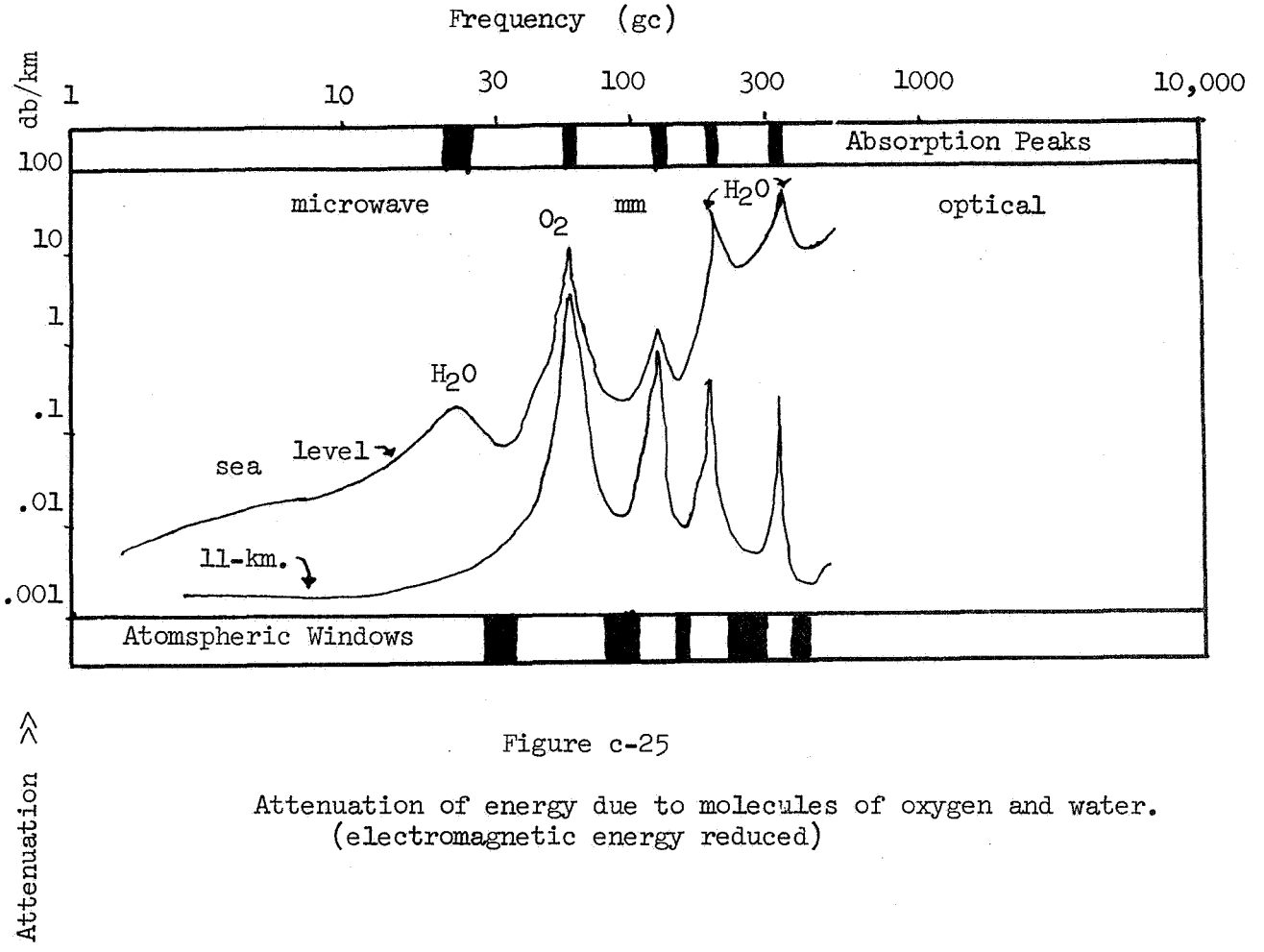

Figure c-25

Attenuation of energy due to molecules of oxygen and water. (electromagnetic energy reduced)

of such a system is loss of several db during modulation. Also, the modulator is limited to several hundred khz of bandwidth where this mission's goal of 10^7 bits/sec is necessary for real time picture reception.

A different approach to the problem of modulating mm-wave radiation is to look at the interaction of molecular gases to such radiation. Since a gas is composed of electric dipoles which collide with one another as well as the wall of the container, torques can be induced via electric fields. By intensifying the field to saturation, amplification, as well as modulation of an incoming signal, could be obtained. This system would be highly reliable because of its high predictability.

Tolerances

Perhaps the key devlopmental problem to adequate mm-wave communication is the amount of deviation from perfection that components operating in this frequency range may have; in a word, tolerance. One can begin to appreciate the problem of designing components from their microwave predecessors when dimensions of 0.060 inches for mm-waves come from a dimension of 3.0 inches in the microwave region.

Tolerances of $\pm$ 0.0005 inches are needed for operation. Waveguides have a particular problem in this region. A waveguide skin depth is on the order of 9 microinches. The surface finish is supposed to be smoother than this. This would indicate a tolerance not to exceed 5×10^{-7} inches.[25]

Add to this noise figures ranging from 10 db on up and one can appreciate the size of the task to make mm-wave generation feasible and practical.

Detection

Again, two different routes have been followed in the development of techniques for mm-wave detection. These methods have been developed with an eye to where millimeter waves stand on the continuous energy spectrum as well as to what has been accomplished using microwaves and lasers.

Watkins-Johnson has built a detector for the 70 - 100 gc region which amplifies with a noise figure of 14 to 18 db. Solid state devices such as germanium and indium antimone semiconductors operating at low temperatures have proven to be the best types of detectors in the mm-wave region. In addition, there have been developed varactor diodes and masers for use as "quiet" detectors. Westinghouse has developed the most successful maser amplifier for the purpose of detection by using a pumping frequency of 65 gc and a signal frequency of 96 gc. Noise figures run about 2 db for solid state masers.[25] Varactor diodes operating at 50 gc have been successful with noise figures down to 5 db.

It should be apparent that mm-waves are nearly in the optical range, therefore, quasi-optical techniques for detection are in the making. Improved fabrication techniques and materials should eliminate most difficulties now encountered.

Reception

Formulas for the minimum power requirements from a distance (D) of 93×10^6 miles using a gain of 50 db and receiving a signal of strength (P_r) 10^{-8} watts on a 5 foot parabolic antenna (A_r) indicate that, with no losses considered, a 100 watt transmitter (P_t) could be used.

$$P_t = \frac{4\ (\pi)\ D^2\ P_r}{\text{Gain} \times A_r} \qquad \text{where } A_r = 0.2025\ (\pi)\ A^2$$

It should be noted that losses (L) are multiplicative terms in formulas in which they appear.

$$P_t = \frac{P_r\ D^2\ L1\ L2\ L3\ (\pi)^2}{0.17\ A^2_{trans}\ A^2_{received}} \qquad \text{(Ref. 25)}$$

Slight loses will therefore have large effects on transmitted power. Remembering that efficiencies are low for most systems in the mm-wave reion because of the need for extremely high tolerances, it becomes evident why mm-waves have not been used to date in space craft communication systems.

ALTERNATE DOWNLINK SYSTEM

An alternate method of communication from the Mars probe to earth will be with S-band microwave, the frequency presently used for deep space telemetry. Within the present state-of-the-art, transmitting the 10^7 bits/sec required for this mission is a formidable problem.

The following approximate calculations will help to assess the requirements for the 10^7 bit/sec data rate.

The power received is given by

$$P_r = P_t \frac{G_t A_r}{4\pi R^2 L}$$

where

P_t = transmitted power

R = transmitted distance

L = system losses

G_t = transmitting antenna gain = $0.5 \left(\frac{\pi d}{\lambda}\right)^2$

A_r = area of receiving antenna

d = the antenna diameter

The noise power is given by

$$P_n = kTB$$

where

k = Boltzmann's constant (1.4×10^{-23} watt sec/^oK)

T = the noise temperature seen by the receiver (50^oK)

B = bandwidth ($5 + R_b$)

R_b = the data rate in bits/sec

A signal to noise ratio of $S/N = \frac{P_r}{P_n} \geq 10$ db., is required to receive meaningful data with a 3 db safety margin.

At the present time, the values for the above parameters are as follows:

G_t = 42 db (18 ft. parabolic disk)

A_r = 3×10^3 sq. meters (210 ft. Goldstone antenna)

R = 2×10^{11} meters

L = 10 db

Power Requirements For Various Antennas Table c-12

data rate 10^7 bits/sec

transmitting antenna	210 ft.	600 ft. ground antenna
18 ft.	32kw	1kw
50 ft.	2.3kw	70watts

data rate 10^6 bits/sec

transmitting antenna	210 ft.	600 ft. ground antenna
18 ft.	3.2kw	100watts
50 ft.	230watts	7watts

Using these values and $\frac{P_r}{P_n} = 10$, we find:

$$P_r = P_t \times 1.1 \times 10^{-17}$$

$$P_n = R_b \times 3.5 \times 10^{-21} \text{watts}$$

$$R_b = 310\ P_t$$

with $R_b = 10^7$ bits/sec

then $P_t = 32$ KW

This power is much too high for use on a spacecraft and, therefore, the other parameters must be improved to make this type of system feasible.

It should be possible to improve the antenna gain by using deployable or inflatable balloon-type antennas. Work is now being done in these areas and significant improvements may be obtained in antenna design in time for use on this project.* If a 50 ft. diameter antenna were developed, the gain for the antenna would be given by:

*See Antennas.

$$G_t = 0.5\left(\frac{\pi d}{\lambda}\right)^2 \simeq 54 \text{ db.}$$

for $R_b = 10^7$ bits/sec

$P_t = 2.3$ kw.

Another possible improvement appears if the size of the receiving antenna could be increased. If a 600 ft. antenna could be constructed, the transmitted power required would be reduced by a factor of 30 over that obtained for the 210 ft. antenna and still maintain the same data rate.

It is not likely that any significant improvement can be made in the coding to reduce bandwidth or that the required S/N could be reduced since the S-band receivers are now refined to a noise temperature of $17^{\circ}K$.

Transmitters

The transmitter capable of such high power on board a spacecraft is a problem which could be solved by using a large number of travelling wave tubes (TWT) in parallel. However, at an efficiency of 30-40%, the absolute maximum out put power for this mission would be on the order of 2.5 KW. This would mean, if no antenna advances are made, the maximum data rate would be 7.5 x 105 bits/sec, and even this would represent a large heat dissipation problem.

However, it is quite possible that a 50 ft. antenna will be available for use by the time of this mission. If this is the case the S-band system could use 10 250 watt TWT's in parallel and achieve the desired data rate of 10^7 bits/sec. The use of 10 tubes in parallel gives reliability to the system because even with 50% failures, a data rate of 5×10^6 could be maintained. The bit rates and power required for various antenna systems are shown in Table 12. A system such as this would require a refinement in our present knowledge of deep space heat dissipation. Large heat sinks could not be used due to interference with the solar cells and camera.

Due to the high power requirements and the large antenna sizes that are necessary for this project, the laser system was decided upon. However, if large antennas can be developed, a 10^7 bit/sec S-band microwave system would be entirely possible.

REFERENCES

1. Airborne Instruments Laboratory, "High-sensitivity Infrared (10.6) Heterodyne Receivers, Parts I & II", IEEE Spectrum, June, 1968, p. 5, July, 1968, p. 5.

2. Baird-Atomic, "Electro-optic Light Moculators, KDP, ADP, KDP", June, 1967.

3. EG&G Electronics Products Division, "Data Sheet AV-102 Silicon Avalanche Photodiode", November, 1967.

4. Ealing Optical Services, "Ealing-TFP Interference Filters", Ealing Catalogue 1968-1969, p. 142.

5. EMI Electronics Limited, "EMI Photomultiplier Tubes".

6. ITT Industrial Laboratories, "S-25 Photocathode", ITT News Letter, January, 1968.

7. Anderson, L. K. and McMurtry, B.J., "High-Speed Photo-detectors", Applied Optics, October, 1966, p. 1573.

8. Chapoton, C.W. and White, J.W., "Deep-Space Optical Communications", Communication Satellite Systems Technology, Vol. 19, AIAA, May, 1966 p. 909.

9. Fowles, Grant R., Introduction To Modern Optics, pp. 36-43, 191-193.

10. Fusica, James A., Space/Aeronautics, "Laser Communications", May, 1964, p. 59.

11. Gray, A.H., "Memoes on Tracking and Ranging", Emerson Electric, December, 1967 - May, 1968.

12. Heidbreder, G.R., "PCM Noise Considerations", UCSB, June, 1968, p. 1.

13. Horan, J.J., "Spacecraft Infrared Imaging", IEEE Spectrum, July, 1968, p. 66.

14. Kalil, F., "Optical & Microwave Communications", NASA TN D-3984, June, 1967, p. 1.

15. Kerr, J.R., "Microwave-Bandwidth Optical Receiver Systems", IEEE Proceedings, October, 1967, p. 1686.

16. Landry, John, Graduate Student, University of California at Santa Barbara.

17. Lozin, N.G., "Pointing In Space", Space/Aeronautics, August, 1966, p. 76.

18. Nelson, Donald F., "The Modulation of Laser Light", Scientific American, Vol. 218, Number 6, June, 1968, p. 17.

19. Otten, K.W., "Optical Communications", Aerospace Electronics, November, 1962, p. 39

20. Richards, G.P. and Bisignani, W.T., "Redundancy Reduction/Course-Fine Encoded Video", IEEE Proceedings, October, 1967.

21. Shumate, M., et. al., "Weather Dependent Data Links", NASA/JPL Task #125-22-02-01, July, 1967, pp. 1-79.

23. Sommers, H.S. and Gatchell, E.K., "BLIP Conditions In Optical Communications", IEEE Proceedings, February, 1967, p. 189.

24. Stiffler, J.J., "Telecommunications", Space Technology, NASA SP-69, Vol. 5.

25. Johnson, Robert, E., "The Millimeter Wave Compromise", Space/Aeronautics, Vol. 44, July, 1965, pp. 62-68.

26. Senitzky, B., "Use of Gases on Millimeter Wave Devices", Vol. 10, November, 1967.

27. Dickens, L.E., "Millimeter Wave Diodes For Harmonic Power Generation", IEEE Transactions on Microwave Theory and Techniques, Vol. 15, No.2, January, 1967.

APPENDIX D: SCIENCE PAYLOAD

APPENDIX D (Continued)

MULTI-SPECTRAL LINE SCAN CAMERA

Light Intensities and Detection

The multispectral scanner detects reflected sunlight from the surface of Mars. The power incident over a wavelength band of $\Delta\lambda$ from a ground cell of a length a on a side gathered by a lens or mirror of diameter D is given by

$$P_i = a^2 D^2 P_o \rho \gamma^2 \frac{\Delta\lambda}{8h^2} \cos^2\psi$$

where P_o = incident power on the surface
ρ = the surface reflectivity
γ = the atmospheric transmittance
ψ = the sun vertical angle
r = altitude of the satellite

The surface reflectivity varies with the composition of the surface from ~.05 to more than .5. Unfortunately the most interesting areas are likely to have a low reflectivity. For a sample calculation ρ = .1 seems reasonable, and an atmospheric transmittance of 0.8 is conservative for any of the bands used in our proposal. From the selected orbit, the average sun zenith angle will be approximately 70°. The altitude is 2×10^{-12} meters and the bandwidth = .1μ or more. Solar power incident on Mars is about .48 the level at 1AU, or about 750 watts/m^2. Using these numbers $P_i = 6.36\times10^{-12}$ watts, which represents more than 10^6 photons/sec. At the shortest wavelength involved, this level is more than sufficient for detection at the prescribed scan rate. Pictures in all bands at a usable signal to noise ration can be expected for most of the orbit.

The light to be detected is subject to optical attenuation in the optical fibers and mirrors. The attenuation can be calculated from known reduction and packing factors of the optical system.

$$\sigma = P_1 P_2 \sigma_1 \sigma_2 \sigma_3$$

P_1 = .67 = the packing factor on the image plane, and P_2 = .65 = the packing factors of the multiple bundles. These packing efficiencies can be computed from the geometry of the plane and are a measure of the reception efficiencies.

$$P = \frac{\pi r^2}{d^2}$$

is the reduction factor of the image fiber optics which is a function of the total length and diameter. σ_2 and σ_3 are reduction factors for the mirrors, lenses and prisms.

$$\sigma_1 \sigma_2 \sigma_3 = .90 \text{ for the system}$$

These parameters yield a total system reduction of 36.4% or σ_T = .364.

Data Bit Rates

The data transmission rate is determined from

$$B.R. = Nn\,C,$$

where N is the number of cells covered in a unit time, n is the number of bands to be transmitted, and C is the bits per data point. The data transmission rate of the communications link was given at 10^7 bits/sec Within this remarkably liberal constraint the data production rate parameters had to be optimized to yield the most return for the received data.

We assumed that the raw data could be compressed by a factor of 3. This figure is conservative by present day standards, however, state-of-the-art in this area indicated that 5 is not an unreasonable figure. The 6 bit format over five channels was selected. The wavelengths of these channels lie well within the capability of the optical system to resolve to the prescribed two meters, represent the spectrum near the solar peak, and the regions of most intense interest for photographic investigation. Using the 5 band and bit format the data rate is 3.0×10^{-1} N bit/sec., where N is given by the resolution cell dimension, ground velocity and swath width.

$$N = \frac{VL}{a^2}$$

where $V = 3.2\times10^3$ m/sec., $L = 10^3$ m, and $a = 2$m. For the given numbers our point rate is 8×10^5 points/sec. The overall data production rate is 2.4×10^7 bits/sec. Applying a compression factor of 3 to this rate yields a bit rate of 8×10^6 bits/sec. for transmission.

Mars is a low contrast object over most of the surface. The 6 bit word was selected as being sufficient since 5 bands are detected. This gives a sufficiently fine shading differential and still retains a reasonable dynamic range. The use of an 8 bit word was investigated but was rejected as too fine a 5 band system, although there is no way to be sure of the informational redundancy of a particular code when little or no information is available about the nature of the object being scanned.

The particular coding procedure and word length selected is considerably less critical as a system constraint than illumination and point rate considerations, thus considerable latitude can be allowed in a preliminary design. Nevertheless the 6 bit word seems reasonable from past experience.

Object Image Scanner Comparison

Primarily, two alternatives were open for consideration as methods for photocoverage of the Martian surface; Multi-spectral scanning and vidicon or more traditional television techniques (frame pictures). The advantages of the scanner are:

1. Compatibility with real time transmission

2. Higher grade information

a. parallel, point by point production and correlation of the spectral bands.

b. greater flexibility in choice of optical apparatus.

c. the possibility of utilizing considerably more sensitive detectors than can be used in the vidicon camera.

The advantages of the vidicon camera are:

1. Simple construction and operation yielding a high reliability

2. Variable field of view and resolution

3. Easily variable information production rate.

In order to choose between the two systems a projection of our knowledge of Mars in the 1975-80 period was required. It was assumed after investigation that a coarse photosurvey of the planet would have been accomplished prior to this mission.

Our assumptions on the prior work that would have occurred led us to believe that the emphasis of our mission should lie in obtaining high-grade, high-resolution photographs of the surface areas most important in Martian investigation at the expense of reduced coverage.

The light levels obtainable from the desired orbit indicated that either long exposure times or restrictively large optical systems would be dictated by the use of vidicons.

These considerations led us to the selection of the multispectral scanning concept.

Image Versus Object Scanning

Several existing systems and proposals were examined to determine their adaptability to our mission requirements. The most representative of these were the Hughes Multispectral point scanner and the Stanford Earth Resources Satellite proposal. The Hughes design was developed in conjuntion with the Applications Technology Satellite. It utilized a vibrating mirror object scanner. The Stanford Group proposal used an image scanner system employing a high speed motor system. It was decided that the motor scanner was a better choice for our mission because of the speed limitations inherent in oscillating a large mirror. Also an oscillating mirror system suffers from duty cycle limitations that make it incompatible with real time transmission for continuous coverage.

A sample calculation clarifies the disadvantage of the object scanner. With a ground velocity of 3.2 km./sec. 2 m. resolution dictates 1600 lines scanned per second. Using a nominal value of 10 channels before restrictive detection complexity becomes a constraint, this requires a mirror scan rate of 160 Hz. It is unclear how this could be accomplished using a mirror of the size required (1.5x1.2 m.). This high scan rate could also be the source of linearity problems near the edges of the mirror.

The use of the Stanford concept allows with some modification the use of more channels for scanning than need be detected. For example, in our actual design the image falls on 16 channels; however, because of the scanning arrangements only 4 separate detector packages are required to detect the light on all sixteen channels.

The scanning motor of the Stanford proposal camera rotates at relatively high RPM (10000). Our system reduces this figure somewhat through the use of more channels and the reduced orbital velocity at Mars; however, this problem of high speed rotating devices maintaining the fine tolerances with a reliability required by this mission has yet to be solved and is an area of research requiring investigation.

Calculation of Focal Plane Image Sizes and Fiber Optic Acceptance Angles

The calculation of focal plane sizes and fiber optic acceptance angles is routine. The sizes of the fiber optical tubes and the half angles involved for this system are all intentionally conservative and well within the state-of-the-art. The separation distance between the image fibers and the scanning fibers was increased to as large a figure as was felt reasonable. This was done to minimize the technical problems of close tolerance maintenance in the rotating scanning system. However, these problems are still important and must be further investigated. Proposals of rotating scanners of higher speed and more critical tolerance intervals have been made and represent an important field of investigation in multispectral scanning.

Calculation 1:

Size of focal plane and fiber optics in plane if 2m resolution and 1 km swath width is desired.

size of plane = $\frac{w}{h} F$

w = 1 km = swath width
h = 200 km = satellite altitude
F = 4.8 m = focal length

size of plane = 2.4 cm

Calculation 2:

size of resolution element in image plane = $\frac{a}{h} F$

a = 2 m = size of ground resolution cell
F = 4.8 m = focal length
h = 200 km = satellite altitude

size of resolution element in image plane = 48 μ

Calculation 3:

fiber optic pipes used for scanning

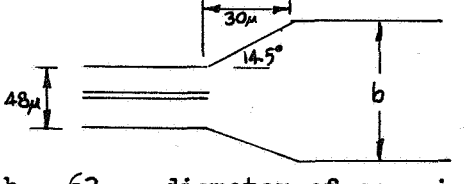

b = 63 μ = diameter of scanning fiber optic pipes

$b = d + 2c \sin\theta$
b = diameter of scanning fiber optic pipe
d = 48 μ = size of image on image plane
$\theta = 14.5^\circ$ = dispersion of light out of fiber optics which is the same as the light entering. This angle is a function of the size of the aperature over the focal length

Vidicon Video Subsystem for Extremely Fine Resolution Photography

The use of the large diameter primary mirror in the Multi-Spectral Line Scan system was dictated by illumination restrictions arising from high speed scanning requirements. The resolvency of the scanning system cannot, unfortunately, be made to match the optical diffraction limit of such a system; however, the size of the mirror is such that the system offers attractive possibilities for extremely high resolution photography.

The diffraction limit of a telescope lens system is a function of the diameter of the primary mirror. The angular resolvancy is given by

$$\theta = \frac{1.22\lambda}{D}$$

this yields for the 120 cm mirror an angular resolvency of 0.5μ radians at a wavelength of 0.5μ. This angle subtends an arc length of 10 cm on the surface of Mars at an altitude of 200 km.

The light intensity from such a small area precludes scanning to this resolution; however, if a vidicon were introduced at the image plane and the camera was servo controlled to remain fixed on this point, a high resolvency image could be obtained.

The illumination from 20x20 cm ground cell gathered by the primary mirror indicated that the telescope must be maintained on the object for a considerable length of time. Using approximate figures of 300μ amp/lumen scene brightness at one foot lambert and neglecting considerations arising from time exposure problems, the time required to form an image of signal to noise ratio compatible with the communications data link is on the order of one to ten seconds. This would require extremely accurate servo control of the camera platform and scanning mirror. At 200 km the mirror angular velocity is about 1°/sec. This would have to be accurate to 0.5μ radians or one part in 10^5 to be maintained for one to ten seconds. This problem offers an attractive area of research and development for future work. The high tracking accuracy required is very close to that required by the laser communications system. Thus there exists a possibility of slaving the camera to the communications servo mechanism.

Band Selection

The selection of sensor bands and bandwidths for the Multi-Spectral Line Scanner is controlled by considerations of signal strength, transmission and detection properties, and information and scientific value. From the standpoint of Martian surface studies, visible and near-infrared radiation offer the best regions for resolution and comparison of physical structures of the planetary surface. From the standpoint of signal strength, radiation near the solar peak must be used to obtain a detectable image at the given resolution, height, scanning rate, etc. of the designed camera. An examination of the Mars spectral irradiance curve shows that maximum irradiance occurs at the solar peak of $.5\mu$ and this remains at a usable level to about 2.0μ. Thus, from sensitivity restrictions, if reasonable small bandwidths ($.05 - .2\mu$) are to be used, we must confine our scanner to this region.

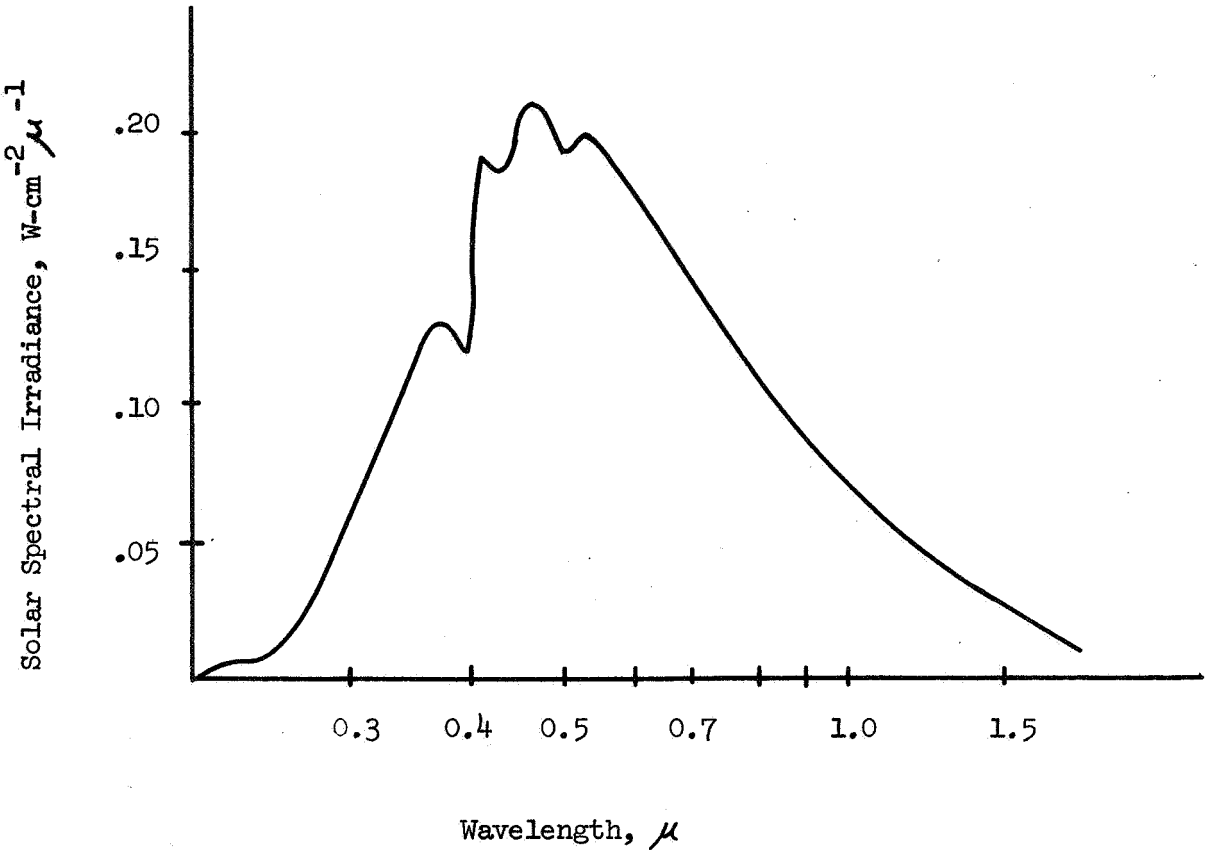
Solar Spectral Irradiance, W-cm^{-2} μ^{-1}
.20
.15
.10
.05
0.3
0.4
0.5
0.7
1.0
1.5
Wavelength, μ

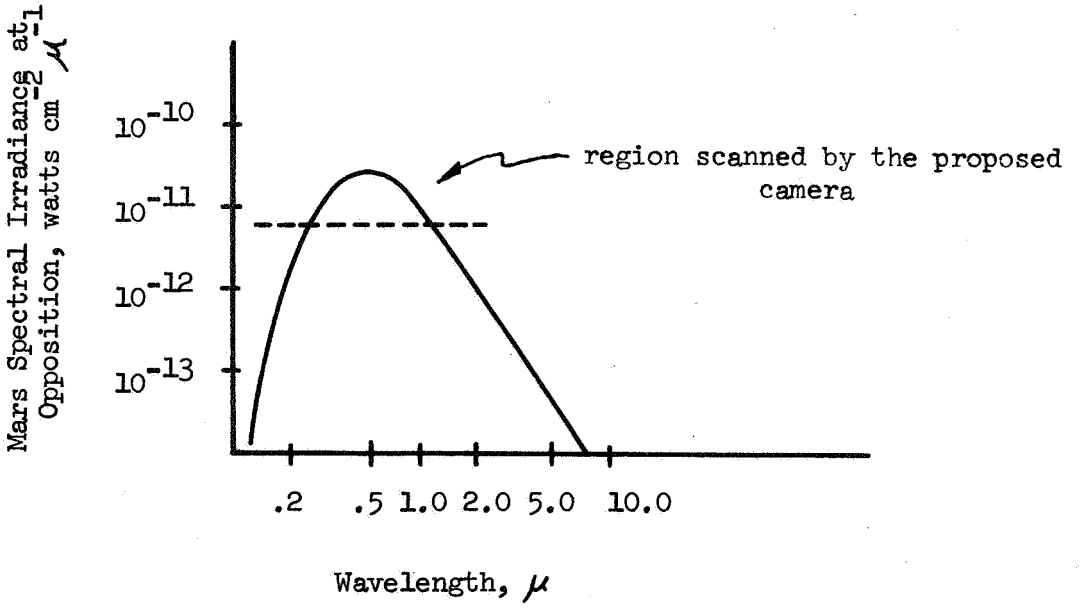
Mars Spectral Irradiance at Opposition, watts cm^{-2} μ^{-1}
10^{-10}
10^{-11}
10^{-12}
10^{-13}
region scanned by the proposed camera
.2
.5
1.0
2.0
5.0
10.0
Wavelength, μ

Figure D-1

Current technology in fiber optics indicates that reasonable transmittance in a single fiber can be maintained from .4μ to a little over 1.1μ.

In order to avoid restrictive complexity in the scanning apparatus, it was decided to limit the total bandwidth that could be transmitted in one fiber. On this basis, it was decided that the bands would extend from .45μ to ~1.1 - 1.2μ .

Five bands for detection over these wavelengths were selected for two reasons:

1) Signal levels in bands much less than .1μ in interval would be difficult to detect with sufficient S/N of projected photo-multiplier devices.

2) The use of more than five bnads would result in greater scanner and detector complexity and communications problems than the additional data provided would be worth.

The bands were allocated into three visible, .45 - .55μ, .55 - .65μ, .65 - .75μ, and two near-infrared, .75 - .9μ and .85 -1.2μ.

These bands would permit observation of the surface and lower atmosphere in three colors. The .45 - .55μ band would also allow observation of fine structures in the "blue haze," if such exist. Also, the reflectivities of most suspected Martian surface materials are reasonably high in one or more of these wavelength channels.

The overall sensitivity of the camera could be increased through the combination of two or more of these bands, lying adjacent to each other, onto one photomultiplier. This could result in an image formed on the dark side of the planet if the scan rate were reduced somewhat; however, this instrument can only work well over the sunlit regions of the planet.

The possibility of including a longer wavelength band using cooled detectors and scanning techniques other than fiber optics was considered. One such proposal was made for a 10 - 12.5μ band which would be scanned behind a slit on the image focal plane. This bandwidth would be to much lower resolution than the optical and near-IR radiation (~50 - 100μ). This proposal was rejected because it was unclear what value could be derived from such a system that could not be essentially gained from IR radiometric techniques. Experiments yielding temperature maps and IR atmospheric readings would already have been performed or are provided for elsewhere.

The size of the image plane is such that considerably more detection equipment could be placed there than is called for in the basic Multi-Spectral Line Scan design.

One addition that was proposed was a correlated Lidar altimeter that would produce range and altitude information parallel to the image scanner and to the same horizontal resolution. This proposal is discussed elsewhere in the report.

LASER RADAR PROFILE MAPPING SYSTEM

The following pages represent an analysis of the proposed laser radar mapping system. This includes a brief discussion of general theory, an analysis of the important parameters, and various conclusions reached from the analysis. Five radar systems were investigated—incoherent side-looking radar, coherent synthetic-aperature side-looking radar, bistatic radar, pulsed laser radar, and frequency modulated continous wave laser radar. The later, FM-CW laser radar has been chosen as the best system and the analysis follows. A discussion of the other systems mentioned follows this main report.

Theory

Before any design can begin, one must know some general theory of radar mapping. The following represents a cursory examination of the basic principles.

Like conventional radar, laser radar transmits a wave that will propagate through space (or atmosphere, but, of course, with absorption and scattering) until it encounters the target. The target will scatter the laser wave in all directions. Some of the energy, however, will return to the receiving antenna where it can be analyzed. The distance, R, from the transmitter to the target is given by $R = \frac{MCT \sin \phi}{\sin \theta + \sin \phi}$ (ref 1)

Where M is the propogation constant of the media
C is the velocity of light
T is the time of travel
θ, ϕ are the reference angles for pointing and receiving the beam

The only critical unknown is the time of travel, T. For the proposed 200 km synchronous orbit, T would be approximately 1.33 milliseconds. There are various schemes of determining the time or getting around of directly computing this quantity.

In the proposed frequency modulated continuous wave optical radar (FM-CW), the transmitter frequency is changed as a function of time in a known manner. Assume that the transmitter frequency to be modulated is a triangular frequency modulated waveform as shown in Figure D-2.The dashed line in the figure represents the return signal. If the local frequency signal, which has a time delay T', is heterodyned with the return signal in a mixer, a beat frequency will be produced. The beat frequency is a measure of the target range. If the frequency is modulated at a rate of f_m over a range Δf, the beat frequency is

$$f_b = (T - T') \, 2 \, f_m \Delta f \qquad \text{(ref 2)}$$

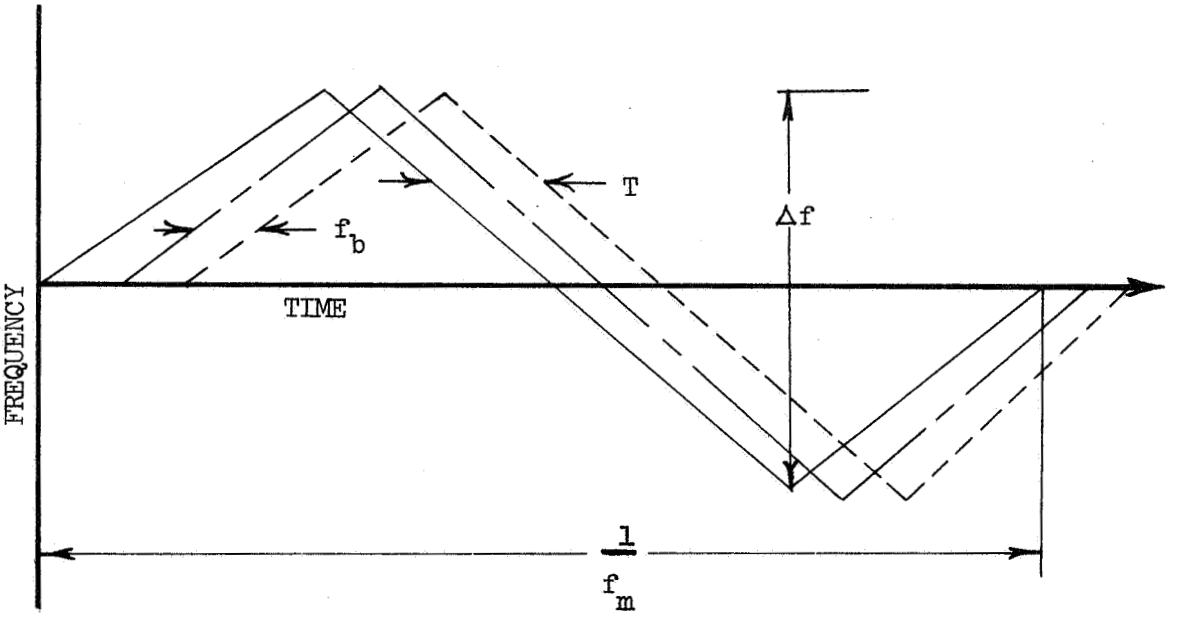

——————— Transmitted signal

— — — — Received echo

——————— — Local oscillator signal

Figure D-2 Frequency Time Relationship in FM-CW Laser Radar

Substituting for T in (1) yields

$$R = \frac{MC \sin \phi}{\sin \theta + \sin \phi} \left(\frac{f_b}{2 f_m \Delta f} + T' \right)$$

Thus the measurement of the beat frequency determines the range R.

Another important application of lidar is that it can measure the rotation speed of a body to high accuracy. This is accomplished by observing the Doppler shift of the returning carrier waveform. The Doppler shift f_d is given by

$$f_d \approx \frac{2 V_r}{\lambda} \quad \text{(ref 3)}$$

where λ is the carrier wavelength

V_r is the radial component of the velocity of the target

But V_r is related to the angular rotation of the target by

$$W = \frac{V_r}{\theta (h+r)} \quad \text{(ref 4)}$$

where θ is the instantaneous elv. angle of the scanner

h is the orbit altitude

r is the radius of the target

Therefore, substituting for V_r in (4) gives

$$W = \frac{f_d \lambda}{2\theta (h+r)}$$

Thus measurement of the Doppler frequency shift determines the angular velocity of the target.

Transmittance of the Atmosphere

Absorption, turbulance, and scattering are the three main sources of energy loss encountered in propagation of electromagnetic waves through the atmosphere. A light beam passing through the atmosphere suffers both absorption and scattering. The attenuation in a pure atmosphere consisting only of permanent gases is caused by scattering from the gas molecules and is proportional to the inverse fourth power of the wavelength. Consequently, the attenuation of a 1 micron laser could be reduced by 1/81 by raising the wavelength to 3 microns. The absorption bands of CO_2 occur at 2.7 μ, 4.3 μ, 15 μ, and for O_3 they occur at 4.3 μ, 9.6 μ, and 14.2 μ. Fig. D-3 shows the spectral irradiance outside the terrestrial atmosphere of Mars. There seems to be a window in the 2.3 u to 3.5 μ range. Consequently, a wavelength range of 2.3 μ to 2.6 μ or 2.8 μ to 3.5 μ would be the best choice for laser operation in the Martian atmosphere. Shorter wavelengths (.4 μ to 1.2 μ) were not considered because of the possible interference with the proposed multi-spectra system.

The present state of the art of CW lasers shows CaF_2 Dy^{+2} doped laser (.75 watts) operates on the 2.36 μ wavelength, CaF_2 U^{3+} doped laser (1 watt) operates on 2.5 μ wavelength, Xe gas laser operates on 3.5 u wavelength, and He Ne gas lasers operate on many wavelengths in the required bands, but with only low power.

Figure D-3 Spectral Irradiance of Mars

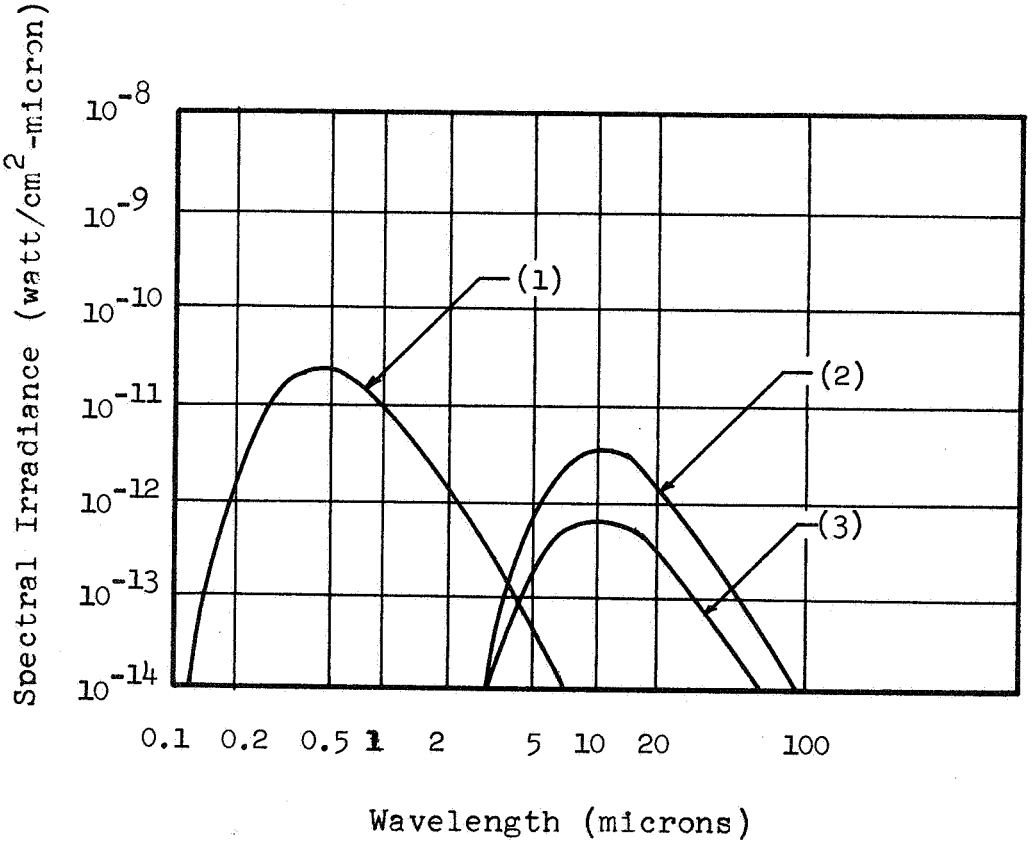

(1) Calculated irradiance from Mars, at brightest, due to sun reflectance only.

(2) Calculated irradiance from Mars, due to self-emission only. Superior planet at opposition.

(3) Calculated irradiance from Mars, due to self-emission only. Superior planet at quadrature.

Proposed System

General Description

The system to be considered is shown in Fig. D-4 It is a frequency modulated continuous wave (FM-CW) laser altimeter. The transmitter has a laser source, a modulator, and an optical transmission system. The modulator is also connected to a local oscillator through a delay line, which feeds into the mixer of the receiver. The receiver has an optical receiver scanning system, an optical amplifier, a mixer, amplifier, discriminator, and processing system.

In the transmitter, the laser source generates a light beam with a power of P_t (λ) watts, which acts as the carrier for the modulation. The modulator imparts to the light beam a variation which contains the information in a bandwidth of Δf Hz. The optical system has a transmittance which accounts for the losses of the system, and optical gain, G_t, which normalizes the power in the beam to that from an equivalent isotropic radiator. $G_t = \frac{4\pi}{\Omega}$, where Ω is the solid half-power beamwidth of the transmitter beam and given by $\Omega = \frac{\pi \theta_d^2}{4}$, where θ_d is the angular resolution.

The optical receiving system collects and focuses the power to the amplifier which in turn is fed into the mixer. The local oscillator signal acts as the reference signal required to produce the beat frequency. The beat frequency signal is amplified and fed into a frequency discriminator. The discriminator output is a voltage proportional to frequency and is continous rather than discrete. This is followed by a signal to digital conversion unit.

Pointing Optics

The transmitted beam will be directed towards the surface of the planet by focusing the laser beam through a lens and onto a rotating warped conical mirror. The light impinges on the side of the cone and reflects off at a predetermined angle and down on the planet. Any given element of the cone will have a specified slope; thus giving a particular direction to the reflection. The cone, of course, will be warped since each element will have a different slope. The cone will be rotated at a speed that will give the required sweeping rate. Fig. D-5 gives a rough idea of what is to be desired.

Scanning Optics

The scanning system will be quite similar to that of the multispectral camera system. For 2m resolution with a swath width of 1 km, there must be at least 2000 fiber optics. These fiber optics will be scanned 1600 times per sec. This figure corresponds to a motor speed of 96,000 rpm which is quite high. This speed can be reduced by a factor of eight by packing the fiber optics in a quarter circle instead of a full circle and adding another scanner motor (let each scanner scan 1000 fiber optics) and switching system. Future work should, however, be done in trying to reduce the scan rate by other methods. Once

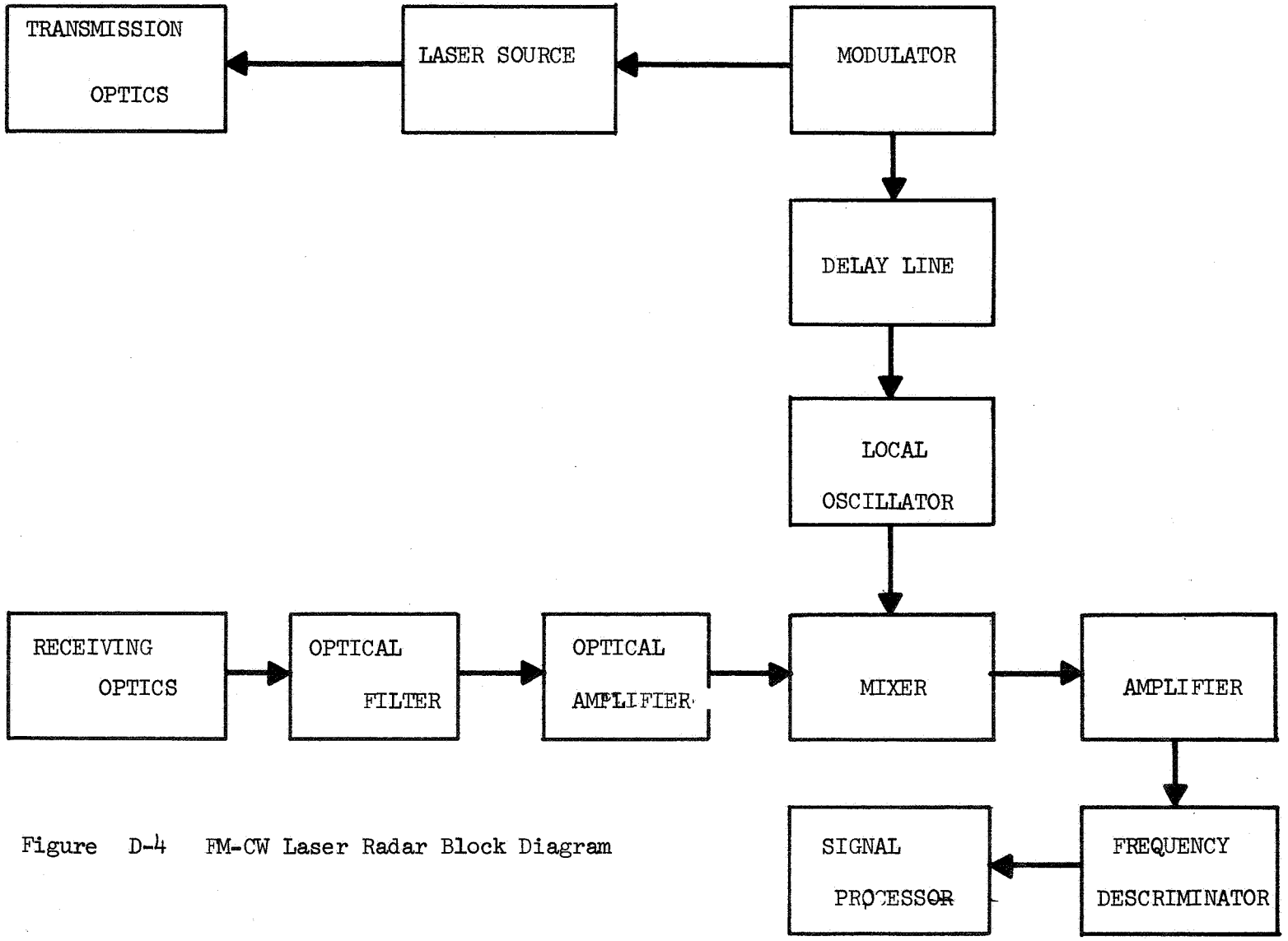

Figure D-4 FM-CW Laser Radar Block Diagram

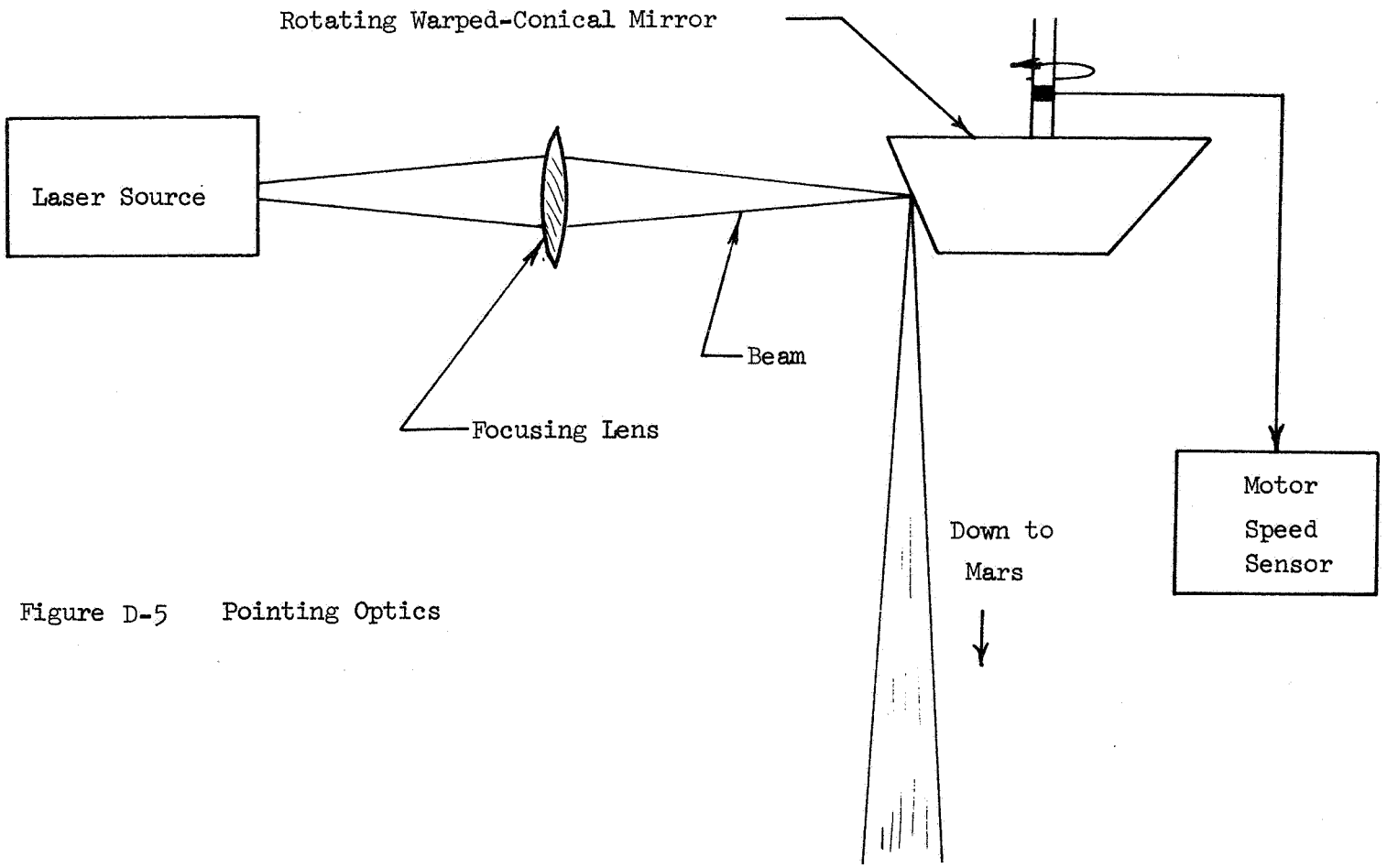

Figure D-5 Pointing Optics

the fiber optic has been scanned, it is fed by other fiber optics to the detector. Figure D-6 shows the optical scanner system.

The possibility of using the scanning system of the multi-spectral camera system to monitor the return signal of the laser has been investigated briefly. It does seem quite feasible and thus some of the redundancy of the observation systems could be reduced. Also, it would be possible to achieve a more positive correlation between the laser and camera maps. This system is contained in abstract form in the appendix.

Stability Requirements

Since the data rate can be continous using the FM-CW altimeter, the platform stability must be within to $\frac{1}{2}$ beamwidth of the optical systems. This requires a continuous platform stability of 1 second arc (in roll and pitch) for receiver and transmitter optical and laser components. The yaw stability is less critical and will be governed by communication restraints.

Transmitting Optics

It was decided to use 2 meter resolution to be consistent with the multi-spectral system and thus give good correlation possiblities. For a 200 km orbit, 2 seconds of arc beamwidth is required. These requirements are well within the present state of the art of optics.

Receiving Optics

The aperature arc of the primary collecting parabolial mirror will be taken as 1 square meter (which is in full agreement with the multi-spectral system), and with a hyperbolical secondary mirror forming a pseudo-Cassegrainian reflective optical system. The optical system transmittance was taken as .6 which includes the losses in a 10 Angstrom optical filter to exclude background noise lying outside the spectral region occupied by the returned laser signal.

For the detector, a Bolometer or cooled semi-conductor could be used. Phototubes with the present state-of-the-art give practically no response for any wavelength greater than 1u. A responsivity of .4 $\mu a/\mu w$ and rise time of 10^{-11} seconds with a dark current of 10^{-9} amps were chosen as values that could be expected by the next 10 years. Photomixing will be accomplished by photomultipliers. Traveling-wave phototubes and photodiodes are also possible choices.

Proposed System Parameters

The following system parameters represent the proposed FM-CW laser radar profile mapping system.

Figure D-6 Receving Scanning System

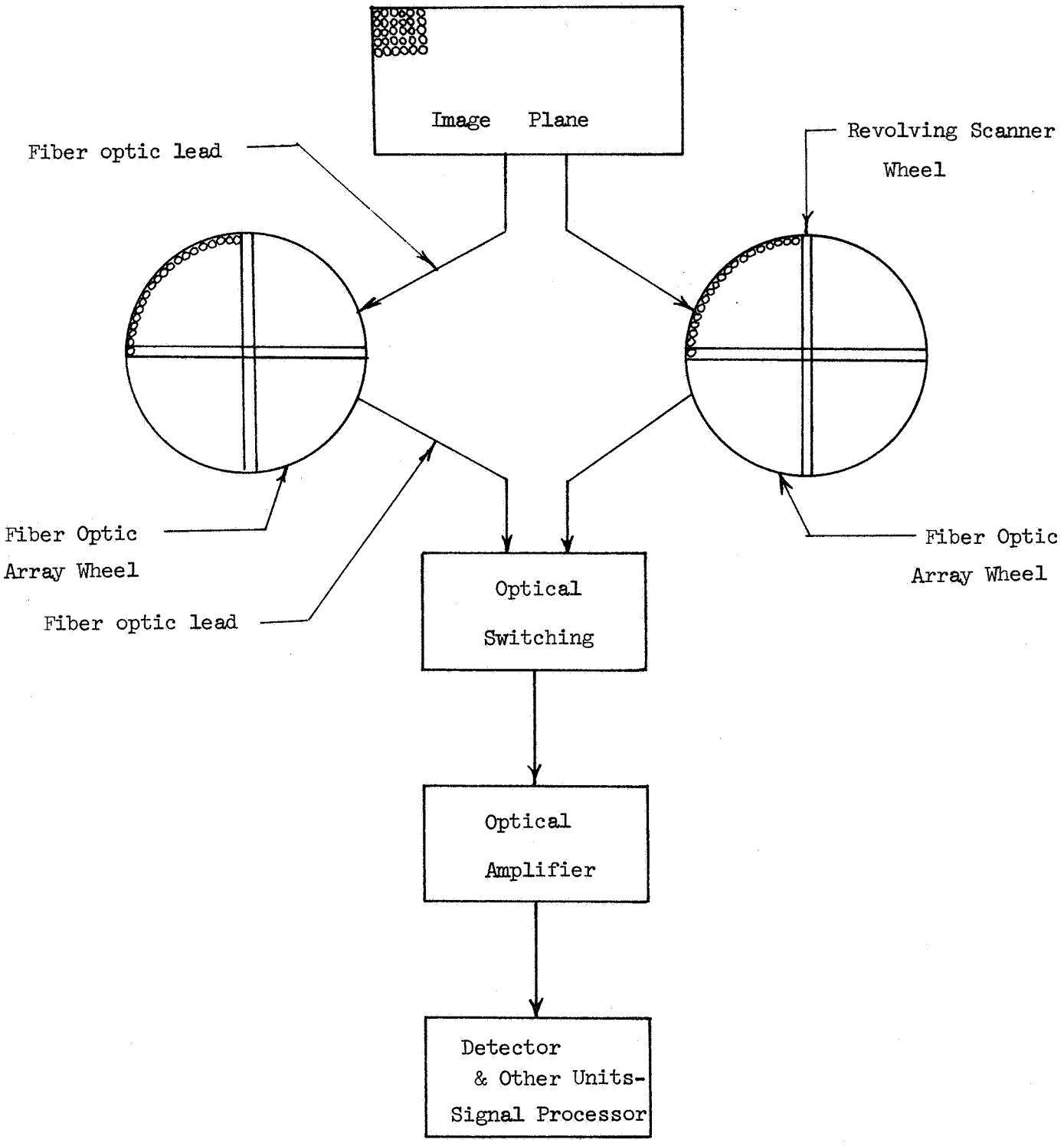

SYSTEM PARAMETERS

Velocity of Spacecraft (V)	3.44 km/sec
Altitude of Spacecraft (h)	200 km
Transmitting Aperture Beamwidth (β)	2 seconds
Transmitting Optical Transmittance (n_t)	0.9
Receiver Light Amplifier Gain (G)	30 db
Receiver Optical Transmittance (n_r)	0.6
Receiver Aperture Area (A_r)	1.0 m^2
Signal-to-Noise Ratio (γ)	10
Operating Wavelength (λ)	2.5 μ
Modulation Frequency (f_m)	1.14 khz
Ground Resolution (r_R)	2.0 m
Atmospheric Transmittance (T)	0.90
Ground Reflectance (p)	.03
Detector Responsivity (R)	.40 μamp/μ watts
Data Rate (DR)	800 k $\frac{\text{res.elm}}{\text{sec}}$
Bandwidth (Δf)	10 mhz
Swath Width (W)	1 km
Range Accuracy (Δr)	1.5 cm
Scanner Rate (ζ)	96 K rpm

INPUT POWER REQUIREMENTS

Transmitter

CW Laser.....	$\frac{3.08 \text{ watts}}{.005 \text{ efficiency}}$	617 watts
Modulator.....		25 w

Receiver

CW Laser Amplifier.....	$\frac{.2 \text{ watts}}{.001 \text{ efficiency}}$	200 w
Optical Laser Oscillator....	$\frac{.1 \text{ watts}}{.001 \text{ efficiency}}$	100 w
Photomixer, Amplifier, & Discriminator.....		50 w
Processor (Spectrum analyzer and coding).....		100 w
Servomechanisms.....		10 w
	Total	1102 w

The receiver electronic circuit components are all solid state.

SYSTEMS WEIGHT

Transmitter

Optical System (lens & rotating mirror)	15 lb
CW Laser	50 lb
Modulator	1 lb

Receiver

Pseudo-Cassegrainian Reflector Optical System (an aperture of 1.17 m and made of coated beryllium metal, parabolidial mirror)	20 lb
CW Laser Amplifier	10 lb
Optical Local Oscillator	10 lb
Photomixer detector (Bolometer), Delay Line, Amplifiers, Discriminator	50 lb
Indicator or Converter	50 lb
Optical System Pointing Servomechanism	10 lb
Total	216 lb

SYSTEM PHYSICAL SIZE & VOLUME

Transmitter

Transmitter Optics (lens & rotating mirror).....	1.0 ft^3
CW Laser with Modulator (10 inches diameter and 3 feet long).....	1.6 ft^3
Laser Power Supply.....	1.5 ft^3

Receiver

Pseudo-Cassegrainian Optical System with photomixer (3.2 ft dia. & 3 ft long.....	7.7 ft^3
Laser Optical Amplifier (4 in dia. & 10 in long)...	125 in^3
Laser Local Oscillator (4 in dia. & 10 in long)....	125 in^3
Laser Power Supply.....	2 ft^3
Amplifier, Delay Line, Discriminator.....	1 ft^3
Processor or Indicator Unit.....	1.5 ft^3
Total	18.5 ft^3

System Calculations

The velocity of the spacecraft will be taken as 3.44 km/sec for a 200 km sun synchronous (85%) orbit. The usual desired signal-to-noise ratio of 10 will be assumed. Receiver light amplifier gain will be 30 db. for present state-of-the-art amplifiers. Atmospheric transmittance of Mars will be taken as .9 which is reasonable since the atmosphere is thin and a 2.5 μ wavelength provides little absorption of the wave. Receiver and transmitter optical transmittances will be taken as .6 and .9, respectively, which are conservative estimates, considering the present state-of-the-art.

Tramsmitting Aperture Beamwidth

A high resolution of 2 meters is desired with a swath width of 1 km. This means that the beam can only diverge 2 m after traveling 200 km or

$$\beta = \frac{r_R}{h} = \frac{2m}{200\,km} = 1 \times 10^{-5}\ radians$$

We also know that

$$\beta = \frac{k_2 \lambda}{D}$$

where k_2 is equal to 1.22

D is the diameter of the mirror if a focusing mirror were used

Hence,

$$D = \frac{k_2 \lambda}{\beta} = \frac{(1.2)(2.5 \times 10^{-6})\ m}{1 \times 10^{-5}\ rad} = 30\ cm$$

Bandwidth

The bandwidth is a critical factor. It must be made large enough to compensate for the Doppler shift, i.e.,

$$\Delta f > f_d$$

By having a large bandwidth, extremely high range measurements can be made, but high laser power results since the required laser power is directly proportional to the size of the bandwidth. Consequently, the bandwidth will be made as small as possible to meet power restraints.

The Doppler shift frequency is given by

$$f_d = \frac{2 V_m s}{\lambda}\left(\frac{1}{r} + \frac{1}{h}\right)$$

where V_m is the circular surface velocity of Mars

s is half of the swath width w.

Therefore,

$$\Delta f > \frac{(2)(3.548\ \frac{km}{sec})(500\,m)}{2.9 \times 10^{-6}\,m}\left(\frac{1}{3415\,km} + \frac{1}{200\,km}\right) = 7.5\ mHz$$

Hence, let Δf = 10 mhz for the system.

Modulation frequency

The area that must be observed per sec is

$$\dot{A} = VW = (3.20\ \tfrac{km}{sec})(1\ km) = 3.20\ \tfrac{km^2}{sec}$$

Therefore the time spent on each resolution element (2mx2m) is

$$T_{res} = \frac{A_{res}}{\dot{A}} = \frac{4m^2}{3.20\ \frac{km^2}{sec}} = 1.25\ \mu sec.$$

We should want to count about 40 cycles in this period of the beat frequency. Hence,

$$f_b = \frac{40}{T_{res}} = \frac{40}{1.25\mu sec} = 32\ mHz.$$

We know that

$$f_b = (T-T')2 f_m \Delta f$$

Assuming that $T-T' = 1.4$ millisec for a 200 km altitude, then

$$f_m = \frac{f_b}{(T-T')2\Delta f} = \frac{34.5\ mHz}{(1.4\ msec)(2)(10\ mHz)} = 1.14\ kHz$$

Data rate

The data rate is just the inverse of T_{res}, the time spend on each resolution element. Therefore,

$$DR = \frac{1}{T_{res}} = \frac{1}{1.25\mu sec} = 800\ K\ \frac{resolution\ elements}{sec}$$

If it is desired to have a four bit word or in other words, a 16 gray level scale, then

$$DR = 3.2\ mega\ bits/second$$

Ground reflection

A ground reflection coefficient of 0.03 was chosen as a reasonable value for reflection of laser light. This value was based on Table D-1. Although the reflectances are for wavelengths ranging from .48μ to .58μ, these values should represent ball-park figures of what can be expected. A more detailed study can be made later in determining the correct reflection values. It might be noted that possibly by measuring the return intensity of the laser light, it might be possible to determine some characteristics of the ground of Mars. This method is used in conventional radar to determine the dielectric constant of the material.

TABLE D-1 Visible Reflectance of Various Large Areas or Objects on the Earth

Type	Reflectance (%)
Inland waters	3-10
Oceans	3-7
Snow	70-86
Ice	75
Buildings	9
Limestone	63
Concrete	15-35
Calcereous rocks	30
Field (plowed)	20-25
Granite	12
Coniferous forest	3-10
Mountain tops (bare)	24
Deciduous forest	10-15
Sand	24
Meadow (dry grass)	3-8
Clay soil	1.5-15
Grass (lush)	15-25
Ground bare (rich soil)	7.5-20
Field crops	7-15

Fiber Optics

The minimum number of fiber optics is given by

$$N = \frac{4W}{r_R} = \frac{(4)(1)\text{ km}}{2\text{ m}} \approx 2000$$

Scanner Rate

The scanner rate is given by

$$\dot{\theta} = \frac{V}{r_R} = \frac{3.20\ \frac{\text{km}}{\text{sec}}}{2\text{m}} = 1.60 \times 10^3\ \text{times/sec}$$

Therefore, 2000 fiber optics must be swept 1600 times per second. If the fiber optics were placed in a circle, this would correspond to a rotational rate of

$$\dot{\theta} = 96{,}000\ \text{rpm}$$

Power requirements

The signal-to-noise ratio expression will be derived and, from this, the power required can be computed. To calculate the signal power available at the mixer, we define the spectral radiance of the source N_λ as the radiant power per unit solid angle per unit wavelength interval omitted from the source. For the laser,

$$N_\lambda = \frac{P_t}{\Delta\lambda_t \Omega_t A_t}$$

where $\Delta\lambda_t$ is the laser's transmittance beamwidth
P_t is the power of the transmitting source

A_t is the area of the transmitting source

Ω_t is the solid angle of the transmitter beam represented by $\Omega_t = \frac{\pi}{4}\theta_d^2$ in which θ_d is the half power beamwidth.

Consider the wavelength interval λ and $\lambda + d\lambda$. If the emitting aperture has an area A_t, the differential flux density within a beam at a distance R is

$$dP = \eta_t T \frac{A_t}{R^2} N_\lambda d\lambda$$

where the factor η_t accounts for the losses of the transmitter optics at wavelength λ and T is the factor accounting for the transmittance of the atmosphere. The power reflected back by the radar by the ground is given by

$$dP = \eta_t T \frac{A_t}{R^2} N_\lambda \frac{\pi}{4}(\theta_d R)^2 \frac{\rho}{\pi} d\lambda$$

Assume for the purpose of this calculation that the reflectivity of the ground follows the cosine law distribution into the hemisphere. The power input to the mixer is the product of G, A_r/R^2, dP, and η_r, where G is the gain of the light amplifier, A_r is the receiving aperture area, and η_r is the factor which accounts for losses in the receiver optics at wavelength λ. Thus

$$dP_r = G \eta_r \eta_t T^2 \frac{A_r}{R^2} \frac{A_t}{R^2} N_\lambda \frac{(\theta_d R)^2}{4} \rho d\lambda$$

Substituting into for N yields

$$dP_r = \frac{A_r}{\pi R^2} \frac{G \eta_t \eta_r T^2 \rho P_t(\lambda) d\lambda}{\Delta\lambda_t}$$

The detector output will be a voltage or current which is proportional to the input flux. Let the responsivity of the detector be given by $R(\lambda)$. For a photoemissive detector, the photocathode current i is

$$di = R(\lambda) dP_r$$

Substituting the expression for dP_r in the above equation, one obtains

$$i_{peak} = \frac{A_r G}{\pi R^2} \int_{\lambda_1}^{\lambda_2} \frac{R(\lambda) \eta_t \eta_r T^2 \rho P_t(\lambda) d\lambda}{\Delta\lambda_t}$$

The root means square signal current is given by

$$(\bar{i}_r^2)^{1/2} = \frac{i_{peak}}{F_1}$$

where F_1 depends on the type of modulation used. The average signal current is given by

$$I_r = \frac{i_{peak}}{F_2}$$

where F_2 depends on the type of modulation used.

There are three important sources of noise in this type of system: background, detector, and photon noise. The background noise arises from the reflection of the sun's energy by Mars. Detector noise is caused by various noise sources within the particular detector used.

Photon noise is due to the random emission and arrival of photons. For this system, as long as the photocurrent produced by the local oscillator is larger than the dark current or the photocurrent induced by the background, it is possible to achieve a signal-to-noise ratio determined by the noise in the signal. Thus for the purpose of this study, the system will be assumed to be photon noise limited.

The statistical emission of electrons at the photocathode gives rise to shot noise. The value of the noise current is given by the familar Schottky formula $\overline{i_N^2} = 2eI\Delta f$

where I is the average photocathode current. It will be assumed that $I=I_r$ for our study. The signal-to-noise ratio is given by

$$\frac{S}{N} = \gamma = \frac{\overline{i_r^2}}{\overline{i_N^2}}$$

Substituting for the above expressions and solving for P_t yields

$$P_t = \frac{2\gamma F_1^2 e \Delta f \pi R^2}{F_2 A_r G R_\lambda \eta_t \eta_r T^2 \rho}$$

Assuming that γ is 10 and we use frequency modulation ($F_1 = 2\sqrt{2}$, $F_2=2$), then

$$P_t = \frac{(2)(10)(8)(1.6\times10^{-19}\,\text{coul})(10^7\,\text{Hz})(\pi)(2\times10^{-5}\,\text{m})^2}{(2)(1\,\text{m}^2)(10^3)(.4\,\frac{\text{amp}}{\text{watt}})(.9)(.6)(.9)^2(.05)}$$

$$= 3.08\ \text{watts}$$

A special note might be made at this time concerning why frequency modulation was chosen above amplitude modulation. By employing frequency modulation, a substantial improvement in signal-to-noise ratio is obtained. This improvement is given by

$$\left(\frac{S_o}{N_o}\right)_{FM} = 3\beta^2\left(\frac{S_o}{N_o}\right)_{AM}$$

where $\beta = \frac{\Delta f}{f_m}$. The signal-to-noise ratio of 10 (which is actually for the AM case) may be increased by 20 to 30 db for wide band FM or low modulation frequency. Consequently, the power estimate is a conservative estimate and should not be regarded as being too large for satellite capabilities.

Range accuracy

The ultimate accuracy of the FM-CW laser altimeter depends upon the combined error of two factors: the measurement error and geometrical resolution accuracy. Measurement error, of course, will depend upon the signal-to-noise ratio, accuracy of the frequency measuring device, the residual path length error caused by circuitry, errors caused by multiple reflections, and the frequency error due to the turn-around of the frequency modulation. A common error that is computed is the fixed error (due to discrete frequency measurement).

$$\Delta r = \frac{150\ \text{m}}{\Delta f\ (\text{mHz})}$$

Thus for our system

$$\Delta r = \frac{150}{10} = 15\,m$$

This error can be reduced by 1/1000 with the frequency modulation discriminator used. Hence,

$$\Delta r = 15\,mm$$

The geometrical resolution error is given by

$$\Delta r = R\left(\frac{1}{2}\theta_d^2 + \frac{5}{24}\theta_d^2 + \dots\right) = 10\,\mu$$

Thus our limiting error is the measurement error =1.5 cm.

Conclusion

The FM-CW Laser Radar Profile Mapping System can perform a very useful function aboard the Mars orbiting satellite. A land profile map is essential if landing missions are desired. The advantages of laser radar have been made clear. The disadvantages can certainly be rectified in the years to come before the orbiter is launched. Future work must be concentrated in building more powerful laser transmitters and amplifiers. The power requirements of the FM-CW lidar system at the desired wavelengths are high, but with the present trend in laser technology, there is no reason to doubt that they will not be attained in the next five years. Also further research is needed in developing accurate servo techniques and platform stability mechanisms. The laser must be able to sweep at high speeds if fine resolution maps are desired.

Other Systems Investigated

Pulsed Laser Rangefinders

Much of the research effort on laser rangefinders is classified information, so the basic principles and similarities to the FM-CW laser altimeter will be discussed.

A block diagram of the pulsed laser rangefinder is given in Figure D-7. The transmitting system consists of an optical pointing and focusing system, a pulsed laser source, and a rotating G-spoiler. The receiving system contains a Cassegraining optical system with appropriate systems for scanning, detecting, amplifying, counting, and processing the signal.

The absolute range is determined by the high speed counter, but relative height of surface objects in the beam width is determined by comparing the transmitted with the return pulse. The master oscillator determines the data rate of relative height measurements. Since the output of pulsed laser waveforms are non-repeatable, this type of laser altimeter must take data on each pulse. Since the pulsed laser must be used in the scanning mode, dwell time on any particular element is small thus requiring a high pulse rate. These pulse rates are on the order of mega pps. In the present state-of-the-art, pulsed lasers are restricted to pulse rates of a few kilo-pps. However, pulse rates on the order of 10 mega-pps are hoped for in the future. GaAs lasers offer bright possibilities. Future research is needed, however, to obtain the desired pulse rates and high peak powers required by this system.

Parameters

System parameter calculations were made. Most of the system parameters remained the same as far as comparing them to the FM-CW laser parameters. Only new parameters or changed parameters are given, thus refer to the FM-CW laser section for system parameters that are not reported.

Bandwidth

For good pulse fidelity, the receiver bandwidth must be about 100 mhz. Amplitude modulation is chosen which means that we must have a high signal-to-noise ratio. Doppler effects were not investigated in this appraisal.

Power Requirements

The modified equation for pulsed laser altimeters is:

$$\hat{P}_t = \frac{\gamma F_1 \pi R^2 2e \Delta f}{F_2 A_r \eta_t \eta_r T^2 \rho R_\lambda}$$

Substituting the parameter values into this expression yields:

$$\hat{P}_t = \frac{(10^3)(2\sqrt{2})(8)(2\times10^{-5}\,m^2)(2)(1.6\times10^{-19}\,coul)(10^8)\,Hz}{(2)(1\,m^2)(.9)(.9)(.9)^2(.03)(4\,amp/watt)} = .720\ mwatts$$

$$= 720\ Kw$$

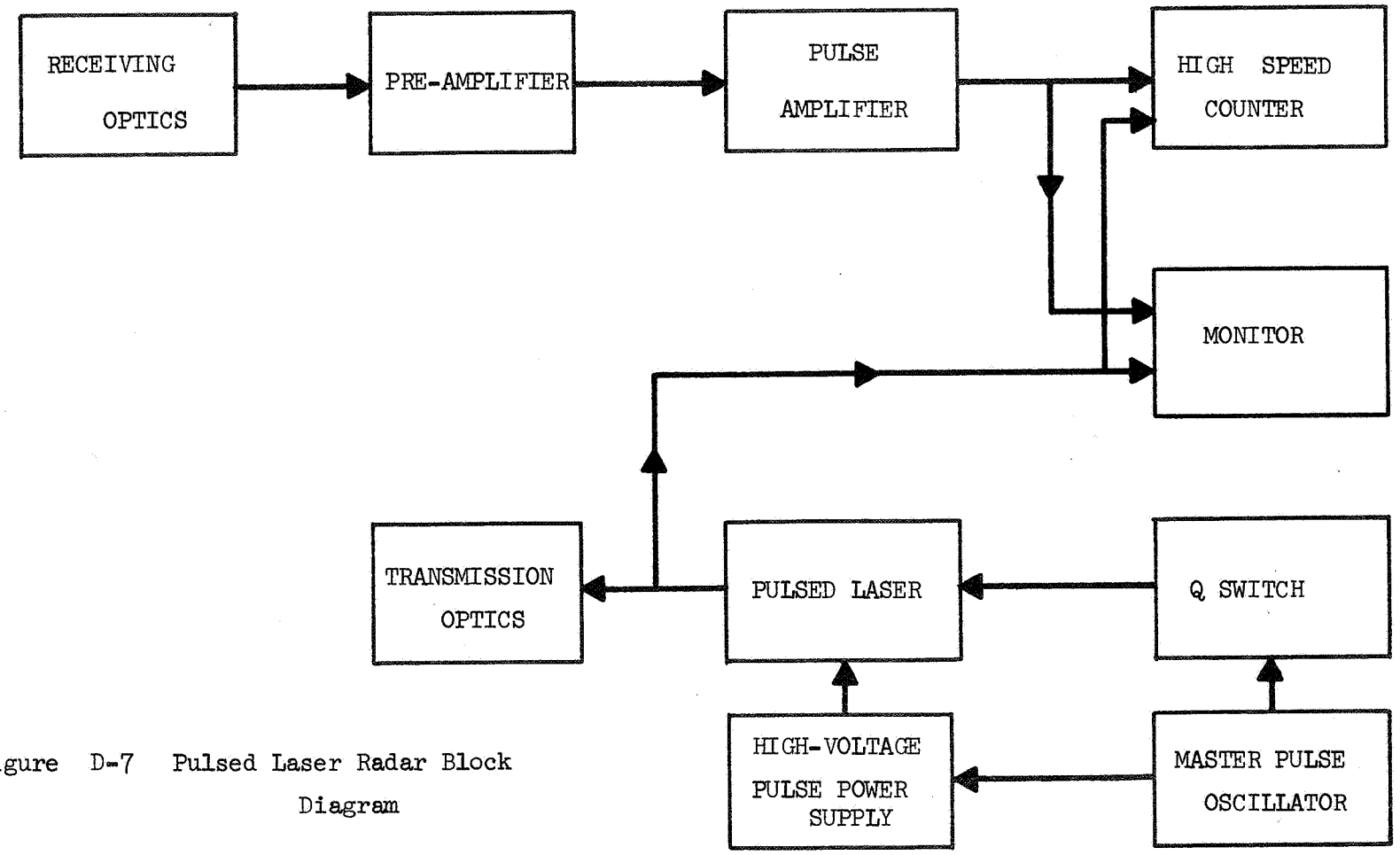

Figure D-7 Pulsed Laser Radar Block Diagram

SYSTEM PARAMETERS

Signal-to-Noise Ratio (γ) . . . . . 30 db

Ground Resolution (r_R) . . . . . 2 m

Bandwidth (Δf) . . . . . 100 mHz

Required Pulse Repetition Frequency (prf) . . . . . .800 k pps

Required Laser Output Power (P_t) . . . . . 720 kw

Data Rate (DR) . . . . . 800 k $\frac{\text{resolution elements}}{\text{sec}}$

Range Accuracy (Δr) . . . . . .6-1 m

Approximate System Power Requirements (1000 pps - low power). . 350 watts

Approximate System Weight . . . . . .150 lb

Approximate System Volume . . . . . 13.5 ft^3

Range Accuracy

The ultimate accuracy of a pulsed laser rangefinder depends upon the error in measuring pulse stretching of the received pulse as compared to the transmitted pulse. Using trained A-scope operators and having dual beam presentation, the relative accuracy can be made 1/10 of the rise time of 20 nanoseconds which means a range accuracy of .6 meters. Laser altimeters (pulsed) will be limited by electronic amplifier bandwidth and shorter detector response times.

Pulse Repetition Frequency

The pulse repetition frequency minimum is simply the number of resolution elements observed per second. That is:

$$PRF = \frac{1}{T_{res}} = \frac{1}{1.25\mu sec} = 800\ Kpps$$

Bistatic Radar Profile Mapping

Bistatic radar can be a very important tool in mapping when weight, data rate, and power requirements are critical. Bistatic radar as opposed to monostatic radar has its receiving and transmitting stations placed at different locations. Figure D-8 gives the two possible configurations for a satellite-earth bistatic arrangement.

Earth-based Transmitter

The first system has its basic virtues in having the capability of transmitting high powers and thus higher resolution potential. Earth-based transmitters can send megawatt pulses or 400 k watt continuous wave transmission as at the NASA/JPL Deep Space Instrumentation Facility at Goldstone, California. Consequently, large radar transmitters are not needed on a satellite to obtain profile maps of a planet. The resolution capabilities are on the order of a few miles. The system does, however, have the disadvantage of still needing a receiving system, signal processor, and data communication link to earth. The signal processing and data link are not critical systems, but receiving apparatus must have sufficient capabilities to receive a signal that has traveled 200 million miles and rebounded off of a planet. Calculations show that the present state-of-the-art has these capabilities provided power requirements and ultimately weight restraints are not critical. If the receiving system does meet the standards discussed, relatively good profile maps can be made although satellite monostatic radar would produce far superior maps.

The system resolution is given by:

$$r_R = \sqrt{\frac{\gamma F_o K T B R_{em}^2 R_{ms}^2}{P_t G_t G_r \lambda^2 \rho}}$$

where P_t is the power transmitted
R_{em} is the distance between the earth and Mars
R_{ms} is the range between Mars and the satellite
P is the reflection coefficient
F_o is the noise factor
γ is the signal-to-noise ratio
K is Boltzmann's constant

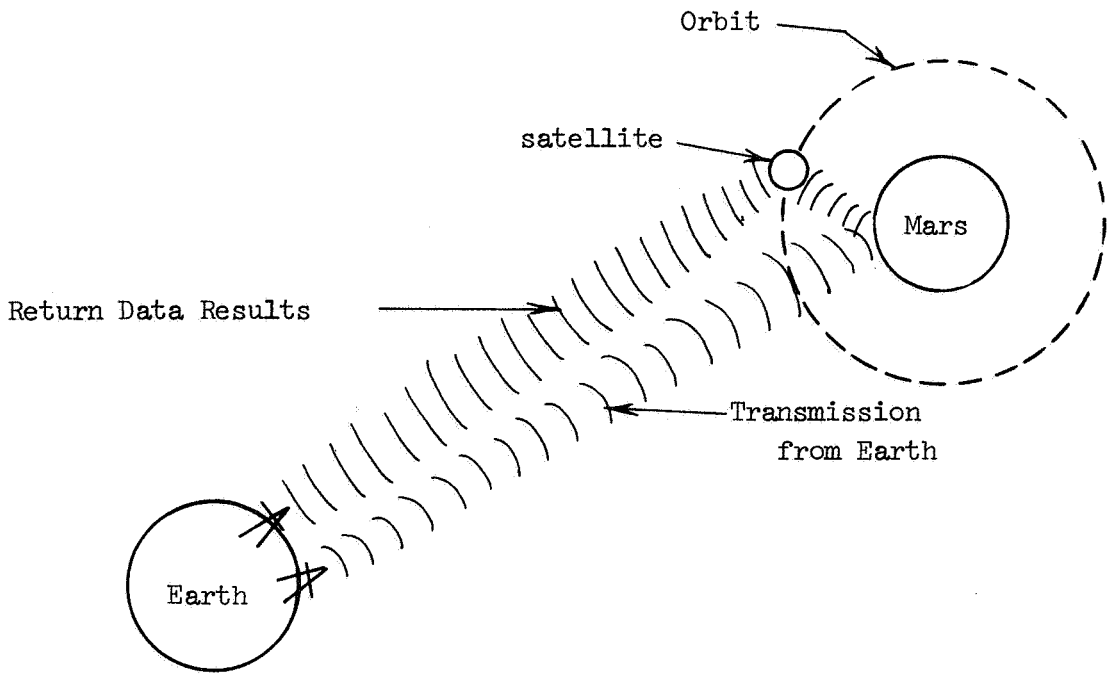

Case I.

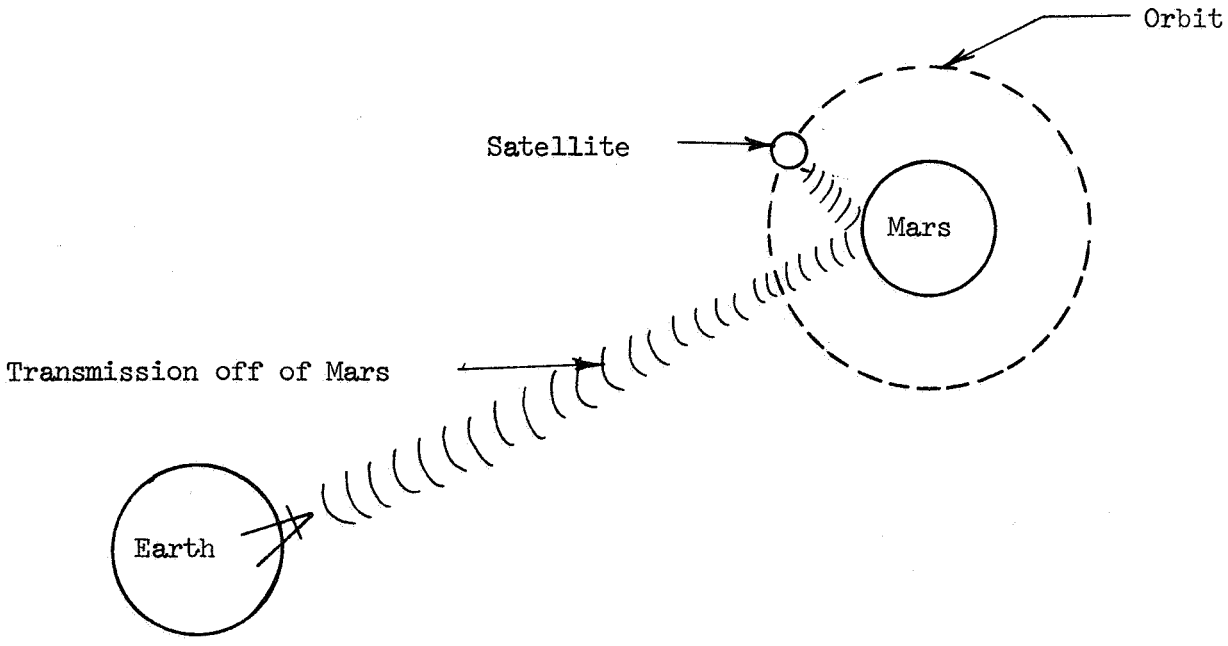

Case II.

Figure D-8 Bistatic Radar

T is the system temperature
B is the pre-detection bandwidth
G_t, G_r are the transmitter & receiver gains
λ is the wavelength of transmission

Assuming that P_t is 400 kw and λ is 12.5 cm (Goldstone parameters), the resolution can be calculated. The other parameters are standard and are discussed in the next section. Therefore:

$$r = \sqrt{\frac{(10)(10)(1.38\times10^{-23}\ \frac{\text{watt-sec}}{^\circ K})(30^\circ K)(10^3)(2\times10^8\ \text{mi})^2(2\times10^5\ \text{in})^2}{(4\times10^5\ \text{watt})(10^5)(10^7)(1.25\ \text{m})^2(10^{-2})(10^{-4})}} = 1.63\ \text{mi}$$

Data rate calculation is totally dependent on how many resolution elements are to be observed since the transmitter will be operated in the CW mode The higher the data rate the better the correlation between successive pictures.

Satellite-based Transmitter

This system seems more advantageous than the earth-based system since no signal processing or data telemetry is required. The system merely requires a transmitter and an antenna to direct the signal. However, the power output has to be lowered because satellite power systems do not have advanced earth capabilities. This, of course, reduces the resolution. Also, the transmitter can no longer work in a CW mode, but is pulsed to achieve high powers (10-100 kw). Consequently, the data rate is no longer continuous which gives less correlation of data. System weights are reduced by more than 50% and system size is reduced accordingly.

Assuming the transmitter can produce 50 k watts peak power, the satellite will have 1/8 the power of an earth-based system. This will decrease the resolution to:

$$r_R = \frac{1.63\ \text{mi}}{\sqrt{1/8}} = 4.62\ \text{mi}$$

The data rate is dependent upon the velocity of the craft, transmission bandwidth, and the angle of elevation assuming the antenna is inclined. The development of the data rate formula is in the next section. The data rate is given:

$$DR = \frac{2mV\times\tan\theta}{wc\ k_3^2} = \frac{2(5)(3.2\ \frac{\text{km}}{\text{sec}})(4)(1)}{(10^{-5}\ \text{sec})(3\times10^8\ \frac{\text{m}}{\text{sec}})(1.1)^2} \approx 40\ \frac{\text{bits}}{\text{sec}}$$

where x is the gray level
This value is merely a ball-park figure since the above formula is not entirely applicable to the bistatic system. However, the data rate is small and represents no problem with handling techniques.

Side-looking Radar

The last two systems to be discussed involve side-looking radar technology. This technology is comparatively young to the radar world, and much of it is of classified nature. Consequently, this report will concentrate on the theoretical nature of radar.

In a side-looking radar system a transmitting antenna in the satellite sends a short pulse of microwave energy out one side of the satellite (45° elevation angle). The energy strikes a roughly circular area

on the ground, and a receiving antenna collects the energy reflected back to the satellite. The greater the distance from the spacecraft to any portion of the target, the greater the time delay in return of the reflected signal. By accurately measuring the time delay, side-looking radar differentiates the echoes that return to it from various small concentric rings. Each ring represents the locus of all points within the large circle that are roughly equidistant from the plane.

Within any ring there is a spot just opposite the spacecraft that moves along at the same speed as the spacecraft. At any given time, the distance from the spacecraft to all other points on the ring is either increasing or decreasing. Here the Doppler effect comes into play: the frequency of the reflected signal changes according to whether the spacecraft is approaching a given point or receding from it. As a result, the microwave energy reflected back to the spacecraft from such points differs in frequency from the energy transmitted to them. The radar receiver is designed to accept energy of approximately the same frequency as the initial pulse and to reject significantly different frequencies.

Because of the two disciminating effects — one depending on the time delay and the other on the Doppler shift — the radar receiver accepts at any given instant only the energy that meets two conditions: that it be from the narrow ring within which the time delay is such that the energy is at that instant striking the receiving ring that is directly opposite the spacecraft. Together the two discriminating features provide the synthetic-aperture. This technique greatly improves the spatial resolution of the system.

Incoherent Side-looking Radar

Incoherent radar has its prime usage where gross mapping is desired and where fine resolution is not required. In incoherent radar systems, the system azimuth resolution expressed as a distance varies directly with the system azimuth beamwidth and range to the target, while the range resolution is only a function of the velocity of the spacecraft, the elevation angle, and the pulse width. Hence, radar antennas usually have the optimum horn configuration to obtain equal resolution in both directions.

An incoherent system operating at the short wavelength end of the radar spectrum is optimized for some purposes, since such a system will provide the best system resolution for a given antenna aperture. A wavelength of 8.6 mm (35 ghz) was consequently chosen. This wavelength has been used in airborne radar mapping systems and has functioned quite well.

In choosing an antenna system, there were three possible configurations for three distinct reasons: (1) Use an optimum horn that will provide 2 m resolution in both range and azimuth directions so as to be consistent with the multi-spectral camera system; (2) Use an optimum horn that will give good resolution for an antenna no larger than 22 feet; and (3) Use the 10 ft parabolic antenna proposed for lander communication as a radar antenna, but of course, suffer the loss of equal resolution in range and azimuth directions (unless the range resolution is decreased by increasing the pulse width). For the first system, it is found that

the optimum horn will have an azimuth beamwidth of approximately 5000 ft which is too large for satellite purposes. The second system will provide 500 meter resolution in all directions using an optimum horn with 22 ft azimuth beamwidth. This system will also reduce the power requirements by a factor of .003 compared with the third system. Finally, the third proposal will provide 21 m range resolution and 1 km azimuth resolution using a 10 ft parabolic antenna. Because antenna sizes are critical and redundancy of antenna systems is not desired, the last system probably provides the best system resolution.

The parameters for the system using the 10 ft parabolic antenna were calculated assuming a 200 km orbit and 3.2 km/sec relative ground velocity of the satellite. A ground reflection coefficient of -40 db was chosen as a suitable reflection minimum for a wavelength of 8.6 mm. Refer to Table D-2 for these parameters.

The peak power requirement for the radar system can be determined from the classic radar equation:

$$P_r = \frac{P_t G^2 \lambda^2 \sigma}{(4\pi)^3 R^4}$$

where P_t is the peak power transmitted
G is the antenna gain
λ is the transmission wavelength
σ is the radar cross section
R is the range to the target

The system noise power is given by:

$$P_N = F_o K T B$$

where F_o is the system noise factor
K is Boltzmann's constant
T is the system temperature
B is the predetection bandwidth

If we let the signal-to-noise ration, S/N, equal γ, then:

$$\frac{S}{N} = \gamma = \frac{P_r}{P_N} \quad \text{or} \quad P_r = \gamma P_N$$

or:

$$P_t = \frac{(4\pi)^3 R^4 \gamma F_o K T B}{G^2 \lambda^2 \sigma}$$

But the radar cross section is given by:

$$\sigma = \eta r_A r_R$$

Where η is the ground reflection coefficient
r_R is the range resolution
r_A is the azimuth resolution

For side-looking radar (noncoherent), the azimuth resolution is just equal to the length of ground wetted by the antenna beamwidth in the azimuth direction, i.e.,

$$r_A = K_3 \beta_A R$$

where K_3 is a constant
β_A is the azimuth beamwidth

and therefore:

$$\sigma = \eta r_R K_3 \beta_A R$$

Thereforethe peak power transmitted is simply

$$P_t = \frac{(4\pi)^3 R^3 \gamma F_o K T B}{\eta G^2 \lambda^2 K_3 \beta_A r_R}$$

TABLE D-2

CHARACTERISTICS OF INCOHERENT

SIDE-LOOKING RADAR

Operating Frequency (f)	35 ghz
Operating Wavelength (λ)	8.6 mm
Antenna Parameters (parabolic	
a. Aperture Beamwidth (β)	3.44×10^{-3} radians
b. Elevation Angle (θ)	45°
c. Altitude (h)	200 km
d. Gain (G)	50 db
e. Diameter (D)	10 ft
Velocity of Spacecraft (V)	3.2 km/sec
Pulse Repetition Frequency (prf)	15 pps
Pulse Width (w)	.1 microseconds
System Predetection Bandwidth (B)	10 mhz
Nominal Range Resolution (r_R)	21.2 m
Nominal Azimuth Resolution (r_A)	1.07 km
Illuminated Ground Swath Width (W)	1.38 km
Required Transmitted Peak Power (P_t)	.310 kw
Required Transmitted Average Power (P_a)	33 w
Required System Data Rate (DR)	.880 $\frac{\text{res. elm.}}{\text{sec}}$
Approximate System Volume	15 ft^3
Approximate System Weight	<100 lbs

The range resolution of the system is a function of the system pulse width, w, and the angle of elevation of the antenna, θ. In other words:

$$r_R = \frac{wc}{2\sin\theta}$$

where C is the velocity of light.

which gives

$$P_t = \frac{(4\pi)^3 R^3 \gamma F_0 KTB\, 2\sin\theta}{\eta G^2 \lambda^2 K_3 \beta_A wc}$$

Using the system bandwidth pulse width constraint,

$$BW \approx 1$$

the peak power can now be given:

$$P_t = \frac{2(4\pi)^3 h^3 \gamma F_0 KT \sin\theta}{\eta G^2 \lambda^2 K_3 \beta_A w^2 c \cos^3\theta}$$

where h is the altitude

Using basic identities, it may be presented in two more forms

$$P_t = \frac{(4\pi)^3 h^3 \gamma F_0 KT}{\eta G^2 \lambda^2 K_3 \beta_A w r_R \cos^3\theta}$$

$$P_t = \frac{2(4\pi)^3 \gamma F_0 KT h^2 W \tan\theta}{\eta G^2 \lambda^2 K_3 \beta_A \beta_R W^2 c}$$

where β_r is the azimuth beamwidth
W is the swath width

If it is desired to have a high range resolution, then the pulse width must be made smaller which in turn increases the predetection bandwidth which increases the noise in the system. To maintain a γ of 10, the peak power of the transmitter must be increased. With the present state-of-the-art, a pulse width of .1 microseconds was chosen to give good resolution and maintain a small power requirement.

The azimuth and range beamwidths are equal since we are using a parabolic antenna. The beamwidth apertures are given by:

$$\beta_A = \beta_R = \frac{K_2 \lambda}{D} = \frac{(1.2)(8.6\text{ mm})}{10\text{ ft}} = 3.44 \times 10^{-3}\text{ radians}$$

where K_2 is a constant
λ is the wavelength
D is the diameter of the ant.

The range resolution is simply:

$$r_R = \frac{wc}{2\sin\theta} = \frac{(.1\times10^{-6}\text{ sec})(3\times10^{8}\text{ m/sec})}{2\sin 45^\circ} = 21.2\text{ m}$$

while the azimuth resolution is just:

$$r_A = \frac{K_3 h \beta_A}{\cos\theta} = \frac{(1.1)(2\times10^{5}\text{ m})(3.44\times10^{-3}\text{ rad})}{\cos 45^\circ} = 1.07\text{ km}$$

where K_3 is a constant
h is the satellite alt.

The system predetection bandwidth is related to the pulse width by:

$$BW \approx 1, \text{ or } \quad B = \frac{1}{w} \le \frac{1}{10^{-7}\text{ sec}} = 10\text{ mHz}$$

The pulse repetition frequency is given by:

$$prf = \frac{m V_r \cos\theta}{K_3 h \beta_A} = \frac{(5)(3.2\text{ km/sec})\cos 45^\circ}{(1.1)(200\text{ km})(3.44\times10^{-3}\text{ rad})} = 15\text{ pps}$$

where V_r is the spacecraft vel. relative to the ground
m is an integer constant

The illuminated ground swath width is given by

$$W \approx \frac{h\beta_R}{\cos^2\theta} = \frac{(200\ km)(3.44 \times 10^{-3}\ rad)}{\cos^2 45^\circ} = 1.38\ km$$

Knowing the preceding parameters, the peak power can now be calculated. That is:

$$P_t = \frac{(2)(4\pi)^3(n)(10)\left(1.38 \times 10^{-23}\ \frac{joules}{^\circ K}\right)(300^\circ K)(200\ km)^2(1.38\ km)(\tan 45^\circ)}{(10^9)(10^{11})(8.6\ mm)(1.1)(3.44 \times 10^{-3}\ rad)^2(10^{-14}\ sec)\left(3 \times 10^8\ \frac{m}{sec}\right)} = 310\ kw$$

The average power is simply

$$P_a = \frac{10 P_T V_r \sin\theta}{c} = \frac{(10)(310\ kw)(3.20\ km/sec)\sin 45^\circ}{3 \times 10^8\ m/sec} = 33.1\ watts$$

The data rate for this system was derived and found to be:

$$DR = \frac{2mV_r \tan\theta}{wc k_3^2} = \frac{(2)(5)(3.2\ km/sec)\tan 45^\circ}{(10^{-2}\ sec)(3 \times 10^8\ m/sec)(1.1)^2} = 880\ \frac{resolution\ elements}{sec}$$

Coherent Synthetic-Aperture Side-looking Radar

Coherent or synthetic-aperture radar shows much promise as a remote sensor operating from an orbiting platform when high resolution measurements are required. This is due to the fact that the system resolution is not a function of range to the target or of the portion of the microwave spectrum in which the system operates.

With conventional radar techniques if one wishes to have fine linear azimuth resolution at long ranges, the required antenna length can be on the order of hundreds or thousands of feet. The synthetic-aperture technique offers a way around this problem. The spacecraft would carry a small, side-looking antenna, producing a beam that is relatively wide in the azimuth direction, which scans the terrain by virtue of the spacecraft motion. The antenna is carried by the spacecraft to a sequence of positions which can be treated as if they were the positions occupied by the individual elements of a linear antenna array. At each such position, the antenna radiates a pulse, then receives and stores the reflected signal. These stored data are then processed in a manner analagous to the coherent weighted summation carried out in a large linear array. The processed signal bears a quantitative similarity to those which would be obtained if a large antenna were used; in particular, the resolution and the signal-to-noise ratio are greatly improved by the signal processing.

Since the peak power required varies inversely with the cube of the wavelength, it is important that the wavelength chosen is not too small. However, it can not be made large since the data rate is directly proportional to it. Consequently, a wavelength of 3 cm (10 ghz) was chosen. Much work has already been done with X-band (3 cm), and as a result, little development would be required if this system were to be used.

If the 10 ft. parabolic antenna for communication with the lander is used and 2 m resolution is required, the transmitter would be required to produce a peak power of approximately 90 mega watts with a pulse width of 4.7 nano-seconds. The data rate is on the order of

10^{-11} resolution elements per second. These values are not attainable with the present state-of-the-art. Consequently, the system resolution was increased to 25 m to lower power requirements.

The system parameters were calculated and appear in Table D-3. As one can see, most of the figures are reasonable except for the data rate. Since real time transmission is desired, this rate is entirely too large. If the maximum data rate is a few mega bits per second, the system resolution will have to be approximately 500 m with the 10 ft antenna or possibly 400 m with a 20 ft. antenna.

The antenna beamwidth can be calculated using the now familiar equation,

$$\beta_A = \beta_R = \frac{k_2 \lambda}{D} = \frac{(1.2)(3\text{ cm})}{10\text{ ft}} = 1.18 \times 10^{-2}\text{ radians}$$

The system pulse width, w, can be determined by assuming the system resolution to be 25 m,

$$w = \frac{2 r_a \sin\theta}{c} = \frac{(2)(25\text{ m})(\sin 45^\circ)}{3 \times 10^8\text{ m/sec}} = .118\ \mu\text{sec}$$

One of the system restraints, namely $D \geq \frac{2F k_2 V_r}{(prf)}$, determines the pulse repetition rate.

$$(prf) = \frac{2F k_2 V_r}{D} = \frac{(2)(1)(1.2)(3.2\text{ km/sec})}{10\text{ ft}} = 2.52\text{ kpps}$$

The predetection bandwidth is simply the reciprocal of the pulse width (bandwidth restraint).

$$B \approx \frac{1}{w} = \frac{1}{.118 \times 10^{-6}\text{ sec}} = 8.5\text{ mHz}$$

To calculate the peak power required, the following equation will be used:

$$P_t = \frac{(4\pi)^3 R^4 \gamma F_0 KTB}{G^2 \lambda^2 \sigma} = \frac{(4\pi)^3 R^4 \gamma F_0 KTB}{\eta G^2 \lambda^2 r_R r_A}$$

This expression was derived in the side-looking radar calculations in this appendix. A coherent radar system has the advantage of being able to integrate many return signal pulses (signal phase information is used) from a target. For a system integrating n pulses, the signal power increases with n^2. The advantage of this integration technique is the fact that noise power increases linearly with the number of integrated pulses (the noise power resulting from a random noise process). The number of pulses, n, which are processed is a function of the system pulse repetition frequency, prf, the system azimuth beamwidth, β_A, the range of the target, R, and the antenna velocity, V, and can be expressed in the form

$$n = \frac{R \beta_A (prf)}{V}$$

However,

$$\beta_A = \frac{k_2 \lambda}{D_A} \quad \text{and} \quad R = \frac{h}{\cos\theta}$$

TABLE D-3

CHARACTERISTICS FOR SYNTHETIC-APERTURE SIDE-LOOKING RADAR

Operating Frequency (f)	10 ghz
Operating Wavelength (λ)	3 cm.
Antenna Parameters (parabolic)	
a. Aperture Beamwidth (β)	1.18×10^{-2} radians
b. Elevation Angle (θ)	45^{o}
c. Altitude (h)	200 km
d. Gain (G)	10^{5} or 50 db
e. Diameter (D)	10 ft.
Velocity of Spacecraft (V)	3.20 km/sec
Pulse Repetition Frequency (prf)	2.52×10^{3} pps
Pulse Width (W)	.118 microseconds
System Predetection Bandwidth (B)	8.5 mhz
Nominal Range Resolution (r)	25 m
Illuminated Ground Swath Width (W)	4.72 km
Required Transmitted Peak Power (P_t)	30.1 kw
Required Transmitted Average Power (P_a)	$1.6 \times 10^{9} \frac{\text{res. elm.}}{\text{sec.}}$
Approximate System Volume	$20\ ft^{3}$
Approximate System Weight	150 lbs

Thus, the peak power is given as

$$P_t = \frac{(4\pi)^3 R^4 \gamma F_0 K T B}{\eta G^2 \lambda^2 r_A r_R n} = \frac{(4\pi)^3 h^3 \gamma F_0 K T B D_A V}{\eta G^2 \lambda^2 K_2 (prf) r_A r_R \cos^3\theta}$$

Using the system bandwidth pulse width restraint,

$$Bw \approx 1$$

and using the resolution condition $r_R = \frac{wc}{2\sin\theta}$, the peak power is

$$P_t = \frac{(4\pi)^3 h^3 \gamma F_0 K T V D_A c}{2\eta G^2 \lambda^2 r^3 K_2 (prf) \sin\theta \cos^3\theta} \qquad \text{where } r = r_A = r_R$$

with this restraint:

$$r \geq \frac{D_A}{2FK_2} \geq \frac{V}{(prf)}$$

Therefore, substituting the parameter values into the peak power expression yields

$$P_t = \frac{(4\pi)^3 (200\,km)^3 (10)(10)(1.38\times10^{-23}\,joules/^\circ K)(300^\circ K)(3.2\,km/sec)(10\,ft)(3\times10^8\,m/sec)}{(2)(10^{-4})(10^{10})(3\,cm)^2(25\,m)^3(1.2)(2.52\times10^3\,\frac{p}{sec})(\sin 45^\circ)(\cos^3 45^\circ)} \approx 30.3\ kw$$

The average power is given by

$$P_a = P_T\, w\, (prf) = (30.3\ kw)(1.18\times10^{-7}\,sec)(2.52\times10^3\,\tfrac{p}{sec}) = 9\ watts$$

and the system data rate is expressed as

$$(DR)_{max} = \frac{ch\lambda K_2}{D_A r^2 \sin\theta} = \frac{(3\times10^8\,m/sec)(2\times10^{-6}\,m)(3\,cm)(1.2)}{(10f_0)(25\,m)^2(\sin 45^\circ)}$$

$$(DR)_{max} = 1.6\times10^9\ \frac{\text{resolution elements}}{sec}$$

Conclusion

All the systems investigated have their different advantages and disadvantages. If any particular system must be chosen as the proposed design, then the exact function of the system and the system restraints must be made clear. It was felt that the following system conditions were desired:

1. Average power must be less than 2 kw and peak powers should be less than 100 kw.
2. Data rate maximum is 10^7 bits/sec.
3. Antenna size should be limited to no more than the 10 ft. parabolic antenna for lander communication.
4. Weight should not be critical (less than 500 lbs.).
5. High resolution, preferably 2 m, is desired.

From the analysis, it has been shown that the FM-CW laser radar meets all of these requirements. Two meter resolution can be achieved with the present state-of-the-art. The most research needed in developing this system will be devoted to the scanning system and light amplifier system. But it is felt that these systems will be developed and more powerful lasers will be built in the next ten years.

Pulsed laser radar has good prospects, but the high pulse rates required for satellite radar make it hardly feasible. If spot-check high resolution measurements are required, then pulsed laser radar will be worth development.

Bistatic radar is only used when weight and power requirements are critical. Its resolution capabilities are quite limited. Since this proposed mission will have been preceded by two or three exploration missions, poor resolution maps will not be desired.

Side-looking radar, of course, has been a tremendous boon to airborne surveillance. However, its future does not lie in space satellite mapping systems. Power requirements are too large, and bulky antennas introduce too many design problems.

However, coherent synthetic-aperture side-looking radar does have a potential future. If optical data processing and reduction techniques can be developed to a high degree, then coherent radar has a bright future. High resolution and accurate ranging can be accomplished by such a system.

Even though coherent radar mapping is presently being used in Earth observation, it is felt that the potential of laser radar is too great not to be developed. Reliability and accurate ranging are only a matter of development and can be done within the next ten years.

ACKNOWLEDGEMENTS

Spectra-Physics Inc., Mountain View, California.

Dr. Glen Wade, Department of Electrical Engineering, University of California, Santa Barbara.

BIBLIOGRAPHY

Anonymous, "New Laser Altimeter Earmarked for 1968," Aerospace Technology, vol. 21, no. 57, Sept. 11, 1967.

_____, Preceedings of the Fourth Symposium on Remote Sensing of Environment, University of Michigan, Ann Arbor, Michigan, December 1966.

_____, A Review of Space Research, National Academy of Sciences ——National Research Council, Pub. 1079, State University of Iowa, June 17-August 10, 1962.

_____, Priority Analysis of Manned Orbital Research Applications, Volume II, Stanford Research Institute, Stanford University, September 1965.

_____, "Remote Sensing of Natural Resources," Scientific American, vol. 218, no. 1, January 1968.

_____, Peaceful Uses of Earth Observation Spacecraft, prepared under Contract No. NASw-1084, University of Michigan, Ann Arbor, Michigan, Vol. III, 1965.

Bell, D. T., Jr. and Kidd, E. T., "Ultrasonic Devices for Coherent Optical Systems," 1967 SWIEECO Record, IEEE 19th Annual Southwestern Conference & Exhibition, Dallas, Texas, April 19-21, 1967.

Brown, W. M., "Synthetic-Aperture Radar," Transactions on Aerospace & Electronic Systems, vol AES-3, no. 2, March 1967.

Carpenter, R. L., Study of Venus by CW Radar —— 1964 Results, NASA Technical Report No. 32-963, March 1966.

Cutrona, L. J., "On the Application of Coherent Optical Processing Techniques to Synthetic-Aperture Radar," Proceedings of the IEEE, vol. 54, no. 8, August 1966.

Elion, H. A., Laser Systems & Applications, Pergamin Press, London, 1967.

Fowler, J. and Schlafer, J., "A Survey of Laser Beam Deflection Techniques," Proceedings of IEEE, vol. 54, no. 10, October 1966.

Gray, L. D., "Transmission of the Atmosphere of Mars in the Region of 2u," University of California Press, Los Angeles, November 23, 1965.

Miller, B., "Air Reconnaissance Aided By Line-Scanning Laser," Aviation Week & Space Technology, April 26, 1965.

Muhleman, D., Goldstein, R., and Carpenter, R., A Review of Radar Astronomy——Parts I, II, NASA Technical Report No. 32-824, January 30, 1966.

Thomas, P. G., "Multi-Function Airborne Radar," Space/Aeronautics, vol. 47, no. 2, February 1967.

Tyler, G. L., "Bistatic-Radar Detection of Lunar Scattering Centers with Lunar Orbiter," Science, vol. 157, July 14, 1967, pp. 193-5.

Tyler, G. L., "The Bistatic, Continuous Wave Radar Method for the Study of Planetary Surfaces," Journal of Geophysical Research, vol. 71, no. 6, March 15, 1966.

CAMERA-RADAR SCANNER HYBRID

The prospect of combining scanning equipment for both the multi-spectral camera and the laser radar system is quite desirable. It not only reduces the redundancy of the entire observation system, but allows bit-by-bit correlation between camera pictures and laser profiles. If the two systems are separate, then each system requires a scanning motor and a large parabolic mirror receiver system and servos. It also requires servo data from both systems; thus increasing data rate problems.

The accuracy of contour maps is improved when one scanning system is used since it is then possible to determine quickly which picture corresponds to which altitude reading. Data processing and probability of error is reduced substantially, too.

Probably, the most feasible method of combining the two systems is simply to add the 2000 fiber optics of the laser scanning system to the 32,000 fiber optics of the camera system (fiber optics of each system are of different material). Since the scanning mechanism of the laser is sequential, each fiber optic must be sampled sequentially. This, of course, presents a problem with channeling the camera system. There is a possible solution in that the 16 channel system could be abolished; thus raising the scanning motor speed back up to 96 krpm. This can be reduced by a factor of 4 or 8 by placing the fiber optics in a quarter circle or half a quarter circle. The motor speed could also be reduced by a factor of 2 by adding one more scanning motor and a switching network. (Refer to Figure D-9) If this packing has already been done, then the fiber optics must be placed in smaller arc angles of the scanner. This eventually causes the system diameter to increase, but not substantially.

With this sort of a system, both the multi-spectral camera and radar would be receiving light from nearly the same spot on Mars. All six bands (5 camera bands and 1 laser band) would record their findings sequentially, giving bit-by-bit correlation between systems.

The critical factors governing the above system are dependent on fiber optic packing and on available motor technology. Both areas need research if the system is to function well.

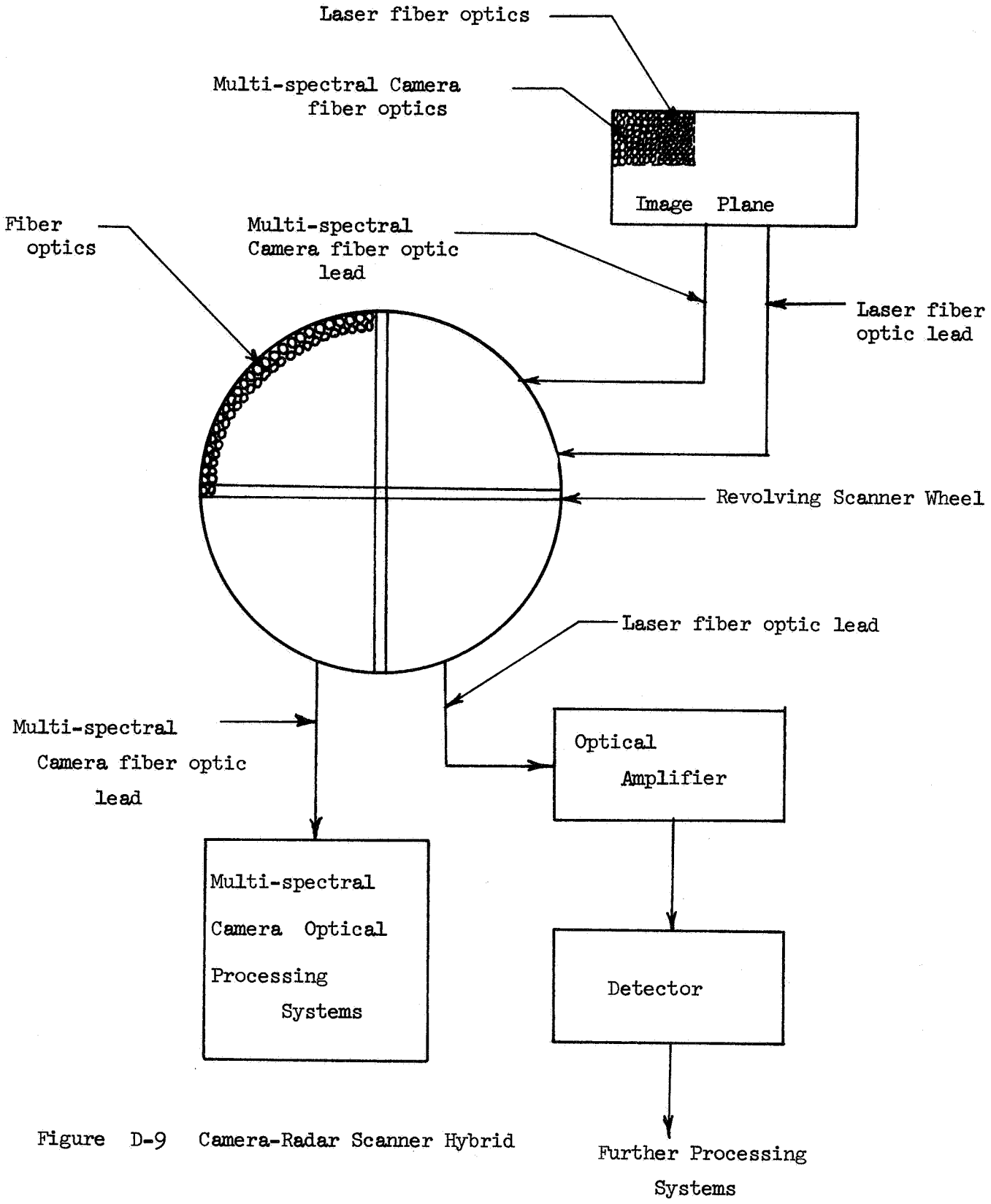

Figure D-9 Camera-Radar Scanner Hybrid

MOBILE SURFACE LABORATORY - DETAILED DESCRIPTION

This mission has included a roving lander in its overall configuration to further aid in data acquisition. The following is a general description of that system.

The system selected is, to a great extent, that speculatively designed by McDonnell Astronautics in conjunction with A.C. Electronics (GM) of Santa Barbara. To these corporations, and some very helpful engineers at the Jet Propulsion Laboratory at Pasadena, go a great deal of thanks for their assistance.

The roving vehicle itself, known as the Mobile Surface Laboratory (MSL), is a six wheeled vehicle carrying its own power supply, communications system, and an on-board computer. All six wheels are drive wheels, each being driven by an ac induction motor. The overall surface length is about 160 inches (13.3'), the width is 70 inches, the tire diameter is 40 inches, and it weighs 1900 pounds at liftoff. Four 75 watt Radioisotope Thermionic Generators (RTG) provide the power.

Figure D-10 is a conceptual view of the MSL.

This configuration is what A.C. called the 6x6 semiflexible MSL, since the first four wheels carry the rigid-body laboratory, and the last two carry the power supply. The forward section is connected to the rear trailer by flexible hollow rods that are telescoped at liftoff. A full description of this telescopring follows later. A pitch limiter prevents extreme or dangerous motion of the rear section.

The tires are ten inches wide and not pneumatic, but rather are a complex of intermeshed wires about the size of piano wire and made of titanium alloys. Capable of withstanding one earth g, these non-rigid wheels allow maximum mobility in soft, grannular soils.

The turning radius of the MSL is 15.2 feet, and both the front and back two wheels are capable of steering rotations of over 20 degrees. Torsion bar suspension is provided for all wheels not only for dynamic loading on the surface, but also for liftoff loading. The main structures are a titanium-vanadium or titanium-aluminum alloy, and stand 17 inches off the ground on Mars. It has a top speed of 1.5 km/hr. and a range of about 100 kilometers.

The laboratory portion of the MSL maintains communications with the orbiter (which relays information to Earth) at a rate of 50,000 to 200,000 bits per second via a 36 inch high-gain dish antenna which is the most prominent member on the top of the vehicle. Also present is an atmospheric instrumentation mast capable of composition measurements,

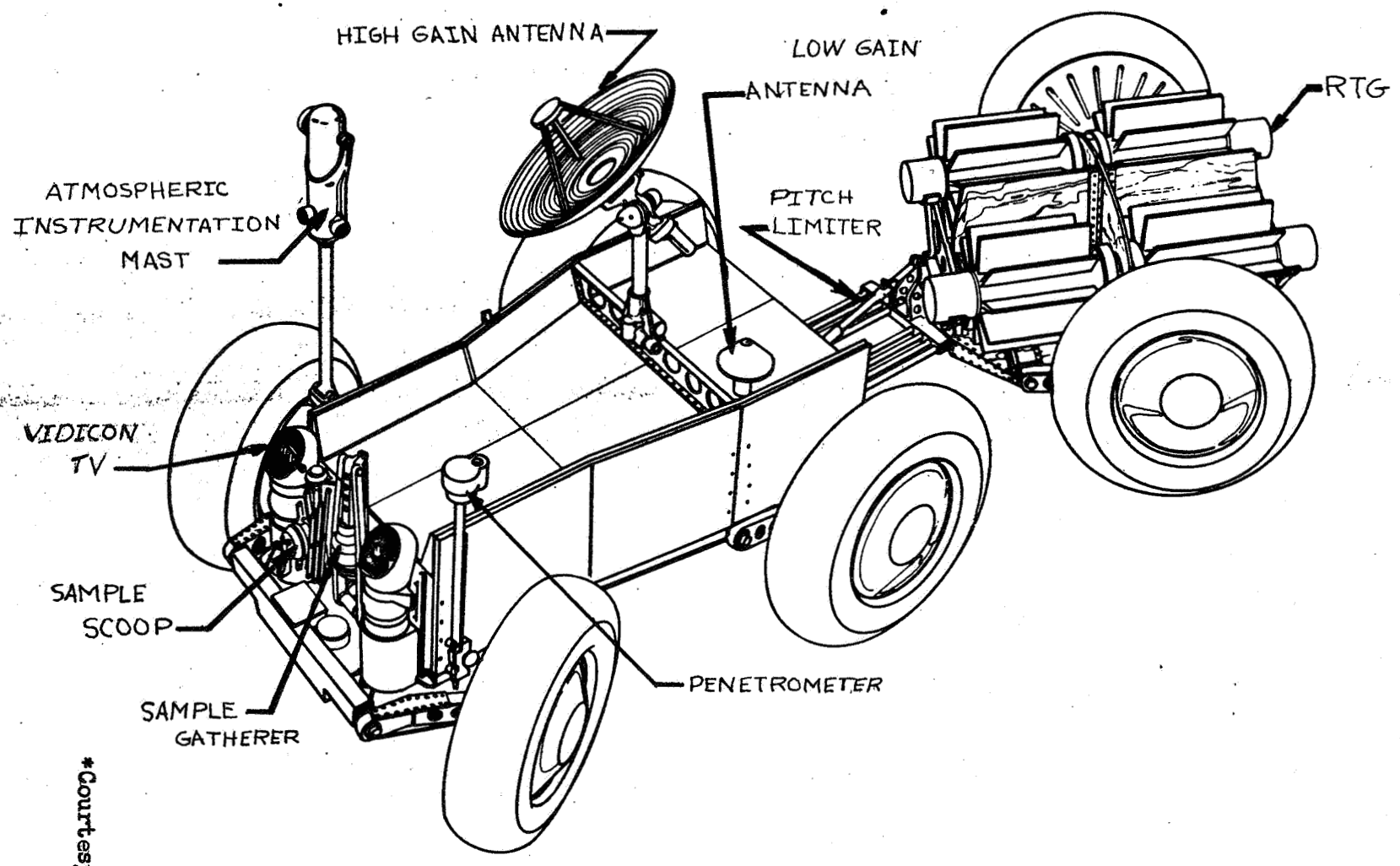

Fig. D-10 **Mobile Surface Laboratory Concept**

*Courtesy of A.C. Electronics, Santa Barbara

wind speed and direction determination, and possible a small particle (dust) sampler, along with a penetrometer for the testing of soil consistency, elastic modulus, etc. The two large "headlight-like" devices at the front of the vehicle are actually vidicon TV cameras which can be used not only for the detection of movement, but also for guidance and navigation either by earth-controllers or an on-board decision making computer. Mounted on the front portiong of the MSL is a sample scoop, much like that on Surveyor. Near it is located a sample gatherer capable of inhaling soil samples directly to the interior portion of the lab.

The interior laboratory details, although sketchy and not yet fully designed, would include a gas chromatograph, a mass spectrometer, a growth chamber to measure metabolism of any bacteria which may be present, and chemical reagents used in the experiments. An infrared sensor would be present, along with temperature sensors and a core drill. The lab may even have storage space for hermitically sealed samples of virgin soil to be picked up by early human explorers. Electromagnetic and magnetic flux could be measured with the appropriate instrumentation. Seismology devices could also be included. The elctronic gear needed for operation (computer, communications, experiment power, etc.) would also be stored in the laboratory volume of about 43 cubic feet. Other apparatus could include an acoustical monitor, UV detectors, and ray detectors, amino acid and lipid analyzers, macromolecular detectors, etc. Needless to say, not all of the mentioned volume will be available, since adequate insulation to keep the interior at 50 degrees Centigrade must be, and is, provided. The vehicle is also provided with various sensors capable of detecting obstacles which it may not be able to surpass, or which may be dangerous to the structure. These sensors may include radar and infrared radiometers, in conjunction with the T.V. On-board computers will be programmed to the extent that decisions can be made as to what action should be taken by the vehicle should an obstacle interfere with its motion. If the decision cannot be made, the system would request guidance from earth.

The lander is stowed in approximately the same position as the Surface Laboratory in Figure D-11. Figure D-12 shows a more general geometrical idea of the actual stowage. The flexible portion of the frame is telescoped "in" such that the rear tires of the front section touch and even deflect the two trailer wheels. The wheels are not the supporting members, since liftoff acceleration would exceed their designed strength. The torsion bars do, however, help absorb the loading on the frame.

The requirement of keeping the lander sterile during flight has necessitated the use of a "sterilization canister" to contain the landing system and to biologically insulate it from the rest of the capsule. This sterilization canister is shown in Figure D-11. The canister could conceivably contain a gaseous mixture designed to keep the mechanism sterile, but since elaborate investigation of this concept is lacking, no decision has been made regarding its use.

Although the lander and supporting system are mounted in a different way (see Figure 5-2, Spacecraft Design Summary), Figure D-13 demonstrates

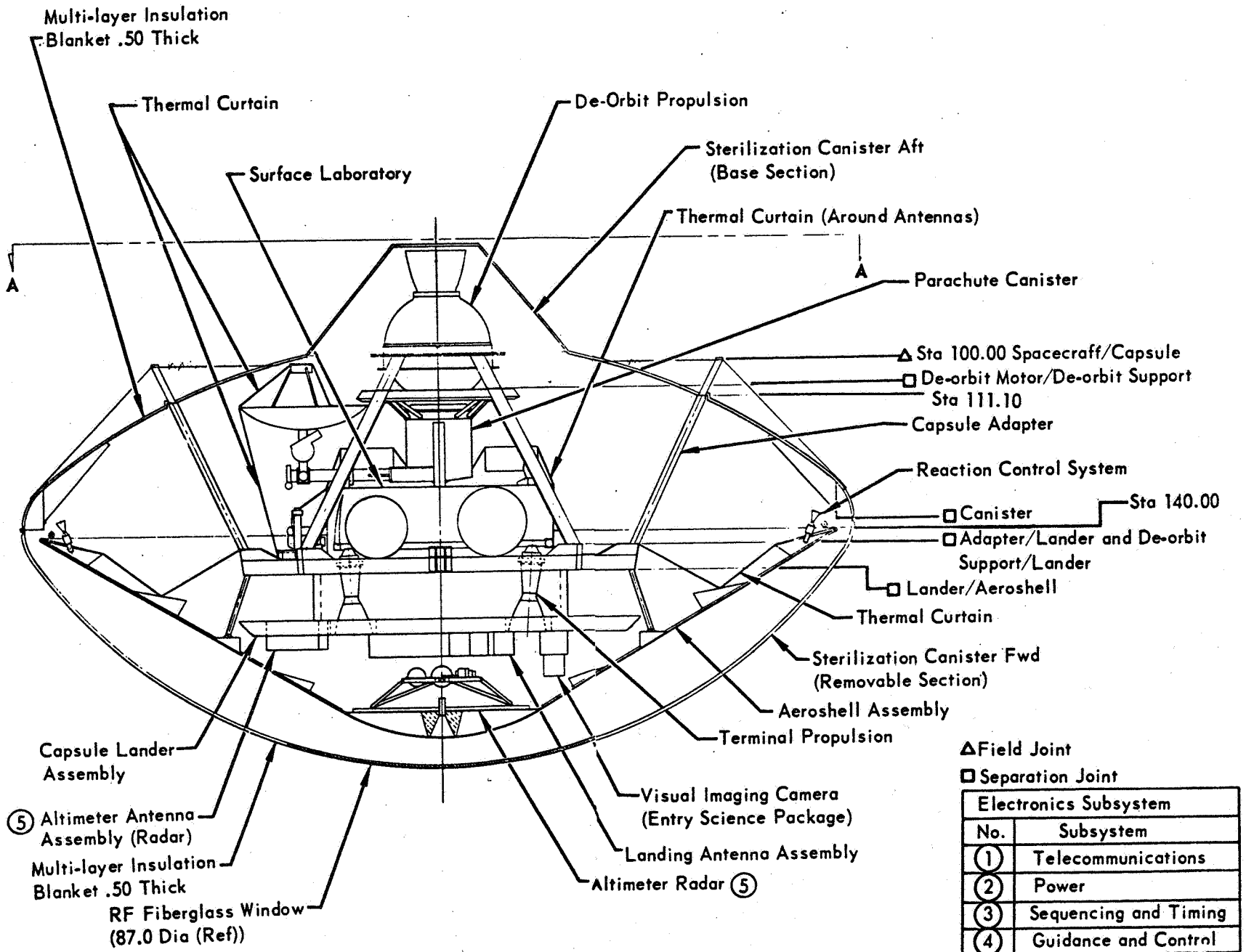

Electronics Subsystem	
No.	Subsystem
1	Telecommunications
2	Power
3	Sequencing and Timing
4	Guidance and Control
5	Radar

Figure D-11

*Courtesy of McDonnell Astronautics

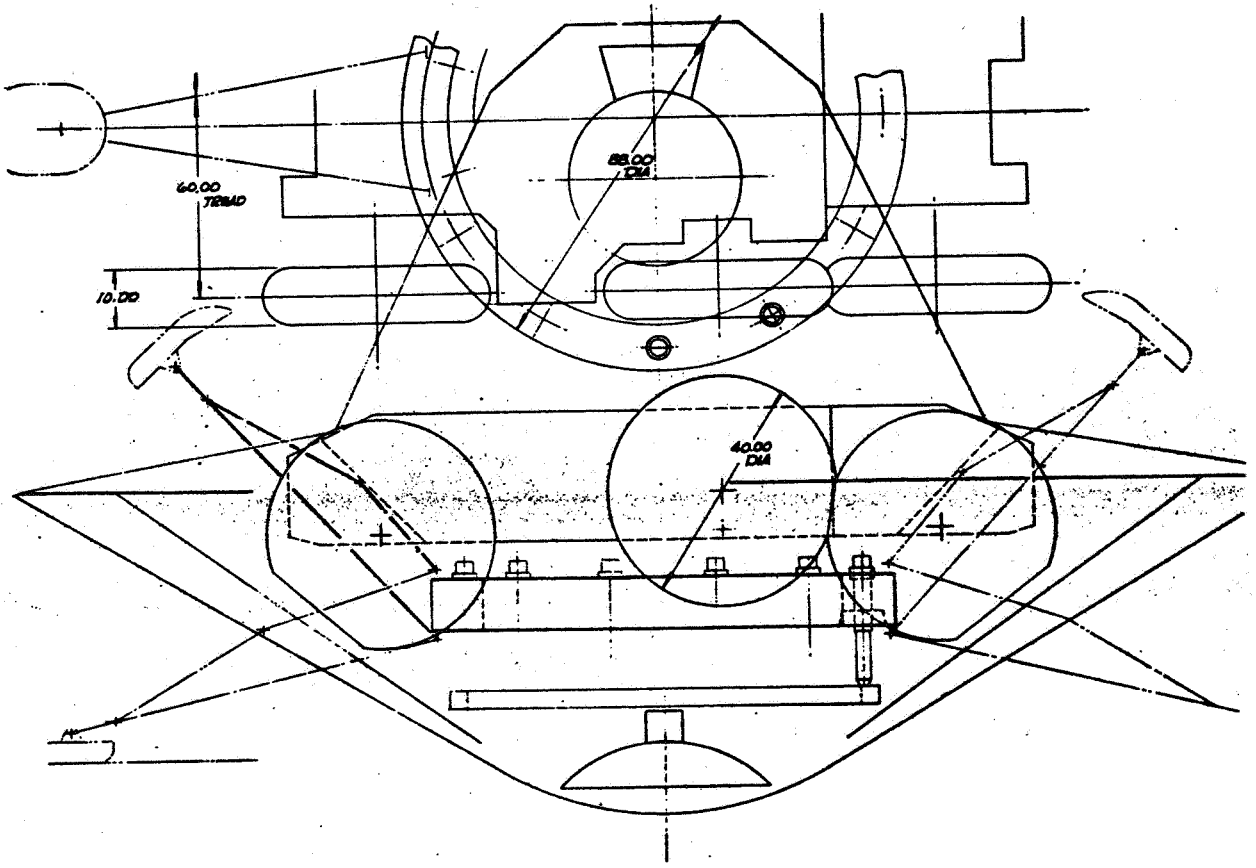

*Courtesy of A.C. Electronics, Santa Barbara

Fig. D-12 Mobile Surface Laboratory, Semiflexible 6x6 Concept Stowage

CAPSULE BUS STAGING SEQUENCE

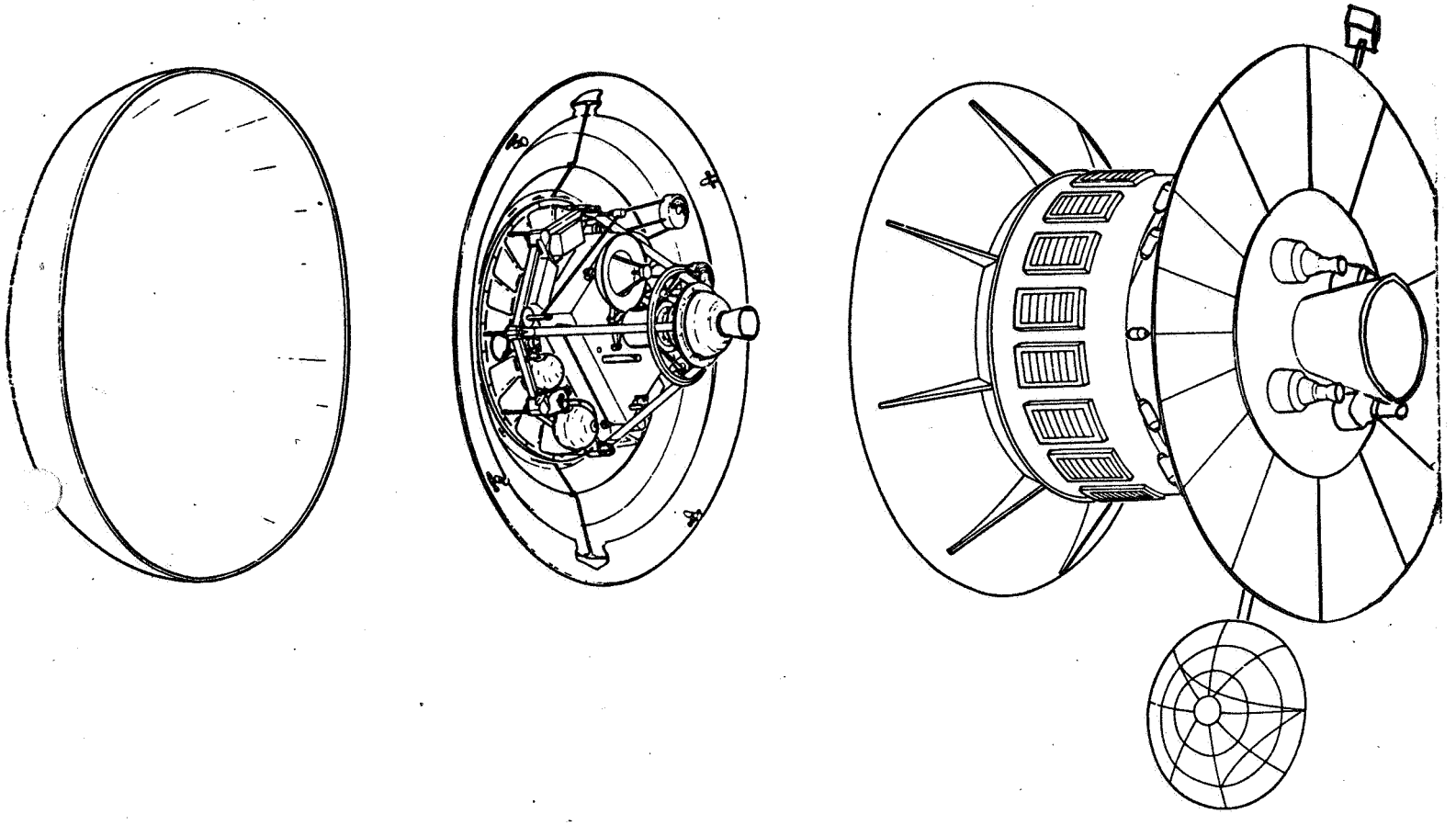

(1) FORWARD CANISTER SEPARATION
- Redundant CESD Severs Canister Attach Bolts in Tension
- Also Provides Energy to Separate Canister
- Separation Velocity > 1.25 Ft/Sec

(2) CAPSULE BUS SEPARATION
- Fire Eight Explosive Bolts at Adapter/ Capsule Lander Interface
- Operate Pitch and Yaw Thrust Chambers to Separate
- Separation Velocity = 1.25 Ft/Sec.

(3) SPACECRAFT IN ORBIT
- Aft Canister Remains on Spacecraft
- Adapter Remains Attached to Aft Canister.

Figure D-13
*Courtesy of McDonnell Astronautics

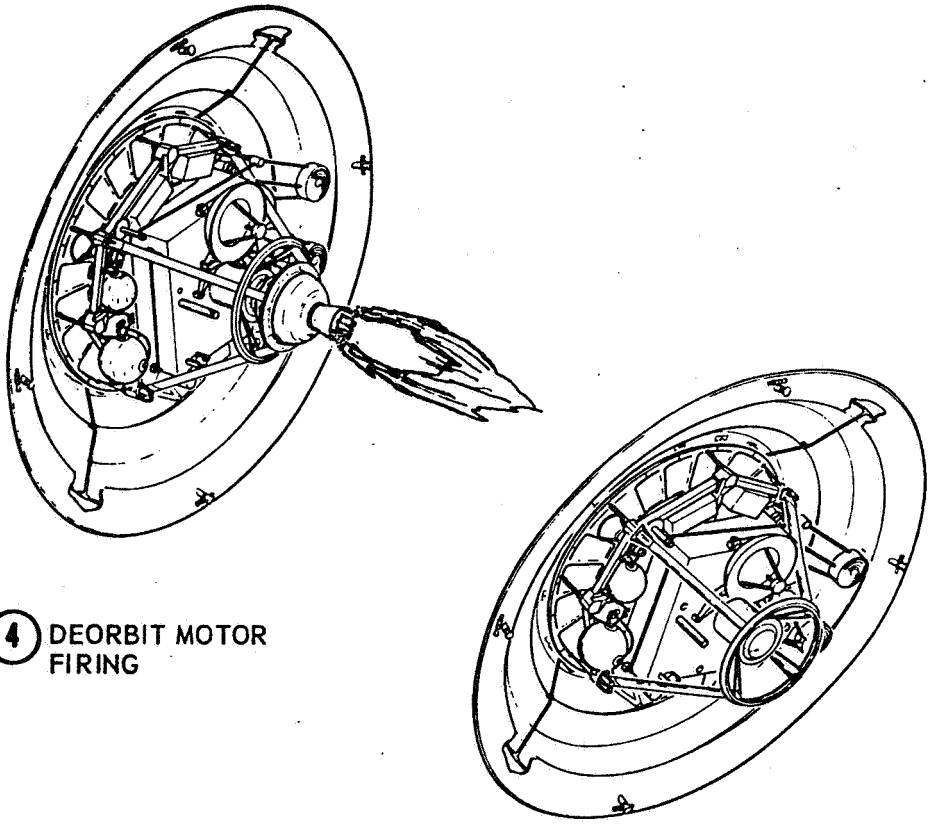

(4) DEORBIT MOTOR FIRING

(5) DEORBIT THRUST CUTOFF
- Fire One Explosive Bolts which Releases Nozzle from Case

(6) DEORBIT MOTOR SEPARATION
- Fire Four Explosive Bolts to Release Spent Motor Case and Upper Support Structure
- Separated by Springs in Each Strut

Fig. D-13 (cont'd)
*Courtesy of McDonnell Astronautics

CAPSULE BUS STAGING SEQUENCE
(Continued)

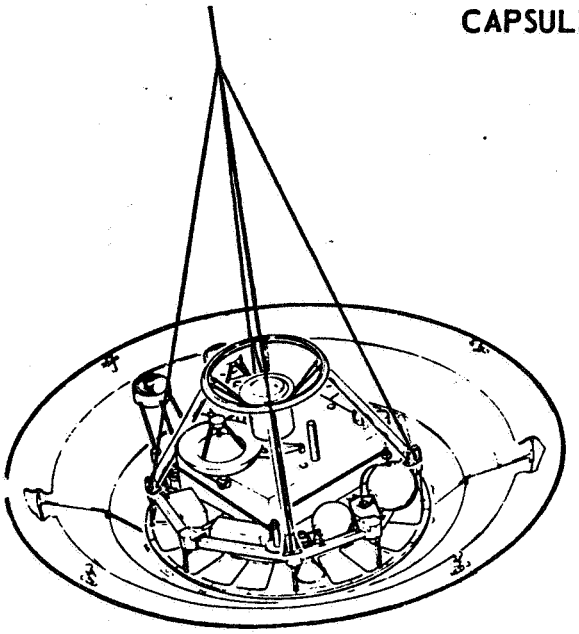

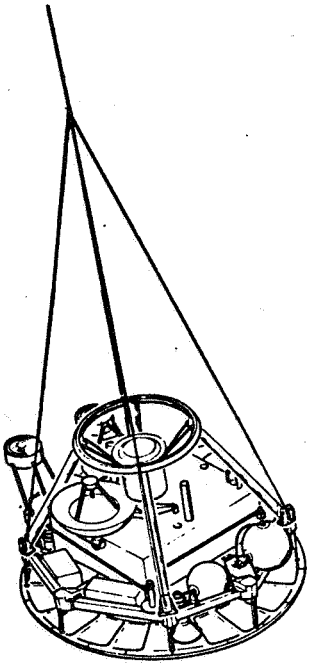

(7) PARACHUTE DEPLOYMENT
- Parachute Deployed by Catapult Firing Straight Aft § 100 FT/Sec Deploy Velocity
- Parachute Disreefed by Firing Four Pyrotechnic Actuated Reefing Cutters

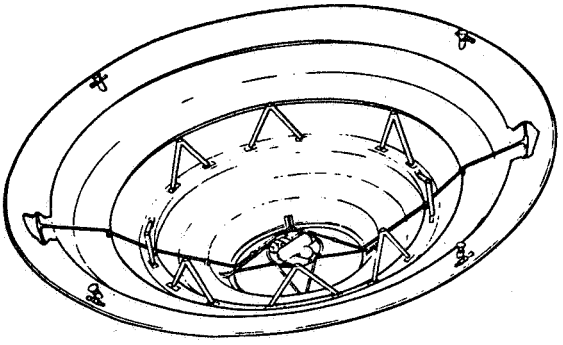

(8) AEROSHELL SEPARATION
- Fire Four Explosive Bolts at Capsule Lander Aeroshell Interface
- Sequence at 8.0 Sec After Parachute Deployment

Fig. D-13 (cont'd)
*Courtesy of McDonnell Astronautics

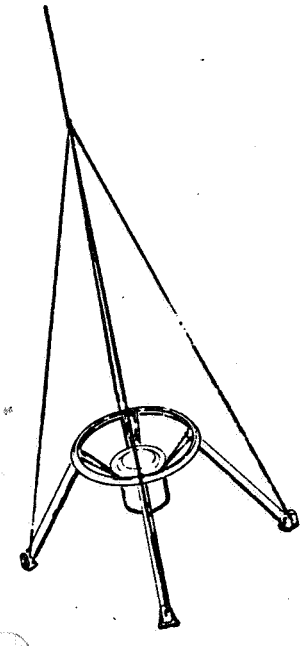

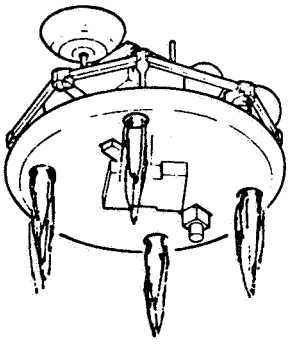

(9) PARACHUTE SEPARATION
- Ignite Terminal Propul System – Low Thrust
- Ignition Altitude is 5000 Feet
- After Successful Ignition, Fire Four Explosive Bolts at Base of Lower Support Structure

*Courtesy of McDonnell Astronautics

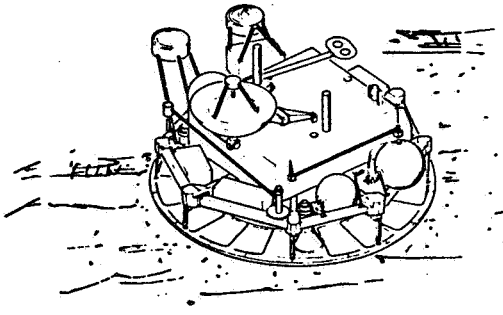

(10) LANDING
- Terminal Propulsion Terminated at 10 Feet
- Impact at $V_{v\,max}$ = 20 fps and $V_{h\,max}$ = 10 fps
- Surface Conditions Per Constraints Document
- Extend Stabilizing Blocks Released by Single Bolt Cutter Spring Actuated, Mechanically Locked

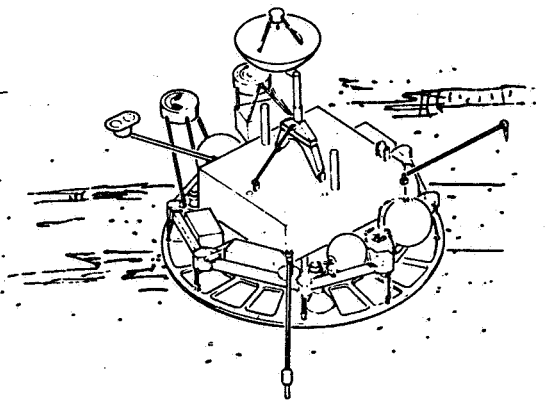

(11) LANDING OPERATION
- Capsule Bus System Shut Down
- Surface Laboratory in Operation – All Equipment Deployed.

Fig. D-13 (cont'd)

the various features of entry and deployment. Even though the orbiter bus used is a Voyager type, and the landed equipment is not mobile in the depicted example, the same procedure (with a few minor exceptions) is carried out for landing the MSL. The first of these exceptions is the attitude of the lander after pyrotechnic devices have released the forward canister and the capsule itself. The capsule, by using vernier engines mounted on the rim of the aeroshell, will be oriented in correct retro-fire attitude. After retro-fire, the capsule may either be flipped into correct entry attitude if its aerodynamic center is more aft than its center of gravity, or, if this fails, by re-use of the verniers. The second exception occurs at point 10 of Figure D-13, where the MSL's front 4 wheels are freed. They pull forward "de-telescoping" the connection rods between the laboratory and trailer, which are subsequently locked in this position by spring-loaded pins. The rear wheels are then released and the MSL crawls neatly from the landed platform without requiring ramps. Once deployed, its sensors and sampling equipment are ready for use.

During the time of entry the lander may acquire data concerned with experiments as atmospheric temperature gradient, composition, and radar location pinpointing. The entire landing sequence is controlled by radar determined altitude, and the expected time of available experiment-entry time is four and one half to nine minutes.

The time and position at which the lander is deployed are largely left to the discretion of the earth controllers. The determination of the exact position of the injected vehicle (bus + lander) and seasonal condition of the surface may require the lander to stay aboard from two days to two weeks. Assuming the Mariner 71 mission to be a success, much critical information (temperature) about the polar caps will be known, possibly justifying the placement of the rover in a boundary zone between the famed orange and purple zones of Mars. It could then acquire data from both of these zones with its high mobility.

The present state-of-the-art leaves several questions to be answered concerning the ultimate design of the of the lander system. These include a method of termal control and balance on or near the RTG's. Much of the steering mechanism in the trailer may have to be shielded from the four RTG power sources. The RTG's can produce temperatures of 500 degrees centigrade in these areas.

Much more performance data on vehicle dynamics is needed to complete the study and, of course, the sterilization problem still looms as the main obstacle to many designs. The sophistication-reliability tradeoff is a very significant feature of the on-board computer system, since it must make decisions regarding path obstacles as well as overseeing experiments. However, if the lander did not carry a decision making system, it would seem that much time would be lost in transmission time between Mars and Earth when the lander came near an obstacle, which it will undoubtedly do several times in one move.

The major philosophy overriding McDonnell's design is one of continued use of reliable hardware, i.e., the manipulation of Appollo and post-Appollo hardware into as many systems as possible. This forms the

basis for a claim of higher reliability, more standarization, and lower costs. This is probably the outstanding feature of the system, and is the foundation of its selection.

At this point it may be well to recap the history of the lander concept with regards to our mission.

One must only recall that the purpose of any space mission is to provide not only information that is scientifically suggestive, but information that is also conclusive and somewhat redundant. With this idea in mind, and with a knowledge of our present technology, it is only natural to consider a lander of some sort on a Mars mission scheduled a decade from now. To this end, a stationary vehicle, known as the Automated Biological Laboratory (ABL) was studied in great detail. However, as weeks wore on, suddenly the concept of a roving vehicle was evolved. This arose mainly from the realization that the retro-burn of any lander would possibly destroy all life that was present in the near vicinity of the laboratory, thus leaving a scientifically sound decision about life on Mars an impossibility. Since time was somewhat limited, and these systems possess a great deal of complexity, a system that was presented in greater detail and which had had more testing to its name seemed a logical choice. However, this choice is not as haphazard as it may seem. The General Electric Company had suggested another system, not as sophisticated nor in such detail. The main disadvantage with this lander (as it appeared in early reports) was its requirement of a hinged platform that could swing 180 degrees to deploy the vehicle. This of course adds weight to supporting structures and increases chances for mechanical failure.

There are also possible future uses for various components of the chosen system. For example, the aft portion of the sterilization canister could someday feasibly be used as a high gain dish attenna, since it is of the correct shape and provides no useful purpose once the lander itself is de-orbited. A pointing problem, possible overcome with hinges, is its only limitation.

The inevitable conclusion reached in a study of any landing system is that in a design of such sophistication and intricacy, the possibility of failure of part and/or all of the mechanism is a very real problem. In this design, where the lander plus entry system accounts for 7000 to 8000 pounds of the liftoff payload, the question of reliability is especially critical. Yet one need only consider the comparitive worth of the data returned from the lander and the high resolution camera to surmise that the information value-to-reliability quotient is much higher for the lander system, and hence explains its equal priority rating with the camera.

INFRARED SPECTROMETER - ALTERNATE DESIGN

In researching the topic of IR detectors, it was noted that the diffraction grating was often rotated slightly in order to extend the wavelength range of the detector. This technique was avoided because the fast ground-speed of the orbiter would cause the detection of different portions of the spectral region over different areas of the planet.

It was also noted that the plane mirror was often pivoted so that the planetary surface could be scanned. The problem that arises is that this scanning will decrease the amount of time radiation falls on the detectors, thus rendering the bolometers ineffective as they do not have as low a time constant as photodetective material.

In addition, or as an alternative, to the proposed system, which will operate from the orbiting spacecraft, a similar system might be incorporated into the proposed lander, weight and spacial limitations permitting. Such a system will then enable the proposed experiments to be conducted during the descent phase of the lander.